SMALL MOLECULES AND FUNCTIONALIZED PEPTIDES TO STUDY PROTEIN PRENYLATION

A DISSERTATION
SUBMITTED TO THE FACULTY OF
UNIVERSITY OF MINNESOTA
BY

JEFFREY SCOTT VERVACKE

IN PARTIAL FULFILLMENT OF THE REQUIREMENTS
FOR THE DEGREE OF
DOCTOR OF PHILOSOPHY

ADVISOR: MARK D. DISTEFANO

SEPTEMBER 2016

Acknowledgements

Pursuing a doctorate in chemistry is a demanding and difficult challenge. I owe a debt of gratitude to several individuals for helping me achieve this goal and for making the process more enjoyable than imagined.

First, I would like to thank my mother and father for their unconditional support, sacrifice, and encouragement as I pursued my education. Thank you to my family and friends for always being a phone call away when times were tough.

To the MDD group, both past and present, for their friendship, inspiration, and advice. Thanks to Kelly Kyro who helped get my feet wet in lab, to Dan Mullen who educated me on peptide synthesis and HPLC purification, and Yen-Chi Wang who was an endless supply of organic synthesis knowledge.

I have also had the opportunity to collaborate with several talented research groups, both in and outside of the University of Minnesota. I would like to acknowledge Dr. Christine Hrycyna at Purdue and her graduate students, Kalub Hahne, Amy Funk, Patty Wiley, and Erh-Ting Hsu for their efforts in using my compounds to study Ste24 and Icmt. I would like to acknowledge Dr. Carol Williams at the Medical School of Wisconsin and her team members Nathan Schuld, and Patrick Gonyo for their work with studying my materials with SmgGDS proteins. To Dr. Marco Pravetoni in the Medicine Department for the opportunity to make drug-peptide conjugates.

Most of all, I would like to thank my advisor, Mark Distefano, for his inspiration, motivation, and enthusiasm. Without his leadership, I am sure my time in graduate school wouldn't have been as gratifying or successful.

Preface

Please note the following:

Chapter 2, in part, was previously published: Hahne, K.; Vervacke, J. S.; Shrestha, L.; Donelson, J. L.; Gibbs, R. A.; Distefano, M. D.; Hrycyna, C. A. Evaluation of substrate and inhibitor binding to yeast and human isoprenylcysteine carboxyl methyltransferases (Icmts) using biotinylated benzophenone-containing photoaffinity probes. *Biochem. Biophs. Res. Commun.* **2012**, *423*, 98-103

Chapter 3, in part, was previously published: Vervacke, J. S.; Funk, A. L.; Wang, Y.-C.; Strom, M.; Hrycyna, C. A.; Distefano, M. D. Diazirine-Containing Photoactivatable Isoprenoid: Synthesis and Application in Studies with Isoprenylcysteine Carboxyl Methyltransferase *J. Org. Chem.* **2014**, *79*, 1971-1978

Abstract

Post-prenylation processing enzymes Rce1, Ste24, and Icmt function to increase the hydrophobicity of prenylated proteins and assist in targeting them to cellular membranes. Rce1 and Ste24 are CAAX endoproteases that cleave the –AAX residues off the C-termini of prenylated proteins that are then methylated by Icmt. Many prenylated proteins play key roles in the progression of cancer, such as the prenylated G-protein family Ras. Most therapeutic efforts in this area focused on preventing protein prenylation by inhibiting the prenyltransferase enzymes. However, other means of preventing oncogenic signal transduction can be accomplished by disrupting the function of Rce1, Ste24, and Icmt. This thesis focuses on the synthesis and application of small molecules and functionalized peptides to study isoprenoid recognizing enzymes.

In order to evaluate Icmt's topology, mechanism of methylation, and substrate recognition, isoprenoid-containing photoactivatable analogues were developed that crosslink to residues in or near the reactive sites. Initial studies focused on the synthesis and evaluation of benzophenone-containing peptide probes that resemble the natural, prenylated substrate. After the functionalized peptides were determined to be substrates, UV wavelength photolysis was used to cross-link the benzophenone moiety to adjacent Icmt isoprenoid binding site residues. To improve the efficiency of the substrate recognition and enhance labeling of Icmt, a new diazirine isoprenoid analogue was developed. Additionally, the peptide backbone was modified to contain both a biotin moiety and a fluorophore for facile in-gel fluoresces detection of the crosslinked material. These improvements should assist the ability for the cross-linked active site to be

determined for Icmt after proteolysis and LC-MS-MS analysis, a task that has yet to be solved.

Ste24p has two different proteolysis roles in the maturation of the yeast mating pheromone, **a**-factor. The first site is the CAAX motif, while the second site is upstream toward the N-terminus, each having a unique amino acid sequences. As a way to observe the reaction kinetics of both sites, peptide analogues that contain a fluorescent donor-quencher pair were developed. By monitoring the increase in fluorescence upon proteolysis, reaction kinetics of both cleavage positions were determined.

To explore the pool of cellular proteins that recognize isoprenoid diphosphates, photoaffinity isoprenoid diphosphate analogues were synthesized. Two types of isoprenoid diphosphate derivatives were developed: diphosphate and phosphonophosphate. Each of the derivatives contain a diazirine motif as the photophore. The diphosphate analogue was shown to be an alternative substrate for both yeast and mammalian farnesyltransferase. The photoaffinity phosphonophosphate analogues were proven to be inhibitors of farnesyltransferase, demonstrated the ability to label isoprenoid binding proteins SmgGDS-607 and SmgGDS-558, and should be suitable for identifying unknown binding partners in future cellular lysate labeling experiments.

Lastly, effort was put forth to synthesize a small molecule inhibitor for Icmt. The inhibitor incorporates both substrates recognized by Icmt: a prenylcysteine carboxylate, and the methyl donor *S*-adenosine methionine. In order to make the bisubstrate molecule an inhibitor, the appendage between the two substrates is through an amide bond that replaces the cysteine carboxylate moiety. It is hypothesized that by combining both

substrates into one entity, the bisubstrate compound will bind more efficiently with Icmt and enhance inhibitor potency. The bisubstrate inhibitor was shown to inhibit mammalian Icmt, but had little effect on the yeast homologue.

Table of Contents

List of Tables

List of Figures

List of Schemes

Chapter 1: Synthetic Probes for the Analysis of Enzymes Involved in the processing of Prenylated Proteins

1.1 Introduction to Protein Prenylation

Many proteins and peptides found in eukaryotic biological systems are translated in an immature state. Expressing proteins in an inactive form is advantageous for the cellular system, allowing the cell to control when and where full maturity is reached. Before obtaining full utility within the cell, proteins require one or more enzymatic transformations known collectively as post-translational modifications (PTMs).[1] PTMs are carried out by a wide range of cellular enzymes, and account for the manipulation of multiple different functional groups.[2] A particular post-translational modification of growing interest for its potential use in cancer treatments is known as protein prenylation.[3] Prenylation renders the target protein more hydrophobic, enabling the prenylated protein to anchor itself to the cellular membrane, and is essential for membrane-associated functions involving protein-protein interactions, signal transduction, and cellular homeostasis regulation.[4] Among the many translated proteins in a mammalian host, roughly 2% of the proteome is prenylated.[5] A specific family of prenylated proteins, known as the Ras superfamily, has been the primary focus for anti-cancer research, due to studies linking Ras mutations with approximately 30% of known cancer.[6]

Ras, whose name is derived from Rat Sarcoma,[7,8] is a superfamily of small g-proteins (GTPases) that bear a prenylated C terminus.[9] GTPases are monomeric proteins that participate in guanosine triphosphate (GTP) exchange and act as molecular switches

in signal transduction cascades by alternating between an inactive GDP-bound form and an active GTP-bound state.[10] The primary function of the Ras enzymes is to regulate gene expression, along with cytoskeletal assembly, intracellular vesicular trafficking, and nucleocytoplasmic transport.[11] The translation of mutations in the Ras genes that cause constitutive activation of the enzymatic function results in abnormal cell growth and division.[10-12] Of the three members of the Ras superfamily (H, N and K),[13] K-Ras is often found mutated in cancer, especially in the pancreas.[14] Crucially, transformation of both wild type and mutated Ras proteins cannot be reached until a CAAX signal motif is completely processed,[3] providing the opportunity to design methods to inhibit cancer-linked mutations.

A CAAX motif is the last four amino acids at the C terminus of a protein: C, cysteine; A, an aliphatic amino acid; and X, any amino acid. In order to reach complete maturity, the CAAX sequence undergoes three enzymatic structural modifications, known as the isoprenylation pathway (Figure 1.1).[15-21] The initial step is prenylation, the attachment of an isoprenoid moiety to the cysteine amino acid residue through a thioether linkage. Enzymes farnesyltransferase (FTase) and geranylgeranyltransferase (GGTase) catalyze the covalent attachment of the cysteine's free thiol with either *all-trans*-farnesyl (C15) or *all-trans*-geranylgeranyl (C20) pyrophosphate, respectively.[22-24] Specificity between the two enzymes is determined by the identity of the terminal X amino acid of the CAAX motif.[25] The second step, endoproteolysis, is the removal of the -AAX tripeptide from the C-terminus by Ras converting enzyme (Rce1) and zincmetalloprotein Sterile 24 (Ste24).[26,27] The final step of the CAAX transformation is the methylation of

the newly revealed C-terminal cysteine carboxylate by isoprenylcysteine carboxyl methyltransferase (Icmt).[28,29] The complete series of modifications to the CAAX sequence increases the hydrophobicity of the protein, and facilitates membrane localization.

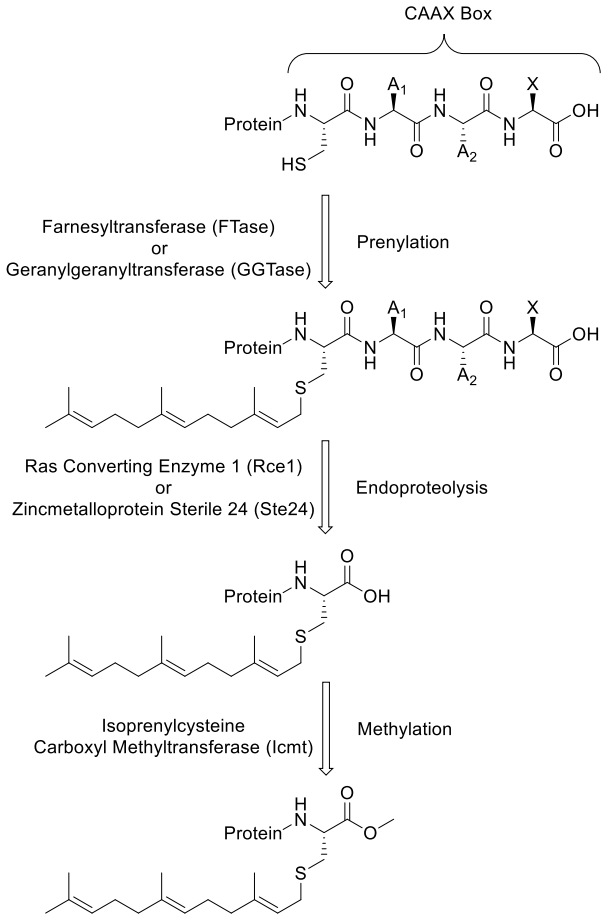

Figure 1.1. Isoprenylation pathway: prenylation by FTase or GGTase; endoproteolysis by Rce1 or Ste24; methylation by Icmt.

Due to the important role CAAX proteins play in the biogenesis of cancer, research has centered on developing CAAX processing inhibitors. The most successful anti-cancer agents thus far have been farnesyltransferase inhibitors (FTIs) which prevent farnesylation of these proteins.[5,30] Unfortunately, Ras proteins were found to become

alternatively prenylated with geranylgeranyl isoprenoids in the presence of FTIs, limiting treatment effectiveness for Ras-induced tumors. Because of this alternative prenylation phenomenon, disruption of the proteolysis and methylation steps in the isoprenylation pathway have been considered as a possible cancer treatment strategy. The following reviews the small molecule tools used to define substrate specificity, inhibit enzymatic activity, and explore structural characteristics of Rce1, Ste24, and Icmt.

1.2 Ras Converting Enzyme 1 (Rce1) and Zincmetalloprotein Sterile 24 (Ste24)

1.2.1 Background

Following isoprenoid attachment along the isoprenylation pathway is endoproteolysis of the last three amino acids in the CAAX motif (Figure 1.1). In mammalians there are two enzymes that perform this function: Ras converting enzyme 1 (Rce1)[31] was the first to be characterized, followed by zincmetalloprotein sterile 24 (Ste24).[32] Both enzymes are localized in the endoplasmic reticulum (ER) and contain seven transmembrane a-helices (TMH), with Rce1 (329 AA) being slightly smaller than Ste24 (457 AA).[33] Although some overlap occurs in substrate recognition, Rce1 is exclusively responsible for the processing of the Ras superfamily, while recent findings contradict assumptions that prelamin A was the only substrate for Ste24.[34,35] Despite being analogous in function, only Ste24 contains the zinc binding motif, HEXXH, characteristic of zinc-dependent metalloproteases,[36] while Rce1 has no sequence typical of any of the well-defined protease classes.

Efforts targeting the proteolysis step of prenylation are supported by studies showing that K-Ras and H-Ras activity was attenuated when the genes encoding Rce1

were deleted.[36,37] Deletion of the gene encoding Rce1 in mice to further study the endoproteolytic processing of Ras proteins resulted in embryonic lethality late in gestation (following day 15.5) or shortly after birth.[38] Similarly, phosphodiesterase 6 transformation and localization was impacted, causing a reduction in mice photoreceptor cell viability and ability to respond to light.[39] Moreover, fibroblast cells derived from the Rce1-deficient mice embryos were not carboxymethylated, the final step in the processing of Ras proteins which requires prior proteolysis. Most importantly, Rce1-deficient cells were unable to process farnesylated H-Ras, N-Ras and K-Ras or geranylgeranylated K-Ras proteins which became mislocalized within cells to the cytoplasm.[31,38] Mislocalization indicated that Rce1 was essential for the proper membrane association of Ras proteins, which is a requirement for enzymatic activity. Proper functioning of Ste24 has also been shown to be crucial for proper nuclei structure.

The nuclear lamina is composed of lamin filaments and associated membrane proteins that provide structural integrity to most eukaryotic nuclei.[40] Of the three types of lamin proteins, lamin A and B are translated with C-terminal CAAX motifs that require the isoprenylation pathway modifications to reach maturity.[41-43] Interestingly, prelamin A is endoproteolyzed 15 residues upstream from the C-terminal by Ste24, after carboxymethylation by Icmt, to release lamina A into the nucleoplasm.[36] If prelamin A or Ste24 undergo mutations that block this cleavage, prelamin A accumulates in the nuclear membrane, causing a class of disease called laminopathy.[41] Depending on the impact of the mutation on Ste24 activity levels, laminopathy severity can range from skin or bone abnormalities up to Hutchinson-Gilford progeria syndrome or restrictive dermopathy.[42,44-

[47] Although disrupting endoproteolysis activity can be beneficial for controlling Ras associated diseases, laminopathy symptoms highlight the importance for selectively inhibiting Rce1 while leaving Ste24 unaffected. To approach this difficult challenge, the scientific community worked heavily with Rce1 and Ste24 enzymes found in yeast.

The yeast homologues Rce1p and Ste24p have catalytic function and cellular localization that is similar to mammalian endoproteases, making them ideal candidates for comparison studies.[33,48] While it was initially thought that Rce1p was the only ER localized endoprotease, later work in Saccharomyces cerevisiae (S. cerevisiae) found two splice variants of the protease, leading to the discovery of Ste24p.[26,27] Ste24p performs the proteolytic cleavage of the C-terminal CAAX motif from the precursor peptide of **a**-factor, a yeast mating pheromone.[49] Additionally, Ste24p performs an unrelated N-terminal cleavage on the **a**-factor precursor peptide, an event which normally takes place after the C-terminal modification is complete,[50] but is not dependent upon completion.[51] Like Ste24, Ste24p possesses a consensus zinc metalloprotease motif, requires zinc for optimal activity, and is inhibited by zinc chelating compounds such as 1,10-phenanthroline.[52,53] Rce1p is also capable of cleaving the C-terminus of the **a**-factor precursor as well as other yeast CAAX proteins.[34] Unlike Rce1, sequential analysis of Rce1p identified invariant residues reminiscent of a consensus HEXXH motif found in metalloproteases;[54,55] however, these findings don't rule out the possibility of an undiscovered protease mechanism.[56] Due to the lack of structural details on the membrane-bound proteases, an array of small molecule and peptide based tools have

been developed to explore substrate specificity and structure-activity relationships (SAR) for these enzymes.

1.2.2 CAAX Protease Substrates

Substrate recognition for Rce1p and Ste24p is dependent upon the presence of an isoprenylated CAAX sequence at the C-terminus of a protein or peptide.[15] Although the tetra amino acid sequences undergo endoproteolytic cleavage most efficiently, isoprenylated tri (CXX) and di (CX) amino acid sequences are also found to undergo cleavage at the scissile bond.[57] Interestingly, *N*-acetyl-*S*-farnesyl-cysteine-amide is not processed, confining substrate recognition to a dipeptide across the scissile bond. Dipeptides whose C-terminus was a methyl ester weren't recognized, adding the requirement of a C-terminal carboxylate functionality.[58] The specificity of the amino acids in the CAAX sequence was also explored.

Using a tetrapeptide library that varied at the positions downstream to the prenylated cysteine in the CAAX motif (CA_1A_2X) (Figure 1.1), the specificity of each position was determined. Studies found that the endoproteases prefer large hydrophobic residues in both the A_1 and A_2 positions.[59] Small hydrophobic residues, or hydrophilic, uncharged residues in both the A_1 and A_2 positions are also recognized. Endoprotease activity was not found when the substrate peptide contained nonnative D amino acids at any position in the CAAX sequence, emphasizing stereoselectivity for substrate recognition.[58] Varying the length of the isoprenoid appended to the tetrapeptide showed that farnesylated peptides where processed more readily compared to the geranylgeranylated versions.[54] Most importantly, it was found that specific sequences

were only processed by one of the proteases, demonstrating that Rce1p and Ste24p had distinct substrate selectivity.[54]

1.2.3 CAAX Protease Inhibitors

Initial inhibitor design for the endoproteases began when commercially available protease inhibitors for cysteine (E-64 and leupeptin), serine (APMSF and aprotinin), aspartyl (pepstatin), and metalloproteases (phosphoramidon, EDTA) failed to block complete activity.[60] As a starting point, *N*-acetyl-*S*-farnesyl-cysteine (AFC) **1.1,** and *N*-*tert*-butyloxycarbonyl-*S*-farnesyl-cysteine (BFC) **1.2** (Figure 1.2), were explored as product based inhibitors, but results showed mild effects.[60] Using the BFC scaffold, a series of derivatives were developed that replaced the carboxylate moiety with several other functional groups: primary alcohol, aldehyde, ketone, statine, and difluorostatine. All derivatives proved to be inactive, with the exception of the aldehyde analogue, **1.3** (Figure 1.2), which was a low micromolar competitive inhibitor.[60] This finding suggested that the mechanistic mode of proteolysis was serine or cysteine based, because aldehyde analogues are known to be potent transition state derivatives that mimic the tetrahedral intermediates through either the hydrate form of the aldehyde, or by a complex with the active site serine or cysteine amino acid.[61] In an attempt to enhance potency, peptide based inhibitors were designed.

The first peptide based inhibitors were designed from the carboxyl terminus of retinal transducing, AFC-Val-Ile-Ser, a tetrapeptide known to be a substrate for endoproteolytic activity[62]. Di, tri, and tetrapeptide substrates were constructed that contained a statine motif **1.4** (Figure 1.2) in place of the scissile bond, and tested against

the proteases.[60] Each of the peptides tested as inhibitors, with potency increasing as sequence length increased, consistent with substrate activity for the endoprotease.[57] Similar results with other pseudopeptides led to the conclusion that modifications in which cleavage at the scissile bond is prevented will generate active inhibitors. In attempts to purify the mammalian endoproteases, a more potent class of inhibitor was revealed.

Working with the classical protease labeling agent, halomethyl ketones, the first irreversible inhibitor of endoprotease activity was discovered. Treatment with *N*-tosyl-phenylalanine-chloromethyl ketone (TPCK), was found to block protease activity, presumably by alkylating the active-site residue.[63] However, *N*-tosyl-lysine-chloromethyl ketone (TLCK), a specific irreversible inhibitor of the serine based protease trypsin and trypsin-like enzymes, did not inhibit the enzyme activity under the same conditions. Competition experiments with the reversible inhibitor **1.4** prevented unrecoverable loss in proteolysis activity when co-treated with TPCK; however, pretreatment with TPCK in the experiment resulted in no proteolysis activity upon recovery. These findings support the view that TPCK is a specific active-site-directed irreversible inhibitor, and suggest the mechanistic mode of proteolysis to be cysteine based.

Efforts to improve chloromethyl ketone inhibitor potency afforded two farnesylcysteine analogues: *N*-*tert*-butyloxycarbonyl-*S*-farnesyl-cysteine-chloromethyl ketone (BFCCMK) **1.5** (Figure 1.2), and *N*-*tert*-benzyloxycarbonylglycylgylcyl-*S*-farnesyl-cysteine-chloromethyl ketone (ZGGFCCMK). While both farnesylcysteine analogues were affective, BFCCMK had the strongest inhibitor effect, presumably by

mimicking the wild type substrate to a higher extent.[63] Additional improvement to BFCCMK was afforded years later by replacing the farnesyl moiety with a dodecyl group and the thioether connectivity with a methylene unit.[64] Removing the thioether unit produced a more biologically stable linkage and increased cell permeability, enhancing the inhibition affect. These results provide further evidence of a thiol based proteolysis mechanism and suggest that the farnesylcysteine moiety, or a close mimic, is crucial for potent and selective inhibitor design.

Similar to the chloromethyl ketone, acyloxy methyl ketone analogues were studied as endoprotease inhibitors. Envisioned to chemically alkylate the catalytic residue, peptidyl (acyloxy)methyl ketone (AOMK) **1.6** (Figure 1.2), showed that both yeast Rce1p and Ste24p were inhibited upon treatment.[65] Peptidyl AOMKs were initially an intriguing discovery because they inhibited both Rce1p and Ste24p to a similar extent, lacked the farnesylcysteine motif, and the inhibition effect was thought to be tunable based on the stability of the acyloxy leaving group.[65] Years later, while studying the structural elements that contribute to the inhibitor properties of AOMK toward Rce1p and Ste24p, inhibition was found for dipeptides lacking the acyloxy functionality.[66] This finding suggested that the inhibition observed was from reversible, noncompetitive binding, unrelated to the formerly mentioned chloromethyl ketone analogues. Although unfortunate, the result supported the theory that Rce1p is not a cysteine protease.

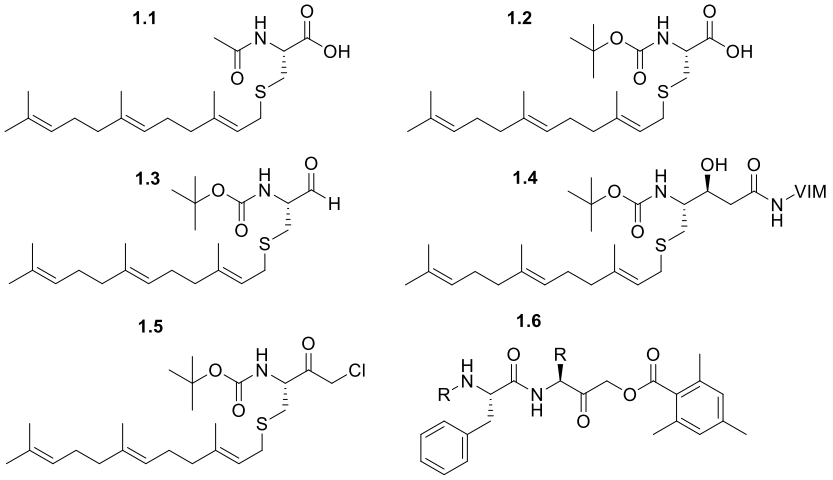

Figure 1.2. Early inhibitors of Rce1 and Ste24: AFC **1.1**, BFC **1.2**, AFC-Aldehyde **1.3**, BFC-Statine-VIM peptide **1.4**, BFCCMK **1.5**, Dipeptide-AOMKs **1.6**.

Non-peptidic, non-prenylic small molecules have also been developed as endoprotease inhibitors. The first studies of this type used a bisubstrate approach by incorporating a farnesyl mimetic conjugated though a linker to a peptidomimetic motif for the inhibitor design. Out of the 16 analogues tested, the most potent was a cinnamyl prenyl mimetic appended though a β-Ala linker to a benzenesulfonamide motif as an A_1A_2-mimetic, indicating that the X-amino acid is of minor importance, **1.7** (Figure 1.3).[67] Interestingly, many of the analogues showed inhibitor effects to the prenylation enzyme, PFTase, but didn't affect the subsequent methylation enzyme, Icmt. This advancement toward more drug-like inhibitors was further developed with the aid of high-throughput screening.

Using high-throughput screening methodology the NCI DTP Diversity Set library was tested for inhibitors of Rce1p. Out of the 1981 compounds 46 were found to be inhibitors, of which 9 passed a secondary screening protocol. Many structure similarities were observed for the lead compounds: three contained a diphenylmethane motif, two

were hexachloro-substituted bicycloheptene based, two were nearly identical mercury-based, multi-cyclic ring structures containing purine nucleoside substructures, and the remaining had a pyridine and hydrazinecarbothioate core. All of the compounds were determined to have low micromolar inhibition effects, with the most potent, NSC1011 **1.8** (Figure 1.3), having an IC_{50} value of 9 μM. Inhibition of Rce1p *in vitro* persisted through washing treatment, suggesting that the compounds are irreversible competitive inhibitors.[68] *In vivo* tests with the lead compounds have been shown to displace GFP-Ras2p reporters upon treatment in yeast, while displaying low cytotoxicity to the treated cells.[69] The majority of the lead compounds were also shown to inhibit Ste24p and the yeast methyltransferase, Ste14p.[68,69] Although promiscuous, this study yielded compounds that represent new and useful tools for the *in vitro* and *in vivo* characterization of Rce1p.

Most recently, advancement in the selectively of Rce1 non-peptidic, non-prenylic small molecule inhibitors has been demonstrated. Using a design based on the endoprotease inhibitor **1.8**,[68] a library of 58 analogues was developed in an attempt to increase specificity for Rce1 over Ste24. Several of the 8-hydroxylquiolin based analogues caused reduction in Rce1 activity *in vitro* (IC_{50} < 10 μM), exhibited low cell toxicity, and induced mislocalization of EGFP-Ras from the plasma membrane in human colon carcinoma cells.[70] Surprisingly, some of the inhibitors, particularly the 8-hydroxylquiolin derivative **1.9** (Figure 1.3), were more effective at mislocalizing K-Ras compared to a potent farnesyltransferase inhibitor (FTI). Similar inhibition results with **1.9** and the non-metal chelating 1-naphthol derivative, **1.10** (Figure 1.3), infers that Rce1

may not be a zinc metalloprotease. Most importantly, **1.9** and other 8-hydroxylquiolin based analogues that tested positive for Rce1 failed to inhibit Ste24. This study presents a new guideline for effective Rce1 inhibitor design and demonstrates SAR differences between Ste24 and Rce1.

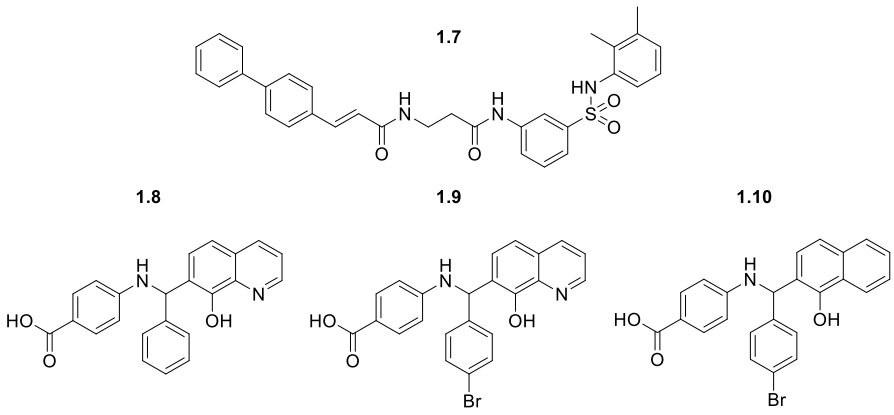

Figure 1.3 Non-preptidic, non-prenyl based Rce1 and Ste24p inhibitors: original bisubstrate inhibitor **1.7**, NSC1011 **1.8,** 8-hydroxylquiolin derivative **1.9**, 1-naphthol derivative **1.10**.

Inhibition experiments of Ste24 with HIV protease inhibitors (HIV-PIs) have been performed with varying success.[71-73] Using GFP fusion forms of prelamin A, inhibition effects of lopinavir (LPV), Tipranavir (TPV), and ritonavir (RTV) on Ste24 activity were explored by *in vitro* treatment of transfected HEK293 cells. Western blots using antibodies against GFP, and prelamin A clearly showed evidence of the accumulation of prelamin A upon treatment with HIV-PIs. To verify that Ste24 was being inhibited, the HIV-PIs were treated *in vitro* with yeast cells and **a**-factor processing was quantified in a coupled endoproteolysis/methylation assay, affording IC_{50} values in the low micromolar range.[71,73] Interestingly, in a follow-up study with the potent HIV-PI Darunavir, no Ste24 inhibition or prelamin A accumulation was found.[72] Given the fact that the HIV protease

is a known aspartyl protease, it is perplexing how LPV, TPV, and RTV interacts with the zinc dependent protease and only minimally with Rce1.

1.2.4 CAAX Protease Photoactive Probes

Structural characterization of membrane-bound proteins has been limited, due to their hydrophobic nature and low cellular abundance. A solution to this challenge is offered by the technique known as photoaffinity labeling. Photoaffinity labeling is employed to identify noncovalent interactions between molecules, including protein-ligand and protein-protein complexes. By incorporating a photoactive motif into protein substrates or ligands, the site of interaction with the protein is captured upon UV photolysis, covalently bonding the interacting partners together. After enrichment and proteolysis of the bound complex, the crosslinked segments can be identified and used to map substrate binding sites,[74] or potentially reveal unknown binding partners.[75] To address these membrane-bound limitations with Rce1p, photoaffinity peptides and isoprenoid analogues were designed.

To date, only two attempts have been reported to characterize Rce1p by utilizing the photoaffinity labeling strategy. Both studies designed peptide based probes that mimicked the C-terminal sequence of the Ras protein K-Ras4B, KSKTKC(Fr)VIM. The first study analyzed Rce1p though the use of photoactive isoprenoid analogues appended to the K-Ras4B peptide in place of the farnesyl group on the CAAX motif. Several isoprenoid analogues incorporating the photocrosslinking motifs aryl azide, diazotrifluoropropionate, and benzophenone have been successful in labeling experiments with the prenyltransferase enzymes; however, due to their superior stability

properties,[76,77] only benzophenone-containing derivatives were employed. Using a fluorescent based assay, Rce1p was shown to recognize and process peptide **1.11** (Figure 1.4), a peptide substrate prenylated with a benzophenone isoprenoid, though slower than the wild type farnesylated peptide.[56] Given the recognition of **1.11** by Rce1p, peptide **1.12** (Figure 1.4), bearing a biotin moiety at the N-terminus, was synthesized to crosslink Rce1p. Using the biotin as a handle, the ability of **1.12** to label Rce1p was demonstrated via streptavidin pull-down, SDS–PAGE, and Western blot analysis.[56] Labeling of Rce1p with **1.12** was shown to be reduced by competition with the farnesylated version of the peptide. Taken together, these results demonstrate that benzophenone-containing peptides can serve as substrates for Rce1p and suggest that the enzyme is being labeled in the isoprenoid binding site.

Enhancement in crosslinking was shown in the subsequent study, where benzoylphenylalanine (Bpa), **1.13** (Figure 1.4) was incorporated in the backbone of the peptide.[78] Rce1p substrate determination for **1.13** was verified by monitoring cleavage by HPLC and product detection by MS. Interestingly, moving the Bpa moiety to different positions in the peptide sequence resulted in varying crosslinking efficiency not dependent on the proximity of Bpa to the scissile bond. Bpa crosslinking results suggest that residues upstream of the CAAX motif are in contact with Rce1p, a notion overlooked by previous substrate and inhibitor work with Rce1p. By increasing the labeling efficiency of substrate photoprobes, further structural information on Rce1p may be obtained via isolation and characterization of the covalent enzyme–probe complex.

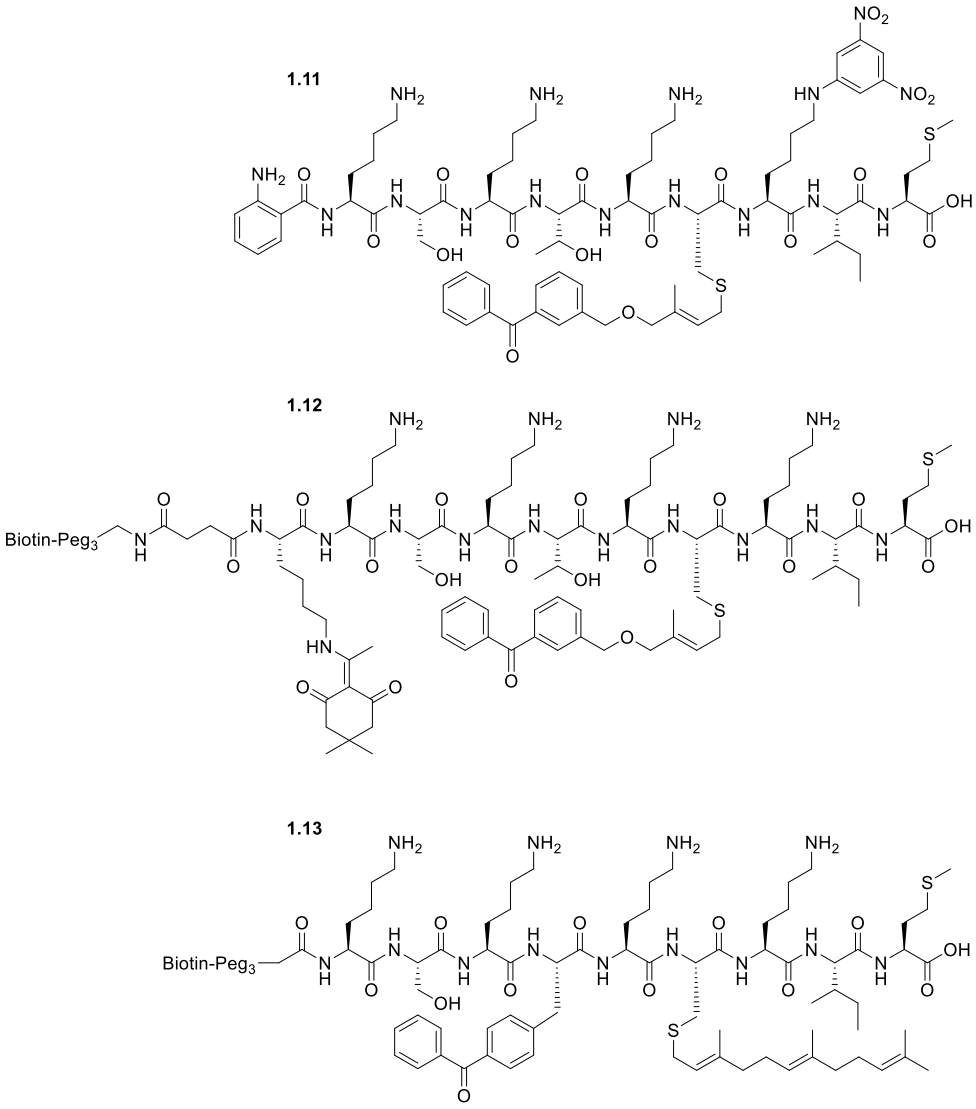

Figure 1.4. Rce1 photoaffinity labeling peptide probes: Self-quenching fluorescence assay probe **1.11**, K-Ras4b-C_5-Benzophenone probe **1.12**, K-Ras4b-Bpa probe **1.13**.

1.2.5 Perspective and Conclusion

The development of small molecule and peptide based compounds to study Rce1 and Ste24 have largely been centered on substrate-product design. Given the potential of inhibiting Rce1 as a cancer therapeutic, while avoiding Ste24 associated laminopathy syndromes, non-prenylic small molecule inhibitors are an attractive alternative for

selectively attenuating Rce1 activity. However, studies have shown that Rce1 activity is crucial for the proper functioning of other vital cellular enzymes,[39,79] which may limit the applicability of Rce1 inhibitors as a therapy strategy. Undoubtedly, new compounds will be pursued to further explore the structure and function of the endoproteases.

Advancement in x-ray crystallography has afforded three-dimensional crystal structures of Ste24 and Ste24p.[80,81] These images have shown the presence of a voluminous membrane-enclosed hallow chamber containing several fenestration. The chamber size and number of entry points presents a challenging puzzle for defining their role in Ste24's substrate selectivity and dual proteolysis function. X-ray studies in combination with photoaffinity labeling compounds should aid in mapping the structural features of Ste24 that are associated in the processing of substrates.

1.3 Isoprenylcysteine Carboxyl Methyltransferase (Icmt)

1.3.1 Background

Isoprenylcysteine carboxyl methyltransferase (Icmt) catalyzes the methyl esterification of C-terminal isoprenylcysteine generated after proteolysis of the CAAX motif (Figure 1.1).[82,83] Like its yeast homologue Ste14p, Icmt and Ste14p are putative polytopic membrane proteins that have been shown to be localized in the ER,[84] which is unique among *S*-adenosyl-methionine (SAM)-dependent methyltransferases.[85] Kinetic analysis showed that Icmt follows a Bi Bi mechanism, with SAM binding initially followed by the prenylated substrate.[86,87] Yeast and human Icmt share 41% sequence identity,[88] which contains a novel tripartite consensus motif that has been shown to be

crucial for enzymatic function.[89] Ste14p and Icmt contain multiple transmembrane α-helices, with Ste14p having 6 segments and Icmt containing 8 segments. The two additional N-terminal segments in Icmt are thought to play a regulatory role.[90] Catalytic function and substrate recognition is mutual between the homologues, with Icmt shown to recover methylation activity in yeast Ste14pΔ mutants.[85]

Icmt and Ste14p behave as metalloenzymes,[88,91] although by what mechanism and metal is still in question. Incubation with the metal chelator 1,10-phenanthroline and Zircon caused Icmt to lose activity, but treatment with the water-soluble chelator EDTA had no effect on enzymatic activity. Similarly, treatment of Icmt with chelator nitrilotriacetic acid (NTA) showed little inhibition, but conjugation of NTA though a lysine linker to a hydrophobic compound, such as cholesterol, eliminated activity.[92,93] Collectively, these findings suggest that the metal ion is located in a hydrophobic segment of the enzyme.

The discovery of Icmt began with the isolation of a peptide that contained an isoprenylcysteine methyl ester C-terminus from two fungi, *Tremella mesenterica* and *Tremella brasiliensis.*[94,95] Nearly a decade later, the yeast gene for Ste14p was uncovered after the identification of the yeast mating hormone, **a**-factor, that bared the isoprenylcysteine methyl ester functionality.[28,29,96] The discovery of yeast Ste14p ignited the search of its mammalian homologue, Icmt, that was first found in bovine retinal rod outer and rat liver cells.[97-99]

The methyl esterification reaction has several important physiological roles in protein function and cellular homoeostasis.[26,27,100,101] The conversion of a negatively

charged carboxylate to a methyl ester renders the C-terminus more hydrophobic and enhances the partitioning of the protein to the cell membrane, facilitating proper cellular localization.[27,100,101] Carboxyl methylation has been suggested to protect the precursor poly peptide from proteolytic digestion.[26] The methyl esterification of proteins also aids in the proper recognition of plasma and intercellular membrane receptors, and mediating protein-protein interactions.[100,101] As an example highlighting the requirement for proper enzymatic function by Icmt, mice embryos lacking Icmt were shown to die ten days into gestation, exhibiting abnormal cell structure and division.[102] Although the function of Icmt is important in the development of mammalian cells, significant effort has been devoted toward targeting Icmt as an anti-cancer therapeutic.

Efforts to target the methylation modification in the prenylation pathway began when studies showed that Ras protein activity was attenuated in cells that lack Icmt.[103,104] It was found that Icmt deficiency in embryonic stem cells caused mislocalization of K-Ras away from the plasma membrane and trapped it within the cytoplasm, while wild type cells showed proper plasma membrane association.[103] In addition, inactivation of Icmt in a mouse fibroblast cell line resulted in inhibition of cell growth and reduced oncogenic transformation of K-Ras and its downstream receptor B-Raf.[104] More recently, down regulation of Icmt in mice dispositioned with progeria showed recovery in phenotype characteristics and increased lifespans.[105] From these studies, it is clear that Icmt is critical for proper membrane targeting and biological function of Ras proteins, and a promising target in oncogenesis research.[106]

1.3.2 Icmt Substrates

Icmt substrate recognition is dependent upon the incorporation of an isoprenylcysteine moiety. Using Icmt isolated from rat liver, the binding affinity for the synthetic peptide LARYKC was studied in the non-prenylated, *S*-geranylated, *S*-farnesylated, and *S*-geranylgeranylated forms.[97] As predicted, Icmt only recognized the prenylated substrates, with farnesylated (K_m = 2.2 μM) and geranylgeranylated (K_m = 10.9 μM) peptides having the strongest binding. It is important to note that the geranylated derivative had a substantial decrease in affinity to the enzyme when compared to farnesyl and geranylgeranyl versions, suggesting a minimum 15-carbon length of the isoprenoid moiety for optimum substrate recognition.[97] Additionally, modifying the sulfhydryl moiety to an n-alkyl derivative also decreased the affinity of the substrate, highlighting the importance of the conjugated, rigid isoprenoid structure.[97]

Several studies with *N*-acetyl-*S*-farnesyl-cysteine (AFC) **1.1** (Figure 1.2) and the longer *N*-acetyl-*S*-geranylgeranyl-$_L$-cysteine (AGGC) have found them to be good substrates for recognition by Icmt.[86,88,101,107,108] K_m values for AFC (7 μM) and AGGC (20 μM) are within an order of magnitude compared to the peptide substrates,[97] signifying that the majority of substrate specificity is dependent upon the spatial relationship between the isoprenoid moiety the carboxylic group. The stereoselectivity of Icmt was also tested with $_D$-AFC and racemic DL-Homocysteine, which were shown to be non-substrates and only mild inhibitors of Icmt.[98] Interestingly, the unmodified amino version of AFC, farnesylcysteine (FC), wasn't a substrate but acted as an inhibitor of Icmt, suggesting that a peptide like modification of the amino group is required for

substrate activity.[98] These findings led researchers to believe that the minimal recognition element for Icmt was an amino acetylated, isoprenylated cysteine moiety.

Removal of the amino group from AFC, creating *S*-farnesyl thiopropionic acid (FTP) **1.14** (Figure 1.5), was shown to be recognized and methylated by Icmt.[98] FTP was found to have a K_m of 14 μM, similar to that of AFC, thereby reducing the minimal structure requirement for Icmt recognition. *S*-farnesyl thioacetic acid (FTA) **1.15** (Figure 1.5), one methylene unit shorter between the carboxylic and thiol functionality than FTP, resulted in loss of substrate activity;[98] however, FTA did test as a potent competitive inhibitor to Icmt with a K_I of 3.9 μM. Overall, discovery of FTP helped simplify inhibitor synthesis by eliminating amino acid chirality, reducing molecular weight, and increasing ligand efficiency.[109] To refine substrate requirements for Icmt, heteroatom derivatives were examined.

Using AFC and FTP as templates, a series of heteroatom analogues were designed to test the substrate specificity of Icmt. The role of the thioether connectivity in AFC was first studied by oxidation of the sulfur atom to the racemic mixture of sulfoxide diastereomers. Neither of the sulfoxide analogues were substrates of Icmt, but tested as a mixture to be competitive inhibitors.[98] Additionally, racemic selenium derivatives of AFC and FTP were tested to be substrates but had a large K_m and smaller V_{max}. Only weak substrates for Icmt were afforded when replacing the sulfur atom in oxo and amino analogues of FTP.[98] Several years later, the thioether moiety in AFC was exchanged with a methylene unit, desthio-AFC **1.16** (Figure 1.5), which lacked both substrate and inhibitor activity for Icmt.[110] The thioether moiety in FTP was also replaced with a

triazole group. Triazole-FTP **1.17** (Figure 1.5) lost substrate activity, but tested as a potent competitive inhibitor.[111] Taken together, these works demonstrate the importance of the thioether moiety in Icmt recognition, and establish its importance in future inhibitor designs. Many inhibition studies have been performed in an attempt to further understand the nature of Icmt substrate specificity.

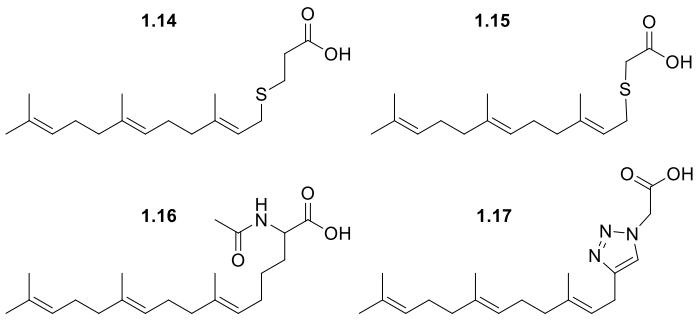

Figure 1.5. Small molecules to study Icmt substrate specificity: FTP **1.14**, FTS **1.15**, desthio-AFC **1.16** and Triazole-FTP **1.17**.

1.3.3 Icmt Inhibitors

Initial Icmt inhibition studies worked with AFC and AGGC, utilizing their competitive inhibitor and cell-permeable properties, while avoiding inhibition of other cellular methyltransferases.[98,107,112-114] Treatment of cells with AFC and AGGC induced an array of biological effects thought to be caused by specifically inhibiting Icmt. Examples included a decrease in methylated Ras proteins, disruption of signaling for insulin releasing, interruption of the Ras signaling pathway, and interference of superoxide release in human neutrophils.[114-120] Conversely, it was shown that AFC and AGGC induced cellular effects that are unrelated to the inhibition of Icmt,[117,121,122] indicating that AFC and AGGC were most likely dominant inhibitors of prenylcysteine-

dependent interactions not exclusively limited to Icmt. Nevertheless, due to their important impact on the mislocalization of Ras, and endothelial cell apoptosis,[102,104] analogues of AFC and AGGC were pursued.

Based on the FTP framework, a series of rigid carboxylic acid analogues were designed as small molecule Icmt inhibitors. Using thiosalicylic acid in place of thiopropionic, *S*-farnesyl thiosalicyclic acid (FTS) was synthesized that restricted carboxylate and thiol functionalities to a cis confirmation by the aromatic ring, limiting the degree of rotational freedom while maintaining the two carbon spacer in FTP. In cell free inhibition studies, FTS was shown to be a competitive inhibitor of Icmt (K_I = 2.8 μM), and also caused mislocalization of human Ras in transformed Rat1 cells.[123] Additional structural isomers of FTS resulted in a decrease in inhibition activity as well as the exchange of the thioether linkage to a secondary amine. Adding chloro and fluoro substituents to the aromatic ring had varying effects. Halogens at the 5-position maintained comparable inhibitor activity to FTS, but at positions 3 and 4 considerably diminished inhibition.[124] Unfortunately, *in vivo* inhibition assays with FTS showed only mild inhibitor effects on Icmt, leading to the conclusion that like AFC, FTS was a dominant inhibitor of prenylcysteine-dependent interactions.[125]

Based on the findings that AFC acted as a substrate and FC did not, design and synthesis of Icmt inhibitors that varied functionality at the amide position were pursued. The first series of amino-FC derivatives were synthesized by acylation of the free amine with various acid anhydrides and evaluated on human platelet methyltransferase. FC analogues incorporating a *N*-isobutyl or *N*-isovaleryl were found to be substrates for

Icmt, but increasing the steric bulk to *N*-(Trimethylacetyl)pivaloyl or *N*-Benzoyl eliminated substrate activity.[122,126] Interestingly, when glycine spacers were inserted between FC and the benzolyl motif, substrate recognition was recovered.[126] These findings suggested that Icmt has a steric limit in proximity to the isoprenoid recognition site.

The amide-substituted FC approach for inhibitor design was expanded a decade later through the development of a 23-member analogue library. Library screening results supported the previous finding, demonstrating that only small alkyl derivatives were substrates for Icmt, while also identifying a modest inhibitor, adamentyl-FC **1.18** (Figure 1.6).[127] Streamlining the amino-substituted FC approach by implementing solid-phase synthesis, o-phenoxyphenyl FC (POP-FC) **1.19** (Figure 1.6) was identified to be a potent Icmt inhibitor (IC_{50} = 4.3 μM).[128] The discovery of **1.19** is perplexing due to the lack of inhibitor activity found for N-Benzoyl-FC. Additionally, a library of sulfonamide-substituted FC analogues was synthesized and evaluated, resulting in another potent inhibitor, 2-thienyl-sulfonamide-FC (IC_{50} = 4.3 μM) **1.20** (Figure 1.6).[129] Taken together, these works demonstrate that Icmt might have a more spatially robust binding site than was earlier assumed.

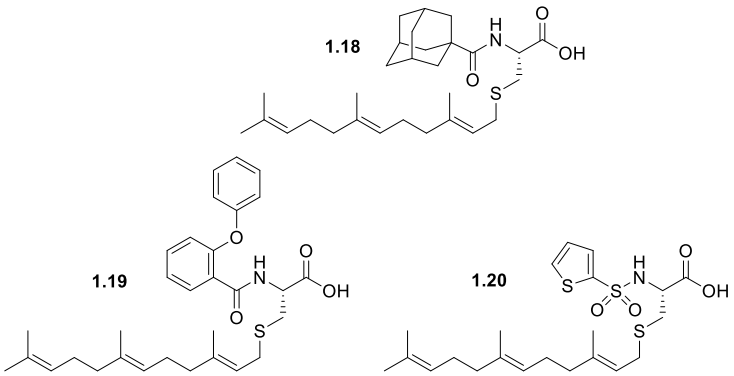

Figure 1.6. Amino-substituted FC Icmt inhibitors: Adementyl-FC **1.18**, POP-FC **1.19,** 2-thienyl-sulfonamide-FC **1.20**.

To more accurately understand the role of the isoprenoid motif in Icmt substrate recognition and potentially uncover effective inhibitors, farnesyl-modified AFC analogues were explored. The first studies tested two AFC analogues: one containing an isobutenyl substitution at position 3 of AFC (3-iBAFC) **1.21**, the other replacing the terminal isoprene domain with a biphenyl motif (3MB-AFC) **1.22** (Figure 1.7). Results showed 3-iBAFC was an inhibitor of Ste14p but a substrate for Icmt.[130] In contrast, 3MB-AFC acted as a mild mixed-mode inhibitor of Icmt with the competitive component being more dominant (IC_{50} = 259 μM).[130] Follow-up studies showed that a derivative of 3MB-AFC that incorporated a C_8 alkyl tail, compound **1.23** (Figure 1.7), in place of the terminal biphenyl motif increased Icmt inhibition (IC_{50} = 35 μM).[111] The most potent inhibitor was reported when amide-substitution with o-phenoxyphenyl was linked to 3MB-AFC, creating POP-3MB-FC **1.24** (Figure 1.7), with a IC_{50} value of 2.5 μM.[128] These efforts highlight several important findings: the correct (E)-geometry of the first isoprene must be maintained for efficient recognition, hydrophobic substitutions in the

farnesyl motif at or beyond position 3 are tolerated, and yeast and human Icmt have distinct substrate specificities.

A more recent farnesyl-modified approach evaluated triazole containing analogues of FTP. Using the well-characterized azide-alkyne click chemistry, a library of 21 triazole-FTP analogues was synthesized and tested as inhibitors for Icmt. Of these triazole-FTP analogues, the most potent inhibitor of Icmt *in vitro* (IC_{50} = 0.8 μM) incorporated a triazole in place of the second isoprene unit connected by a two methylene spacer to a *para* substituted biphenyl motif (TAB) **1.25** (Figure 1.7).[131] The lead compound was also shown to displace GFP-K-Ras from the membrane in transfected PaTu-8902 cells. Analogues with alterative orientations of the biphenyl moiety or fewer methylene units in the spacer decreased inhibition affect, highlighting the importance of the flexibility and linearity in the isoprenoid chain. Compound **1.25** represents the first Icmt inhibitor with submicromolar efficiency, possessing lower molecular weight than previous compounds, and exhibiting improved ligand efficiency.

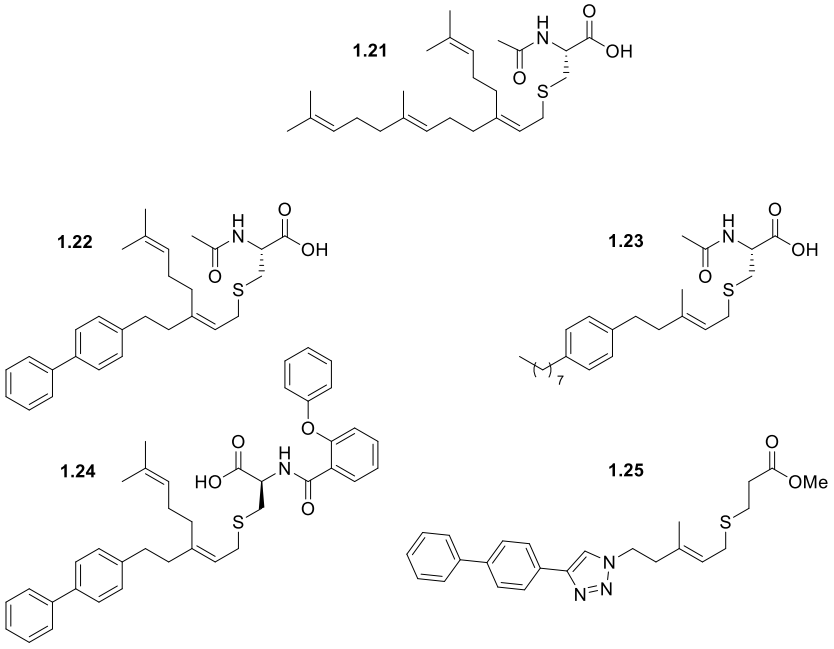

Figure 1.7. Isoprenoid-substituted FC Icmt inhibitors: 3-iBAFC **1.21**, 3MB-AFC **1.22**, C_8 alkyl tail **1.23**, POP-3MB-FC **1.24**, TAB **1.25**.

Another class of Icmt inhibitors that has been researched extensively is based off the byproduct *S*-adenosylhomocysteine (SAH) **1.26** (Figure 1.8). During methyl esterification catalysis, Icmt consumes *S*-adenosylmethionine **1.27** (Figure 1.8) as the methyl donor, releasing SAH and the methylated substrate.[86] SAH has been shown to bind to methyltransferases, consequently acting as a competitive inhibitor of Icmt and other related enzymes.[132] Using strategies to increase cellular levels of SAH, studies have shown its ability to block proliferation of multiple cell types.[133-135] As a recent example, treatment with adenosine dialdehyde inhibited Ras cancer cell proliferation via SAH inhibition of Icmt.[136] Unfortunately, the use of SAH as an Icmt inhibitor is limited by the fact that it also inhibits most cellular methyltransferases.[132,137]

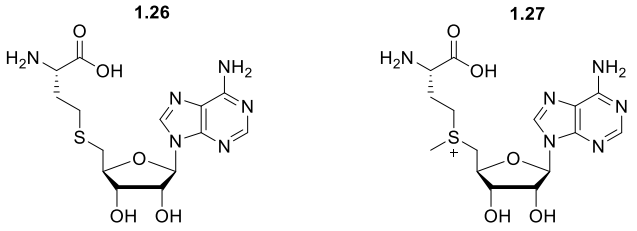

Figure 1.8. Cofactor and byproduct of Icmt methylations: S-adenosylhomocysteine **1.26**, S-adenosylmethionine **1.27**.

Advances in high-throughput screening techniques have allowed new Icmt inhibitors to be found that are not derived from substrate-product based framework. Screening of a small molecule library composed of approximately 10,000 compounds led to the discovery of Icmt inhibitors that shared a unique indole core motif. The lead compound for the indole core inhibitors was coined cysmethynil **1.28** (Figure 1.9).[138] Cysmethynil is a potent time-dependent inhibitor of Icmt with a IC_{50} value of 2.4 μM.[139] Inhibition with cysmethynil is highly Icmt specific and does not inhibit the other prenylation enzymes FTase, GGTase-I, Rce1, and Ste24, or the SAM-dependent DNA methyltransferase.[140] Treatment with cysmethynil has shown Icmt inhibition effects in a variety of different cell lines: induced mislocalization of GFP-K-Ras constructs in MEF, stopped soft agar growth of DKOB8, induced autophagic-dependent apoptosis in PC3, and reduced migration of the highly metastatic MDA-MB-231 breast cancer cell line.[141-145] HPLC methodology for the quantification of cysmethynil effects in mouse plasma has also been achieved.[146] Derivatives of cysmethynil indole core have been developed that offer improved antiproliferative properties.[147] Collectively, these works have shown the utility of the indole class of Icmt inhibitors, and establish a new drug design platform for highly specific inhibition of Icmt.

High-throughput screening has also identified small molecule Icmt inhibitors isolated from natural products. The first natural product inhibitor, spermatinamine **1.29** (Figure 1.8), was discovered form the Australian marine sponge, *Pseudoceratina* sp. Spermatinamine is a symmetrical polyamine alkaloid compound with a bromotyrosyl-spermine-bromotyrosyl sequence. Inhibition studies with Icmt afforded an IC_{50} of 1.9 μM.[148] Additionally, other milder natural product Icmt inhibitors have been found: Aplysamine 6 **1.30** (Figure 1.9),[149] a bromotyrosine like structure similar to spermatinamine from *Pseudoceratina* sp, and a series of prenylated b-hydroxychalcone from *Hovea parvicalyx* root extract.[150] The inhibition potency for spermatinamine and aplysamine 6 led to their total synthesis,[151,152] which would later be improved upon for spermatinamine.[153] It will be interesting to see what future studies on these natural products will expose for Icmt.

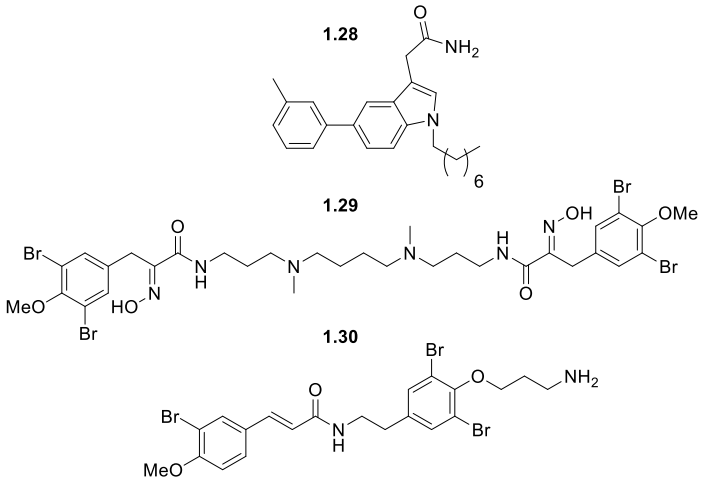

Figure 1.9. Non-isoprenylcysteine Icmt inhibitors: Cysmethynil **1.28**, spermatinamine **1.29**, aplysamine 6 **1.30**.

1.3.4 Icmt Photoactive Probes

Structural characterization of Icmt has been limited due to its membrane-bound nature and low cellular abundance. To generate a model of Icmt and gain insight into its structural features, photoaffinity labeling has been explored. The first reported photolabeling study on human and yeast Icmt worked with isoprenoid analogues that incorporated the photoreactive group benzophenone. A variety of compounds were utilized ranging from small molecule derivatives of AFC that incorporated benzophenone in the isoprenoid structure **1.31**, or in the peptide backbone with noncanonical amino acid Bpa **1.32**, to more complex **a**-factor based peptides prenylated with different benzophenone-containing isoprenoid analogues **1.33** (Figure 1.10).[154] Using an *in vitro* methyltransferase vapor diffusion assay, all of the probes tested as substrates for Ste14p with K_m's comparable to that of AFC. Similar results for Icmt were obtained for **1.31** and **1.32**; however, the **a**-factor probes tested as inhibitors to the enzyme, with the most potent, **1.33,** having an IC_{50} value of 13.7 μM. Most importantly, all of the compounds were shown to crosslink to both Ste14p and Icmt, as confirmed by neutravidin–agarose capture, SDS–PAGE resolution, and immunoblot identification. Although labeling efficiencies varied amongst the analogues, they will be invaluable tools in future efforts to identify and define the substrate binding sites for both yeast and human Icmt.

The most recent photocrosslinking study showed an enhancement in the ability to label Icmt.[155] The improvement in crosslinking efficacy was afforded by the development of a new isoprenoid analogue that contained the diazirine photoactive motif. Using **a**-factor as a scaffold, a trifunctional Icmt labeling probe was designed incorporating biotin,

a fluorophore, and the diazirine isoprenoid analogue **1.34** (Figure 1.10). Substrate testing with Ste14p showed an increase in the binding efficiency of the diazirine probe compared to a trifunctional benzophenone version (K_m 12.2 µM vs 27.8 µM, respectively), and crosslinking to Ste14p was improved by 100%. As compared to the benzophenone analogues, the diazirine version better resembles the natural farnesyl structure and generates a more reactive carbene intermediate than the diradical intermediate produced from the benzophenone photophore. Competition experiments with the wild type farnesylated version of **a**-factor showed a decrease in Ste14 labeling, indicating that the probe was labeling the binding site. The addition of the fluorophore also simplified the detection of crosslinked products. Given the increase in photolabeling and ease of analysis obtained, the diazirine isoprenoid mimic should facilitate the identification of the active-site residues in Ste14p.

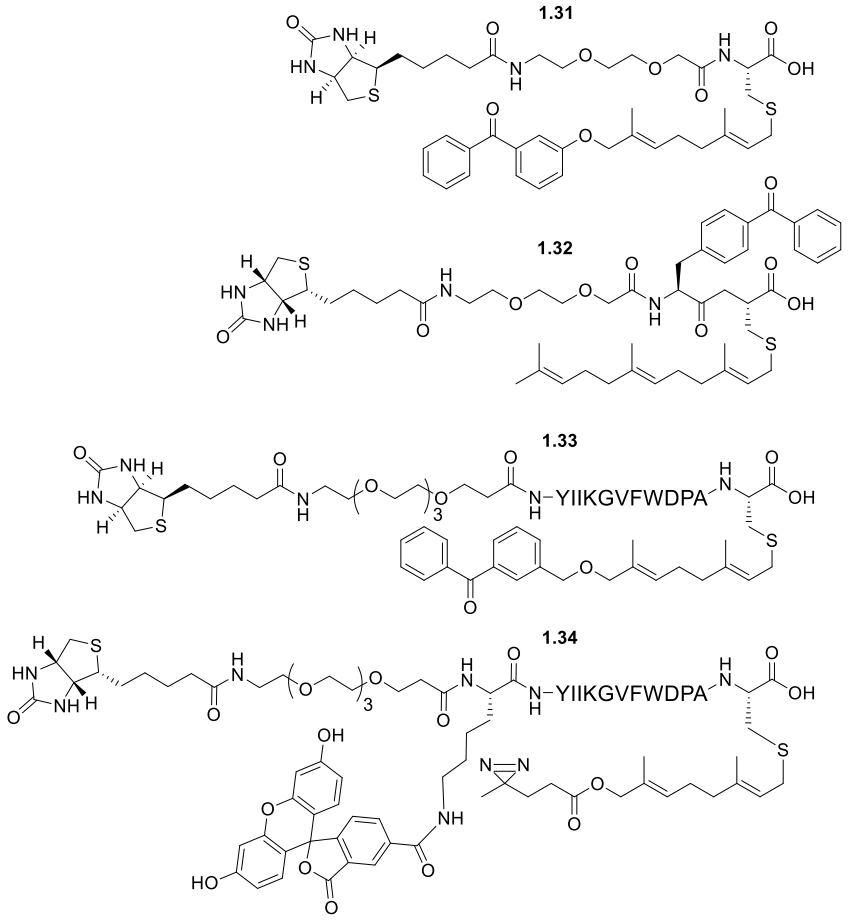

Figure 1.10. Photocrosslinking probes for Icmt: N-Biotin-S-C_{10}-Benzopheone-Cysteine **1.31,** Biotin-Bpa-farnesylcysteine **1.32**, **a**-factor-C_{10}-Benzophenone **1.33**, **a**-factor-C_{10}-Diazirine **1.34.**

1.3.5 Perspective and Conclusion

Given the adverse consequences associated with inhibiting the prenylation endoproteases, advancement of chemical tools to study and control Icmt activity has been a growing target in oncogenesis research. Beginning with simple compounds like AFC, the scientific field has developed a wide range of effective inhibitors based on product-substrate design, to natural product discovery. While no crystal structure has been solved for Icmt, the improvement in photoaffinity labeling compounds, in combination with

enhancement in analysis techniques, should afford a better structural model to Icmt, and aid in future inhibitor design.

Chapter 2: Evalulation of Substrate and Inhibitor Binding to Yeast and Human Isoprenylcysteine Carboxyl Methyltransferases (Icmts) using Biotinylated Benzophenone-containing Photoaffinity Probes

Isoprenylcysteine carboxyl methyltransferases (Icmts) are a class of integral membrane protein methyltransferases localized to the endoplasmic reticulum (ER) membrane in eukaryotes. The Icmts from human (hIcmt) and *S. cerevisae* (Ste14p) catalyze the α-carboxyl methyl esterification step in the post-translational processing of CaaX proteins, including the yeast **a**-factor mating pheromones and both human and yeast Ras proteins. Herein, we evaluated synthetic analogues of two well-characterized Icmt substrates, N-acetyl-*S*-farnesyl-L-cysteine (AFC) and the yeast **a**-factor mating pheromone, that contained photoactive benzophenone moieties in either the lipid or peptide portion of the molecule. The AFC modified compounds were substrates for both hIcmt and Ste14p, whereas the **a**-factor analogues were only substrates for Ste14p. However, the **a**-factor analogues were found to be micromolar inhibitors of hIcmt. Photocrosslinking and neutravidin-agarose capture experiments revealed that both hIcmt and Ste14p were specifically photolabeled with all of the analogues tested to varying degrees Together, these data suggest that the Icmt substrate binding site is dependent upon features in both the isoprenyl moiety and downstream amino acid composition and that hIcmt and Ste14p have overlapping, yet distinct, substrate specificities.

2.1 Introduction

Many eukaryotic proteins are initially synthesized with a C-terminal amino acids CAAX motif that signals a series of post-translational modifications including isoprenylation of the cysteine (C) by either a farnesyl or geranylgeranyl moiety, proteolysis of the –aaX residues and α-carboxyl methyl esterification of the newly exposed cysteine residue.[27,100,101] CAAX proteins include the Ras superfamily of small GTPases,[156,157] Rheb, the nuclear lamins, the Rho family of GTPases and the γ subunits of heterotrimeric G proteins.[3,18,98,101]

The only enzymes known to methyl esterify the α-carboxylate group of CAAX proteins are the isoprenylcysteine carboxyl methyltransferases (Icmts), a family of integral membrane proteins localized to the endoplasmic reticulum (ER).[18,88,101,158-160] Ste14p from *S. cerevisiae*, the founding member of the Icmt family of enzymes, is a 26-kDa integral membrane protein with six putative transmembrane helices.[29,89] The human enzyme, hIcmt, which shares 41% identity and 63% similarity with Ste14p, is a 33-kDa membrane protein with putative eight transmembrane helices.[85,90,130] Interestingly, hIcmt functionally complements the mating defect of a *Δste14* strain by methylating the **a**-factor peptide, suggesting that the enzymes have overlapping substrate specificities.[85] In addition to CAAX proteins and peptides, numerous small molecules such as N-acetyl-*S*-farnesyl-L-cysteine (AFC), N-acetyl-*S*-geranylgeranyl-L-cysteine (AGGC), and farnesyl thioproionic acid (FTP) have been shown to be substrates for both human and yeast Icmts,[112,113] while other compounds have shown specificity for the yeast enzyme.[130]

Aside from these few examples, little is known about the differences in substrate specificity between the yeast and human enzymes, nor is it known how and where substrate binds to these Icmts. A recent 3.4 Å crystal structure of the prokaryotic Icmt ortholog *Ma*-Icmt has been published that revealed important well-conserved structural features of the binding pocket for the co-substrate *S*-adenosyl-L-methionine (SAM).[161] The structure also showed a conserved access tunnel for lipidated substrates that is comprised of residues both in the C-terminal SAM-binding domain and those in the N-terminal half of the protein.[161] The N-terminal half of the protein is thought to confer substrate specificity for lipid substrates. However, poor sequence conservation between *Ma*-Icmt and the eukaryotic Icmts in the N-terminal half precluded a definitive analysis of residues important for binding the isoprene moieties and thus, different approaches must be taken to identify these key amino acids.

Benzophenone-modified substrate analogues have been used previously to interrogate the protein binding sites for farnesyl and geranylgeranyl moieties. The utility of this approach was first demonstrated in experiments designed probe the interaction between the CAAX protein Rho and its regulator RhoGDI. In this study, an isoprenoid containing cysteine analogue bearing the benzophenone label in the lipid itself was used to demonstrate that the isoprene group itself specifically interacts with RhoGDI.[162] Most recently, a series of benzophenone-modified peptide analogues based on the yeast **a**-factor sequence was developed and used to examine the activity of yeast CAAX protease Ras converting enzyme 1 (Rce1p). These experiments demonstrated that yeast Rce1p recognized the modified analogues as substrates and each analogue specifically

photoaffinity labeled the protein.[56,78] Similarly, carboxyl methylated, photoactive analogues of the **a**-factor mating pheromone peptide were shown to functionally interact with the **a**-factor receptor, Ste3p.[163]

In this study, we synthesized and examined several analogues of AFC and farnesylated **a**-factor peptides that contained both a biotin tag and a photoactive benzophenone moiety, either in the isoprene unit or in the peptide region, for their ability to bind and act as substrates or inhibitors of hIcmt and Ste14p. The benzophenone group allowed for specific photoaffinity labeling of the substrate binding site and the biotin moiety allowed for isolation of the labeled protein from a crude membrane mixture. Using kinetic studies, we determined that the AFC analogues were substrates for both enzymes. The **a**-factor analogues were only substrates for Ste14p but were competitive inhibitors of hIcmt. Furthermore, using photocrosslinking experiments followed by isolation with neutravidin-agarose beads, we determined that both Ste14p and hIcmt were labeled by all of the analogues tested, albeit to varying degrees, under saturating conditions.

2.2 Results and Discussion

2.2.1 Probe synthesis. All of the photoactive probes used in the studies described here were prepared via solid phase synthesis (Figure 2.1). For the preparation of the AFC analogues, the compounds were assembled starting with Fmoc-Cys(*S*-t-Bu)-OH that had been immobilized on 2-chlorotrityl resin. Side chain deprotection followed by S-alkylation was used to install either a farnesyl group (for **2.2**) or a benzophenone-based

photolabel (for **2.3**). Photolabel **2.3** was based on a previously described AFC analogue.[162] Fmoc deprotection and subsequent chain elongation using standard solid phase synthetic procedures followed by cleavage under mild acidic conditions afforded the desired probes. For the preparation of the **a**-factor-based analogues, the biotinylated peptide **2.4** was first prepared via standard solid phase synthetic procedures. That compound was then alkylated with the short chain benzophenone-functionalized isoprenoids **2.5a** or **2.5b** to yield **2.7a** or **2.7b**, respectively; similarly, alkylation of **2.4** with **2.6a** or **2.6b** yielded **2.7a** or **2.7b**, respectively.

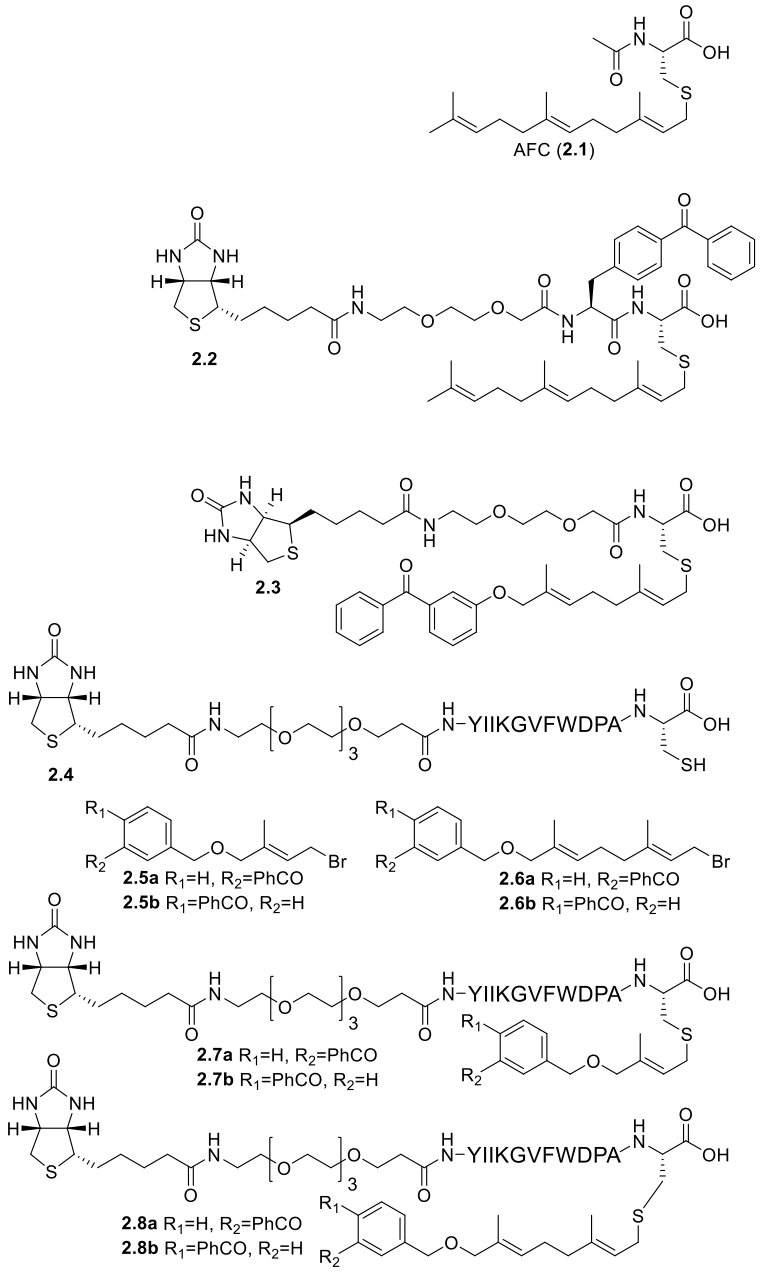

Figure 2.1. Structures of Photoactive Analogues of AFC and the a-factor peptide from *S. cerevisiae.*

2.2.2 All photoaffinity analogues were substrates of His-Ste14p. We first examined the ability of the benzophenone-labeled AFC (**2.1**) analogues (**2.2** and **2.3**) and **a**-factor mimetics (**2.7a**, **2.7b**, **2.8a** and **2.8b**) (Figure 2.1) to act as substrates for yeast

$His_{10}myc_3N$-Ste14p (His-Ste14p) using an *in vitro* methyltransferase vapor diffusion assay. We determined the K_m and V_{max} values for each analogue using crude membrane preparations from yeast expressing His-Ste14p (5µg), using AFC as the positive control.[130] The small molecule photoaffinity compounds based on AFC (**2.2** and **2.3)**, demonstrated similar K_m values to that of AFC (Table 2.1).[130] The **a**-factor peptide photoaffinity analogues with the benzophenone substituted in the *meta* position (**2.7a** and **2. 8a**) also demonstrated similar K_m values to AFC (Table 2.1). Interestingly, the K_m values for the **a**-factor analogues containing a *para*-substituted benzophenone moiety (**2.7b** and **2.8b**) were 2 – 3 times lower than the *meta*-substituted analogues. These data suggest that **2.7b** and **2.8b** interact with the His-Ste14p binding site with higher affinity, possibly as a result of the increased linear and aromatic hydrophobicity of the analogues. AFC and the small molecule AFC-based analogues substrates may demonstrate greater K_m values than the **a**-factor analogues because they lack favorable downstream amino acid contacts with the His-Ste14p substrate binding site. Together, these data suggest that features of both the lipid moiety and the peptide sequence affect binding to His-Ste14p. However, it is important to note that while the isoprene moiety is absolutely essential for recognition by His-Ste14p and other Icmts, the peptide sequence is dispensable,[98] and may serve as a more subtle recognition factor for the selection of substrates *in vivo.*

Table 2.1. Kinetic Parameters for AFC and a-Factor Photoaffinity Analogues as Substrates for His-Ste14p.

Compound	$K_{m(app)}$[a, b, c]	V_{max}[c]
	μM	pmol methyl groups transferred/min/mg
2.1	15.9 ± 0.9[130]	869.6 ± 14.9
2.2	17.9 ± 0.5	2072 ± 112
2.3	18.3 ± 0.4	362 ± 4.2
2.7a	14.6 ± 0.3	762 ± 28
2.7b	6.1 ± 0.6	320 ± 16
2.8a	15 ± 0.2	473 ± 8
2.8b	5.1 ± 0.6	240 ± 3.8

[a] K_m values are apparent because the hydrophobic nature of the substrates precluded accurate determinations of their exact concentrations.

[b]Data are the average of three experiments performed in duplicate ± standard deviation

[c]Values were determined by fitting data to classical (Michaelis-Menten) enzyme-catalyzed curve data using GraphPad Prism 4.

Although the K_m values for **2.2**, **2.3**, **2.7a** and **2.8a** were similar for His-Ste14p, the V_{max} values varied greatly (Table 2.1). Analogue **2.2,** which contains a photoactive a *p*-benzoyl-L-phenylalanine upstream of the cysteine residue, demonstrated the greatest V_{max} (2072 pmol/min/mg). This value was more than 2-fold greater than that of AFC (869 pmol/min/mg), the compound defined as the minimal substrate for Icmts that contains peptide character.[98] These data suggest that His-Ste14p can turn over a substrate containing a bulky hydrophobic moiety next to the lipidated cysteine residue more quickly and may point to a mechanism in which product release is rate limiting. Analogue **2.3** demonstrated the lowest V_{max}, 362 pmol/min/mg, with analogues **2.7a** and

2.8a showing midrange V_{max} values of 473 and 762 pmol/min/mg, respectively (Table 2.1). Analogues **2.7b** and **2.8b**, which had the lowest K_m values, showed the lowest V_{max} values of all the substrates tested against His-Ste14p. This reduction is substrate turnover may be a result of the lower K_m or a decreased ability to release product following the reaction.

2.2.3 AFC photoaffinity analogues were substrates for His-hIcmt but the a-factor photoaffinity peptide analogues were inhibitors. We next examined the ability of these analogues to act as substrates for $His_{10}myc_3$N-hIcmt (His-hIcmt). We performed kinetic analyses to determine the K_m and V_{max} values for each of the analogues and to establish if differences in substrate specificity existed between the yeast and human enzymes (Table 2.2). We found that **2.2** is a substrate for His-hIcmt with a K_m lower than that for AFC and a V_{max} that was only slightly decreased. However, **2.3**, which contains the modified isoprenyl group, was not a substrate for His-hIcmt to any measurable extent and thus, the K_m value is not particularly relevant (Table 2.2). Furthermore, even though the native **a**-factor peptide is a substrate for His-hIcmt,[85] none of the modified **a**-factor analogues displayed any measurable activity (data not shown). However, all of **a**-factor peptides were inhibitors of His-hIcmt, to varying degrees (Table 2.2). Analogues **2.7a** and **2.7b**, which have a shorter 5-carbon isoprene spacer, were poor inhibitors of His-hIcmt (IC_{50} >100 μM) whereas **2.8a** and **2.8b**, which have a 10-carbon isoprene spacer, were relatively potent, displaying IC_{50} values of 25.7 ± 1.6 μM and 13.7 ± 0.8 μM, respectively (Table 2.2). The calculated Ki values for **2.8a** and **2.8b** using the Cheng –

Prusoff method were 13.0 ± 0.8 μM and 7.0 ± 0.4 μM, respectively.[164] These marked differences between the activities of these photoaffinity analogues and His-Ste14p and His-Icmt highlight previously unappreciated substrate specificity differences between the different Icmts. Furthermore, these data suggest that the hIcmt binding site is less tolerant of changes in the isoprene architecture than is Ste14p.

Table 2. Kinetic Parameters for AFC and a-Factor Photoaffinity Analogues as Substrates for His-hIcmt.

Compound	**$K_{m(app)}$[a, b, c]**	**V_{max}[c]**	**IC_{50}[d]**
	μM	pmol methyl groups transferred/min/mg	μM
2.1	10.3 ± 0.5[130]	884 ± 49	N. A.
2.2	5.9 ± 0.5	504 ± 27	N. A.
2.3	3.4 ± 0.3	24 ± 2	N. A.
2.7a	N. D.	N. D.	> 100
2.7b	N. D.	N. D.	> 100
2.8a	N. D.	N. D.	25.7 ± 1.6
2.8b	N. D.	N. D.	13.7 ± 0.8

[a] K_m values are apparent because the hydrophobic nature of the substrates precluded accurate determinations of their exact concentrations.

[b]Data are the average of three experiments performed in duplicate ± standard deviation

[c]Values were determined by fitting data to classical (Michaelis-Menten) enzyme-catalyzed curve data using GraphPad Prism 4.

[d]Values were found by fitting data to variable slope sigmoidal dose-response curve using GraphPad Prism 4.

2.2.4 His-Ste14p specifically interacted with each of the benzophenone-modified analogues. To evaluate the ability of His-Ste14p to be labeled with the analogues, we performed photoaffinity labeling studies. Crude membranes expressing His-Ste14p (100 μg) were incubated with saturating concentrations of each substrate, based on kinetic

parameters, and photocrosslinked with UV light (365 nm) for 40 min.[56] The crosslinked proteins were isolated by neutravidin-agarose capture exploiting the biotin tag on each analogue and resolved by SDS-PAGE. Incubation with AFC served as the negative control and membrane preparations from a *Δste14* deletion strain served as the control for non-specific binding. The proteins were visualized by enhanced chemiluminescence (ECL) following immunoblot analysis. The signal corresponded to the amount of analogue covalently crosslinked to His-Ste14p (Figure 2.2A). Although His-Ste14p was labeled with all of the analogues, it is of note that **2.2** and **2.7a** crosslinked to the protein less efficiently than the other compounds, which labeled His-Ste14p with approximately equal efficiency. Paradoxically, **2.2** was the best substrate for His-Ste14p enzymatically, suggesting that the benzophenone moiety was not in an ideal position in the binding pocket for efficient labeling.

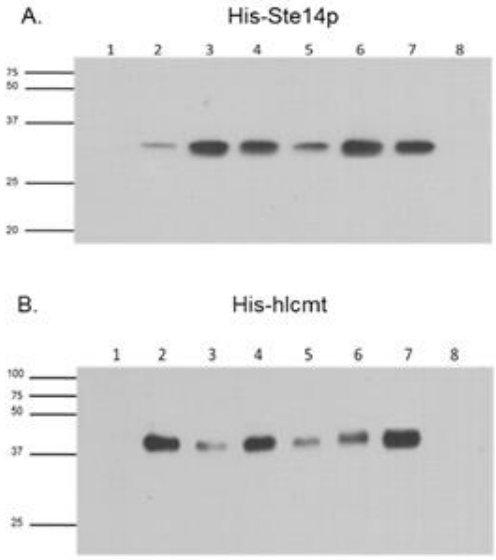

Figure 2.2. Immumoblot of His-Ste14p (A) or His-hIcmt (B) photocrosslinked with benzophenone-containing analogues**. (**100 µg) of crude membrane protein were incubated with each substrate for 40 min on ice under UV irradiation (365nm). The samples were extracted and re-solubilized in RIPA/10% SDS before enrichment using neutravidin-agarose beads. Proteins were eluted, resolved by 10% SDS-PAGE, and visualized as described in *Materials and Methods*. **A: His-Ste14p**: lane 1: 200 µM **2.1**, lane 2:100 µM **2.2**, lane 3:100 µM **2.3**, lane 4: 50 µM **2.7b**, lane 5: 100 µM **2.7a**, lane 6: 50 µM probe **2.8b**, lane 7: 100 µM **2.8a**, lane 8: empty vector (*Δste14*) + 100 µM **2.2**. **B: His-hIcmt**: lane 1: 200 µM **2.1**, lane 2: 50 µM **2.2**, lane 3: 50 µM **2.3**, lane 4: 200 µM **2.7b**, lane 5: 200 µM **2.7a**, lane 6: 200 µM **2.8b**, lane 7: 200 µM **2.8a**, lane 8: empty vector (*Δste14*) + 50 µM **2.2**.

2.2.5 Crosslinking experiments of modified substrates exhibit the ability to covalently crosslink to His-hIcmt. To determine if His-hIcmt interacted similarly with the analogues, crude membrane extracts expressing His-hIcmt (100 µg) were incubated with saturating concentrations of each of the photoactive reagents (200 µM). Samples with His-hIcmt expressing membranes incubated with AFC were used as the negative control and the membrane preparation from the *Δste14* strain was used as a non-specific binding control. All of the samples were crosslinked, enriched, and resolved under the same conditions as described above for His-Ste14p. The amount of each crosslinked

protein was determined by immunoblot analysis followed by visualization by ECL visualized by ECL (Figure 2.2B). These data indicated that all of the analogues labeled the protein but that the degree of crosslinking varied with the structure of these molecules. Analogue **2.2** crosslinked more efficiently than **2.3**, possibly due to the fact that **2.3** was a poor substrate for His-hIcmt (Table 2.2). For the peptide analogues, **2.8a** labeled His-hIcmt most efficiently followed by **2.7b**, **2.8b** and **2.**7**a**. In an effort to determine the nature of inhibition demonstrated by the **a**-factor analogues, we performed competition experiments with His-Icmt and **2.8b** (200 μM) using increasing concentrations of the substrate AFC. The intensity of photolabeling of His-Icmt with **2.8b** decreased with increasing AFC concentration, suggesting that **2.8b** acted as a competitive inhibitor (data not shown). These data suggest that the **a**-factor analogues interact and specifically label residues within the His-Icmt binding pocket

2.3 Conclusion

It is clear from our data that the labeling efficiencies for the benzophenone-containing substrate analogues did not correlate completely to the kinetic data. For example, the **a**-factor peptide that photolabeled His-hIcmt most efficiently was one of the poorest inhibitors (Table 2.2 and Figure 2.2B). Thus, care must be taken not to overinterpret crosslinking data. Since variables such as proximity and orientation of the moiety to the residues in the binding pocket affect the ability to efficiently label a protein,[165,166] the observed variances in crosslinking to His-Ste14p and His-Icmt may be due to the position of the photolabel in the substrate binding site rather than a measure of

their affinity for the enzymes. However, these analogues will be invaluable tools in our future efforts to define the substrate binding sites for both yeast and human Icmts.

2.4 Materials and Methods

2.4.1 Materials. All solvents and reagents used for the solid-phase peptide synthesis of the photoactivatable peptides were of analytical grade and purchased from Peptides International (Louisville, KY), NovaBioChem® (Nohenbrunn, Germany), or Sigma-Aldrich (St.Louis, MO). N-acetyl-*S*-farnesyl-L-cysteine (AFC) was synthesized in the Gibbs laboratory (Purdue University) as previously described.[167] High performance liquid chromatography grade acetonitrile (CH_3CN), dichloromethane (DCM), N,N-dimethylformamide (DMF), trifluoroacetic acid (TFA), and H_2O were purchased from Fisher Scientific (Springfield, NJ), OmniSolv® (Charlotte, NC), or Sigma-Aldrich. NHS-PEG_4-Biotin was obtained from Thermo Scientific (Waltham, MA). The benzophenone-containing isoprenoid bromides; C_5-*meta*-Bp-Br (**2.5a**) or C_5-*para*-Bp-Br (**2.5b**) [(*E*)-(3-((4-bromo-2-methylbut-2-enyloxy)methyl)phenyl)(phenyl)-methanone] and C_{10}-*meta*-Bp-Br (**2.6a**) or C_{10}-*para*-Bp-Br (**2.6b**) [(3-(((2*E*,6*E*)-8-bromo-2,6-dimethylocta-2,6-dienyloxy)-methyl)phenyl)-(phenyl)methanone] were prepared as previously described.[76,162,168-170] HPLC analysis was performed using a Beckman-Coulter system employing series 126 pumps and a series 168 detector. Analytical separations were performed using a Varian (Microsorb-MV C_{18}, 4.6 x 250 mm) column while preparative separations employed either a Phenomenex (Luna C_{18}, 10 x 250 mm) column or a Higgins Analytical (Proto 200 C_4, 250 X 10 mm) column. ESI-MS analysis was

performed using a BioTOFII (Bruker) mass spectrometer. *S*-adenosyl-L-[^{14}C-*methyl*] methionine ([^{14}C]-SAM) was purchased from Perkin Elmer (Waltham, MA). *α-myc* monoclonal antibody, goat *α*-mouse IgG and goat *α* -rabbit IgG were purchased from Invitrogen (Carlsbad, CA). The *α* -Ste14 polyclonal antibody was a gift from Dr. S. Michaelis (The Johns Hopkins University School of Medicine). The neutravidin coated agarose beads and SuperSignal West Pico enhanced chemiluminescence (ECL) was purchased from Pierce (Rockford, IL).

2.4.2 Am-bpBFC BPA Analogue (2.2). The synthesis of the photoactive analogue **2.2** was performed using an adaptation of a solid phase synthetic method developed for the preparation of other AFC analogues.[171] Briefly, Fmoc-Cys(S-*t*Bu)-OH was coupled to 2-chlorotrityl chloride resin using collidine in DMF. was capped with 1% collidine in a solution of 90:10 DCM/MeOH. After the *S*-*t*-butyl protecting group was removed using dithiothreitol (DTT) and diisopropylethyl amine (DIEA), the free thiol was alkylated with farnesyl bromide using DIEA as a base. The Fmoc protecting group was then removed with 20% piperidine in DMF followed by coupling with Fmoc-BPA-OH with HOBt, HBTU, and DIEA in DMF. The Fmoc protecting group was then removed with 20% piperdine in DMF followed by coupling with 2-[2-(Fmoc-amino)ethoxy]ethoxy]acetic acid with HOBt, HBTU, and DIEA in DMF. Deprotection with 20% piperidine in DMF followed by coupling of D-biotin with HOBt, HBTU, and DIEA in DMF and subsequent resin-cleavage with 0.5% TFA in DCM yielded the desired analogue, which was purified by C_{18} RP-HPLC. ESI-MS: calcd for for $C_{50}H_{69}N_5O_9S_2$ $[M+H]^+$: 948.45, found: 946.30

2.4.3 F-bpBFC AFC Analogue (2.3). The synthesis of the photoactive analogue **2.3** was performed using an adaptation of a solid phase synthetic method developed for the preparation of other AFC analogues as noted above and was based on a previously described photoaffinity analogue of AFC.[162] Briefly, Fmoc-Cys(S-*t*Bu)-OH was coupled to 2-chlorotrityl chloride resin using collidine in DMF. The resin was capped with 1% collidine in a solution of 90:10 DCM/MeOH. After the *S*-*t*-butyl protecting group was removed using dithiothreitol (DTT) and diisopropylethyl amine (DIEA), the photoactive isoprenoid (3-(((2*E*,6*E*)-8-bromo-2,6-dimethylocta-2,6-dien-1-yl)oxy)phenyl)-(phenyl)methanone[172] was coupled with the free thiol using DIEA as a base. The Fmoc protecting group was then removed with 20% piperdine in DMF followed by coupling with 2-[2-(Fmoc-amino)ethoxy]ethoxy]acetic acid with HOBt, HBTU, and DIEA in DMF. Deprotection with 20% piperdine in DMF followed by coupling of D-biotin with HOBt, HBTU, and DIEA in DMF and subsequent resin-cleavage with 0.5% TFA in DCM yielded the desired analogue which was purified by C_{18} RP-HPLC. ^{1}H NMR ($CDCl_3$, 500 MHz) 1.43 (m, 2 H), 1.70 (m, 9 H), 2.08 (t, 2 H), 2.22 (m, 4 H), 2.70 (d, 2 H), 2.88 (m, 2 H), 3.00 (dd, 1 H), 3.18 (m, 3 H), 3.33 (m, 1 H), 3.61 (m, 4 H), 3.71 (s, 2 H), 3.97 (d, 1 H), 4.12 (d, 1 H), 4.35 (m, 1 H), 4.42 (s, 2 H), 4.53 (m, 1 H), 4.82 (qt, 1 H), 5.20 (t, 1 H), 5.51 (t, 2 H), 6.71 (s, 1 H), 7.03 (s, 1 H), 7.14 (d, 1 H), 7.34 (m, 3 H), 7.47 (t, 2 H), 7.52 (d, 1 H), 7.58 (t, 1 H), 7.79 (d, 2 H); ^{13}C NMR ($CDCl_3$, 500 MHz) 13.92, 16.13, 25.51, 26.12, 27.72, 27.96, 29.77, 33.23, 35.71, 38.99, 40.40, 51.19, 55.34, 60.31, 62.13, 69.66, 69.78, 70.20, 71.03, 74.15, 115.49, 119.61, 119.94, 122.76, 128.23, 128.63,

129.16, 130.01, 130.97, 132.40, 137.59, 138.76, 139.59, 158.89, 164.78, 170.15, 173.64, 174.57; ESI-MS: calcd for for $C_{42}H_{56}N_4O_9S_2Na$ $[M+Na]^+$: 847.3386, found: 847.3396.

2.4.4 Biotin-Peg$_4$-YIIKGVFWDPAC (**2.4**). Peptide synthesis was carried out using an automated solid-phase peptide synthesizer (PS3, Protein Technologies Inc, Memphis, TN) employing standard Fmoc/HCTU based chemistry. Synthesis began on preloaded Fmoc-Cys(Trt)- Wang resin (0.25 mmol) and the peptide chain was elongated using HCTU/N-Methylmorpholine-catalyzed, single coupling steps with 4 equivalents of both protected amino acids and HTCU for 30 min. Following complete chain elongation, the N-terminal amine was deprotected with 10% piperidine in DMF (v/v) and the presence of the resulting free amine was confirmed by ninhydrin analysis.[173] The resin containing the peptide was washed with DCM, dried in vacuo overnight, weighed, and divided into three portions for further synthesis on a reduced scale. Using 83.0 µmol of peptide, the free amino terminus was biotinylated in DMF (5 mL) with NHS-PEG$_4$-Biotin (49 mg, 83 µmol,) catalyzed by DIEA (14 µL, 8.3 µmol) for 16 h. After acylation, the resin bound peptide was washed thoroughly with DCM and dried in vacuo for 4 h. The peptide was cleaved from the resin along with simultaneous side chain deprotection by treatment with reagent K containing TFA (10 mL), crystalline phenol (0.5 g), 1,2-ethanedithiol (0.25 mL), thioanisole (0.5 mL), and H_2O (0.5 mL) for 2 h at room temperature. The released peptide was collected and combined with TFA washes of the resin before precipitation of the peptide in chilled Et_2O (100 mL). The crude solid peptide was collected by centrifugation, the supernatant was removed, and the resulting pellet was washed 2 times

with cold Et_2O (50 mL) repeating the centrifugation and supernatant removal steps each time. The crude peptide was purified using a semipreparative C_{18} RP-HPLC column with detection at 214 nm and eluted with a gradient of Solvent A (H_20/0.1% TFA, v/v) and Solvent B (CH_3CN/0.1% TFA, v/v). The crude peptide (150 mg) was dissolved in a DMF/H_2O solution (1:5 v/v, 25 mL), applied to the column equilibrated in Solvent A, and washed with 15% Solvent B for 15 min. The peptide was eluted using a linear gradient of (15-55% Solvent B over 1.5 h at a flow-rate of 5 mL/min). Fractions collected were analyzed using an analytical C_{18} RP-HPLC column employing a linear gradient (0-100% Solvent B over 60 min at a flow-rate of 1 mL/min) and detected at 214 nm. Fractions containing peptide product of at least 90% purity were pooled and concentrated by lyophilization to yield 55 mg (37% yield) of a white solid. A small amount (< 1mg) of the resulting purified peptide was dissolved in 10 µl of 0.1% TFA/CH_3CN and diluted 1:50 in a mixture of CH_3CN/H_2O (1:1 v/v) prior to MS analysis. MS was performed using a 50 µL injection and collecting 3000 scans. ESI-MS: calcd $[M+2H]^{+2}$: 942.97, found 943.00.

2.4.5 Biotin-Peg$_4$-YIIKGVFWDPAC(C_5-meta-Bp) (2.7a). Biotin-Peg$_4$-YIIKGVFWDPAC **(2.4)** (10 mg, 5.3 µmol) was dissolved in DMF/n-Butanol/H_2O containing 0.10% TFA (3:1:1 v/v/v, 6 mL)**.** To purify the C_5-*meta*-Bp-Br (**2.5a**) [(*E*)-(3-((4-bromo-2-methylbut-2-enyloxy)methyl) phenyl) (phenyl)methanone][76,168] isoprenoid before reaction, the bromide (8.6 mg, 24 µmol) was dissolved in 0.50 mL of DMF and loaded onto a C18 SepPack® column that had been equilibrated with Solvent A

containing 5% Solvent B. The column was washed with additional Solvent A containing 5% Solvent B (5 mL), followed by Solvent A containing 30% Solvent B (10 mL). The purified bromide, C_5-*meta*-Bp-Br (**5a**), was then eluted from the column with 3.0 mL DMF directly into the reaction flask that contained the dissolved peptide. $Zn(OAc)_2 \cdot 2H_2O$ (5.4 mg, 25 μmol) was then added to initiate the alkylation reaction. After 2 h at room temperature, 2-mercaptoethanol (100 μL, 1.4 mmol) was added to quench the reaction, which was then allowed to stir for an additional 4 h. The reaction was analyzed by analytical RP-HPLC, purified by semipreparative C_{18} RP-HPLC, and identified via ESI-TOF MS. This reaction yielded 2.5 mg (22 %) of the desired alkylated peptide **(2.7a)**. Purity by HPLC: 91 %, ESI-MS: calcd $[M+2H]^{+2}$: 1082.32, found 1082.36.

2.4.6 Biotin-Peg$_4$-YIIKGVFWDPAC(C_5-para-Bp) (2.7b). Biotin-Peg$_4$-YIIKGVFWDPAC **(2.4)** (10 mg, 5.3 μmol) was alkylated with isoprenoid bromide *C_5-para*-Bp-Br **(2.5b),** [(*E*)-(4-((4-bromo-2-methylbut-2-enyloxy)methyl) phenyl) (phenyl)methanone][76,168] (8.6 mg, 24 μmol) using the reaction conditions described above for the preparation **of 2.7a.** This reaction yielded 2.7 mg (24 %) of the desired alkylated peptide **(2.7b)**. Purity by HPLC: 91 %, ESI-MS: calcd $[M+2H]^{+2}$: 1082.32, found 1082.34

2.4.7 Biotin-Peg$_4$-YIIKGVFWDPAC(C_{10}-meta-Bp) (2.8a). Biotin-Peg$_4$-YIIKGVFWDPAC **(2.4)** (10 mg, 5.3 μmol) was alkylated with C_{10}-*meta*-Bp-Br (**2.6a**),

[(3-(((2*E*,6*E*)-8-bromo-2,6-dimethylocta-2,6-dienyloxy)methyl)phenyl)-(phenyl)meth-anone][162,169,170] (10.2 mg, 24 μmol) using the reaction conditions described above for the preparation of **2.7a**. To separate the product from unreacted bromide (**2.6a**), the peptide was suspended in EtOAc (5 mL), recovered by centrifugation, and purified by RP-HPLC (C_4 column). This reaction yielded 3.2 mg (27 %) of the desired alkylated peptide (**2.8a**). Purity by HPLC: 95%, ESI-MS: calcd $[M+2H]^{+2}$: 1116.57, found 1116.58.

2.4.8 Biotin-Peg$_4$-YIIKGVFWDPAC(C_{10}-para-Bp) (2.8b). Biotin-Peg$_4$-YIIKGVFWDPAC (**2.4**) (10 mg**,** 5.3 μmol) was alkylated with C_{10}-*para*-Bp-Br (**2.6b**), [(4-(((2*E*,6*E*)-8-bromo-2,6-dimethylocta-2,6-dienyloxy)methyl)phenyl)-(phenyl)meth-anone][162,169,170] (10.2 mg, 24 μmol) using the reaction conditions described above for the preparation of **2.7a**. Purification of the alkylated product was performed as described for **2.8a.** This reaction yielded 2.9 mg (25 %) of the desired alkylated peptide (**2.8b**). Purity by HPLC: 94 %, ESI-MS: calcd $[M+2H]^{+2}$: 1116.57, found 1116.56.

2.4.9 Yeast strains and crude membrane preparations from yeast cells. His$_{10}$myc$_3$N-Ste14p (His-Ste14p) and His$_{10}$myc$_3$N-hIcmt (His-hIcmt) yeast strains were cloned and expressed as previously described.[88,130] Crude membranes were prepared as described previously with minor modifications.[88] After centrifugation at 100,000 x g, the membrane pellet was resuspended in 10 mM Tris-HCl, pH 7.5, aliquoted, flash frozen in liquid N_2 and stored at -80ºC.

2.4.10 *In Vitro* Methyltransferase Vapor Diffusion Assay. Reactions were performed as described previously.[174] All inhibition studies were completed as detailed earlier.[130] Crude membranes preparations derived from a *Δste14* strain transformed with an empty vector were used as the negative control for these experiments.

2.4.11 Photocrosslinking and neutravidin-agarose pull-down assays. Photocrosslinking assays were performed as described previously, with minor modifications.[56] Briefly, 100 µg of crude membrane preparation expressing either His-Ste14p or His-hIcmt in 100 mM Tris-HCl, pH 7.5 were incubated in the presence of saturating concentrations of the photoaffinity analogues and incubated at 4ºC for 10 min. After incubation, the samples were irradiated with UV light (365 nm) in 96-well plates for 40 min on ice. Following photocrosslinking, unreacted analogue was removed by chloroform/methanol extraction.[175] The resulting protein samples were solubilized in 400 µL of radioimmumoprecipitation assay (RIPA) buffer (25mM Tris-HCl, pH 7.5, 150 mM NaCl, 1% triton X-100, 1% sodium deoxycholate, 0.1% sodium dodecylsulfate) /10% SDS and incubated with 50 µL of a 50% neutravidin/RIPA bead slurry for 2 h at room temperature. Following incubation, the beads were centrifuged at 13,000 x g for 1 min and washed three times with RIPA/10% SDS. The crosslinked protein was eluted from the neutravidin beads by the addition of 50 µL of 2X SDS sample buffer (0.5 M Tris-HCl, pH 6.8, 30% sucrose (w/v), 10% sodium dodecylsulfate (w/v), 3.5 M 2-mercaptoethanol and 0.1% bromophenol blue (w/v)). The His-Ste14p samples were heated for 30 min at 65ºC and the His-hIcmt samples were incubated at room temperature

overnight. The proteins were separated by 10% SDS-PAGE and transferred to nitrocellulose (0.22 μm). The nitrocellulose membrane was blocked at room temperature for 2 h in 20% (w/v) non-fat dry milk in phosphate-buffered saline with Tween-20 (137 mM NaCl, 2.7 mM KCl, 4 mM Na_2HPO_4, 1.8 mM KH_2PO_4 and 0.05% (v/v) Tween-20, pH 7.4) (PBST). The blocked membrane was then incubated for 2 h at room temperature with primary antibody (1:1,000 α-Ste14p) or (1: 10,000 α-myc) in 5% (w/v) non-fat dry milk in PBST for His-Ste14p or His-hIcmt, respectively. The membrane was washed in PBST three times and then incubated for 1 h at room temperature with secondary antibody (1:10,000 goat α-rabbit IgG-HRP for α-Ste14p or 1:4000 goat α-mouse IgG-HRP for α-myc) in 5% (w/v) dry milk in PBST. The membrane was washed three times with PBST and the proteins were visualized using ECL.

2.5 Supporting Information

2.5.1 Characterization of Biotin-Peg$_4$-YIIKGVFWDPAC (2.4)

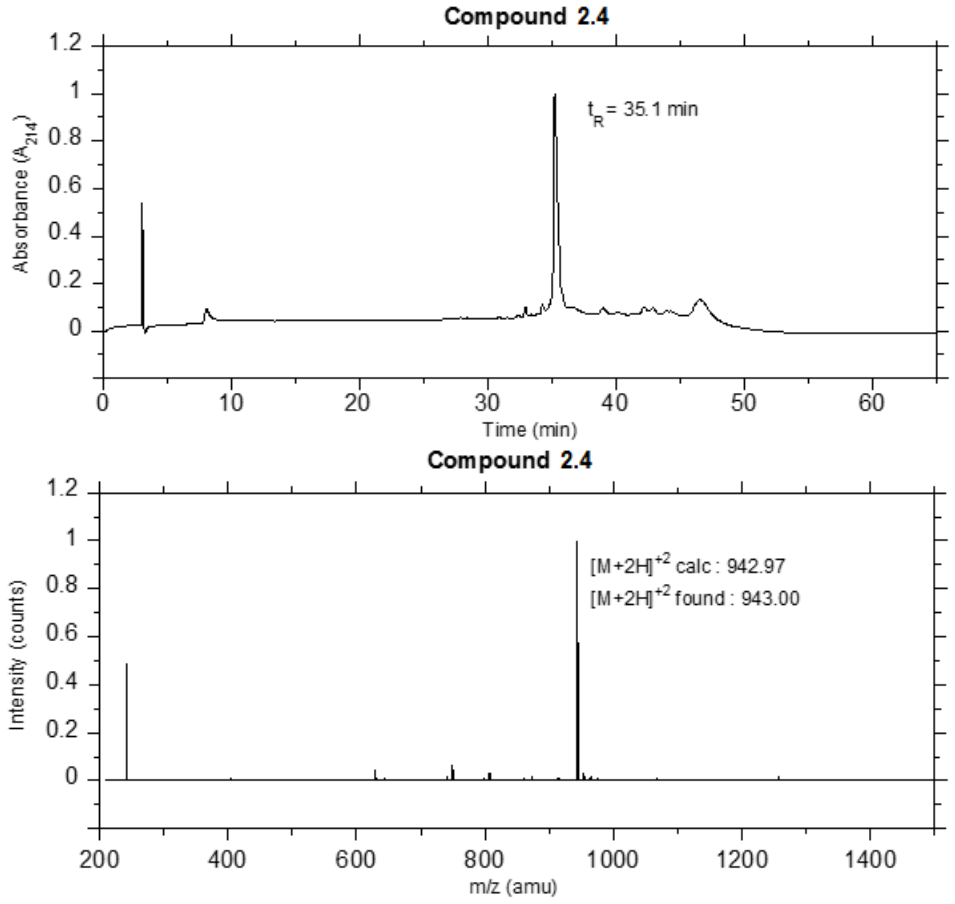

Figure 2.3. Mass spectrum and analytical RP-HPLC chromatogram for peptide **2.4**. Linear gradient 0-100% CH_3CN (0.1%TFA) in 60 min, detected at 214 nm.

2.5.2 Characterization of Biotin-Peg$_4$-YIIKGVFWDPAC(C_5-meta-Bp) (2.7a)

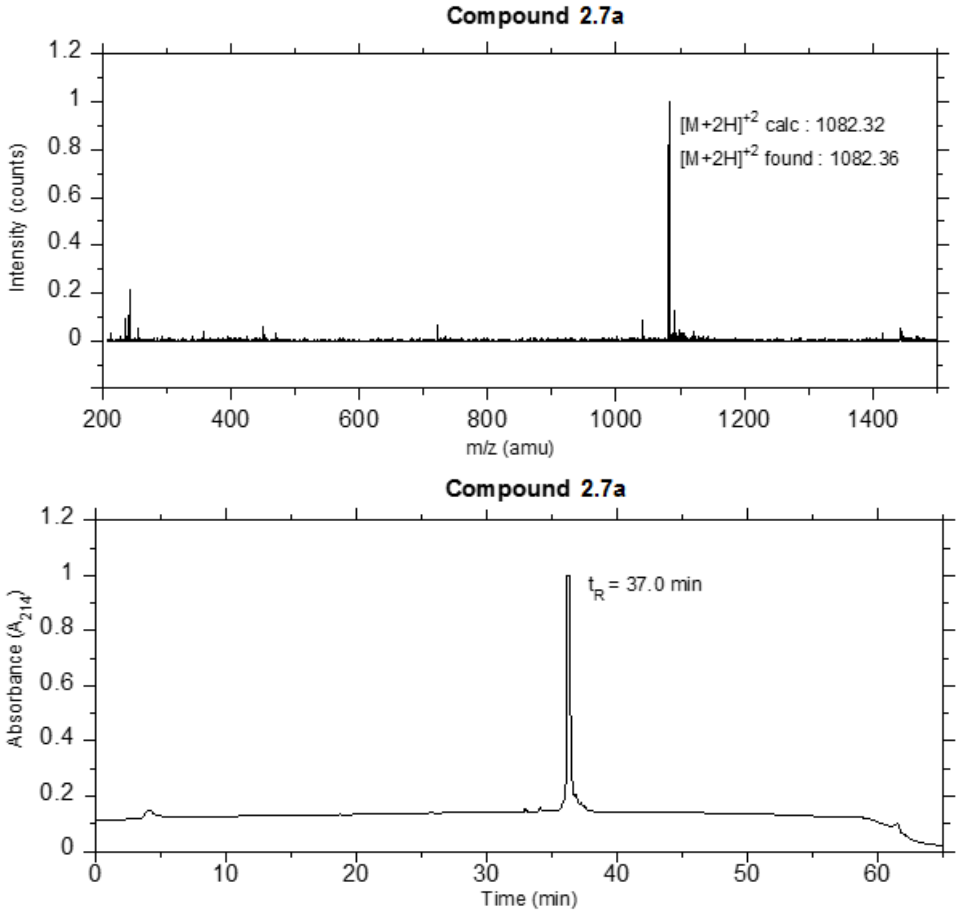

Figure 2.4. Mass spectrum and analytical RP-HPLC chromatogram for peptide **2.7a**. Linear gradient 0-100% CH_3CN (0.1%TFA) in 60 min, detected at 214 nm.

2.5.3 Characterization of Biotin-Peg$_4$-YIIKGVFWDPAC(C_5-para-Bp) (2.7b)

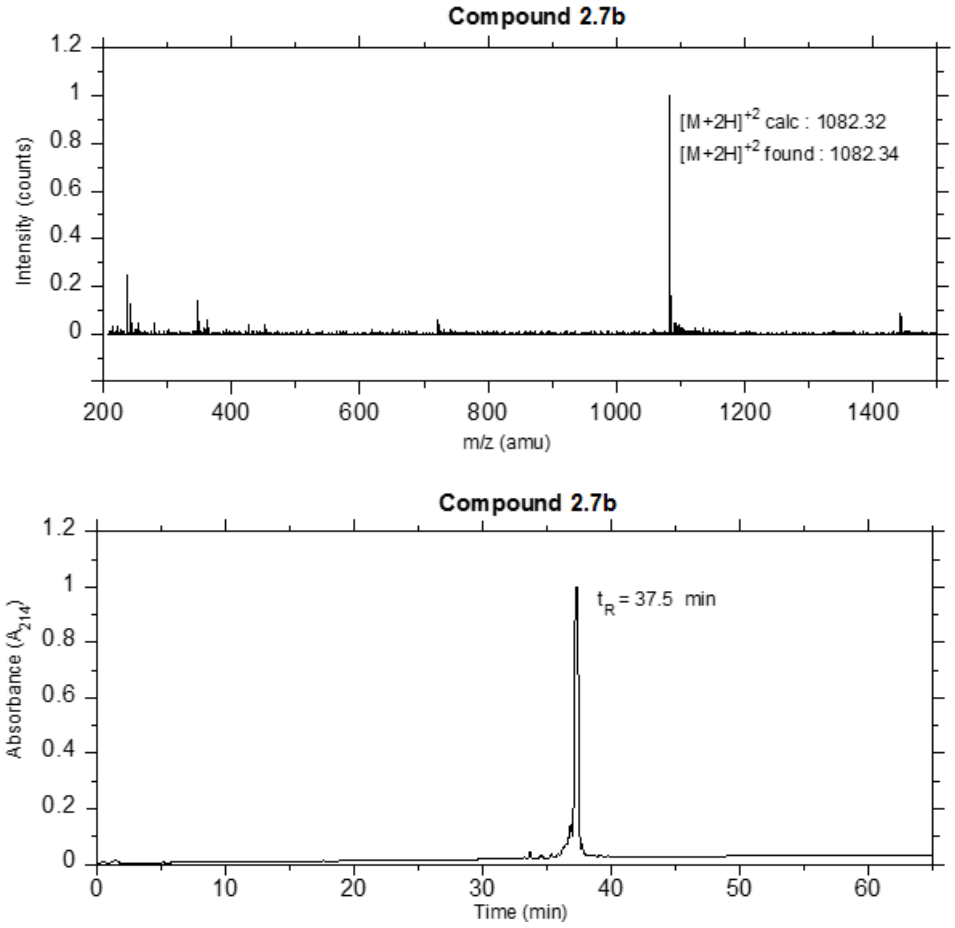

Figure 2.5. Mass spectrum and analytical RP-HPLC chromatogram for peptide **2.7b**. Linear gradient 0-100% CH_3CN (0.1%TFA) in 60 min, detected at 214 nm.

2.5.4 Characterization of Biotin-Peg$_4$-YIIKGVFWDPAC(C_{10}-meta-Bp) (2.8a)

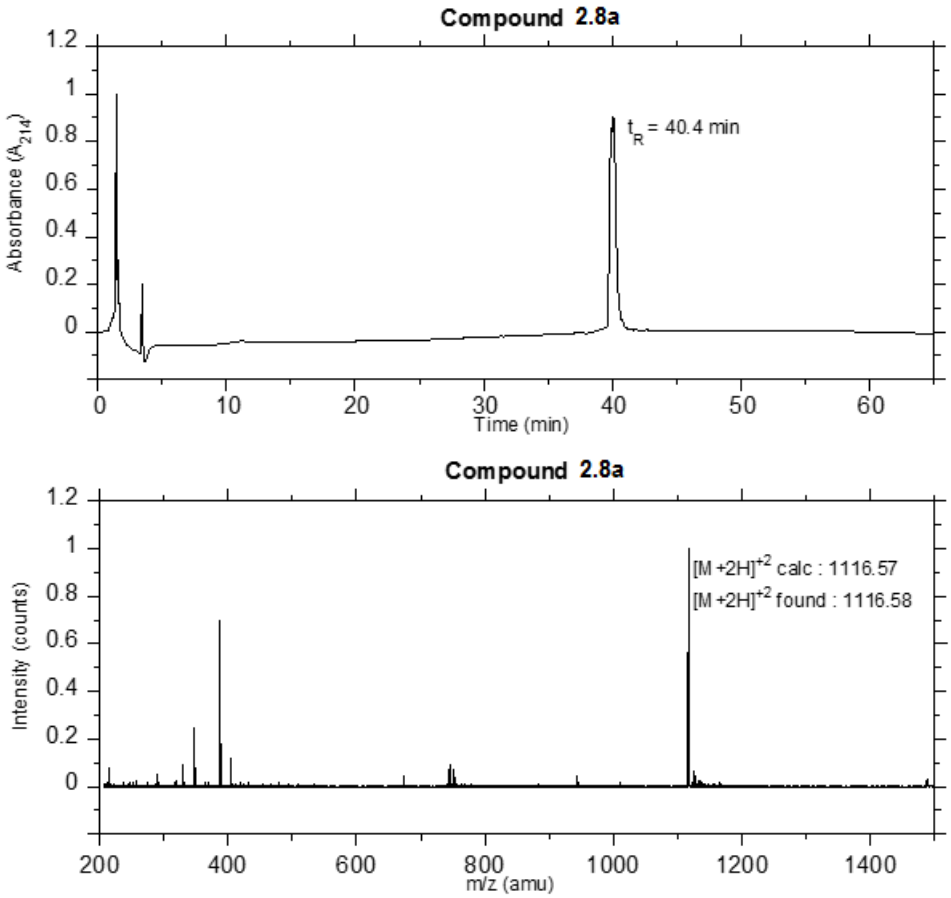

Figure 2.6. Mass spectrum and analytical RP-HPLC chromatogram for peptide **2.8a**. Linear gradient 0-100% CH_3CN (0.1%TFA) in 60 min, detected at 214 nm.

2.5.5 Characterization of Biotin-Peg$_4$-YIIKGVFWDPAC(C_{10}-meta-Bp) (2.8b)

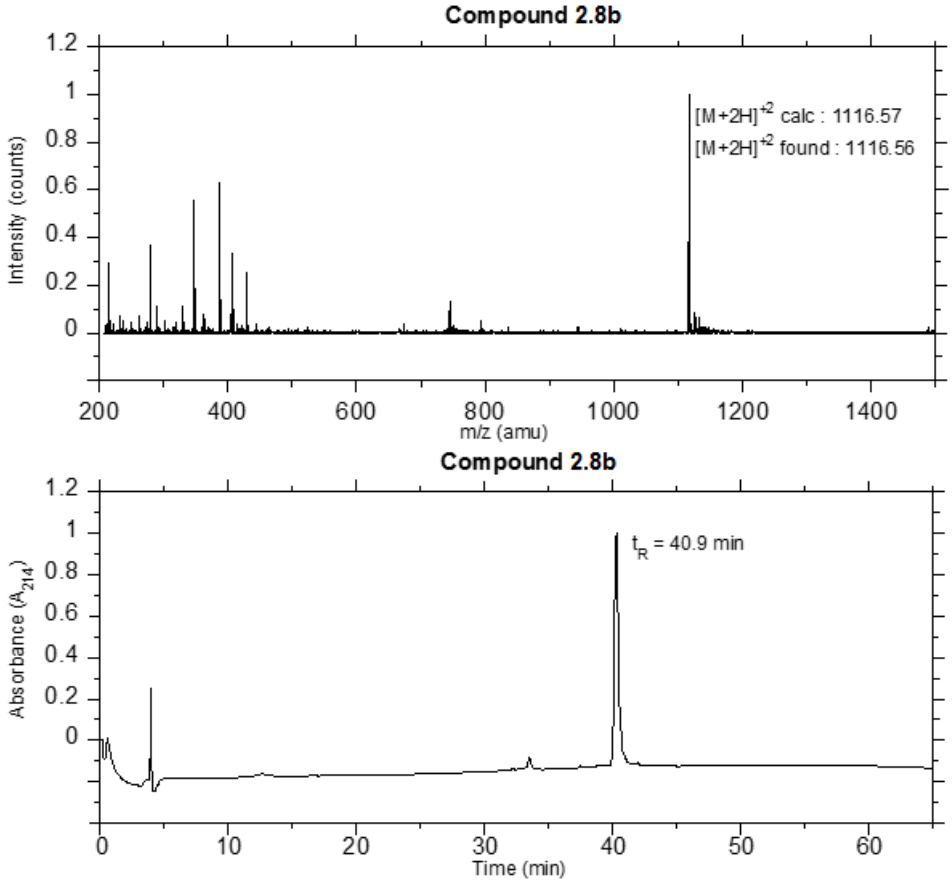

Figure 2.7. Mass spectrum and analytical RP-HPLC chromatogram for peptide **2.8b**. Linear gradient 0-100% CH_3CN (0.1%TFA) in 60 min, detected at 214 nm.

2.5.6 Characterization of Am-bpBFC BPA Analogue (2.2)

Compound 2.2

LS1272#1-15 RT: 0.03-0.39 AV: 15
T: + c ms [150.00-2000.00]
m/z= 170.7-2000.0

m/z	Intensity	Relative
948.3	74864.0	100.00
949.3	34100.7	45.55
623.2	11967.2	15.99
950.3	10377.7	13.86
834.5	7984.9	10.67
548.1	6945.1	9.28
964.2	5697.9	7.61
820.5	5549.7	7.41
1062.4	4750.3	6.35
663.4	4394.5	5.87
962.4	4129.7	5.52
744.3	3347.0	4.47
624.2	2952.3	3.94
551.3	2658.5	3.55
835.6	2470.5	3.30
1063.3	2294.3	3.06
776.4	2175.9	2.91
530.5	2127.9	2.84
1347.4	2003.8	2.68
552.3	1962.0	2.62
664.3	1915.9	2.56
821.5	1859.3	2.48
931.3	1741.1	2.33
971.7	1690.7	2.26
565.9	1664.4	2.22

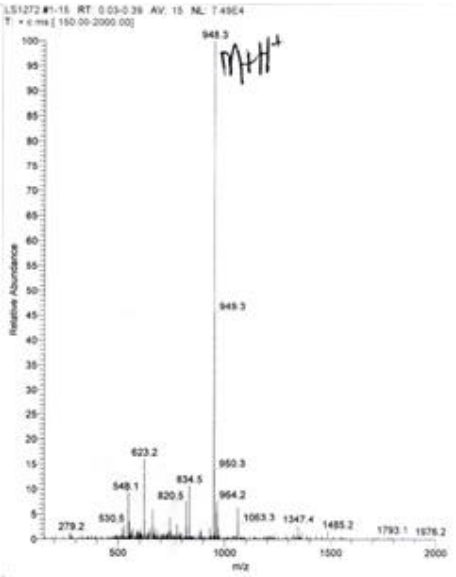

Figure 2.8. Mass spectrum of compound **2.2.**

2.5.7 Characterization F-bpBFC AFC Analogue (2.3)

Compound 2.3

LS112_101102081157#1-20 RT: 0.00-0.37 AV:
T: + c ms [135.00-1300.00]
m/z= 161.1-1300.0

m/z	Intensity	Relative
847.3	33261.2	100.00
733.4	18613.3	55.96
848.3	12691.0	38.16
734.4	7950.4	23.90
749.3	7619.8	22.91
861.4	7096.3	21.33
849.4	6959.6	20.92
763.5	5036.9	15.14
755.4	4725.1	14.21
862.4	4068.8	12.23
721.3	3898.8	11.72
863.4	3498.7	10.52
825.0	3394.9	10.21
756.5	2829.5	8.51
610.4	2650.7	7.97
705.4	2591.9	7.79
595.4	2449.9	7.37
869.4	2432.9	7.31
826.2	2302.6	6.92
821.4	2029.7	6.10
1001.2	1997.2	6.00
596.3	1972.4	5.93
380.6	1944.4	5.85
833.3	1811.0	5.44
718.5	1790.9	5.38

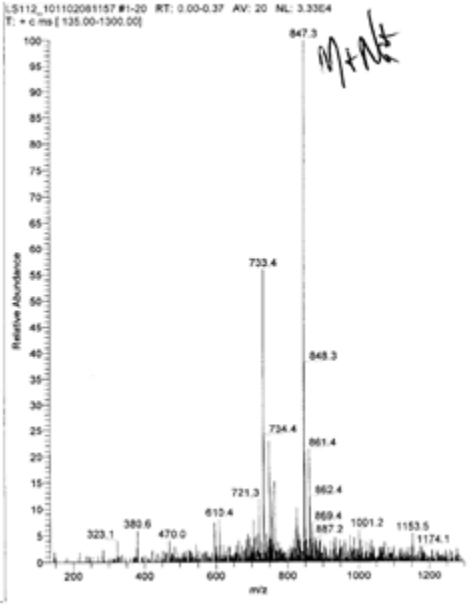

Figure 2.9. Mass spectrum of compound **2.3.**

Chapter 3: A Diazirine-Containing Photoactivatable Isoprenoid: Synthesis and Application in Studies with Isoprenylcysteine Carboxyl Methyltransferase

Photoaffinity labeling is a useful technique employed to identify protein-ligand and protein-protein noncovalent interactions. Photolabeling experiments have been particularly informative for probing membrane-bound proteins where structural information is difficult to obtain. The most widely used classes of photoactive functionalities include aryl azides, diazocarbonyls, diazirines and benzophenones. Diazirines are intrinsically smaller than benzophenones and generate carbenes upon photolysis that react with a broader range of amino acid side chains compared with the benzophenone-derived diradical; this makes diazirines potentially more general photoaffinity labeling agents. In this report, we describe the development and application of a new isoprenoid analogue containing a diazirine moiety that was prepared in six steps and incorporated into an **a**-factor-derived peptide produced via solid phase synthesis. In addition to the diazirine moiety, fluorescein and biotin groups were also incorporated into the peptide to aid in the detection and enrichment of photocrosslinked products. This multifuctional diazirine-containing peptide was a substrate for Ste14p, the yeast homolog of the potential anticancer target Icmt, with K_M (6.6 μM) and V_{max} (947 nmol/min/mg) values comparable or better than **a**-factor peptides functionalized with benzophenone-based isoprenoids. Photocrosslinking experiments demonstrated that the diazirine probe photocrosslinked to Ste14p with observably higher efficiency than benzophenone-containing **a**-factor peptides.

3.1 Introduction

Photoaffinity labeling is a useful technique employed to identify noncovalent interactions between molecules, including protein-ligand and protein-protein complexes. The utility of photoreactive probes to study such interactions is highly dependent upon three criteria, including how closely the photolabeling moiety mimics the native structure, what type of reactive intermediates are formed, and the spatial relationship between the two interacting molecules. The most widely used classes of photoactive functionality include aryl azides, diazocarbonyls and diazirines, and benzophenones, which give rise to nitrenes, carbenes and diradicals, respectively, upon photolysis.[176]

Prenylated proteins are a class of membrane-associated polypeptides that employ a farnesyl, or geranylgeranyl isoprenoid (sometimes two in the latter case) to anchor the proteins into membranes. A three-step process consisting of prenylation, proteolysis and carboxymethylation is frequently required to produce the final mature active proteins. Prenylation is performed by farnesyl- or geranylgeranyltransferases and proteolysis is carried out by Rce1 or Ste24 while carboxymethylation is catalyzed by Icmt, a SAM-dependent enzyme.[101] Attachment of the hydrophobic isoprenoid causes membrane association,[4] and is essential for membrane-associated functions involving protein-protein interactions,[11] signal transduction,[25,174] and cellular homeostasis regulation.[88] Due to the fact that Ras prenylation is required for its proper cellular localization and function,[69] numerous human clinical trials have been conducted to inhibit this critical signal transduction event that is particularly relevant to cancer.[177,178] Importantly, an area of

growing interest is developing inhibitors for the other enzymes in the processing pathway including Icmt, which is localized to the membrane of the endoplasmic reticulum.

Photoactive analogues of farnesyl diphosphate have been used extensively to study the interactions between soluble proteins and their ligands, including isoprenoids and prenyltransferases. This class of photoprobes includes molecules containing aryl azides,[179] diazoesters,[180-183] and benzophenones,[77,168,169,184,185] with the latter being the most commonly employed. Peptides containing these photoactive isoprenoids have also been used to study the interactions between prenylated proteins and their cognate receptors.[162] Recently, we used peptides functionalized with benzophenone-containing isoprenoids in photocrosslinking experiments with membrane-associated proteins that also recognize isoprene moieties, including the Ras coverting enzyme Rce1 and the isoprenylcysteine carboxyl methyltransferase, Icmt, two enzymes involved in the CaaX protein posttranslational processing pathway.[56,154] Although we showed that those enzymes could be successfully photolabeled, the yield of crosslinking was not sufficient to generate quantities of material adequate for mass spectrometric sequencing. In addition, the benzophenone-containing peptides were generally poorer substrates than those incorporating a natural farnesyl group, likely due to the larger size of the benzophenone moiety. To address this size question and potentially increase the yield of crosslinked protein, we wanted to explore the use of smaller isoprene unit surrogates. While a number of diazoester-containing isoprenoid analogues have been previously reported,[168,180,181,185] their synthesis is complicated by the need to use phosgene gas and trifluorodiazoethane.[186] In contrast, diazirines are much simpler to prepare from ketones.

Since diazirines are intrinsically smaller than benzophenones and more closely approximate the size and shape of an isoprene unit, they should be effective isoprenoid mimics; moreover, because they generate carbenes upon photolysis, they also have the potential to react with a wider range of amino acid side chains thereby, increasing photocrosslinking efficiency.

Herein, we describe the synthesis of a diazirine-containing isoprenoid unit (**3**.**1**) (Figure 3.1) and its incorporation into a biotinylated and fluorescently labeled **a**-factor peptide analogue (**3**.**16**) (Figure 3.2); the dodecapeptide, **a**-factor, is a naturally occuring farnesylated peptide found in yeast and known to be generated via methylation by Icmt.[187] The ability of this multifunctional photoactive peptide to bind and serve as a substrate for Icmt was then evaluated using Ste14p, the Icmt from the yeast *S. cerevisiae* as a model enzyme. The diazirine-containing **a**-factor analogue demonstrated an increased V_{max} and lower K_M relative to benzophenone-containing probes. Crosslinking studies showed that the efficiency of photolabeling achieved with the diazirine-based probe was greater than that of benzophenone-containing probes. In contrast to previous work where antibody-based methods were necessary for detection of crosslinked protein, in-gel fluorescence via a fluorophore incorporated into the peptide was used here to successfully detect the crosslinked purified enzyme. These results suggest that such multifunctional diazirine-containing peptides should be useful for identifying active-site residues in Icmts and potentially other enzymes involved in the processing of prenylated proteins.

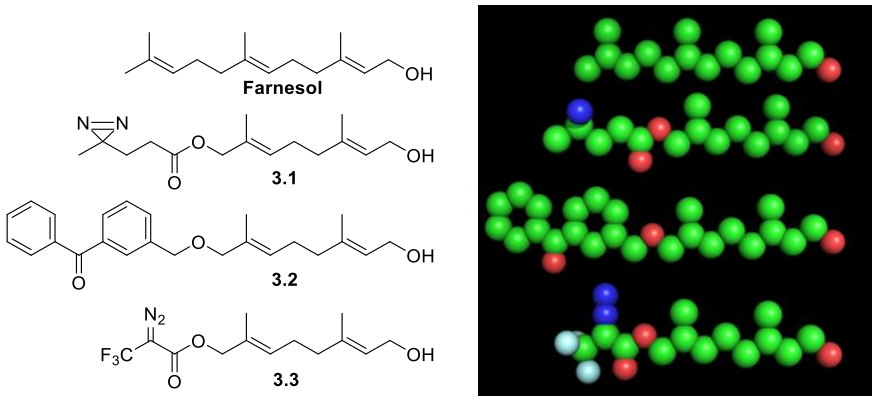

Figure 3.1. Photoactivatable isoprenoid analogues: Left image; Farnesol, Diazirine **3**.**1**, Benzophenone **3**.**2**, DATFP **3.3.** Right image: Space filling models of the isoprenoid analogues. Hydrogen atoms omitted for clarity. Color Scheme: Carbon (green), Oxygen (red), Nitrogen (blue) and Fluorine (white). Spheres are shown at 0.6 VDW radii for clarity.

3.2 Results and Discussion

3.2.1 Design and synthesis of diazirine containing isoprenoid. To prepare the desired multifunctional **a**-factor peptide for *in vitro* kinetic and photocrosslinking analyses of Ste14p, the initial strategy was to first design an isoprenoid moiety containing a diazirine group. Compound **3**.**1** was selected as the target based on the overall similarity in size of the analogue compared with farnesyl diphosphate (FPP). Comparison of **3.1** with benzophenone- and DATFP-containing FPP analogues (**3**.**2** and **3.3**) reveals that **3.1** is closest in size to FPP (Figure 3.1). While potentially less stable than ether-linked analogues such as **3.2**, the ester analogue **3.1** was chosen for ease of synthesis. A convergent strategy was used to prepare **3.1** based on previously published routes for the production of the isoprenoid building block, **3.9**,[185] and the diazirine derivative pentanoic acid **3**.**6** (Scheme 3.1).[188] Coupling of **3.9** and **3.6** in the presence of DIC and DMAP afforded the ester (**3.10**). Removal of the THP protecting group was performed with PPTS in EtOH, followed by conversion of the free alcohol, **3.11**, to the corresponding

bromide, **3.12**, by reaction with CBr_4 and PPh_3. Purification of the bromide was carried out using a small reversed-phase cartridge to minimize decomposition of the allylic bromide on silica gel. The reversed-phase purification also appears to remove colored impurities that interfere with the subsequent peptide alkylation; while this process does not remove unreacted alcohol starting material, that compound does not interfere with the subsequent alkylation chemistry.

Scheme 3.1. Synthesis of a diazirine-containing analogue of a farnesyl group

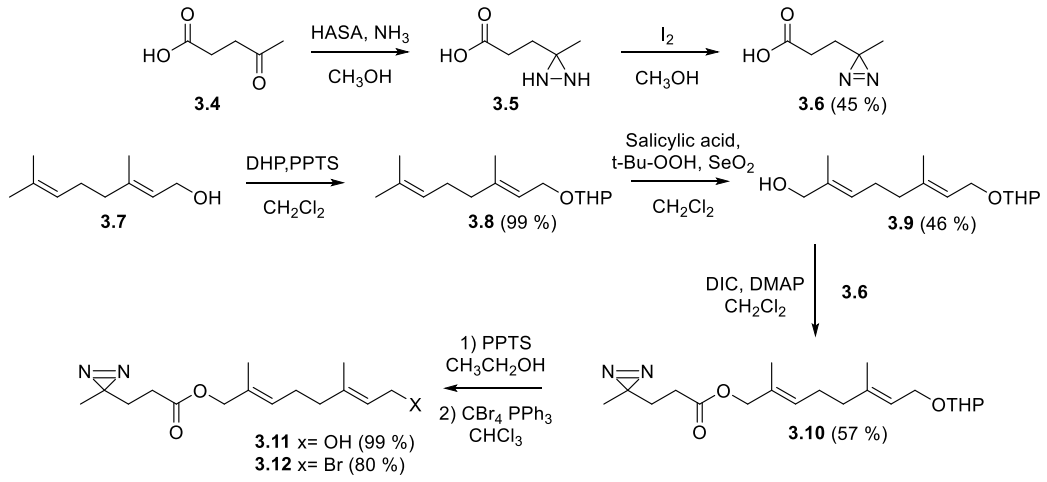

3.2.2 Synthesis of prenylated a-factor. We incorporated the isoprenoid analogue **3.12** into a peptide based on the structure of the farnesylated dodecapeptide mating pheromone **a**-factor, an *in vivo* substrate for Ste14p that is produced via the same three step process as larger prenylated proteins (Scheme 3.2).[187] This peptide (**3.16**) contains a free C-terminal carboxylate to serve as the methyl acceptor in the enzymatic reaction.

Scheme 3.2. Synthesis of prenylated a-factor precursor peptide 3.16

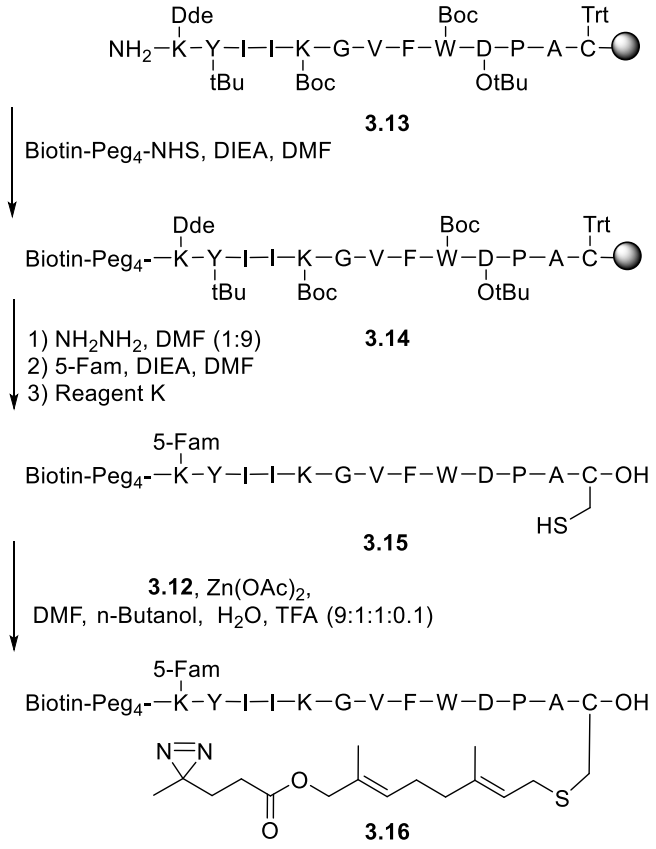

Solid phase peptide synthesis was used to construct peptide **3.13** utilizing standard Fmoc/HCTU coupling conditions. An additional *N*-terminal lysine residue was added to the **a**-factor sequence to provide an additional handle (via the side chain) for fluorophore attachment. After the peptide was elongated, its free *N*-terminus was biotinylated to yield **3.14.** Biotin-Peg_4-NHS was chosen for installation of the biotin label due to its efficient reaction kinetics and inexpensive cost. After specific on-resin cleavage of the Dde protecting group from the side chain ε-amino group of the *N*-terminal lysine with a 10% hydrazine/DMF solution, the resulting free amine was acylated with 5-

carboxylfluorescein succinimidyl ester (5-Fam) in the presence of DIEA to give the fluorescently labeled peptide on resin**.** 5-Fam was chosen as the fluorescent reporter because of its reactivity with primary amines via the succinimidyl ester and its convenient emission wavelength that makes it easy to detect using most commercially available fluorescence scanners. Cleavage from the resin and acidic deprotection was carried out simultaneously by treatment with Reagent K to afford an orange peptide **3.15**, with a C-terminal cysteine bearing a free thiol. It is interesting to note that previous reports have noted that some epimerization of C-terminal cysteine residues can occur when Cys-functionalized Wang resin and Reagent K cleavage conditions are used;[189] however, after RP-HPLC purification, no evidence for epimerization was observed. MS/MS analysis (see Supporting Information) revealed a large ensemble of b-type and y-type fragments consistent with the proposed structure for **3.15**. Alkylation of the free thiol was performed using the bromide **3.12** (1.5 equiv) in the presence of $Zn(OAc)_2$ (0.1 equiv) in acidic DMF to yield the prenylated peptide **3.16** whose identity was determined via ESI-MS and purity confirmed by analytical RP-HPLC (see Figure 3.16). As was observed for **3.15**, MS/MS analysis of **3.16** (see Figure 3.15 and 3.17) showed the presence of a variety of b-type and y-type fragments consistent with the proposed structure for **3**.**16**. Fragmentation via loss of the farnesyl group was also observed as has been previously reported for prenylated peptides.[56,190] The farnesylated control peptide **3**.**17** and benzophenone-containing peptide **3.19** were prepared by a similar procedure while **3.18** was prepared as previously described.

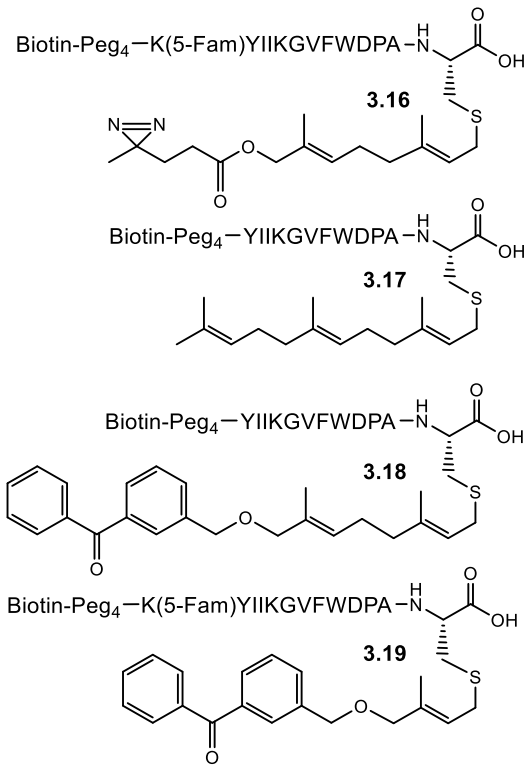

Figure 3.2. a-factor-based peptides for the *in vitro* study of Icmt.

3.2.3 Diazirine-modified a-factor is a substrate for His-Ste14p. To assess the ability of **3.16** to act as a substrate for Icmt, we used a recombinant form of yeast Icmt (Ste14p) that incorporates both a His_{10} tag for purification and a triply iterated *myc* tag to facilitate detection by immunoblot analysis (His-Ste14p).[88] The ability of **3.16** to act as a substrate for His-Ste14p was determined using an *in vitro* methyltransferase vapor diffusion assay. The K_M and V_{max} values (Table 3.1) for **3.16** were measured using crude membrane fractions prepared from yeast expressing His-Ste14p using *N*-acetyl-*S*-farnesyl-L-cysteine (AFC) as a positive control. Comparison of the kinetic parameters obtained for the diazirine **3.16** and the benzophenone-containing analogues **3.18**[154] (previously reported) and **3.19** reveal that of those three probes containing photoactive isoprenoids,

the diazirine manifests the highest V_{max} value and lowest K_M value making it the most efficient substrate. Although the V_{max} for **3.16** was lower than that for a farnesylated analogue of **a**-factor precursor, **3.17**, **3.16** demonstrated a lower K_M value making the catalytic efficiency of **3.16** (V_{max}/K_M = 143) comparable to that of **3.17** (V_{max}/K_M = 157). Both of these values are higher than those obtained for benzophenone-based probes **3.18** and **3.19** (V_{max}/K_M = 52 and 7.0, respectively) suggesting that the smaller diazirine moiety is a superior mimic of an isoprene unit.

Table 3.1. *In vitro* reaction kinetics for **a**-factor peptides methylated by His-Ste14p.

Compound	V_{max}[a] (pmol•min^{-1}•mg^{-1})	$K_{M(app)}$[b] (μM)	V_{max}/K_M[a,b] (pmol•min^{-1}•mg^{-1}•μM^{-1})
AFC[154]	870 ± 15	15.9 ± 0.9	54
3.16	947 ± 4	6.6 ± 0.2	143
3.17	1919 ± 30	12.2 ± 0.1	157
3.18[154]	762 ± 28	14.6 ± 0.3	52
3.19	217 ± 3	27.8 ± 1	7.0

[a] Reported as pmol methyl groups transferred to substrate.
[b] Since these experiments were performed at a single concentration of SAM and the biphasic nature of the membrane suspension makes the concentration of the peptide substrate unknown (due to partitioning into the lipid membranes), these experiments provide only apparent values for K_M.

3.2.4 His-Ste14p crosslinking with the diazirine-modified a-factor. The ability of His-Ste14p to be covalently modified with the diazirine- and benzophenone-modified **a**-factor peptides was assessed via photoaffinity labeling studies (Figure 3.3). Purified His-Ste14p

(0.25 μg) was incubated with 50 μM of each peptide, irradiated with UV light (365 nm) for 30 min on ice and the crosslinked material was resolved by SDS-PAGE. The identity of the Ste14p-**a**-factor conjugate was determined by three different methods: detection of the biotin moiety with NeutrAvidin HRP (Figure 3.3B); detection of His-Ste14 using an α-Ste14p antibody (Figure 3.3C); and ultimately through direct fluorescence detection of the 5-Fam fluorophore (Figure 3.3A).

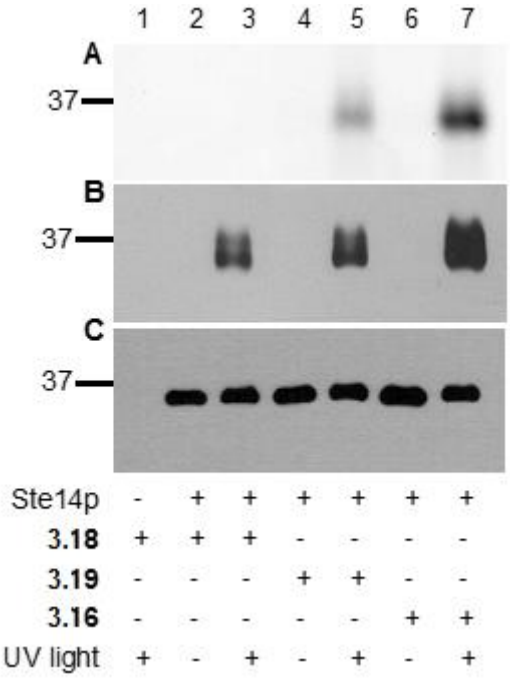

Figure 3.3. Analysis of crosslinking reactions containing purified His-Ste14p and different photoactive probes. (A) Fluorescent imaging; (B) immunoblot analysis with NeutrAvidin HRP; (C) immunoblot analysis with α-Ste14. Experiments were performed with **3.16**, **3.18** and **3.19**. For this experiment, purified His-Ste14p (0.25 μg) was incubated with the probes indicated (50 μM) and irradiated on ice for 30 min followed by fractionation via SDS-PAGE. The resulting gel was visualized using (A) a fluorescence scanner or transferred to a nitrocellulose membrane and visualized using (B) NeutrAvidin HRP or (C) an α-Ste14 antibody. The data shown is from one of three replicates of this experiment.

Following separation of the reaction mixture by SDS-PAGE, immunoblot analysis with an α-Ste14p antibody demonstrated that His-Ste14p was present in each lane at the expected molecular weight (~36 kDa) (Figure 3.3C). UV-dependent photocrosslinking of the probes to His-Ste14p was visualized using NeutrAvidin HRP. Biotinylated His-Ste14p was only present in samples subjected to UV light (Figure 3.3B, lanes 3, 5 and 7). The strongest signal was obtained with the diazirine-containing peptide **3.16**, suggesting that this compound photolabeled His-Ste14p with the highest efficiency. Additionally, UV-dependent fluorescent labeling was also observed using **3.16** and **3.19** (Figure 3.3A, lanes 5 and 7). Probe **3.18** does not contain a 5-Fam moiety and hence could not be visualized in a similar manner. Furthermore, the increased labeling efficiency with **3.16** observed with NeutrAvidin HRP detection was recapitulated with the fluorescence data. This increased labeling, that can be readily visualized via direct fluorescence scanning of the gel, suggests that a larger number of enzyme molecules are crosslinked. These results are in contrast to those previously reported for Rce1 with benzophenone-based probes[56,78] and bode well for future experiments that will be aimed at identifying the site(s) of crosslinking. Moreover, the experimental simplicity of following the crosslinking reactions via fluorescence scanning in lieu of more complicated western blotting or NeutrAvidin HRP detection should greatly facilitate optimization of experimental conditions. Overall, the presence of both a biotin for enrichment and a fluorescent label for direct visualization should make these new probes particularly useful. In addition to the direct analysis of crosslinking reactions shown in Figure 3.3, pull-down experiments

with **3.16** and **3.19** were also performed (see Figure 3.20) showing that the biotin handle could be used to recover the crosslinked products from the reaction mixture.

Comparing the efficiency of crosslinking of His-Ste14p to **3.16**, **3.18** or **3.19**, it is clear that the diazirine probe is the more efficient photoaffinity labeling reagent. Since the crosslinkling experiments were performed with a concentration of each probe that was ~2 – 8 times greater than their individual K_M values, the increase in labeling is likely not attributable to differences in affinities between the different probes. Rather, it must be due either to the increased reactivity of the carbene intermediate generated from diazirine **3.16** compared to the diradical intermediate produced from the benzophenone photophores of **3.18** and **3.19** or greater proximity or more favorable geometry of the peptide in the active site. Currently, additional diazirine- and benzophenone-containing probes are being prepared and we will determine whether the former types always yield higher levels of crosslinking.

Finally, in addition to confirming the formation of the crosslinked protein, the specificity of the photolabeling of His-Ste14p with **3.16** was examined in a competition experiment (Figure 3.4). A biotinylated **a**-factor precursor peptide, **3.17**, was chosen as a competitor, as it was a substrate for His-Ste14p (Table 3.1) and closely mimicked the structure of **3.16** (Figure 3.2). Crude membranes prepared from a *Δste14* deletion strain overexpressing His-Ste14p were incubated with **3.16** in the presence or absence of increasing concentrations of the competitor **3.17** in the presence of UV light (Figure 3.4). Following incubation, the samples were enriched for biotinylated proteins via neutravidin-agarose beads and the proteins were separated by SDS-PAGE. Immunoblot

analysis with an α-Ste14p antibody revealed that the amount of crosslinked His-Ste14p decreased as the concentration of the competitor, **3.17**, was increased from 5 μM (Figure 3.4, lane 3) to 200 μM (Figure 3.4, lane 8). These data suggest that **3.16** is labeling the substrate binding site of His-Ste14p.

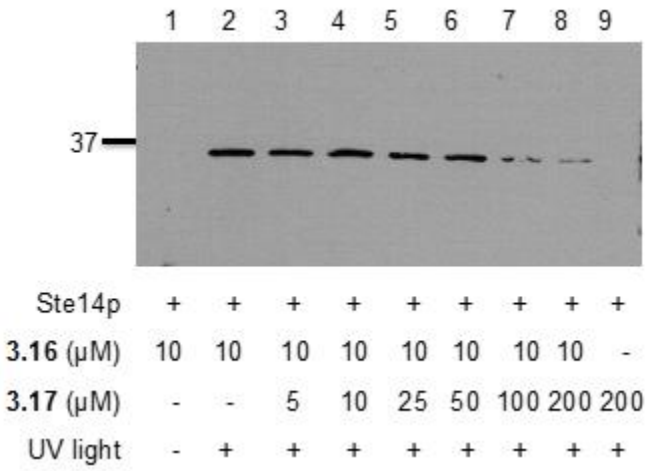

Figure 3.4. Competition of photolabeling of His-Ste14p by **3.16** using a biotinylated **a**-factor precursor peptide **3.17**. For this experiment, His-Ste14p crude membrane protein (100 μg) was mixed with **3.16** and **3.17** at the concentrations indicated and irradiated on ice for 30 min followed by enrichment with neutravidin-agarose beads. The samples are then eluted and resolved via SDS-PAGE. The resulting gel was blotted to a nitrocellulose membrane and visualized using an α-Ste14 antibody. The data shown is from one of two replicates of this experiment.

3.3 Conclusion

Herein, we have described the development and application of a new class of isoprenoid analogue containing a photoexcitable diazirine moiety. The photoactive farnesyl mimic was prepared in 6 steps and incorporated into a multifunctional peptide produced via solid phase synthesis. Kinetic analyses with His-Ste14p showed that the diazirine-containing peptide was an efficient substrate for the enzyme compared to

similar peptides functionalized with benzophenone-based isoprenoids. The diazirine-based probe crosslinked to His-Ste14p upon UV irradiation with an observable increase in efficiency compared to benzophenone-containing peptides. Finally, the incorporation and use of this diazirine-modified isoprenoid in a peptide probe equipped with a fluorophore greatly simplified the detection of crosslinked products. The greater yield of photocrosslinked His-Ste14p coupled with the ease of analysis obtained with this new class of isoprenoid mimics should facilitate the identification of active site residues in His-Ste14p. Such experiments are currently underway for this important membrane protein target. Given their improved features compared with other types of photoactive isoprenoid probes, this new class of analogues should be useful for a variety of studies of enzymes that act on terpene-derived molecules.

3.4 Materials and Methods

3.4.1 General. All solvents and reagents used for the synthesis of the diazirine isoprenoid analogue and solid-phase peptide synthesis of the photoactivatable peptides were of analytical grade and purchased from Peptides International (Louisville, KY), NovaBioChem® (Nohenbrunn, Germany), or Sigma-Aldrich (St.Louis, MO). NHS-PEG_4-Biotin was obtained from Thermo Scientific. The benzophenone-containing isoprenoid bromides; C_{10}-*meta*-Bp-Br (**3.2**) was prepared as previously described.[77,168,169,185] HR-ESI-MS analysis was performed using a Bio-TOF-II (Bruker) mass spectrometer

3.4.2 Synthesis of compound 3.5: 3-(3-methyldiaziridin-3-yl)propanoic acid. Levulinic acid **3.4** (1.61 g, 13.8 mmol, 1 eq) was dissolved in 7 N NH_3 in CH_3OH (13.5 mL, 91.0 mmol, 7 eq). The resulting solution was stirred under N_2 on ice for 3 h. A solution of hydrolxylamine-O-sulfonic acid (1.80 g, 15.9 mmol, 1.2 eq) in CH_3OH (12 mL) was added dropwise at a rate of 1 s^{-1}. The reaction mixture was stirred for 20 h and allowed to warm to rt. N_2 was bubbled through the solution for 1 h to remove NH_3 gas. Vacuum filtration and concentration resulted in a yellow oil that was used in the next step without purification.

3.4.3 Synthesis of coumpound 3.6: 3-(3-methyl-3H-diazirin-3-yl)propanoic acid. The diaziridine **3.5** was redissolved in CH_3OH (10 mL) and stirred on ice for 5 min in a tin foil covered flask. Triethylamine (3.00 mL, 21.5 mmol) was added and allowed to stir for 5 min. Slowly, chips of I_2 were added until the solution remained a brown-red color for longer than 5 min after the last addition. The reaction solution was diluted with EtOAc, washed with 1 M HCl, and with aqueous 10% sodium thiosulfate until the organic layer was colorless. The aqueous layer was further extracted with EtOAc (2x 20 ml). The organic layers were combined, dried over $MgSO_4$, and concentrated to afford the diazirine acid **3.5** as a brown residue (0.785 g, 45%). ^{1}H NMR (300 MHz, $CDCl_3$) δ: 1.05 (s, 3H), 1.73 (t, 2H, J = 6.8 Hz), 2.23 (t, 2H, J = 6.8 Hz); ^{13}C NMR (75.0 MHz, $CDCl_3$) δ: 20.4, 29.2, 30.0, 72.3, 179.1; HR-ESI-MS; calcd for $C_5H_8N_2O_2$ $[M-H]^-$ 127.0513, found 127.0493.

3.4.4 Synthesis of compound 3.8: (E)-2-((3,7-dimethylocta-2,6-dien-1-yl)oxy)tetrahydro-2H-pyran. This compound was prepared via a modification of a previously described procedure.[185] To a solution of geraniol **3.7** (3.11 g, 20.2 mmol, 1 eq) in CH_2Cl_2 (3.5 mL) were added DHP (2.54 g, 30.3 mmol, 1.5 eq) and PPTS (0.502 g, 2.0 mmol. 0.1 eq), and the resulting solution was stirred overnight at rt. The reaction mixture was quenched with saturated aqueous $NaHCO_3$ and extracted with CH_2Cl_2. The organic layer was dried over $MgSO_4$ and concentrated to afford **3.8** as a clear oil (4.79 g, 99%). ^{1}H NMR (300 MHz, $CDCl_3$) δ 1.58 (s, 3H), 1.65 (s, 6H), 1.48 – 1.85 (m, 6H), 2.04 – 2.22 (m, 4H), 3.47 – 3.54 (m, 1H), 3.85 – 3.92 (m, 1H), 3.98 – 4.05 (dd, 1H, J = 7.2, 12 Hz), 4.21 – 4.27 (dd, 1H, J = 6.3, 12 Hz), 4.62 (t, 1H, J = 2.7 Hz), 5.16 (t, 1H, J = 6.3 Hz), 5.39 (t, 1H, J = 6.2 Hz). HR-ESI-MS; calcd for $C_{15}H_{26}O_2$ $[M+H]^{+1}$ 239.1919, found 239.1932

3.4.5 Synthesis of compound 3.9: (2E,6E)-2,6-dimethyl-8-((tetrahydro-2H-pyran-2-yl)oxy)octa-2,6-dien-1-ol. This compound was prepared via a modification of a previously described procedure.[185] The protected geraniol **3.8** was dissolved in CH_2Cl_2 (28 mL). In turn, 70% *t*-Bu-OOH in H_2O (8.5 mL, 60.9 mmol, 3eq), salicylic acid (0.279 g, 2.02 mmol, 0.1 eq), and SeO_2 (0.205 g, 2.03 mmol, 0.1eq) were added, and the resulting solution was stirred overnight at rt. The reaction mixture was quenched with saturated aqueous $NaHCO_3$, extracted with CH_2Cl_2, and dried over $MgSO_4$. After concentration, the residue was purified by flash chromatography (Hexanes: Et_2O, 3:2, v/v) on silica gel to obtain 2.36 g (46%) of alcohol **3.9** as a clear oil. ^{1}H NMR (300 MHz,

$CDCl_3$) δ 1.65 (s, 6H), 1.48 – 1.85 (m, 6H), 2.04 – 2.22 (m, 4H), 3.47 – 3.54 (m, 1H), 3.85 – 3.92 (m, 1H), 3.91 (s, 2H), 3.98 – 4.05 (dd, 1H, J = 7.2, 12 Hz), 4.21 – 4.27 (dd, 1H, J = 6.3, 12 Hz), 4.62 (t, 1H, J = 2.7 Hz), 5.16 (t, 1H, J = 6.3 Hz), 5.39 (t, 1H, J = 6.2 Hz). HR-ESI-MS; calcd for $C_{15}H_{26}O_3Na$ $[M+Na]^{+1}$ 277.1790, found 277.1763

3.4.6 Synthesis of compound 3.10: (2E,6E)-2,6-dimethyl-8-((tetrahydro-2H-pyran-2-yl)oxy)octa-2,6-dien-1-yl3-(3-methyl-3H-diazirin-3-yl)propanoate. To a solution of protected alcohol **3.9** (1.94 g, 7.60 mmol,1 eq) and DMAP (92.8 mg, 0.76 mmol, 0.1 eq) in CH_2Cl_2 (7 mL) was added a solution of the diazirine acid **3.6** (0.97 g, 7.60 mmol, 1 eq) in CH_2Cl_2 (10 mL). DIC (0.959 g, 7.6 mmol0, 1eq) was added and the resulting solution was stirred at rt for 16 hours. The reaction mixture was filtered and concentrated. Purification by flash chromatography (hexanes: EtOAc, 5:1) afforded 1.07 g (57%) of diazirine **3.10** as a clear oil. ^{1}H NMR (300 MHz, $CDCl_3$) δ: 1.03 (s, 3H), 1.48 – 1.85 (m, 14H), 2.04 – 2.22 (m, 6H), 3.47 – 3.54 (m, 1H), 3.85 – 3.92 (m, 1H), 3.98 – 4.05 (dd, 1H, J = 7.2, 12 Hz), 4.21 – 4.27 (dd, 1H, J = 6.3, 12 Hz), 4.46 (s, 2H), 4.62 (t, 1H, J = 2.7 Hz), 5.36 (t, 1H, J = 6.3 Hz), 5.44 (t, 1H, J = 6.2 Hz); ^{13}C NMR (75.0 MHz, $CDCl_3$) δ: 13.16, 16.4, 20.5, 23.7, 25.1, 26.6, 30.6, 32.9, 39.7, 44.2, 63.3, 65.6, 69.3, 72.3, 105.5, 118.5, 130.4, 130.7, 141.8, 173.1. IR (NaCl, cm^{-1}): 2940.69 (s), 2870.41 (m), 1737.07 (s), 1669.76 (w), 1587.67 (w), 1447.34 (m), 1385.74 (m), 1175.14 (m), 1117.30 (m), 1023.15 (m). HR-ESI-MS: calcd for $C_{20}H_{32}N_2O_4Na$ $[M+Na]^+$: 387.2260, found 387.2234.

3.4.7 Synthesis of compound 3.11: (2E,6E)-8-hydroxy-2,6-dimethylocta-2,6-dien-1-yl 3-(3-methyl-3H-diazirin-3-yl)propanoate. To a solution of **3.10** (99 mg, 0.271 mmol, 1 eq) in EtOH (1.60 mL) was added PPTS (6.81 mg, 271 µmol, 0.1 eq). The reaction flask was fitted with a septum and stirred at 60 °C for 4 h. The reaction mixture was concentrated *in vacuo* and purified by flash chromatography (hexanes: EtOAc, 2:1) to afford 75 mg (99%) of diazirine alcohol **3.11** as a clear oil. ^{1}H-NMR (300 MHz, $CDCl_3$) δ: 1.03 (s, 3H), 1.58 – 1.75 (m, 8H), 2.05 – 2.22 (m, 6H), 4.15 (t, 2H, J = 6.0 Hz), 4.47 (s, 2H), 5.38 – 5.45 (m, 2H); ^{13}C NMR (75.0 MHz, $CDCl_3$): δ 13.6, 16.4, 23.5, 26.4, 32.9, 39.7, 44.2, 58.9, 69.3, 72.1, 124.6, 130.4, 130.7, 141.8, 173.1. IR (NaCl, cm^{-1}): 3395.58 (br) 2925.24 (s), 2870.41 (m), 1735.59 (s), 1669.76 (w), 1587.67 (w), 1447.34 (m), 1385.74 (m), 1176.09 (m), 1000.73 (m). HR-ESI-MS: calcd for $C_{15}H_{24}N_2O_3Na$ $[M+Na]^+$: 303.1685, found 303.1649.

3.4.8 Synthesis of compound 3.12: (2E,6E)-8-bromo-2,6-dimethylocta-2,6-dien-1-yl 3-(3-methyl-3H-diazirin-3-yl)propanoate. The diazirine alcohol **3.11** (69.5 mg, 0.247 mmol, 1 eq) was converted to the corresponding bromide in the presence of resin-bound PPh_3 (250 mg, 1.08 mmol, 4 eq) and CBr_4 (350 mg, 1.08 mmol, 4 eq) dissolved in $CHCl_3$ (6 mL). The resulting solution was allowed to stir for 2 h at rt. After the reaction was complete, excess CBr_4 and resin bound PPh_3 were removed from the mixture by passing the reaction through a C_{18} sep-pak column. Removal of the solvent afforded 68.1 mg (80%) of diazirine bromide **3.12** as a clear oil. ^{1}H-NMR (300 MHz, $CDCl_3$) δ: 1.03 (s, 3H), 1.58 – 1.75 (m, 8H), 2.05 – 2.22 (m, 6H), 3.99 (d, 2H, J = 8.4 Hz), 4.47 (s, 2H), 5.39

(t, H, J = 6 Hz) 5.51 (t, 2H, J = 6.1 Hz); ^{13}C NMR (75.0 MHz, $CDCl_3$) δ: 13.6, 15.4, 23.5, 26.4, 30.8, 32.9, 38.3, 44.2, 69.3, 72.1, 123.3, 130.4, 130.7, 143.2, 173.1. IR (NaCl, cm^{-1}): 2925.24 (m), 2870.41 (m), 1736.18 (s), 1656.35 (w), 1586.54 (w), 1446.66(m), 1385.30 (m), 1173.27(m). HR-ESI-MS: calcd for $C_{15}H_{23}BrN_2O_2Na$ $[M+Na]^+$: 366.1941, found 366.1952.

3.4.9 Synthesis of Biotin-Peg$_4$-K(5-Fam)YIIKGVFWDPAC-OH (3.15). Peptide synthesis was carried out using an automated solid-phase peptide synthesizer (PS3, Protein Technologies Inc, Memphis, TN) employing standard Fmoc/HCTU based chemistry. Synthesis began on preloaded Fmoc-Cys(Trt)- Wang resin (0.25 mmol) and the peptide chain was elongated using HCTU/N-Methylmorpholine-catalyzed, single coupling steps with 4 eq of both protected amino acids and HTCU for 30 min. Following complete chain elongation, the peptide's N-terminus was deprotected with 10% piperidine in DMF (v/v) and the presence of the resulting free amine was confirmed by ninhydrin analysis. The resin containing the peptide was washed with CH_2Cl_2, dried *in vacuo* overnight, weighed, and divided into three portions for further synthesis on a reduced scale. Using 83.0 µmol of peptide, the free amino terminus was biotinylated in DMF (5 mL) with NHS-PEG$_4$-Biotin (0.49 mg, 83.0 µmol, 1eq) catalyzed by DIEA (14.4 µL, 8.3 µmol, 0.1 eq) for 16 h. After acylation, the resin bound peptide was washed thoroughly with CH_2Cl_2 and dried *in vacuo* for 4 h. The peptide was then reacted with 5% hydrazine in DMF (5 mL, v/v) to orthogonally remove they Dde protected side chain. After verifying the deprotection was complete by ninhydrin analysis, the peptide was

washed with CH_2Cl_2, dried, and then reacted 5-FAM SE (45 mg, 86.0 µmol, 1 eq) catalyzed by DIEA (14.4 µL, 8.3 µmol, 0.1 eq) overnight. The peptide was cleaved from the resin along with simultaneous side chain deprotection by treatment with Reagent K containing TFA (10 mL), crystalline phenol (0.5 g), 1,2-ethanedithiol (0.25 mL), thioanisole (0.5 mL), and H_2O (0.5 mL) for 2 h at rt. The released peptide was collected and combined with TFA washes of the resin before precipitation of the peptide in chilled Et_2O (100 mL). The crude solid peptide was collected by centrifugation, the supernatant was removed, and the resulting pellet was washed 2 times with cold Et_2O (50 mL) repeating the centrifugation and supernatant removal steps each time. The crude peptide was purified using a semipreparative C_{18} RP-HPLC column with detection at 280 nm and eluted with a gradient of Solvent A (H_20/0.1% TFA, v/v) and Solvent B (CH_3CN/0.1% TFA, v/v). The crude peptide (150 mg) was dissolved in a DMF/H_2O solution (1:5 v/v, 25 mL), applied to the column equilibrated in Solvent A, and washed with 15% Solvent B for 15 min. The peptide was eluted using a linear gradient of (15-65% Solvent B over 1.5 h at a flow-rate of 5 mL/min). Fractions were analyzed using an analytical C_{18} RP-HPLC column employing a linear gradient (0-100% Solvent B over 60 min at a flow-rate of 1 mL/min) and detected at 214 nm. Fractions containing peptide product of at least 90% purity were pooled and concentrated by lyophilization to yield 55 mg (37% yield) of a yellow solid. A small amount (< 1mg) of the resulting purified peptide was dissolved in 10 µl of 0.1% TFA/CH_3CN and diluted 1:50 in a mixture of CH_3CN/H_2O (1:1 v/v) prior to MS analysis. MS was performed using a 50 µL injection and collecting 3000 scans. ESI-MS: calcd for $C_{117}H_{155}N_{19}O_{30}S_2$ $[M+2H]^{+2}$: 1186.0334, found 1186.0453.

3.4.10 Synthesis of Biotin-Peg$_4$-K(5-Fam)YIIKGVFWDPAC(C10-Diazirine)-OH (3.16). Peptide **3.15** (20 mg, 5.3 μmol, 1 eq**)** was dissolved in DMF/n-Butanol/H_2O (0.10% TFA) (3:1:1 v/v/v, 6 mL). The isoprenoid bromide **3.12** (15 mg, 54.5 μmol, 10 eq) was dissolved in 0.50 mL of DMF and loaded onto a C_{18} SepPack® column that had been equilibrated with 5% CH_3CN in aq. 0.10% TFA. The column was washed with 5% CH_3CN (5 mL), followed by 30% CH_3CN (10 mL). The purified bromide was then eluted from the column with 3.0 mL DMF directly into the reaction flask that contained the dissolved peptide. $Zn(OAc)_2 \cdot 2H_2O$ (5.4 mg, 25 μmol, 5 eq) was then added to initiate the alkylation reaction. After 4 h the reaction was analyzed by analytical RP-HPLC, purified by semipreparative C_{18} RP-HPLC, and identified via ESI-TOF MS. This reaction yielded 5.1 mg (21 %) of the desired alkylated peptide **3.16**. Purity by HPLC: 96.1 %, ESI-MS: calcd for $C_{132}H_{177}N_{21}O_{32}S_2$ $[M+2H]^{+2}$: 1317.1223, found 1317.1172.

3.4.11 Synthesis of Biotin-Peg$_4$-YIIKGVFWDPAC(Fr)-OH (3.17). Solid phase peptide synthesis and purification was carried out in the same fashion as described above. Following complete chain elongation, the peptide's N-terminus was deprotected with 10% piperidine in DMF (v/v) and the presence of the resulting free amine was confirmed by ninhydrin analysis. Using 83.0 μmol of peptide, the free amino terminus was biotinylated in DMF (5 mL) with NHS-PEG$_4$-Biotin (0.49 mg, 83.0 μmol, 1 eq) catalyzed by DIEA (14.4 μL, 8.3 μmol, 0.1 eq) for 16 h. After Reagent K cleavage and HPLC purification the free thiol-containing peptide (20 mg, 13 μmol, 1 eq) was prenylated with

farnesyl bromide (10 mg, 65 μmol, 5 eq) using the same conditions as **3.16**. Purity by HPLC: 92.4 %, ESI-MS: calcd for $C_{105}H_{157}N_{17}O_{23}S_2$ $[M+2H]^{+2}$: 1045.0551, found 1045.0499

3.4.12 Synthesis of Biotin-Peg$_4$-K(5-Fam)YIIKGVFWDPAC(C5-*m*-BP)-OH (3.19). Starting with **3.15,** as previously described, the peptide was prenylated using the same conditions and quantities as used for **3.16** with replacement of the isoprenoid analogue **3.12** with C_5-*meta*-Bp-Brthat that was prepared as previously described. [162,168] Purity by HPLC: 94.2 %, ESI-MS: calcd for $C_{136}H_{173}N_{19}O_{32}S_2$ $[M+2H]^{+2}$ 1325.0951, found 1325.0994.

3.4.13 Protein Isolation and *in vitro* Methyltransferase Vapor Diffusion Assays. For experiments using crude protein, membrane preparations from the yeast strain CH2704 overexpressing His-Ste14p were prepared as previously described, with minor modifications.[88,130] Following centrifugation at 100,000 x g for 1 h, the membrane pellet was resuspended in 10 mM Tris-HCl, pH 7.5, aliquoted, flash frozen in liquid N_2 and stored at -80ºC. *In vitro* assays for methyltransferase activity were performed using crude membranes as previously described.[154] In brief, reactions contained crude membrane preparations, 200 μM AFC, 20 μM *S*-adenosyl-L-[methyl-^{14}C]methionine ([^{14}C]SAM) (50–60 mCi/mmol), and 100 mM Tris-HCl, pH 7.5, in 60 μL. The reactions were incubated at 30 °C for 30 min and terminated by the addition of 50 μL of 1 M NaOH, 1% SDS (v/v). Each reaction (100 μL) was then spotted onto a filter paper that

was wedged into the neck of a vial containing 10 mL of scintillation fluid and allowed to diffuse at rt for 2.5 h. The filters were discarded, and the base labile [^{14}C]methyl groups transferred were measured via liquid scintillation counting. For experiments performed with purified His-Ste14p, $His_{10}myc_3$N-Ste14p (His-Ste14p) was expressed in a □*ste14* deletion strain[130] and purified as previously described.[88]

3.4.14 Photocrosslinking and neutravidin-agarose pull-down assays in crude membranes. Photocrosslinking assays were performed as described previously, with minor modifications.[154,169] 100 µg of crude membrane preparation expressing His-Ste14p in 10 mM Tris-HCl, pH 7.5 were pre-incubated with increasing concentrations of the competition peptide before addition of the photolabeling reagent and incubated at 4 ºC for 5 min. The samples were irradiated at 365 nm in 96-well plates for 30 min on ice. The resulting protein samples were solubilized in 800 µL of radioimmunoprecipitation assay (RIPA) buffer (25 mM Tris-HCl, pH 7.5, 150 mM NaCl, 1% Triton X-100, 1% sodium deoxycholate, 0.1% sodium dodecylsulfate)/10% SDS and incubated with 50 µL of a 50% neutravidin/RIPA bead slurry for 2 h at 4ºC. The beads were centrifuged at 13,000 x g for 1 min and washed three times with RIPA/10% SDS. The crosslinked protein was eluted from the neutravidin beads by the addition of 50 µL of 2X SDS sample buffer (0.5 M Tris-HCl, pH 6.8, 30% sucrose (w/v), 10% sodium dodecylsulfate (w/v), 3.5 M 2-mercaptoethanol and 0.1% bromophenol blue (w/v)). Samples were heated for 30 min at 65ºC and subjected to 12% SDS-PAGE and immunoblot analysis.

3.4.15 Photocrosslinking of purified His-Ste14p. 5 µg of purified His-Ste14p in 138 mM MOPS and 1 mM DTT were incubated in the presence of the photoaffinity analogues and incubated at 4ºC for 10 min. The samples were irradiated (365 nm) in 96-well plates for 30 min on ice. Following photocrosslinking, 40 µL of 5X SDS sample buffer (0.5 M Tris-HCl, pH 6.8, 30% sucrose (w/v), 10% sodium dodecylsulfate (w/v), 3.5 M 2-mercaptoethanol and 0.1% bromophenol blue (w/v)) was added directly to the samples. Samples were heated for 30 min at 65ºC and subjected to 12% SDS-PAGE.

3.4.16 Fluorescence Imaging. SDS-PAGE gels were imaged using GE Healthcare Life Sciences Typhoon Trio scanner. Excitation was performed at 488 nm and emission observed with a 520 nm band-pass emission filter (520 BP 40). The images were collected with a pixel size of 50 µm at normal sensitivity with a PMT voltage of 400 V.

3.4.17 Immunoblot Analysis. Proteins from SDS-PAGE gels were transferred to nitrocellulose membranes (0.22 µm) and the membranes were blocked at rt for 2 h in 20% (w/v) non-fat dry milk in phosphate-buffered saline with Tween-20 (137 mM NaCl, 2.7 mM KCl, 4 mM Na_2HPO_4, 1.8 mM KH_2PO_4 and 0.05% (v/v) Tween-20, pH 7.4) (PBST). The blocked membrane was incubated for 2 h at rt with an α-Ste14p (1:500-crude or 1:10,000-pure protein) antibody in 5% (w/v) non-fat dry milk in PBST. The membrane was washed in PBST three times and incubated for 1 h at rt with goat α-rabbit IgG-HRP (1:10,000) in 5% (w/v) dry milk in PBST. Incubation of the membrane with NeutrAvidin HRP (1:5000) was performed in 5% (w/v) BSA in PBST for 3

3.5 Supporting Information

3.5.1 Characterization of compound 3.10

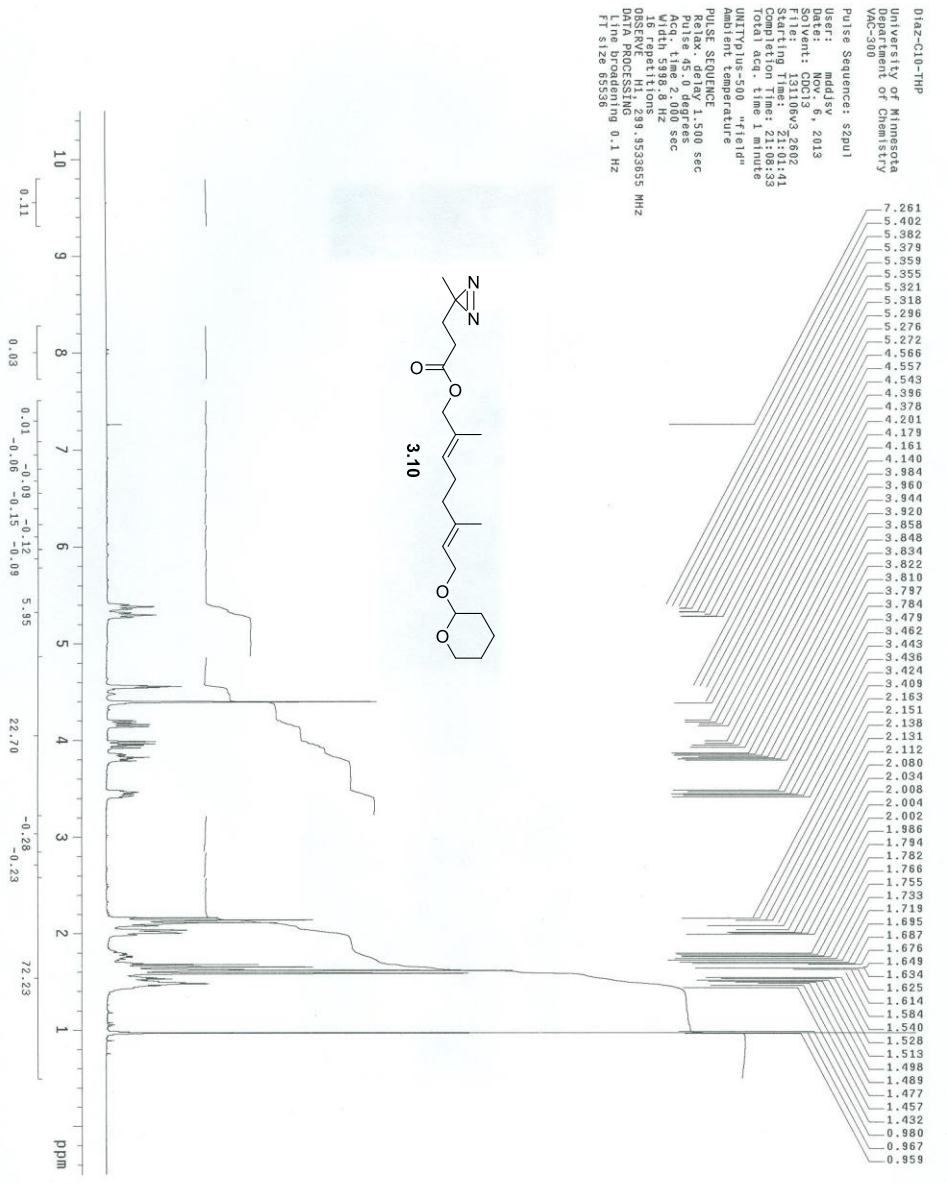

Figure 3.5. ^{1}H NMR spectrum of compound **3.10**.

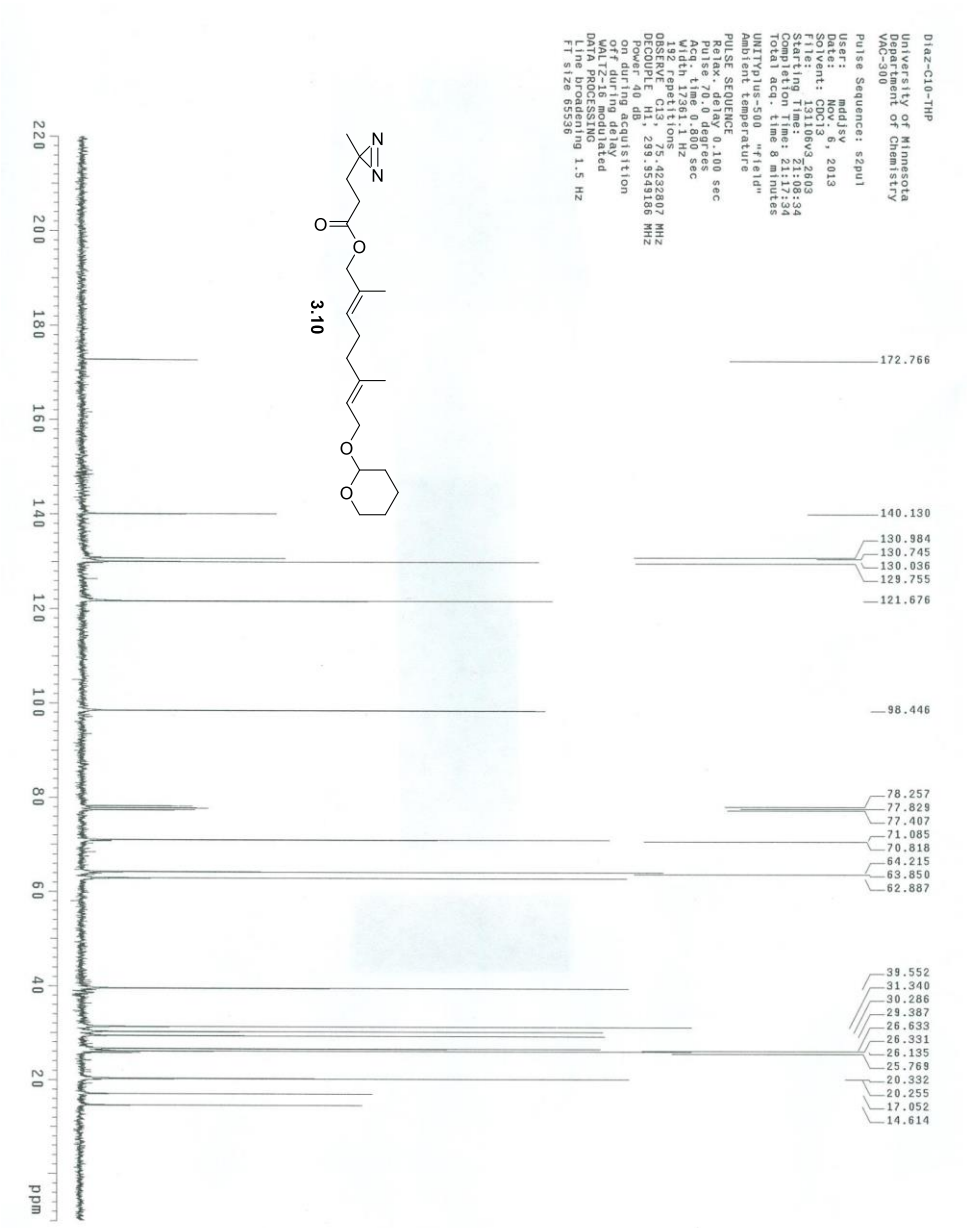

Figure 3.6. ^{13}C NMR spectrum of compound **3.10**.

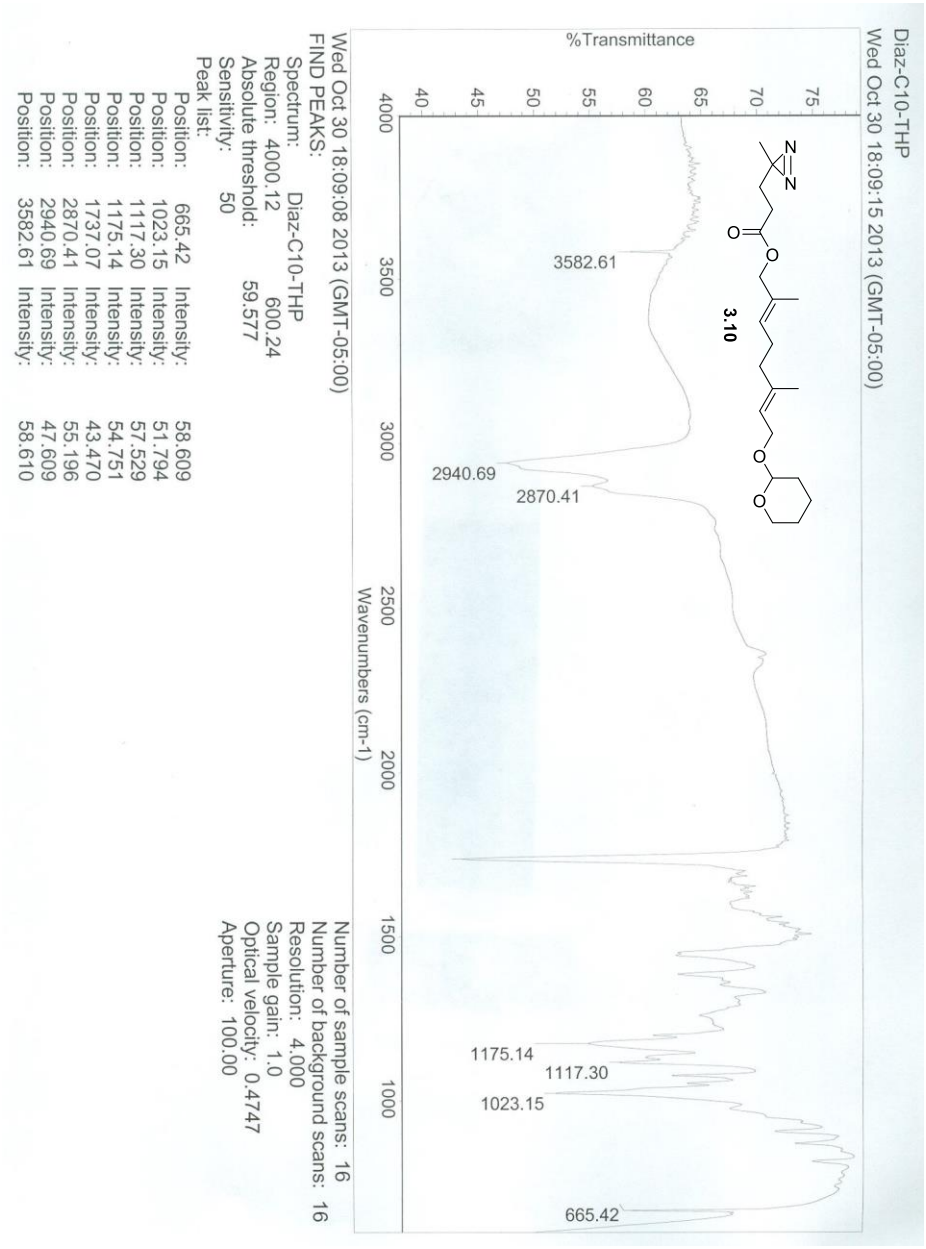

Figure 3.7. IR spectrum of compound **3.10**.

3.5.2 Characterization of compound 3.11

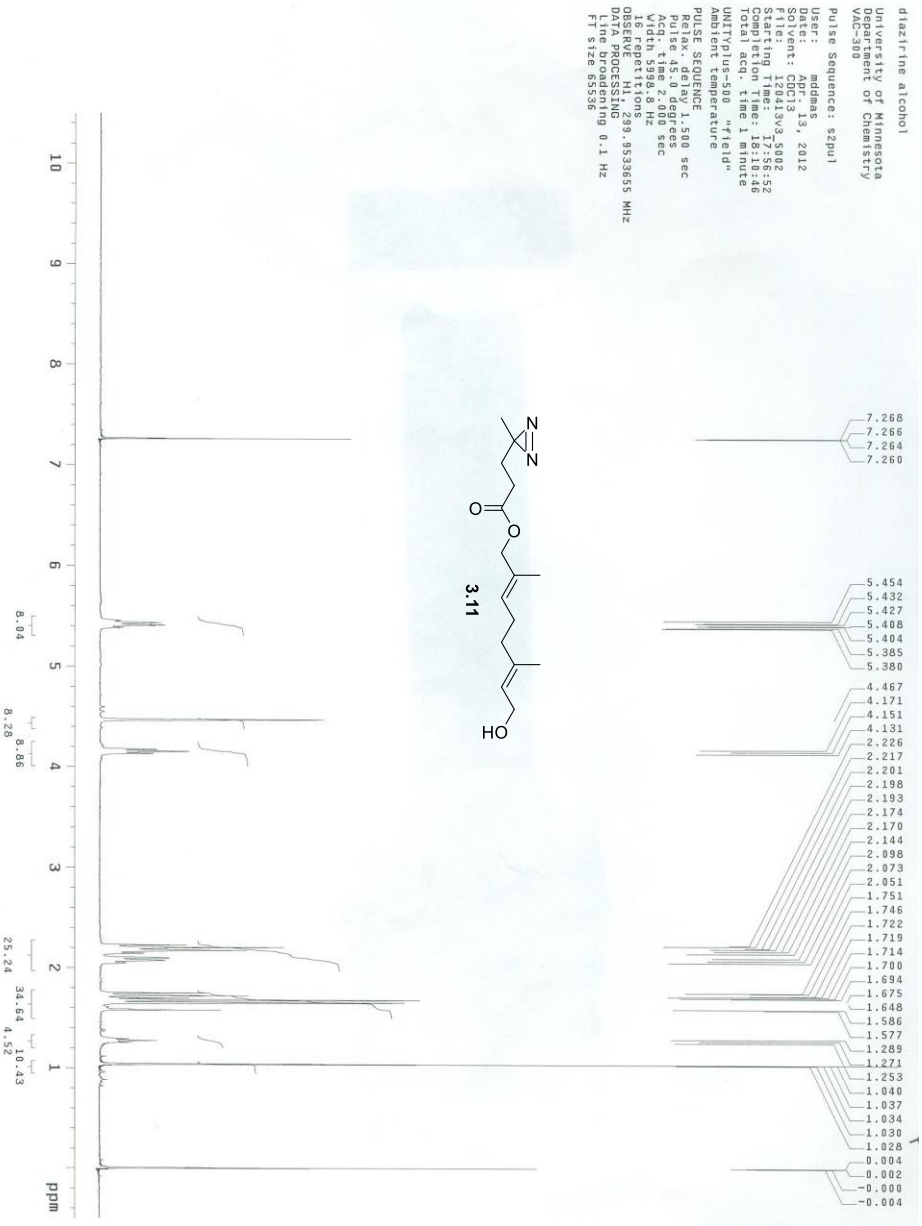

Figure 3.8. ^{1}H NMR spectrum of compound **3.11**.

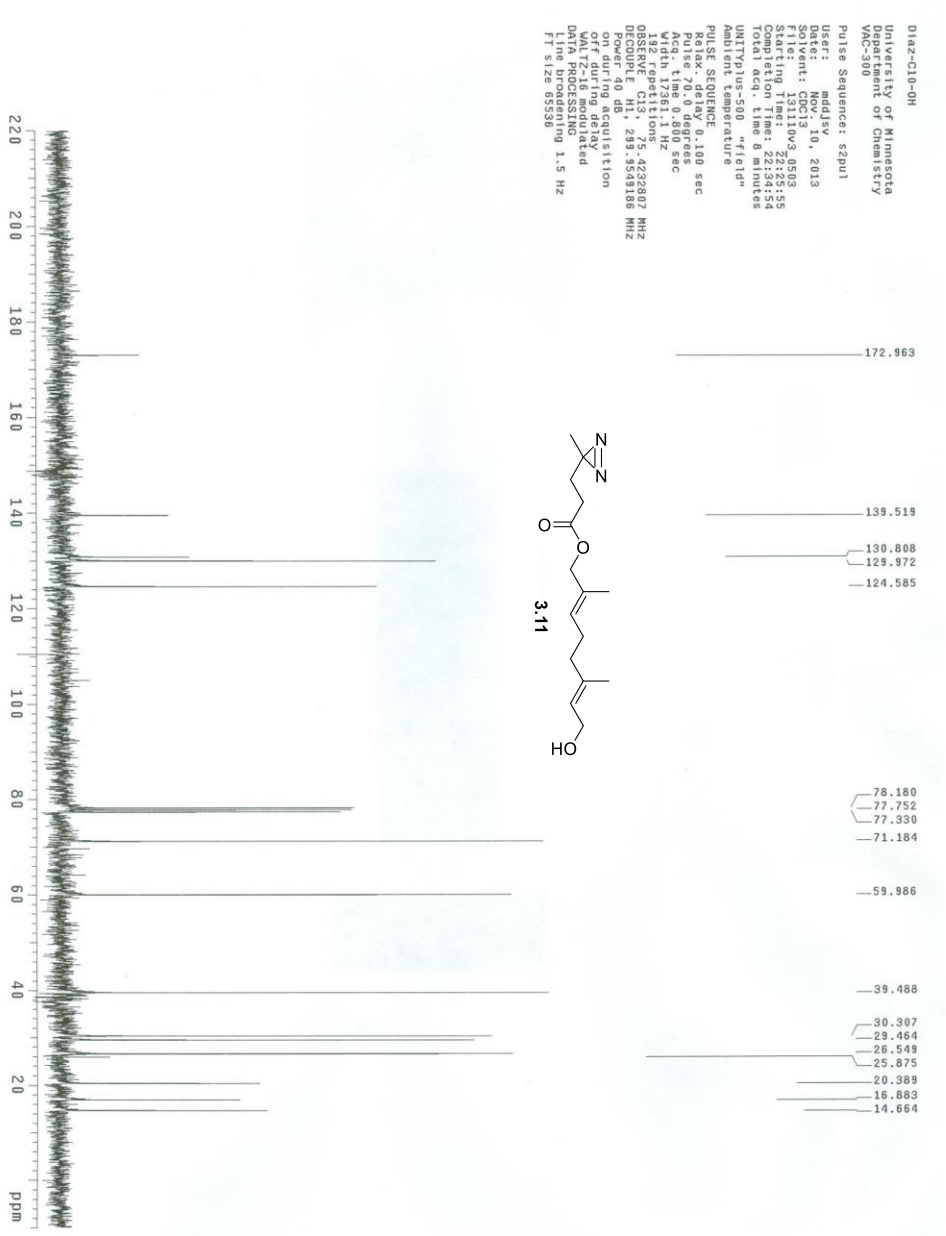

Figure 3.9. ^{13}C NMR spectrum of compound **3.11**.

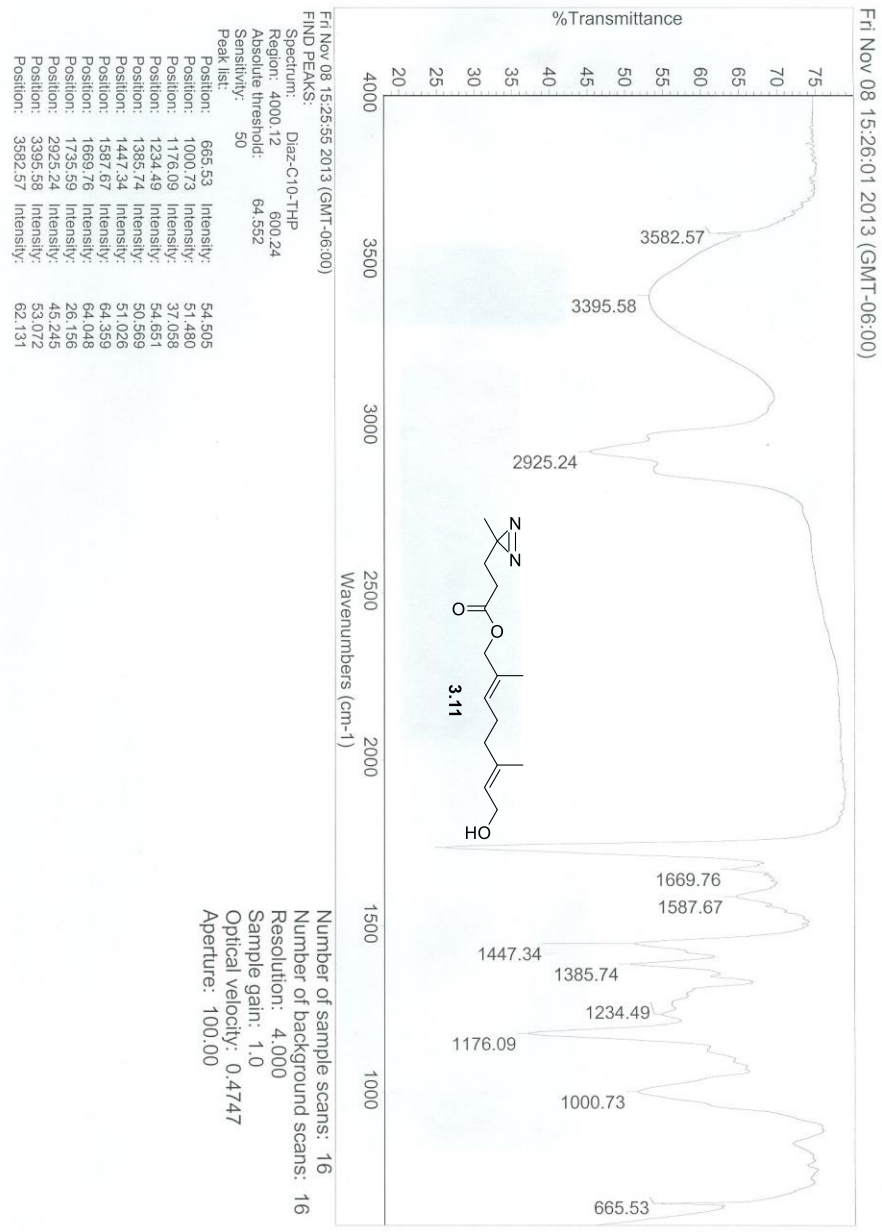

Figure 3.10. IR spectrum of compound **3.11**.

3.5.3 Characterization of compound 3.12

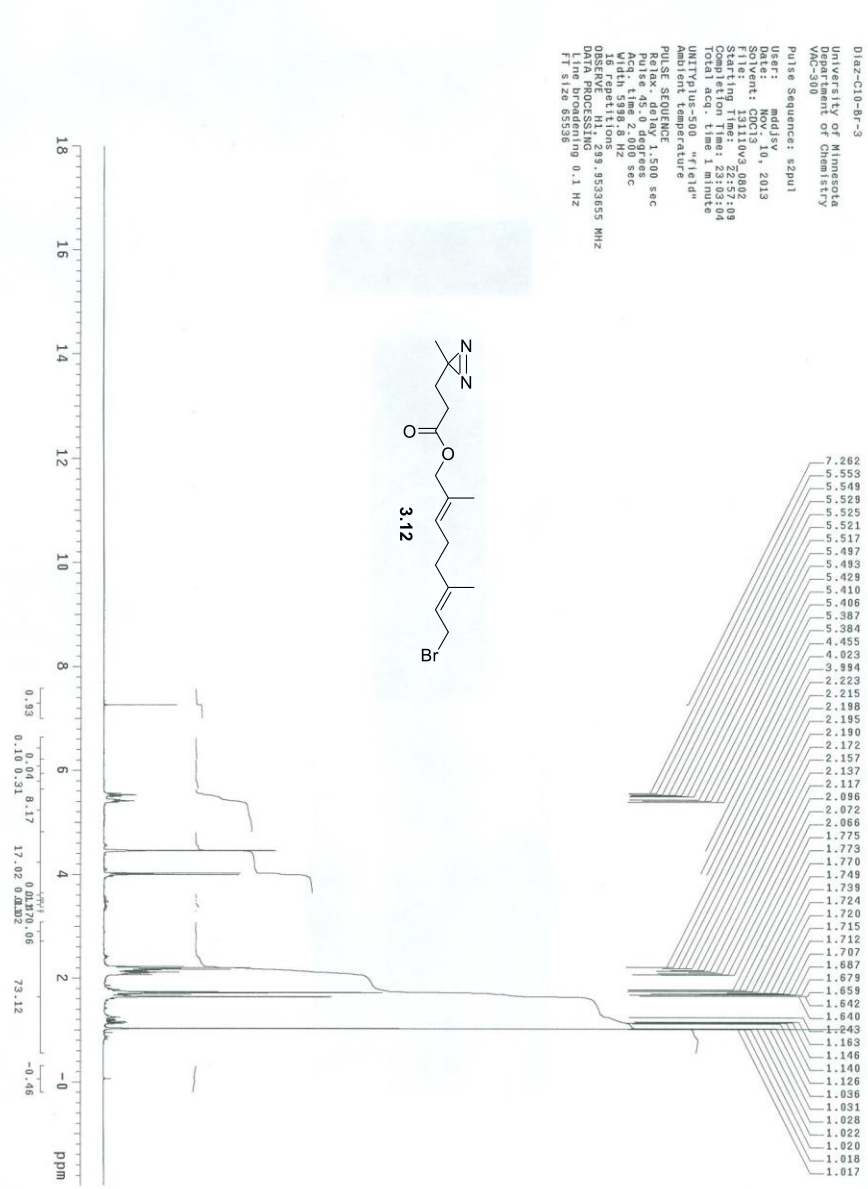

Figure 3.11. ^{1}H NMR spectrum of compound **3.12**.

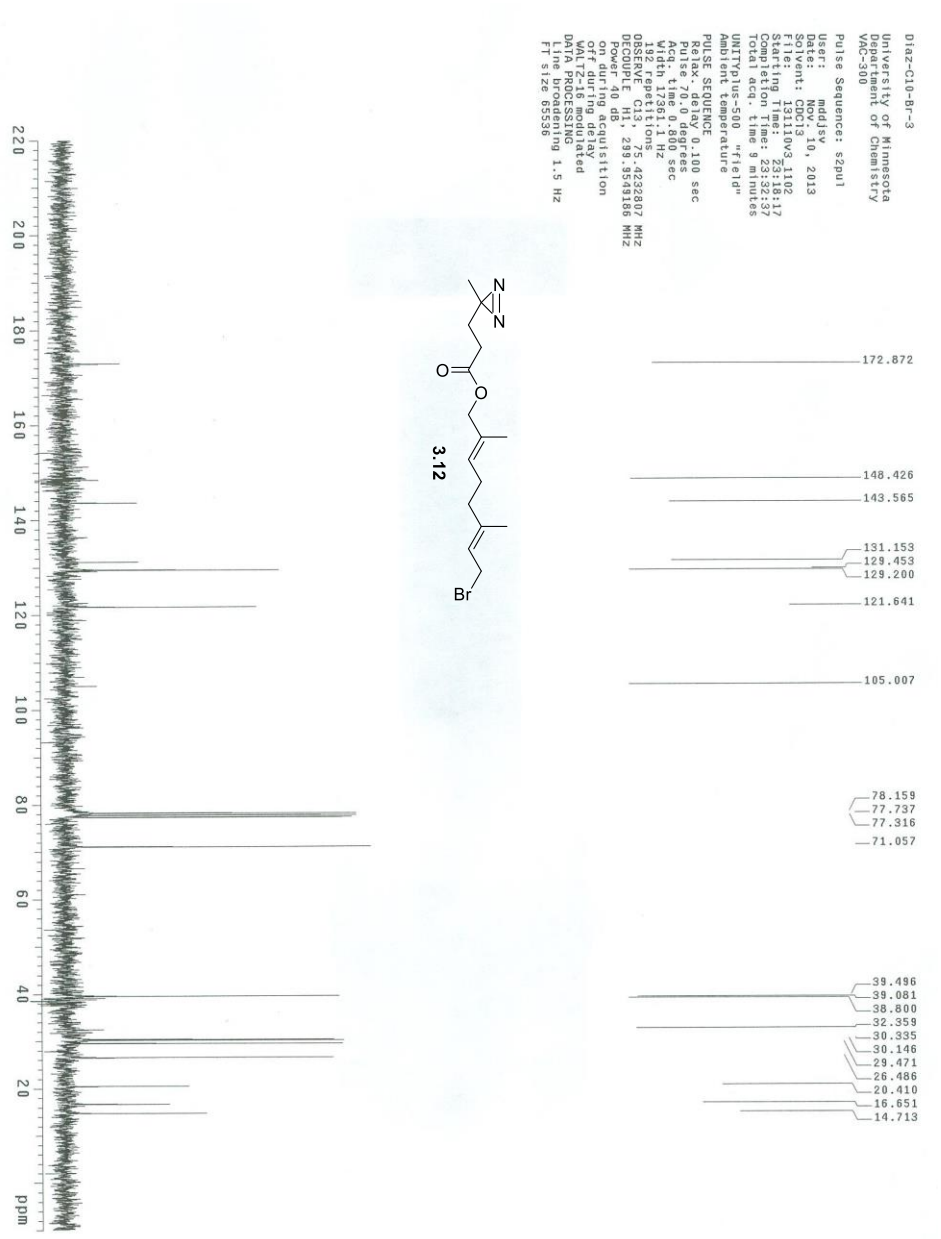

Figure 3.12. ^{13}C NMR spectrum of compound **3.12**.

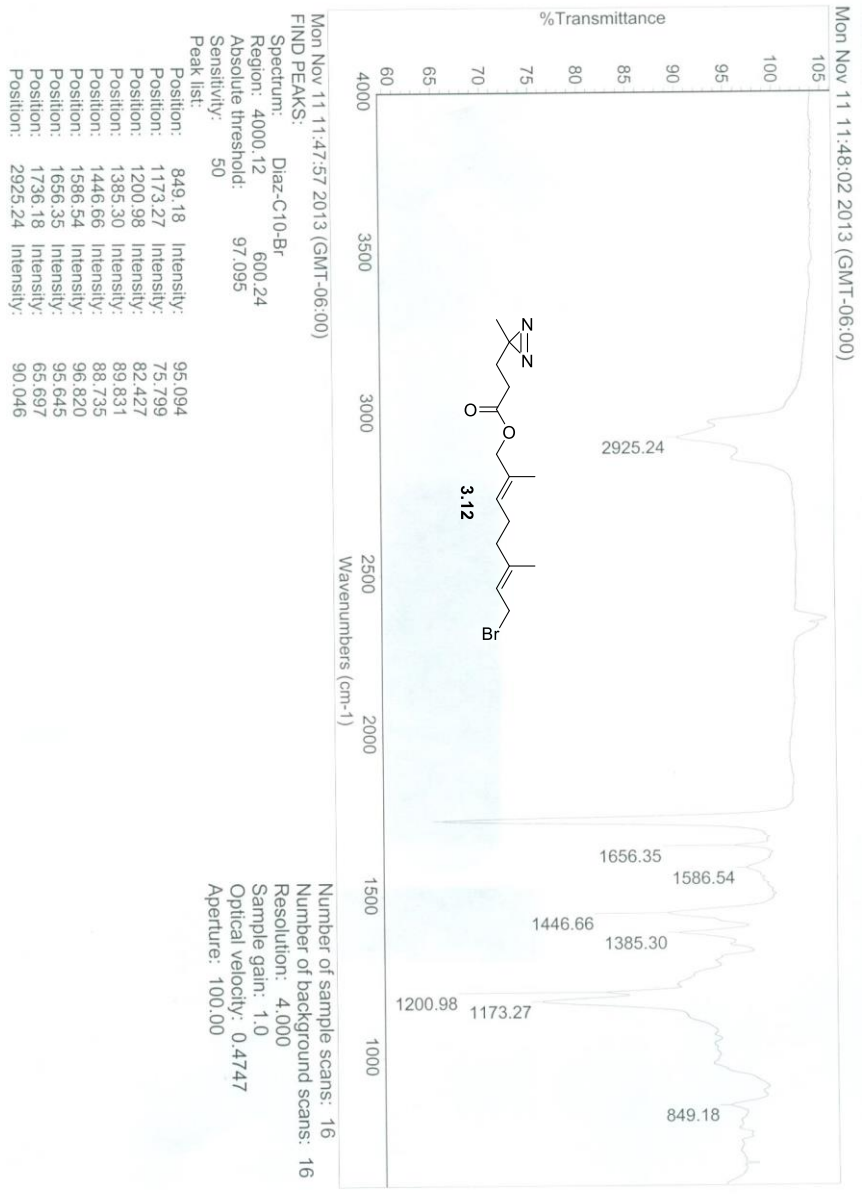

Figure 3.13. IR spectrum of compound **3.12**.

3.5.4 Characterization of Biotin-Peg$_4$-K(5-Fam)YIIKGVFWDPAC-OH (3.15)

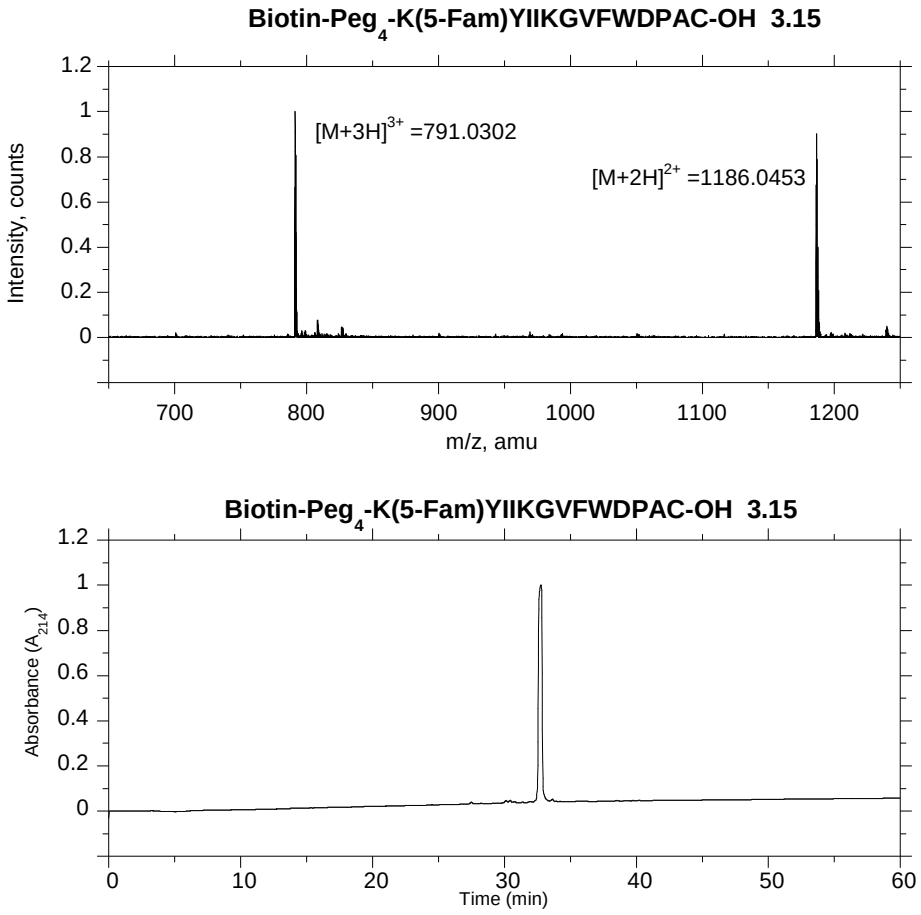

Figure 3.14. Mass spectrum and analytical RP-HPLC chromatogram for peptide **3.15**. Linear gradient 0-100% CH_3CN (0.1%TFA) in 60 min, detected at 214 nm.

Table 3.2. Summary of the ESI-MS-MS fragmentation for peptide **3.15**: -b, loss of 5-((4R)-2-oxohexahydro-1H-thieno[3,4-d]imidazol-4-yl)pentanal ($C_{10}H_{16}N_2O_2S$); -p loss of N-(15-oxo-3,6,9,12-tetraoxapentadecyl)-5-((4R)-2-oxohexahydro-1H-thieno[3,4-d]imidazol-4-yl)pentanamide ($C_{21}H_{37}N_3O_7S$); -h loss of H_2O.

Peptide 3.15

Ion	Calculated	Observed
$[M+2H]^{2+}$	1186.033	1186.030
$[M+2H]^{2+}$-b	958.919	958.915
Y_3	290.129	290.118
Y_4	405.145	405.148
Y_5-h	573.164	573.154
Y_6-h	720.231	720.232
Y_7^{3+}	279.763	279.759
Y_8-p	420.142	420.144
B_3	1123.433	1123.431
B^{2+}	562.215	562.212
B_3^{3+}-h	369.145	369.141
B_4	1236.522	1236.519
B_5-b	1122.516	1122.513
B_7^{2+}	767.867	767.864
B_{10}^{2+}	983.965	983.963
B_{11}^{3+}	694.653	694.651
B_{13}^{2+}	1125.525	1125.523
b	227.100	227.097

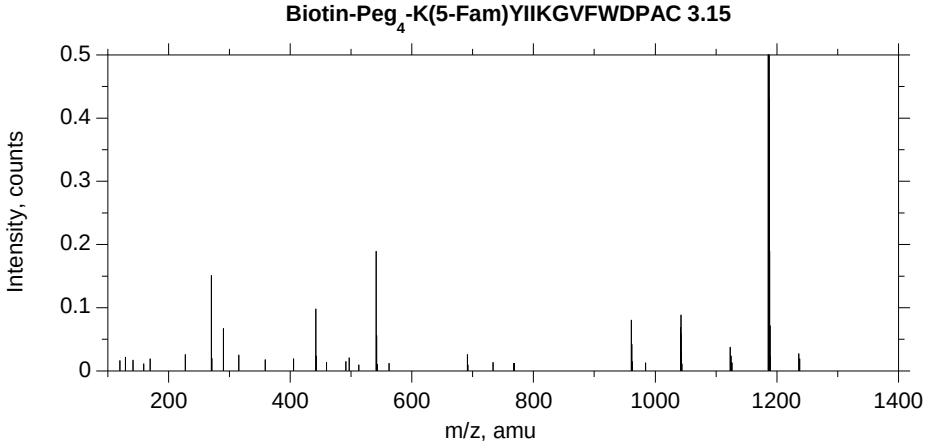

Figure 3.15. MS/MS spectrum of peptide **3.15**.

3.5.5 Characterization of Biotin-Peg$_4$-K(5-Fam)YIIKGVFWDPAC(C10-Diazirine)-OH (3.16)

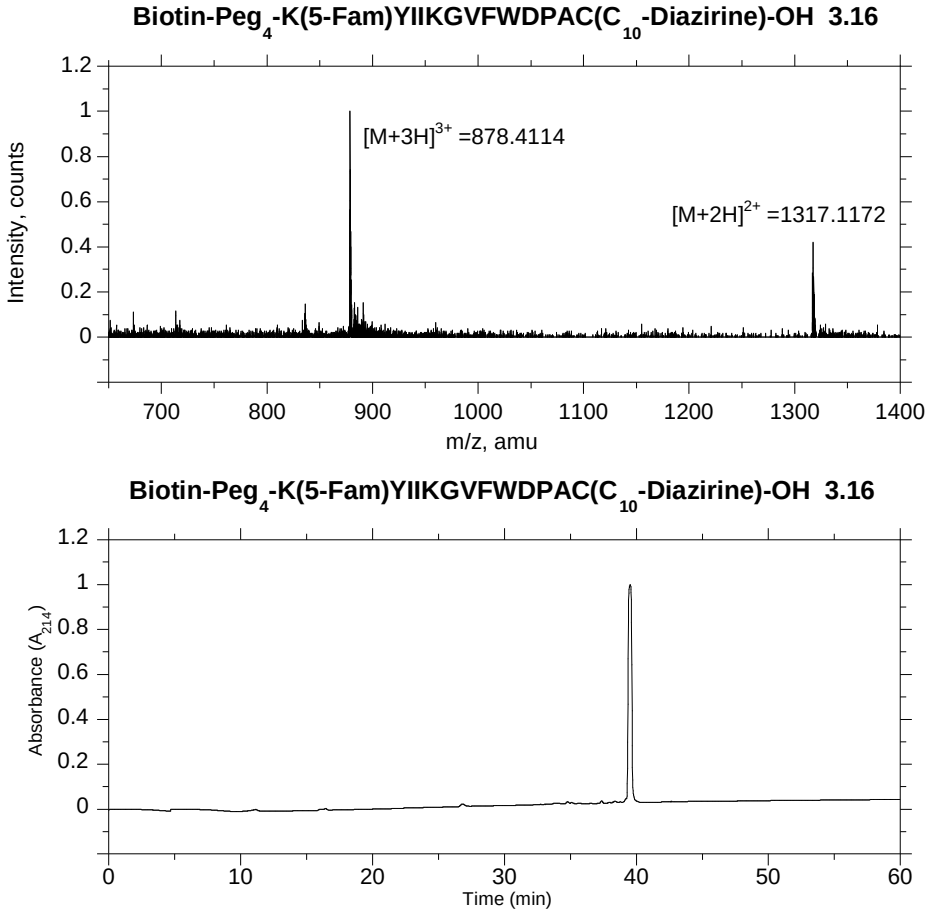

Figure 3.16. Mass spectrum and analytical RP-HPLC chromatogram for peptide **3.16**. Linear gradient 0-100% CH_3CN (0.1%TFA) in 60 min, detected at 214 nm.

Table 3.3. Summary of the ESI-MS-MS fragmentation for peptide **3.16**:-f, (2E,6E)-3,7-dimethyl-8-((3-(3-methyl-3H-diazirin-3-yl)propanoyl)oxy)octa-2,6-dien-1-ylium ($C_{15}H_{23}N_2O_2^+$) -b, loss of 5-((4R)-2-oxohexahydro-1H-thieno[3,4-d]imidazol-4-yl)pentanal ($C_{10}H_{16}N_2O_2S^+$); -p, loss of N-(15-oxo-3,6,9,12-tetraoxapentadecyl)-5-((4R)-2-oxohexahydro-1H-thieno[3,4-d]imidazol-4-yl)pentanamide ($C_{21}H_{37}N_3O_7S^+$); -h, loss of H_2O.

Peptide 16			Ion	Calculated	Observed
Ion	Calculated	Observed	B_3	1123.433	1123.431
$[M+2H]^{2+}$	1317.122	1317.118	B_3^{2+}	562.215	562.212
$[M+2H]^{2+}$-h	1296.396	1296.392	B_3^{3+}-h	369.145	369.141
$[M+2H]^{2+}$-f	1186.033	1186.036	B_4	1236.522	1236.519
$[M+2H]^{2+}$-b-f	958.919	958.915	B_4-b	1009.407	1009.405
Y_2	456.208	456.204	B_5-b	1122.516	1122.513
Y_3	553.126	553.122	B_6^{2+}	739.306	739.302
Y_3-f	290.139	290.135	B_7^{2+}	767.867	767.864
Y_4	668.142	668.139	B_{10}^{2+}	983.965	983.963
Y_5	854.442	854.439	B_{11}^{3+}	694.653	694.651
Y_5-f	591.221	591.218	B_{13}^{2+}	1125.525	1125.523
Y_6	1001.219	1001.216	b	227.100	227.097
Y_9^{2+}	643.327	643.327	f	263.183	263.184

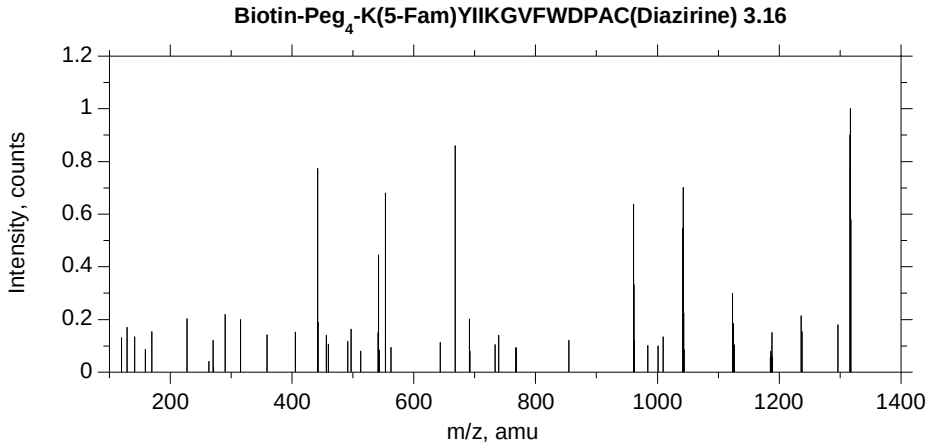

Figure 3.17. MS/MS spectrum of peptide **3.16**.

3.5.6 Characterization of Biotin-Peg$_4$-YIIKGVFWDPAC(Fr)-OH (3.17)

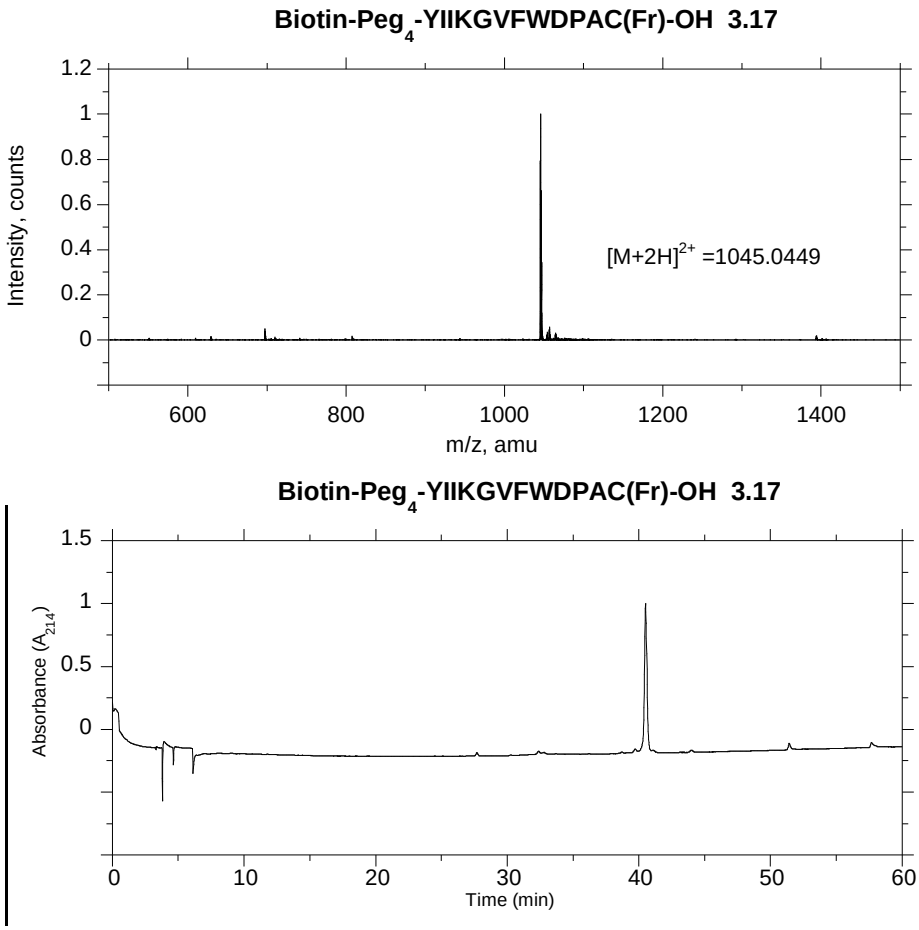

Figure 3.18. Mass spectrum and analytical RP-HPLC chromatogram for peptide **3.17**. Linear gradient 0-100% CH_3CN (0.1%TFA) in 60 min, detected at 214 nm.

3.5.7 Characterization of Biotin-Peg$_4$-K(5-Fam)YIIKGVFWDPAC(C5-*m*-BP)-OH (3.19)

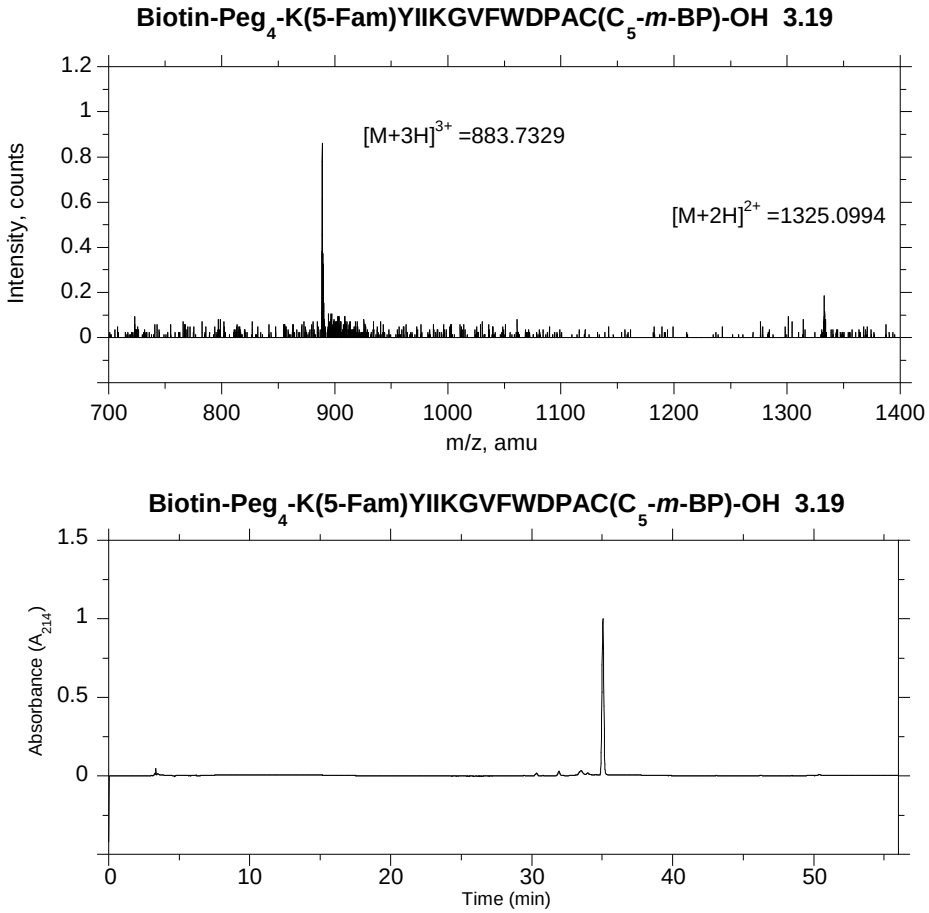

Figure 3.19. Mass spectrum and analytical RP-HPLC chromatogram for peptide **3.19**. Linear gradient 0-100% CH_3CN (0.1%TFA) in 60 min, detected at 214 nm.

3.5.8 Pull-down experiments with 3.16 and 3.19

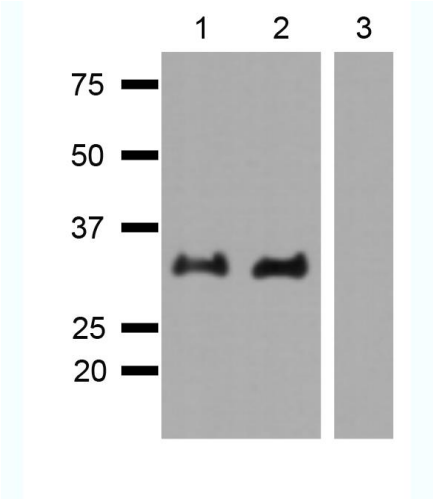

Figure 3.20. Analysis of crosslinking reactions containing purified His-Ste14p and photoactive probes **3.16** and **3.19** after pull-down with streptavidin. For this experiment, crude membrane proteins (100 µg) isolated from yeast were incubated with the probes indicated (50 µM) and irradiated on ice for 30 min followed by pull-down with streptavidin coated agarose beads. After washing the beads, the bound proteins were eluted in SDS loading buffer and fractionated via SDS-PAGE. The resulting gel was transferred to a membrane and visualized using an α-Ste14 antibody. Lane 1: Crosslinking reaction with membranes containing His-Ste14p and 3.**19**; Lane 2: Crosslinking reaction with membranes containing His-Ste14p and **3.16**; Lane 3: Crosslinking reaction with membranes lacking His-Ste14p (deletion strain) and **3.19**.

Chapter 4: Synthesis of Peptides for Evaluating the Activity of Ste24p

4.1 Introduction

Yeast (*Saccharomyces cerevisiae*) is known for its unique mating pattern, accomplished by the secretion of bioactive signaling molecules, fungal pheromones that are divided into two types, **a**-factor and α-factor.[191] These two pheromones are translated as precursor peptides that require multi-step enzymatic processing to progress to their active forms. Due to the presence of a CAAX box motif and an upstream N-terminal cleavage site, studies on **a**-factor provide important information on the posttranslational processing of yeast CAAX proteins.[3]

Similar to the processing of prelamin A found in mammalian cells, **a**-factor is post-translationally modified by the prenylation pathway.[51] As seen in Figure 4.1, **a**-factor undergoes prenylation, endoproteolysis, methyl esterification, and then is subsequently cleaved to reveal the active form of the pheromone.

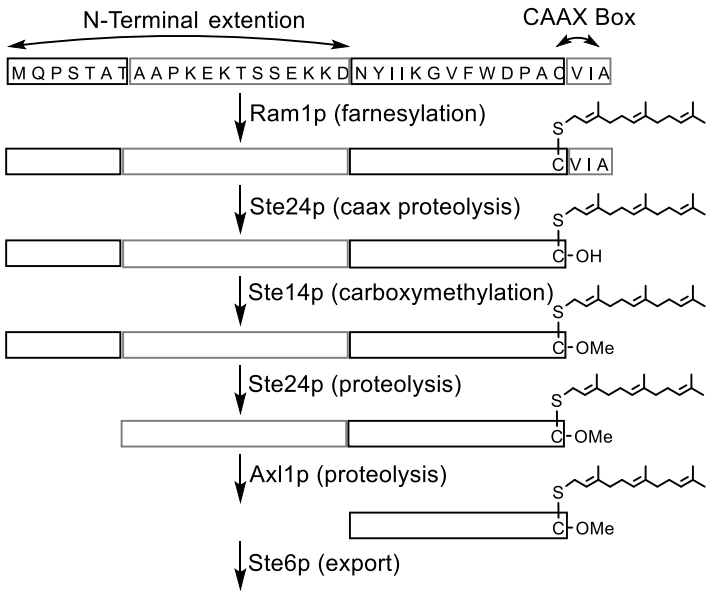

Figure 4.1. Post-translational processing of **a**-factor.

It is interesting that Ste24p is predicted to cleave at two different sites, first at the C-terminal tripeptide and then again upstream in the N-terminal extension. This dual cleavage role suggests that Ste24p's active site can allow for the recognition of two unrelated peptide sequences. It also raises the question of whether the reaction kinetics vary between the different cleavage positions, a concept that has yet to be explored. Having a better grasp of the dual cleavage role performed by Ste24p may help with understanding mammalian Ste24, as it also multiply cleaves its substrate, prelamin A.

The desire to inhibit Rce1 and Ste24 function has led to the development of many assays to monitor the cleavage of the tripeptide from CAAX bearing substrates. Monitoring of Ste24p function in yeast has been largely dominated by coupled assays with Ste14p, using either bioassays to detect the active form of **a**-factor,[163] or a vapor diffusion assay detecting radiolabeled methyl esters.[154] Novel fluorescence based assays have also been developed which can directly monitor proteolysis by Ste24p; however, they are designed to mimic the C-terminal domain of K-RasB4. In order to make a more relevant comparison between Ste24p's proteolysis rate of the two cleavage sites, donor-quencher peptides were designed using **a**-factor as a template. By incorporating 2-aminobenzoic acid (Abz) and 2,4-dinitrophenol (Dnp) at positions across the scissile bonds, direct proteolysis rates can be measured by observing the increase in fluorescence over time. Here we show the synthesis and application of the donor-quencher peptides to study Ste24p.

4.2 Results and Discussion

4.2.1 Design and synthesis of CAAX cleavage probe. The design for a CAAX box cleavage probe started with determining what position in the **a**-factor sequence was suitable to incorporate the fluorescent moiety, Abz, and the quencher, Dnp, which would no longer be attached to the same peptide after Ste24p cleavage. Previous work with Ste24p has shown that Abz-KSKTKCVIQ$_L$-OH is a suitable substrate with a K_M of 10.9 M, and displays a measurable increase in fluorescence upon tripeptide cleavage.[65] When aligned next to the **a**-factor sequence, (Figure 4.2), the attachment of the Abz group falls between the amino acids Val and Phe. This position has been shown to maintain **a**-factor activity upon mutagenesis,[51] making it an attractive location for Abz incorporation. Additionally, placement of Dnp-lysine (Q_L) at the A_2 or X amino acid in the K-Ras4B peptide were shown to be processed by Ste24, with the X position being a superior substrate. With these factors in mind peptide, **4.1** (Figure 4.2), was developed.

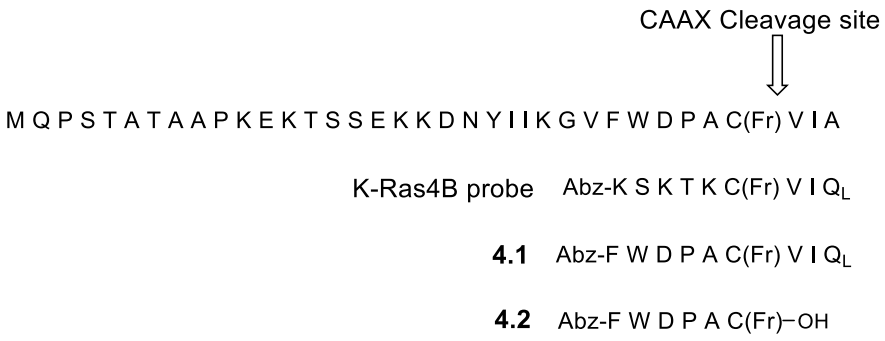

Figure 4.2. Design of fluorescence assay CAAX cleavage probe: CAAX cleavage probe **4.1**, short cleavage standard **4.2**.

Synthesis of peptide **4.1** started with the loading of Fmoc-Lys(Dnp) onto wang resin using DIC and DMAP to facilitate the ester bond formation, **4.3** (Scheme 4.1). After determining the loading of the resin by quantitative-Fmoc analysis, solid phase peptide

synthesis (SPPS) was used to construct the peptide utilizing standard Fmoc/HCTU coupling conditions. The N-terminus was deprotected by treatment with 20% piperidine in DMF, and the free amine was detected by ninhydrin testing. Cleavage from the resin and acidic deprotection was carried out simultaneously by treatment with Reagent K to afford a yellow peptide, **4.4**, with a cysteine bearing a free thiol. After purification of the crude peptide by preparative RP-HPLC, **4.4** was chemically alkylated with farnesyl bromide (3 equiv) in the presence of $Zn(OAc)_2$ (3 equiv) in acidic DMF to yield the prenylated peptide, **4.1**, whose identity was determined via ESI-MS and purity confirmed by analytical RP-HPLC (See Figure 4.8). The cleaved peptide, **4.2**, to be used as a standard in HPLC based assays was prepared similarly; however, Fmoc-Cys(Trt)-Wang resin was used in SPPS as well as an increase in farnesyl bromide and $Zn(OAc)_2$ to afford chemical prenylation.

Scheme 4.1. Synthesis of CAAX cleavage probe

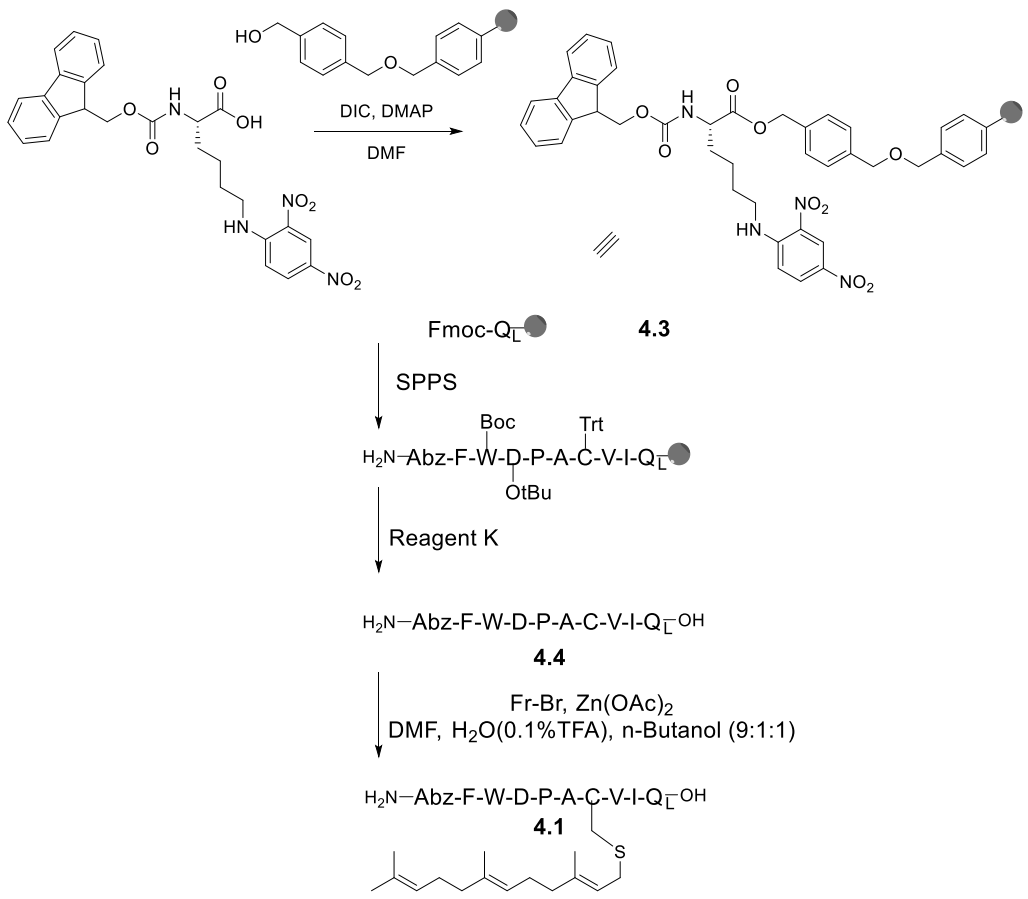

4.2.2 Design and synthesis of N-terminal cleavage probe. Determining the design of the N-terminal cleavage probe once again hinged on the placement of donor-quencher moieties while maintaining recognition by Ste24p. For the sake of synthetic simplicity, the Abz group was chosen to be appended to the N-terminus of the **a**-factor precursor peptide, seven amino acids upstream of the site of cleavage. Placement of the Dnp quencher on the side chain of the furthest upstream lysine residue satisfied the requirement for fluorescence evolution upon proteolysis while also taking advantage of commercially available Lys(Dnp) during peptide synthesis. Moreover, mutational studies have shown that precursor **a**-factor with derivatization at the chosen lysine residue is still

processed by Ste24p.[51] Although the distance between the donor and quencher was extended by two amino acids compared to the known K-RasB4 fluorescence peptide, efforts to synthesize and evaluate the designed peptide, **4.6** (Figure 4.3), were still taken.

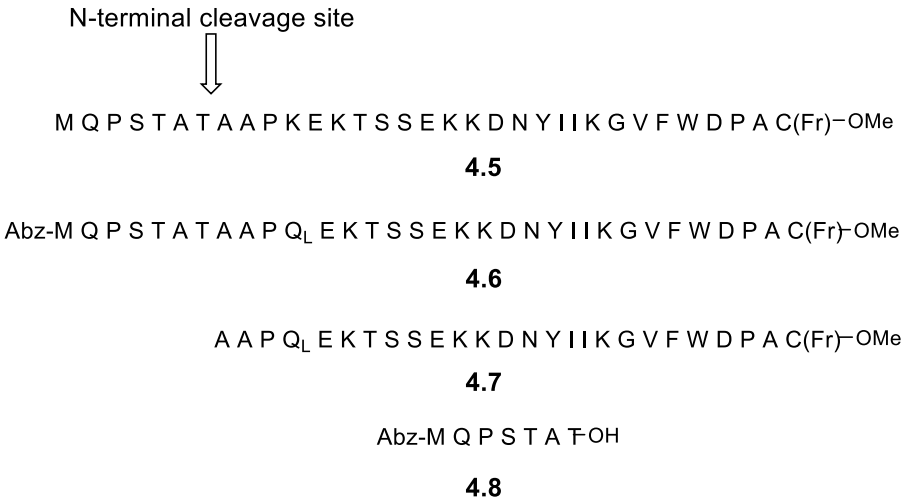

Figure 4.3. Design of fluorescence assay N-terminal cleavage probes: wild type a-factor **4.5**, N-terminal cleavage probe **4.6**, long C-terminal HPLC standard **4.7**, long N-terminal HPLC standard **4.8**.

SPPS synthesis began on Fmoc-Cys(Wang)-OMe resin that was made as previously described,[192,193] and utilized standard Fmoc/HCTU coupling conditions for chain elongation (Scheme 4.2). Upon determination of the free amino N-terminus by ninhydrin testing, the peptide was cleaved and deprotected by treatment with Reagent K. Interestingly, previous reports have noted that some epimerization of C-terminal cysteine residues can occur when Cys-functionalized Wang resin and Reagent K cleavage conditions are used,[194] but after RP-HPLC purification, no evidence for epimerization was observed using the thiol anchoring methodology. Preparative RP-HPLC and subsequent ESI-MS identification yielded a yellow peptide, **4.9**, with a C-terminal cysteine bearing a free thiol and a methyl ester. Alkylation of the thiol was with farnesyl

bromide (3 equiv) in the presence of $Zn(OAc)_2$ (3 equiv) in acidic DMF yielded the prenylated peptide, **4.6**, whose identity was determined via ESI-MS and purity confirmed by analytical RP-HPLC (Figure 4.10). The wild type **a**-factor peptide, **4.5**, and long C-terminal standard peptide, **4.7**, used for a comparative HPLC assay with Ste24p were synthesized in the same fashion, while the Abz containing peptide fragment, **4.9**, started with Fmoc-Thr(Boc)-Wang resin.

Scheme 4.2. Synthesis of fluorescence assay N-terminal cleavage probes

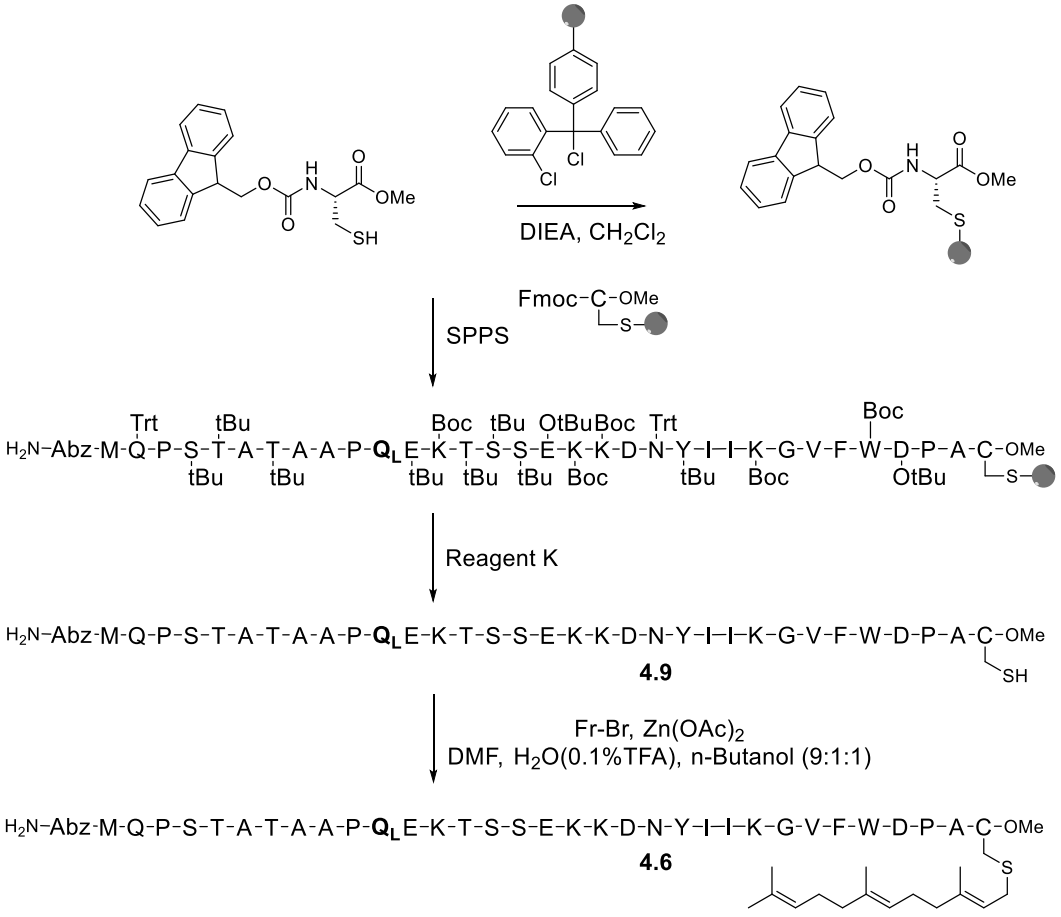

4.2.3 CAAX and N-terminal cleavage probes are substrates for Ste24p. To determine if probes **4.1** and **4.6** were substrates for Ste24p we used an assay that was adapted from an established fluorescence assay with K-Ras quenched substrate.[2,3] Ste24p membranes from yeast (5 μg) was incubated with varying concentrations of quenched substrate, **4.1** or **4.6**, and the fluorescence in the samples was measured at 420 nm every 30 sec for 20 min at 30°C (Figure 4.3). The kinetic values were determined by fitting saturation curve data to Michaelis-Menten equation using Graphpad Prism 4 (Figure 4.4). The fluorescent extinction coefficient was determined by the standard curve of cleavage products, **4.2** and **4.8** (Figure 4.5).

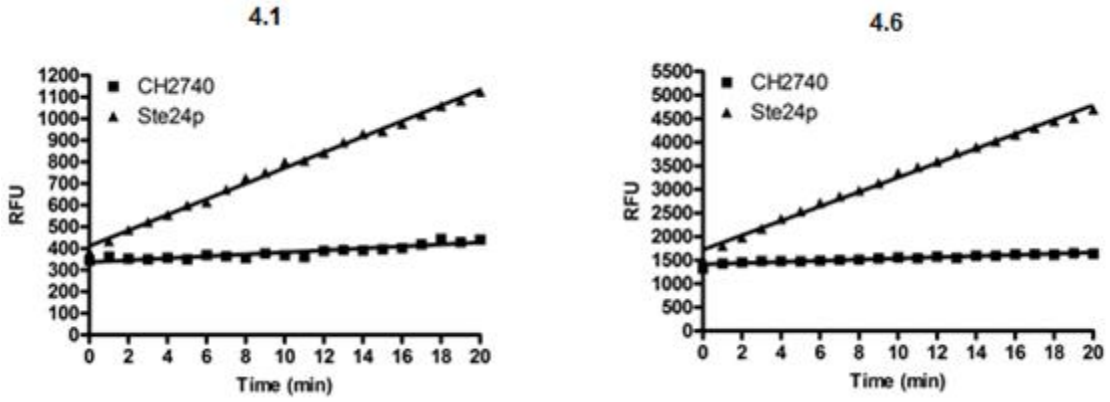

Figure 4.4. Monitoring Ste24p reaction in real time using: Left graph, **4.1**; Right graph, **4.6**. Linear increase in fluorescence measured by Bio-Tek Synergy H4 fluorimeter at 320/420 nm from dequenched peptide was detected. 15 μM of each probe was incubated with yeast Ste24p membranes (5 μg) for 20 min at 30 °C (▲). Control reaction with CH2740 membranes (no Ste24p) showed no increase in fluorescence (■).

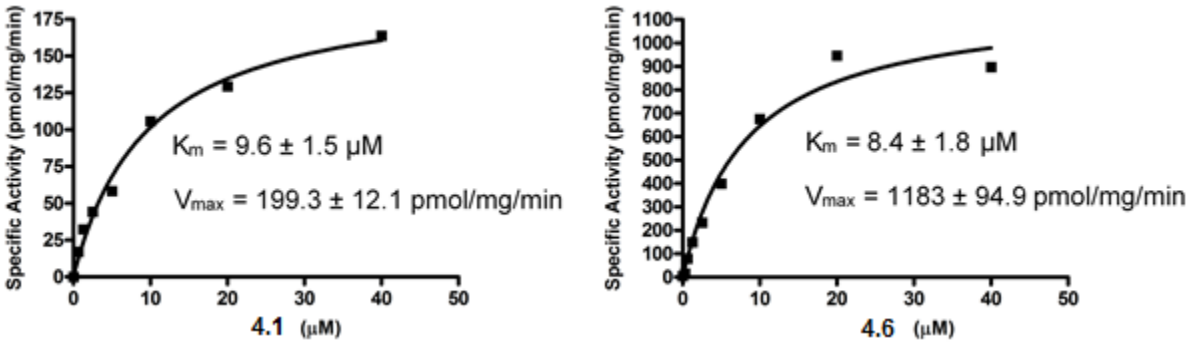

Figure 4.5. Saturation curves for Ste24p proteolysis of **4.1** and **4.6**: Left graph, **4.1**; Right graph, **4.6.** The activity of Ste24p measured from substrate concentrations ranging from 0 to 40 µM. The fluorescent extinction coefficient was determined by the standard curve of cleavage product, **4.2** and **4.8** (Figure 4.6.). Kinetic values were determined by fitting data to Michaelis-Menten equation using Graphpad Prism 4.

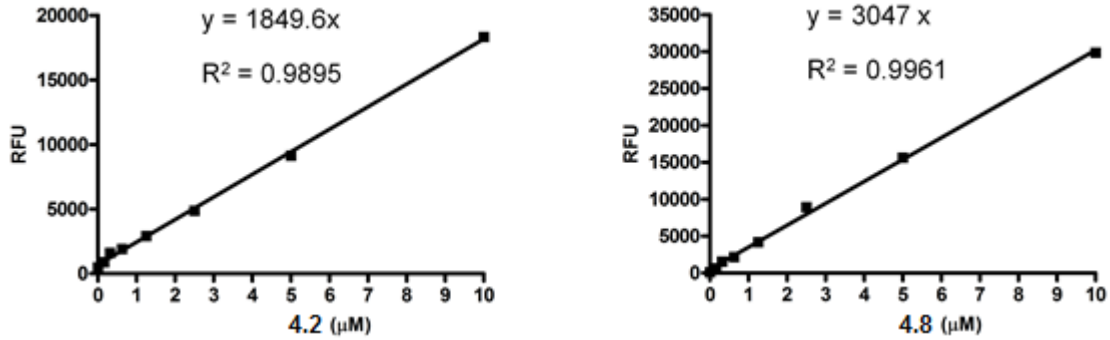

Figure 4.6. Representative calibration curve using **4.2** and **4.8** as standards. Concentrations ranged from (0-10 µM).

As see in figure 4.3, it is clear that in the presence of Ste24p the reaction mixture increases in fluorescence over time, suggesting that peptides **4.1** and **4.6** are recognized and processed by Ste24p. Additionally, in the presence of yeast membrane lacking Ste24p, there is no significant increase in fluorescence, providing evidence that proteolysis of the two quenched peptides is dependent upon Ste24p activity, and not another cellular protease. Comparison of the kinetic parameters obtained for CAAX cleavage probe **4.1** and N-terminal cleavage probe **4.6** reveal that both assay peptides bind equally as well with Ste24p with similar K_M values (Figure 4.4); however, peptide

4.6 is processed at a faster rate than **4.1**, as shown by a V_{max} value that is nearly an order of magnitude greater (Figure 4.4. It is also surprising that the extinction coefficients of the two cleaved products differ, **4.8** being two-fold greater than **4.2** (Figure 4.5), suggesting that aromatic residues in close proximity to the Abz moiety alter its molar absorptivity.

4.3 Conclusion

In this work we described the synthesis and application of fluorescence assay peptides to monitor the dual cleavage role of Ste24p in the processing of precursor **a**-factor. The quenched **a**-factor mimics were prepared in 4 steps via solid phase peptide synthesis on non-commercially available resin. Kinetic analyses with Ste24p showed that the CAAX cleavage peptide was comparable to previously reported K-Ras quenched substrate. Kinetic parameters obtained with the N-terminal cleavage probe are the first to be reported that quantify the secondary cleavage rate of precursor **a**-factor by Ste24p, and showed an enhanced reaction rate over CAAX proteolysis. Monitoring fluorescence of the cleaved standards also revealed a change in the fluorescent extinction coefficient of the Abz fluorophore that appears to be dependent on adjacent aromatic amino acid residues. Given the success in defining the kinetics associated with both cleavage reactions catalyzed by Ste24p, the new class of fluorescence assay peptides should provide a starting platform for the development of similar peptides to study mammalian Ste24.

4.4 Materials and Methods

4.4.1 General. All solvents and reagents used for the synthesis of the fluorescent assay peptides and cleaved products were of analytical grade and purchased from Peptides International (Louisville, KY), NovaBioChem® (Nohenbrunn, Germany), or Sigma-Aldrich (St. Louis, MO). Fmoc-Cys(Wang Resin)-OMe was prepared as previously outlined.[192,193] HR-ESI-MS analysis was performed using a Bio-TOF-II (Bruker) mass spectrometer.

4.4.2 Synthesis of Fmoc-Lys(Dnp)-Wang resin (4.3). Fmoc-Lys(Dnp)-OH (Q_L) (2.0 g, 3.74 mmol, 2 eq) was dissolved in anhydrous CH_2Cl_2 (5 mL) along with Cl-HOBt (0.63 g, 3.74 mmol, 2 eq), DMAP (0.12g, 0.935 mmol, .5 eq), and DIC (0.47 g, 3.74 mmol, 2 eq) in a fritted 6 mL syringe. The resulting solution was allowed to mix on a rotisserie for 10 mins. Wang resin with a (1.62 g, 1.87 mmol, 1 eq) was then added and the resulting mixture was tumbled on a rotisserie overnight. The reaction solution was removed from the syringe by vacuum filtration, and the remaining resin was washed with CH_2Cl_2 and dried *in vacuo* overnight. Loading of Fmoc-Lys(Dnp)-OH onto the resin (0.68 mmol/g) was determined via Fmoc-quantitative analysis.

4.4.3 Synthesis of Abz-FWDPACVIQ$_L$-OH (4.4). Peptide synthesis was carried out using an automated solid-phase peptide synthesizer (PS3, Protein Technologies Inc, Memphis, TN) employing standard Fmoc/HCTU based chemistry. Synthesis began on preloaded Q_L-Wang resin (0.1 mmol) and the peptide chain was elongated using

HCTU/N-Methylmorpholine-catalyzed, single coupling steps with 4 eq of both protected amino acids and HTCU for 30 min. Following complete chain elongation, the peptide's Fmoc-Abz N-terminus was deprotected with 20% piperidine in DMF (v/v) and the presence of the resulting free amine was confirmed by ninhydrin analysis. The peptide was cleaved from the resin along with simultaneous side chain deprotection by treatment with Reagent K containing TFA (10 mL), crystalline phenol (0.5 g), 1,2-ethanedithiol (0.25 mL), thioanisole (0.5 mL), and H_2O (0.5 mL) for 2 hat rt. The released peptide was collected and combined with TFA washes of the resin before precipitation of the peptide in chilled Et_2O (100 mL). The crude solid peptide was collected by centrifugation, the supernatant was removed, and the resulting pellet was washed 2 times with cold Et_2O (50 mL), repeating the centrifugation and supernatant removal steps each time. The crude peptide was purified using a semipreparative C_{18} RP-HPLC column with detection at 220 and 280 nm and eluted with a gradient of Solvent A (H_20/0.1% TFA, v/v) and Solvent B (CH_3CN/0.1% TFA, v/v). The crude peptide (136 mg) was dissolved in a DMF (10 mL), applied to the column equilibrated in Solvent A, and washed with 15% Solvent B until no absorbance was detected at 220 nm. The peptide was eluted using a linear gradient of (15-85% Solvent B over 1.5 h at a flow-rate of 5 mL/min). Fractions containing the desired mass determined by MS analysis were checked for purity by analytical C_{18} RP-HPLC column employing a linear gradient (0-100% Solvent B over 60 min at a flow-rate of 1 mL/min) and detected at 214 nm. Fractions containing peptide product of at least 90% purity were pooled and concentrated by lyophilization to yield a yellow powder 48 mg (35% yield). ESI-MS: calcd for $C_{65}H_{83}N_{14}O_{17}S$ $[M+H]^+$ 1363.5781, found 1363.5753

4.4.4 Synthesis of Abz-FWDPAC(Fr)VIQ$_L$-OH (4.1). Peptide **4.4** (25 mg, 18.3 μmol, 1 eq) was dissolved in DMF/H_2O (0.10% TFA) (9:1 v/v, 10 mL) after which farnesyl bromide (14 mg, 92 μmol, 5 eq) and $Zn(OAc)_2 \cdot 2H_2O$ (20 mg, 92 μmol, 5 eq) was then added to initiate the alkylation reaction. After 12 h the reaction was purified by semipreparative C_{18} RP-HPLC in the same fashion as previously stated, and identified via ESI-TOF MS. This reaction yielded 6.3 mg (22 %) of the desired alkylated peptide. Purity by HPLC: 94.1 %, ESI-MS: calcd for $C_{80}H_{106}N_{14}O_{17}S$ $[M+H]^+$: 1567.7659, found 1567.7598.

4.4.5 Synthesis of Abz-FWDPAC(Fr)-OH (4.2). Peptide synthesis began on Fmoc-Cys(Trt)-Wang resin (0.05 mmol) and followed the same SPPS and purification condition as described above. After Reagent K cleavage and HPLC purification, the free thiol-containing peptide (20 mg, 13 μmol, 1 eq) was prenylated with farnesyl bromide (20 mg, 130 μmol, 10 eq) and $Zn(OAc)_2 \cdot 2H_2O$ (28.1 mg, 130 μmol, 10 eq) with the same reaction conditions previously described. This reaction yielded 3.3 mg (24.5%) of the desired alkylated peptide. Purity by HPLC: 97.2 %, ESI-MS: calcd for $C_{57}H_{72}N_8O_{10}S$ $[M+H]^+$: 1061.5180, found 1061.5153.

4.4.6 Synthesis of Abz-MQPSTATAAPK(Dnp)EKTSSEKKDNYIIKGVFWDPAC-OMe (4.9). Peptide synthesis begin on Fmoc-Cys(Wang)-OMe resin (0.1 mmol) which was prepared as previously described,[192,193] and followed the same SPPS and purification

as described above. Fractions that contained the desired mass and were above 90% pure were pooled and lyophilized giving a yellow powder 138 mg (35% yield). ESI-MS: calcd for $C_{175}H_{262}N_{44}O_{56}S_2$ $[M+3H]^{+3}$: 1314.2894, found 1314.2854.

4.4.7 Synthesis of Abz-MQPSTATAAPK(Dnp)EKTSSEKKDN-YIIKGVFWDPAC(Fr)-OMe (4.6). Peptide **4.9** (75 mg, 19 μmol, 1 eq) was dissolved in DMF/H_2O (0.10% TFA) (9:1 v/v, 15 mL) after which farnesyl bromide (14.5 mg, 95 μmol, 5 eq) and $Zn(OAc)_2 \cdot 2H_2O$ (20.6 mg, 95 μmol, 5 eq) were added and the reaction was mixed for 12 hours. The reaction was purified by semipreparative C_{18} RP-HPLC purification in the same fashion as previously stated, and identified via ESI-TOF MS. This reaction yielded 19.7 mg (25%) of the desired alkylated peptide. Purity by HPLC: 95.2 %, ESI-MS: calcd for $C_{190}H_{286}N_{44}O_{56}S_2$ $[M+3H]^{+3}$: 1382.3521, found 1382.3482.

4.4.8 Synthesis of MQPSTATAAPKEKTSSEKKDNYIIKGVFWDPAC(Fr)-OMe (4.5). Peptide synthesis begin on Fmoc-Cys(Wang)-OMe resin (0.05 mmol) which was prepared as previously described,[192,193] and followed the same SPPS and purification as described above. After Reagent K cleavage and HPLC purification the free thiol-containing peptide (30 mg, 9.6 μmol, 1 eq) was prenylated using the same conditions as seen with **4.6**. This reaction yielded 6.7 mg (21%) of the desired alkylated peptide. Purity by HPLC: 96.4 %, ESI-MS: calcd for $C_{177}H_{282}N_{41}O_{51}S_2$ $[M+3H]^{+3}$ 1287.3391, found 1287.3354.

4.4.9 Synthesis of AAPK(Dnp)EKTSSEKKDNYIIKGVFWDPAC(Fr)-OMe (4.7). Peptide synthesis begin on Fmoc-Cys(Wang)-OMe resin (0.05 mmol) which was prepared as previously described,[192,193] and followed the same SPPS and purification as described above. After Reagent K cleavage and HPLC purification the free thiol-containing peptide (30 mg, 9.6 μmol, 1 eq) was prenylated using the same conditions as seen with **4.6.** This reaction yielded 6.7 mg (21%) of the desired alkylated peptide. Purity by HPLC: 93.4 %, ESI-MS: calcd for $C_{154}H_{233}N_{35}O_{44}S$ $[M+3H]^{+3}$ 1103.9008, found 1103.8942.

4.4.10 Synthesis of Abz-MQPSTAT-OH (4.8). Peptide synthesis begin on Fmoc-Thr(tBu)-Wang resin (0.05 mmol) and followed the same SPPS and purification as described above. Reagent K cleavage and HPLC purification the yield a white solid 22.3 mg (53% yield) Purity by HPLC: 92.8 %, ESI-MS: calcd for $C_{36}H_{55}N_9O_{13}S$ $[M+1H]^+$ 854.3718, found 854.3702.

4.4.11 Crude membrane preparation of yeast Ste24p. Crude membranes containing yeast Ste24p were prepared as previously described.[88] Briefly, late-log phase yeast cells (3-5 A_{600}/ml) were cultured in SC-URA medium at 30°C and harvested by centrifugation at 3,750 × g for 5 minutes at 4°C. The cell pellets were resuspended in lysis buffer (300 mM sorbitol, 10 mM Tris-HCl, pH 7.5, 100 mM NaCl, 5 mM $MgCl_2$, 1% aprotinin, 2 mM 4-(2-aminoethyl)benzenesulfonyl fluoride and 1 mM dithiothreitol) and incubated on ice for 15 minutes. The cells were frozen in liquid nitrogen and thawed at room

temperature twice prior to being lysed by passing through a French press twice at 18,000 psi. The lysates were centrifuged at 500 × g for 10 minutes at 4°C. The resulting supernatant was then centrifuged at 100,000 × g for 1 hour at 4°C to pellet membrane fraction. The pellet was resuspended in 10 mM Tris-HCl, pH 7.5, aliquoted, flash-frozen in liquid nitrogen and stored at -80°C.

4.4.12 In vitro fluorescence-based C- or N-terminal cleavage assays for yeast Ste24p. The assay was adapted from an established fluorescence-based assay with K-Ras sequence based quenched substrate.[65,195] Here we modified the substrates based on **a**-factor sequence to monitor C- or N-terminal proteolysis activity of yeast Ste24p. In brief, yeast Ste24p membranes from yeast (5 μg) and quenched substrates FLQ-CaaX or FLQ-Nterm (various concentrations) were mixed in a 96-well plate with 100 mM Tris-HCl, pH 7.5 and protease inhibitors (10 μg/μl chymostatin, 10 μg/μl leupeptin, 1% aprotinin and 2 mM AEBSF). The fluorescence in the samples was measured at 420 nm every 30 sec for 20 min at 30°C using Bio-Tek Synergy H4 fluorimeter. The collected data were exported and initial linear slopes were graphed and determined by Microsoft Excel. The saturation curves and kinetic values were determined by fitting data to Michaelis-Menten equation using Graphpad Prism 4.

4.4.13 Calibration curve of Abz-FWDPAC(Fr) or Abz-MQPSTAT. The calibration curves were determined by measuring Abz-released fluorescence with 320/420 nm from C- or N-terminal cleavage products, Abz-FWDPAC(Fr) or Abz-MQPSTAT (0 to 10 μM)

in 100 mM Tris-HCl, pH 7.5. The fluorescent extinction coefficients were obtained from standard curves of relative fluorescent units and fixed substrate concentrations for each substrate.

4.5 Supporting Information

4.5.1 Characterization of Abz-FWDPACVIQ$_L$-OH (4.4)

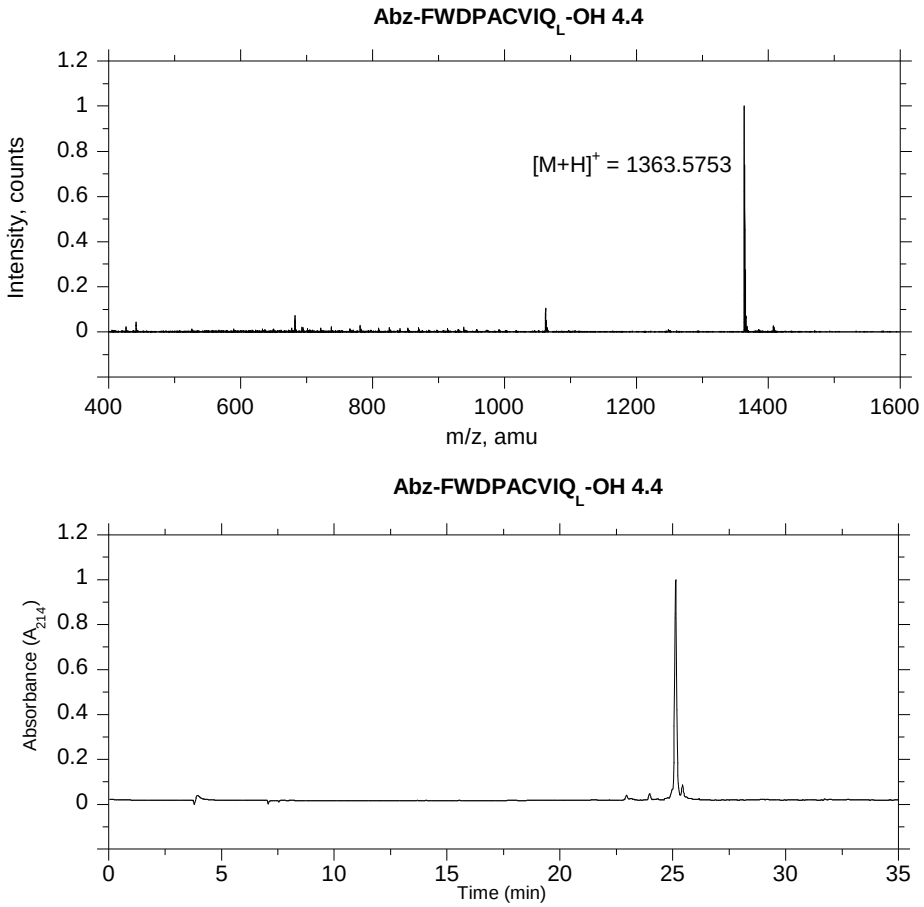

Figure 4.7. Mass spectrum and analytical RP-HPLC chromatogram for peptide **4.4**. Linear gradient 0-100% CH_3CN (0.1%TFA) in 30 min then 100% CH_3CN (0.1%TFA) for 5 min, detected at 214 nm.

4.5.2 Characterization of Abz-FWDPAC(Fr)VIQ$_L$-OH (4.1)

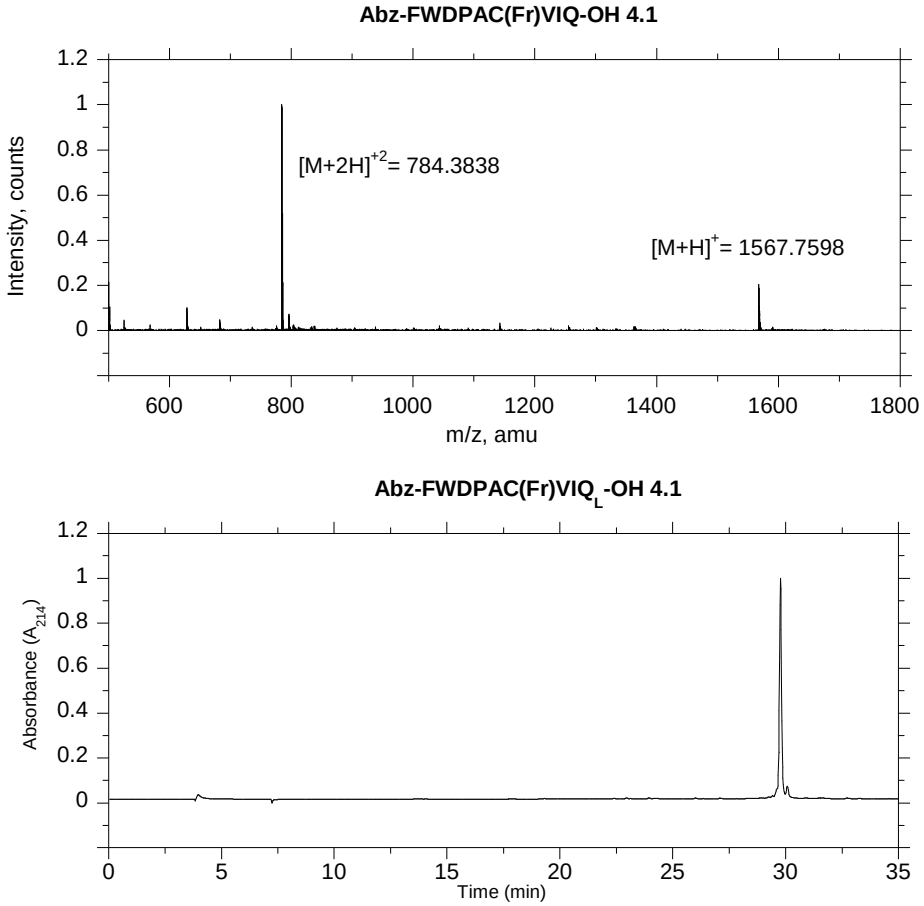

Figure 4.8. Mass spectrum and analytical RP-HPLC chromatogram for peptide **4.1**. Linear gradient 0-100% CH_3CN (0.1%TFA) in 30 min then 100% CH_3CN (0.1%TFA) for 5 min, detected at 214 nm.

4.5.3 Characterization of Abz-FWDPAC(Fr)-OH (4.2)

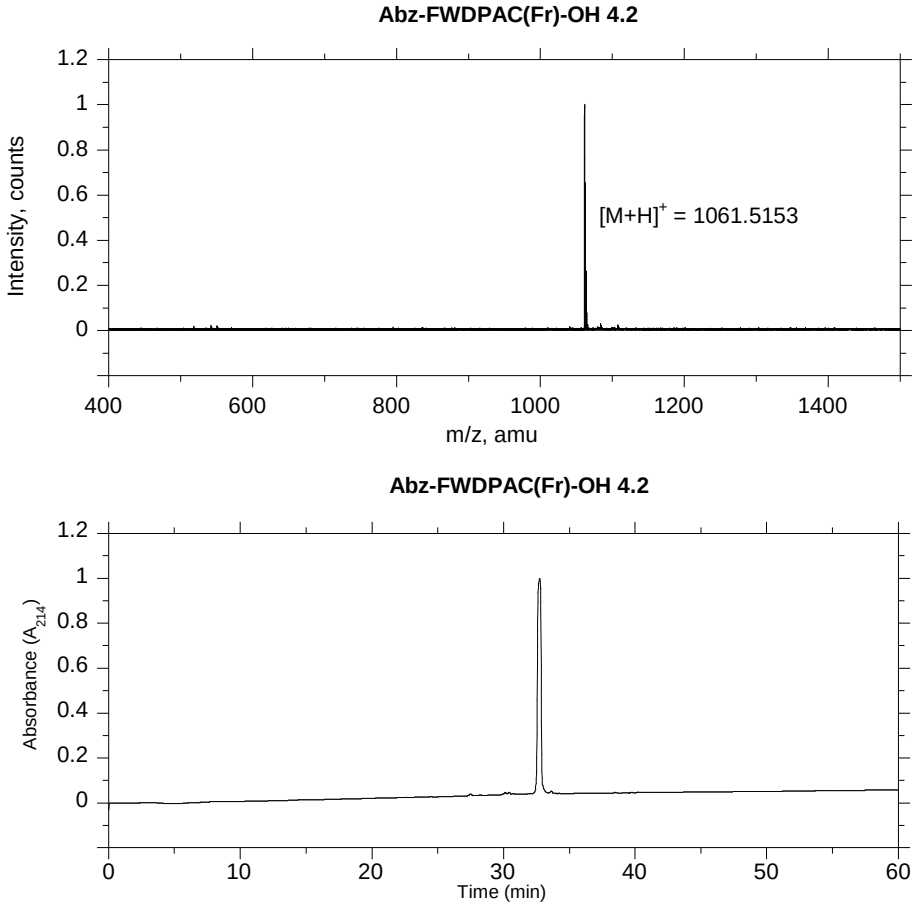

Figure 4.9. Mass spectrum and analytical RP-HPLC chromatogram for peptide **4.2**. Linear gradient 0-100% CH_3CN (0.1%TFA) in 30 min, detected at 214 nm.

4.5.4 Characterization of Abz-MQPSTATAAPK(Dnp)EKTSSEKKDN-YIIKGVFWDPAC-OMe (4.9)

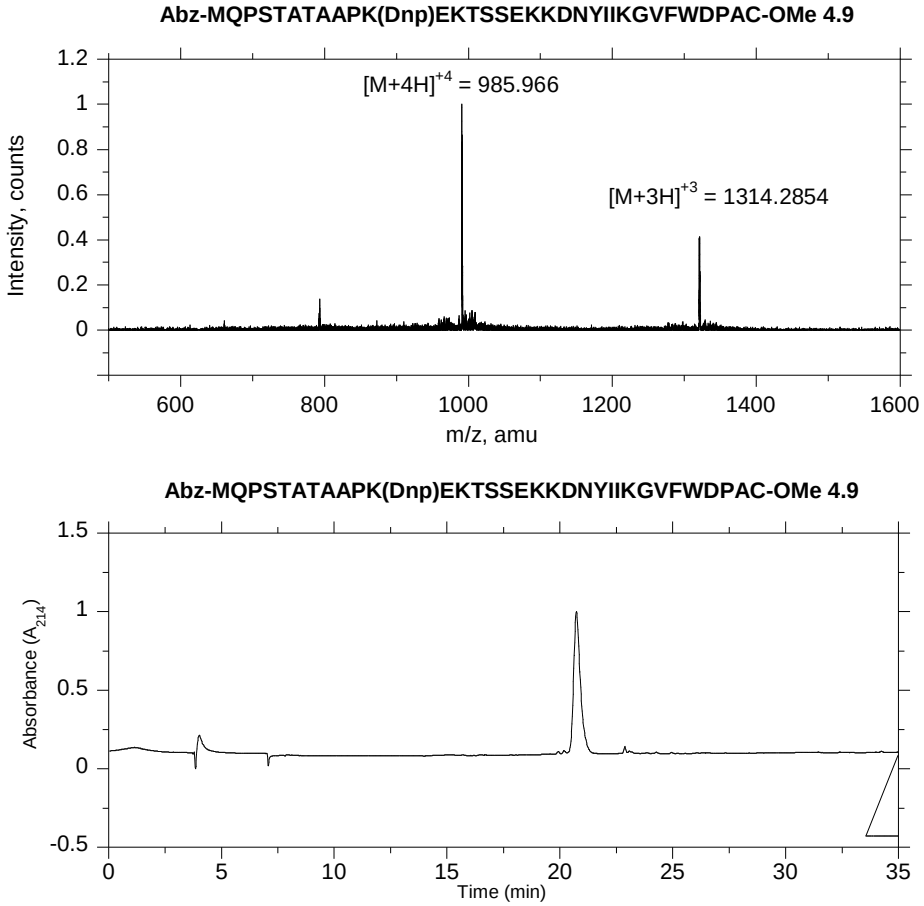

Figure 4.10. Mass spectrum and analytical RP-HPLC chromatogram for peptide **4.9**. Linear gradient 0-100% CH_3CN (0.1%TFA) in 30 min then 100% CH_3CN (0.1%TFA) for 5 min, detected at 214 nm.

4.5.5 Characterization of Abz-MQPSTATAAPK(Dnp)EKTSSEKKDN-YIIKGVFWDPAC(Fr)-OMe (4.6)

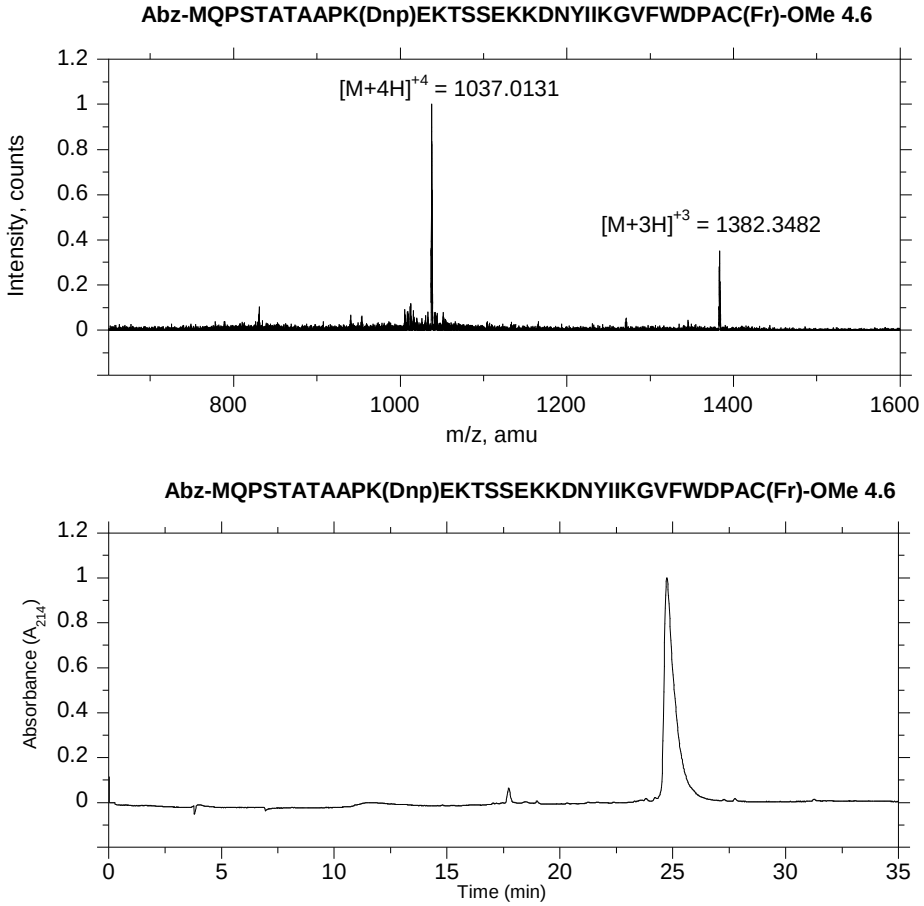

Figure 4.11. Mass spectrum and analytical RP-HPLC chromatogram for peptide **4.6**. Linear gradient 0-100% CH_3CN (0.1%TFA) in 30 min then 100% CH_3CN (0.1%TFA) for 5 min, detected at 214 nm.

4.5.6 Characterization of MQPSTATAAPK(Dnp)EKTSSEKKDN-YIIKGVFWDPAC(Fr)-OMe (4.5)

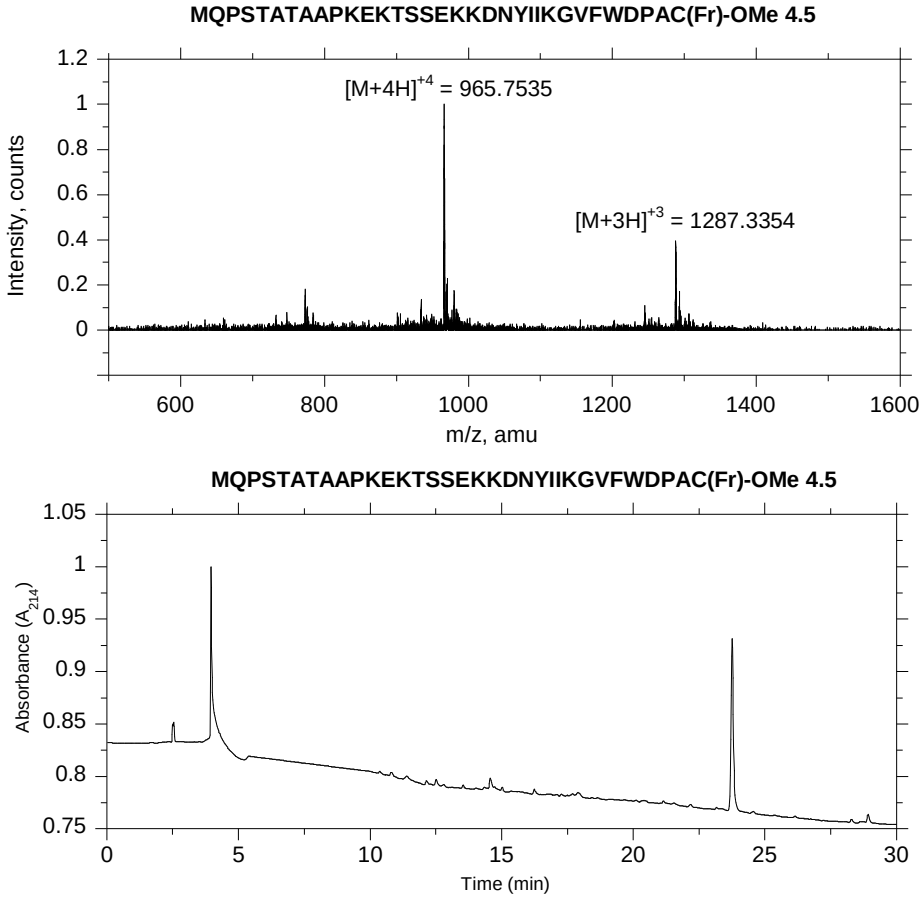

Figure 4.12. Mass spectrum and analytical RP-HPLC chromatogram for peptide **4.5**. Linear gradient 0-100% CH_3CN (0.1%TFA) in 30 min, detected at 214 nm.

4.5.7 Characterization of AAPK(Dnp)EKTSSEKKDNYIIKGVFWDPAC(Fr)-OMe (4.7)

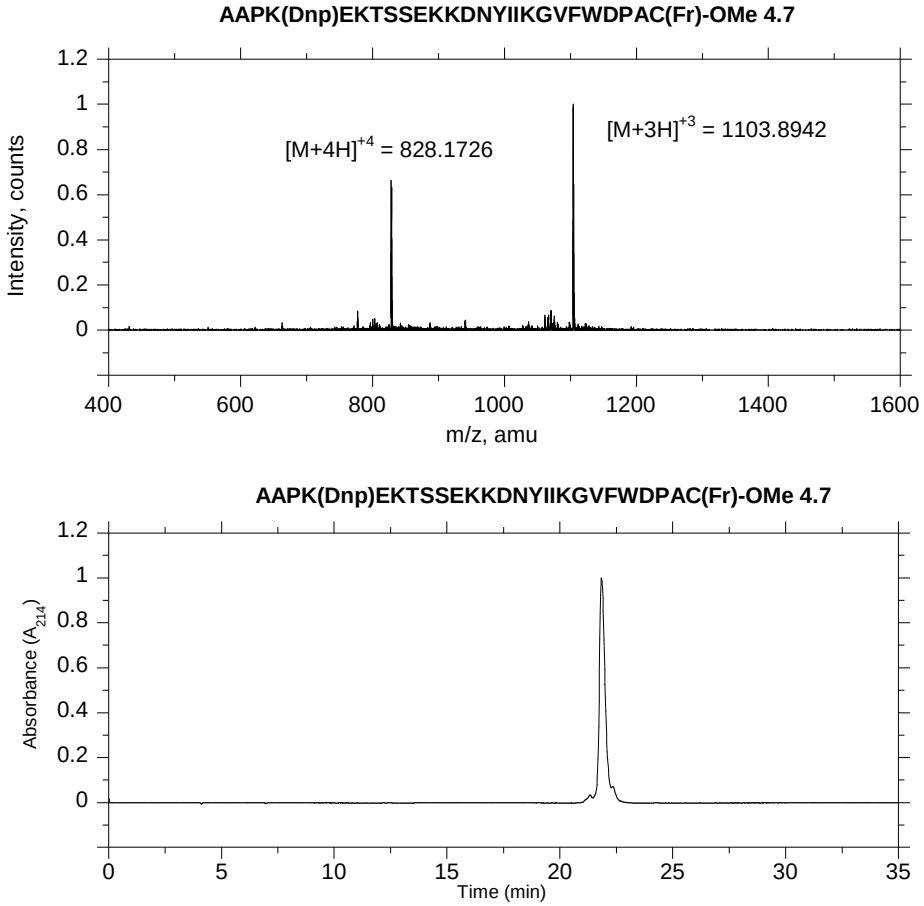

Figure 4.13. Mass spectrum and analytical RP-HPLC chromatogram for peptide **4.7**. Linear gradient 0-100% CH_3CN (0.1%TFA) in 30 min then 100% CH_3CN (0.1%TFA) for 5 min, detected at 214 nm.

4.5.8 Characterization of Abz-MQPSTAT-OH (4.8)

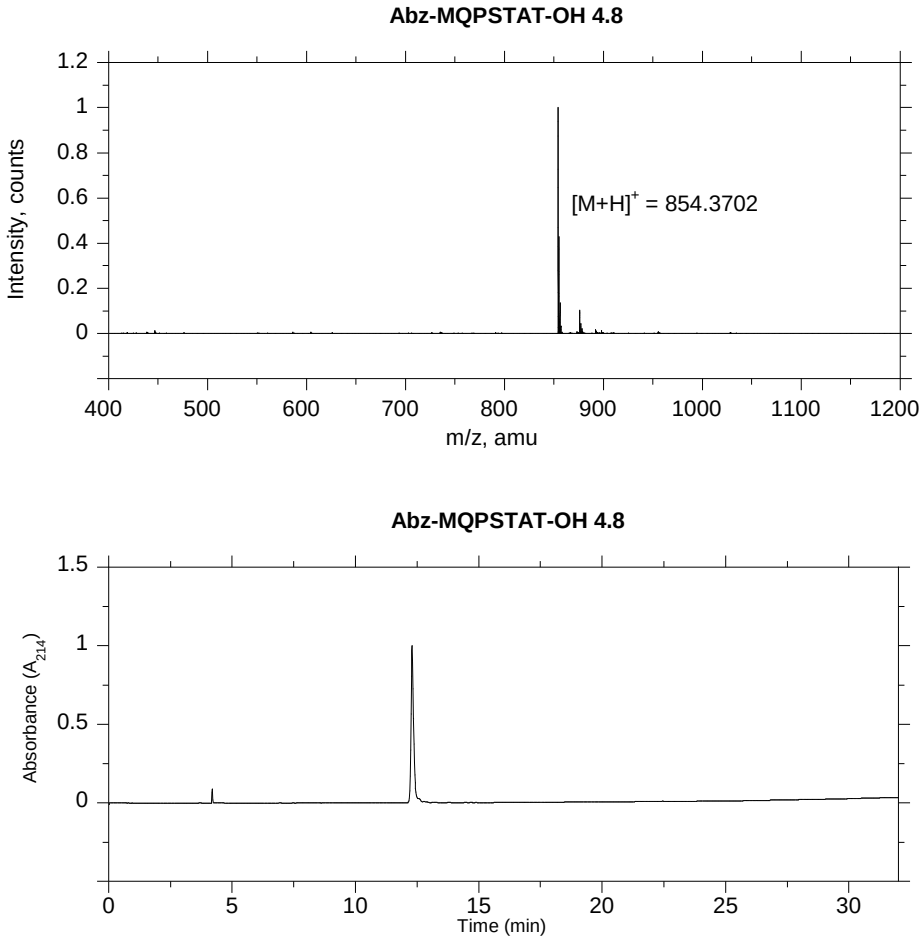

Figure 4.14. Mass spectrum and analytical RP-HPLC chromatogram for peptide **4.8**. Linear gradient 0-100% CH_3CN (0.1%TFA) in 30 min then 100% CH_3CN (0.1%TFA) for 5 min, detected at 214 nm.

Chapter 5: Synthesis and Evaluation of FPP and GGPP Analogues that Incorporate Photoactive Diazirines

5.1 Introduction

Farnesyl diphosphate (**5.1**, FPP, figure 5.1) is an important biological compound that is found in all living organisms. The biosynthesis of farnesyl diphosphate is a well-established metabolic pathway that begins with two 5-carbon isoprene units that cascade, via electrophilic addition followed by elimination, into isoprenoids of varying length.[196] FPP plays a central role as a precursor in the metabolism of an array of essential compounds found in nature. Examples include biopolymers like latex or dolichol,[197,198] sesquiterpene natural products,[199] and side chains to cofactors.[200] Protein prenylation is a post-translational modification that also uses FPP, and the longer isoprenoid geranylgeranyl diphosphate (GGPP), as the lipid donors.[20] Since the discovery that prenylation of mutant Ras proteins is required for transformation,[201] the prenyltransferase enzymes have been a target for anti-cancer drugs.[5,202,203] Given the plethora of important products and the impact that enzymes who use FPP as a substrate have in disease proliferation and prevention,[101] development of chemical tools to study these enzymes is an important area of inquiry. One class of FPP analogue that has had considerable use in this pursuit exploits the technique known as photoaffinity labeling.

Photoaffinity labeling is a technique used to identify noncovalent interactions between molecules, including protein-protein and protein-ligand complexes. Several photoaffinity analogues of isoprenoid diphosphates have been developed to study the enzymes that synthesize FPP, as well as the prenyltransferases that employ FPP as a

substrate. These studies used the photoactive moieties diazotrifluoropropionate,[181-183,186,204-211] or benzophenone,[76,77,168,169,212-215] incorporated into the isoprenoid chain to act as a substitute for FPP. While successful in their intended application, each of the analogues has limitations. DATFP-containing analogues, although good structural mimics of FPP, require prolonged short wavelength UV irradiation for photoactivation and their synthesis is complicated by the need to use phosgene gas and trifluorodiazoethane. Benzophenone-containing analogues are attractive because they are relatively stable and activated by long wavelength UV irradiation; however, enzyme binding efficiency is reduced by their longer and bulkier shape compared to FPP. The benzophenone photophore must also adopt a coplanar arrangement for efficient light absorption, which can be restricted when bound, and produce a diradical upon photolysis that only reacts with a limited group of amino acid side chains. Compounds that utilize the diazirine as the photoactive group proved to be an attractive alternative for several reasons. Diazirines are simple to prepare from ketone precursors, their structure closely approximates the size and shape of an isoprene unit, and when activated by long wavelength UV radiation they produce a carbene intermediate that reacts with a wide range of amino acid side chains. Additionally, work from the Distefano and Hrycyna labs showed that a prenylated **a**-factor peptide, incorporating a diazirine-containing isoprenoid, had increased binding and crosslinking efficiency over a benzophenone variant with the isoprenylcysteine recognition-dependent enzyme, Ste14p.[154,155]

While wild type allylic diphosphate analogues of FPP have been successful substrates, several photoaffinity analogues have been developed that contain

phosphonates.[216-218] The advantage of incorporating a phosphonophosphate to mimic the allyilc diphosphate is that the phosphonophosphate moiety is more stable under acid conditions, affording a longer half-life *in vivo*.[185] The phosphonate linkage is unable to be cleaved by enzymes that use FPP as a substrate. Thus their incorporation produces analogues that act as inhibitors, which may afford increased labeling efficiency or identification of unknown binding partners. Work by Zhao et al. extended the utility of photocrosslinking phosphonophosphate analogues by adding an azide functionality to the phosphate end, allowing for the biorthogonal click reaction with functionalized alkynes to detect or enrich crosslinked product. Upon irradiation of the bifunctional phosphonophosphate analogue in the presence of crude extract from *S. cerevisae* a number of labeled proteins were observed after a pull-down with a click installed biotin handle. Such an approach has pronounced potential for proteomic applications.

Herein, we describe the synthesis of the diazirine functionalized farnesyl diphosphate analogue **5.2** (Figure 5.1) and phosphonophosphate analogues (**5.7** & **5.9**) (Figure 5.2), as well as GGPP phosphonophosphate analogues (**5.8** & **5.10**) (Figure 5.2). Kinetics of compound **5.2** were studied using yeast and mammalian protein farnesyltransferase validating the new FPP analogue as an alternative substrate. Inhibition kinetics with analogues **5.7** and **5.8**, were also determined with yeast PFTase, and will serve as a baseline for saturation conditions in labeling studies to follow. Crosslinking experiments with PFtase and resulting identification of the beta subunit demonstrated the ability of photoaffinity labeling compounds **5.9** and **5.10** to selectively label isoprenoid binding sights. In addition, photolysis experiments with SmgGDS splice variant proteins,

SmgGDS-607 and SmgGDS-558, that promote prenylation and trafficking of GTPases,[219] validated the capability of compounds **5.9** and **5.10** at identifying proteins that recognize but don't utilize isoprenoid diphosphates as substrates.

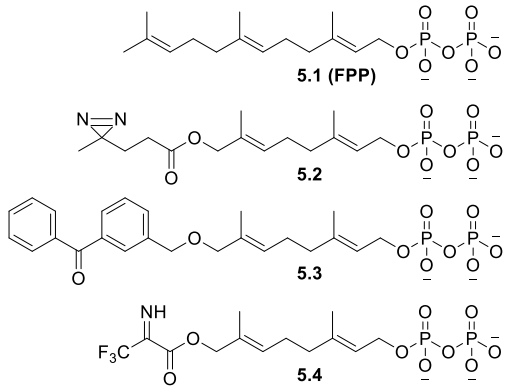

Figure 5.1. Photoactivatable isoprenoid diphosphate analogues: FPP **5.1**, Diazirine **5.2**, Benzophenone **5.3**, DATFP **5.4**.

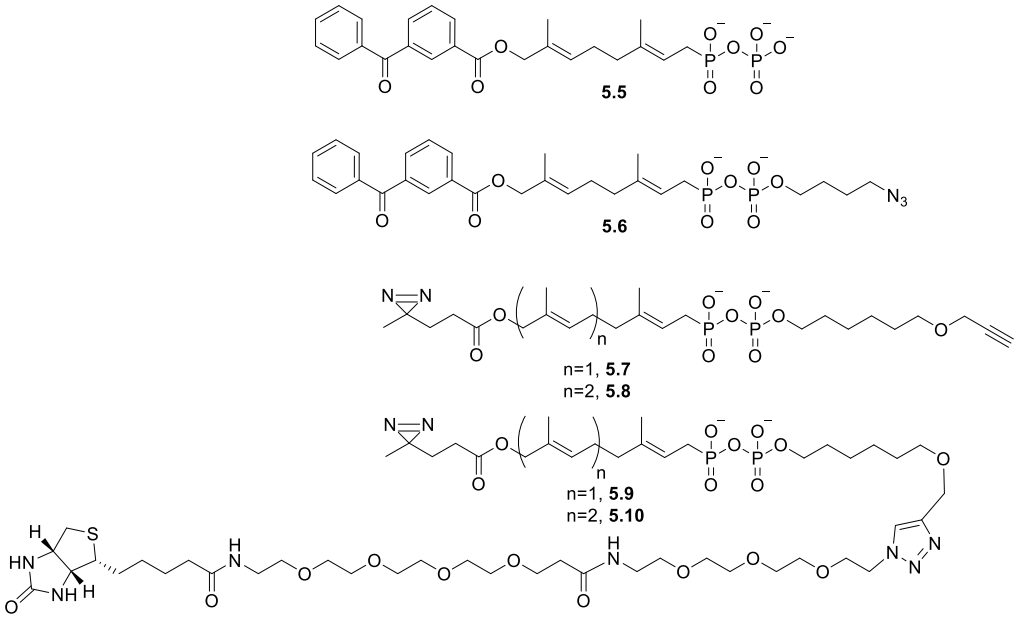

Figure 5.2. Photoactivatable isoprenoid phosphonophosphate analogues: Benzophenone-phosphonate **5.5**, Benzophenone-phosphonophosphate -azide **5.6**, Diazirine-phosphonophosphate -alkyne **5.7** & **5.8**, Diazirine- phosphonophosphate-click-biotin **5.9** & **5.10**.

5.2 Results and Discussion

5.2.1 Design and synthesis of diazirine containing isoprenoid diphosphate. To design a more efficient FPP analogue for photoaffinity labeling studies, the diazirine motif was selected due to its similarity in size to an isoprene unit. Comparison of **5.2** with benzophenone- and DATFP-containing FPP analogs (**5.3** and **5.4**) reveals that **5.2** is closest in size to FPP (Figure 5.1). Although crystal structure studies have shown that ether linkages are the most structurally similar to farnesyl diphosphate, **5.3**,[168] an ester linkage was chosen for ease of synthesis. **5.2** was prepared based on the previously published route to compound **5.18**[155] that utilized a convergent strategy of established compounds **5.16**[215] and **5.13**.[188] Conversion of the free alcohol, **5.18**, to the corresponding bromide was performed by reaction with PBr3. Without subsequent purification, the bromide was then converted to the diphosphate, **5.19**, by displacement with TTBHPP. The final product was obtained by ionic exchange to the NH_4^+ salt and purified by HPLC.

Scheme 5.1. Synthesis of Diazirine-containing FPP analogue

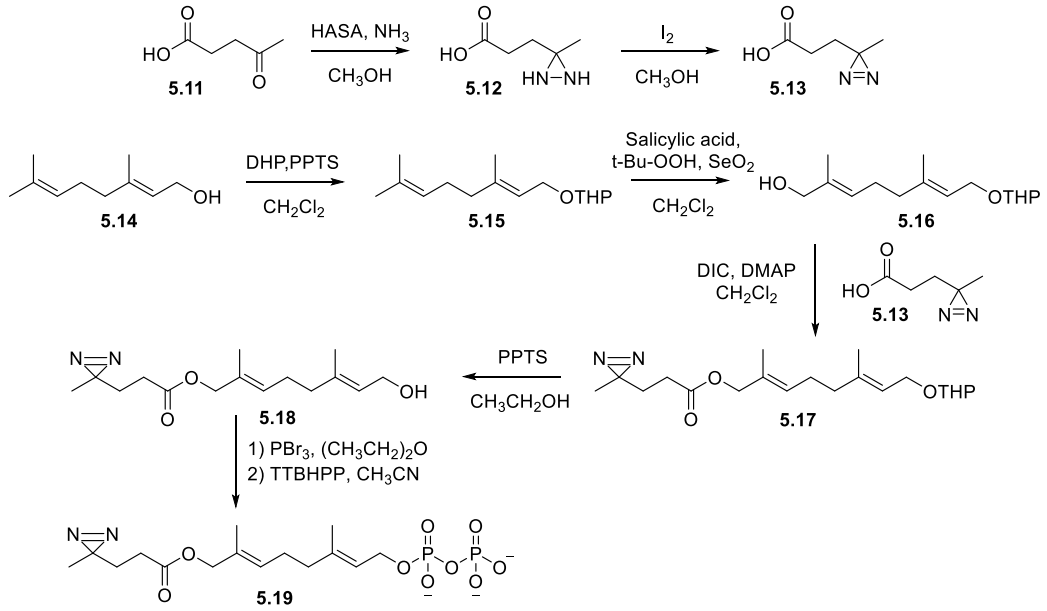

5.2.2 Diazirine analogue is a substrate for PFTase. Initially, a continuous fluorescence assay was used to assess the potential of the new photoaffinity analogue **5.2** as an alternative substrate for yeast protein farnesyltransferase (yPFTase).[220] Incubation of the substrate peptide *N*-dansyl-GCVIA with FPP and yPFTase resulted in a rapid increase in the dansyl fluorescence (Figure 5.3) due to the increase in hydrophobicity upon prenylation **5.20** (Figure 5.4). When analogue **5.2** replaced FPP in the assay, a similar time-dependent increase in fluorescence resulted (Figure 5.3), indicating that the analogue acted as a substrate for yPFTase. Although both assays were performed at the same substrate and enzyme concentrations, the maximum fluorescence differs between the two prenylated products **5.20** and **5.21** due to their differing hydrophobicity. More importantly, the fluorescence increased 12 times slower with **5.2** than FPP, and required a longer reaction time for the complete conversion of the peptide substrate (Figure 5.3). Additionally, the formation of product **5.21**, was verified by large scale enzymatic prenylation followed by MS detection. The prenylated peptide was purified by step chromatography on a Sep Pak cartridge, and high resolution electrospray ionization mass spectrometry (HR-ESI-MS) detected the presence of the prenylated peptide $[C_{46}H_{69}N_8O_{12}S_2]^+$ at 957.4345 m/z, which corresponded closely to the calculated mass of 957.4573 m/z for **5.21**. Having determined that compound **5.2** acts as an alternative substrate for yPFTase, reaction kinetics with the mammalian homologue were pursued.

Scheme 5.2. yPFTase prenylation of substrate peptide *N*-dansyl-GCVIA

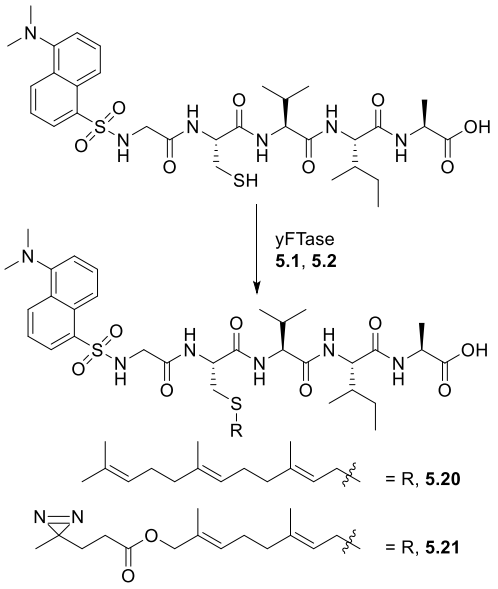

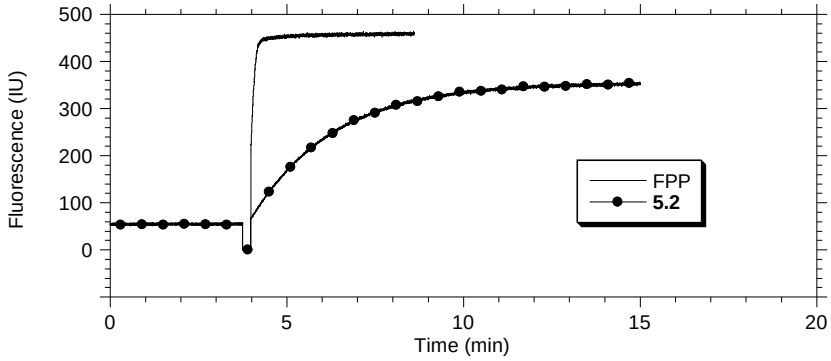

Figure 5.3. Evaluation of diazirine **5.2** as an alternative substrate *S. cerevisiae* protein farnesyltransferase (yPFTase). *N*-dansyl-GCVIA (2.0 μM), yPFTase (70 nM) and FPP (solid line) or **5.2** (●) (10 μM) were used with excitation at 340nm and detection at 504nm.

The kinetic parameters for **5.2** with mammalian PFtase, obtained from the rat (rPFTase), were calculated using the continuous fluorescence assay developed to study human PFTase by Pompliano *et al.*[221]. 50 nM of rPFTase was incubated with N-dansyl GCVLS (2.0 μM) and varying concentrations of **5.2**. The fluorescence assay was

performed in triplicate and the initial velocity was calculated using Microsoft Excel (Figure 5.4). Kinetic values were determined by fitting data to the Kinetic values obtained: V_{max} (1.159 nM/s), K_M (0.254 μM), and K_{cat} (0.0272 s^{-1}). The K_M value is approximately 2-fold higher than that of farnesyl diphosphate. This is likely due to the structure of the diazirine group; although **5.2** is more similar to FPP than previous photoaffinity analogues (**5.3** and **5.4**), it still does not perfectly superimpose the natural substrate. Moreover, pervious kinetics studies with mammalian PFTase using DATFP- and benzophenone-containing FPP substrates failed to produce detectable product formation at the concentration used in the fluorescence assay, requiring large scale prenylation reactions coupled with HPLC detection to quantify prenylated product.[182,207] Given that product formation with compound **5.2** was detectable at the assay concentration, suggests that the smaller diazirine moiety is a superior mimic of an isoprene unit.

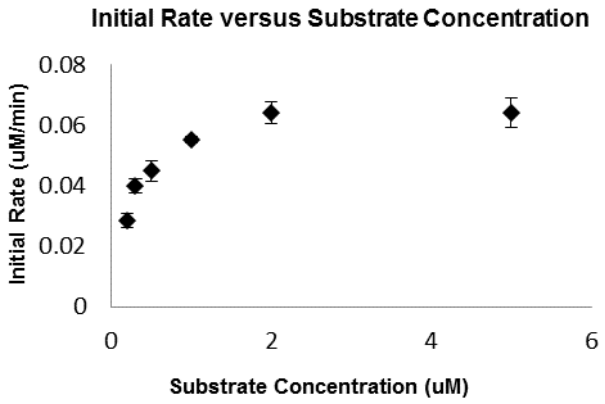

Figure 5.4. Initial reaction rate of rPFTase with **5.2**. rPFTase (50 nM) was incubated with N-dansyl GCVLS (2.0 μM) and varying concentrations of **5.2.** Kinetic values were determined by fitting data to the Michaelis-Menten equation.

5.2.3 Design and synthesis of phosphonophosphate analogues. Having confirmed the ability of the diazirine analogue **5.2** to act as an alternative substrate for FPP with yeast and mammalian PFTases, phosphonate analogues were pursued for their application in protein identification experiments. Pervious phosphonophosphate analogues, **5.5** and **5.6** (Figure 5.2), displayed a substantial increase in stability to acidic hydrolysis, while maintaining the ability to be recognized and photolabel PFTase.[185] Due to the replacement of the phosphoester bond with a phosphonate at the C-1 position, proteins are unable to hydrolyze the C-P bond producing analogues that act as inhibitor, allowing for isoprenoid interacting partners to be identified as reported with **5.6**.[75] With these favorable attributes in mind, phosphonophosphate analogues **5.7** and **5.8** were designed. Similar to **5.6**, compounds **5.7** and **5.8** are envisioned as bifunctional FPP and GGPP derivatives that incorporate the diazirine motif in the isoprenoid structure, and an alkyne functionality across the phosphonophosphate bond.

Synthesis of analogue **5.7** was based on previously published routes for the production of the isoprenoid building block **5.28**[185] and the diazirine derivative **5.13** (Scheme 5.3).[222] Coupling of **5.28** and **5.13** in the presence of DIC and DMAP afforded the ester (**5.30**). Treatment with $(CH_3)_3SiCH_2CHCH_2$ and$(CH_3)_3SiBr$ resulted in clean deprotection of the phosphonate esters to produce **5.32.** Activation with CID followed by addition of phosphate **5.23** produced the coupled phosphonophosphate **5.7**. Purification of **5.7** was performed using RP-HPLC yielding a white powder upon lyophilization. Synthesis of the longer version, **5.8**, followed the same synthetic steps as **5.7**, but began with farnesyl bromide **5.26** in place of geranyl bromide **5.25**. A copper-catalyzed click

reaction with azide **5.35** converted **5.7** and **5.8** into the biotinylated compounds **5.9** and **5.10**, respectively, which isolated by RP-HPLC.

Scheme 5.3. Synthesis of phosphonophosphate analogues

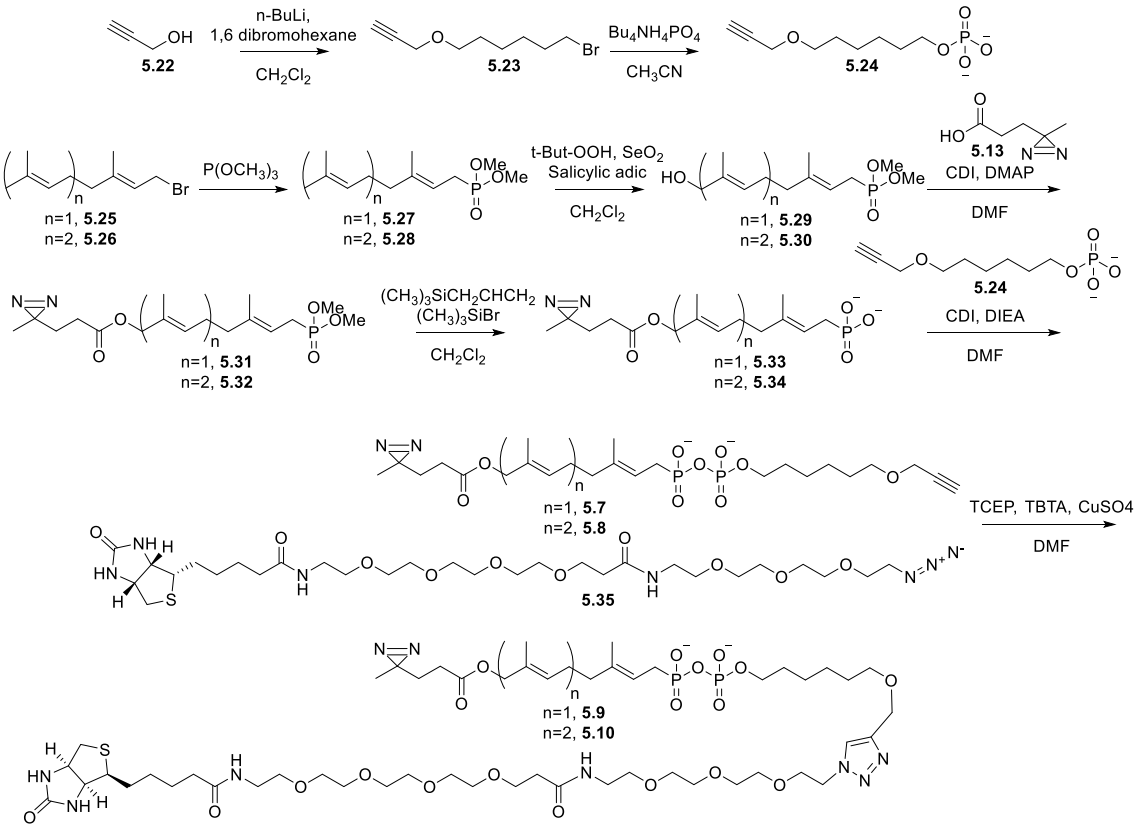

5.2.4 Phosphonophosphate analogues are inhibitors of PFTase. Given the inherent stability of the C−P bond at position C-1, phosphonophosphate **5.7** and **5.8** was tested as a competitive inhibitor of yPFTase. The rate of yPFTase-catalyzed farnesylation of *N*-dansyl-GCVIA was measured in the presence of a fixed concentration of FPP and varying concentrations of **5.7** and **5.8**. An IC_{50} value of 16.99 μM was calculated for **5.7**, and 13.67 μM for **5.8** (Figure 5.3). Comparison with the previously reported

benzophenone-containing phosphonate FPP analogue **5.5**, the bifunctional analogues showed a reduction in the inhibition yPFTase activity **(**Table 5.1). Given the improvement of diazirine-containing diphosphate analogue **5.2** to act as an alternative yPFTase substrate over the benzophonone-containing analogue **5.3**, the decrease in the inhibitor potency for **5.7** and **5.8** must be related to the addition of the alkyne functionality to their phosphate end.

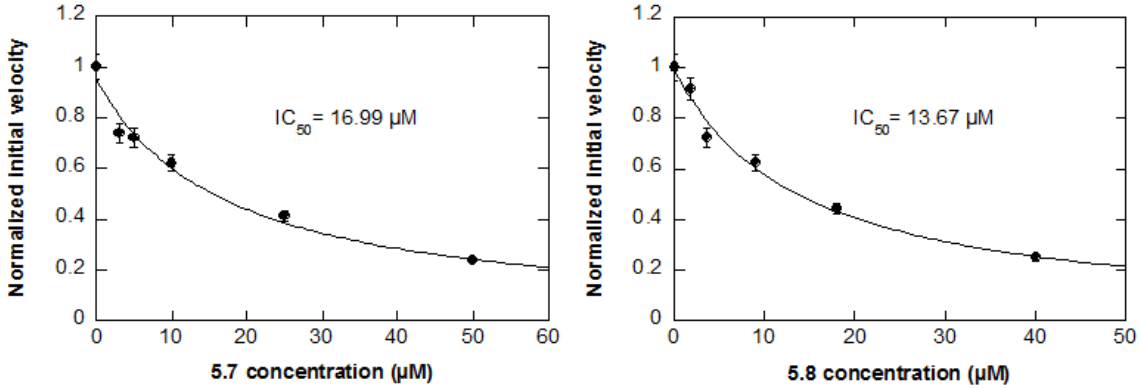

Figure 5.5. Inhibition of yPFTase activity by compounds **5.7** (left) and **5.8**. Inhibition was evaluated using a fluorescence based assay using *N*-dansyl-GCVIA (2.4 μM), FPP (5.0μM), yPFTase (2.0μM) and varying concentrations of compound **5.7** and **5.8**. IC_{50} values were calculated from a plot of the enzymatic rate versus concentration.

Table 5.1. Values for inhibition of yPFTase by diazirine- and benzophenone-based phosphonate isoprenoid diphosphate analogues.

Compound	IC_{50} (μM)
5.7	16.99
5.8	13.67
5.5[185]	0.96

5.2.5 Photolabeling of SmgGDS-607, SmgGDS-558, and rPFTase. The ability of phosphonophosphate **5.9** and **5.10** to crosslink isoprenoid binding proteins was assessed by photoaffinity labeling studies (figure 5.4). Recombinant SmgGDS-607 and SmgGDS-

558 (10 µg) was incubated with compound **5.9** or **5.10** (10 µg) for 10 mins, and then irradiated with UV light (365 nm) for 30 min at a distance of 3 cm. Additionally, rPFtase was also treated with the same conditions and quantities to serve as a positive control. Crosslinked material was isolated with streptavidin beads, precipitated, and resolved by SDS-Page. The identification of the labeled proteins was determined by immunoblotting with antibodies to SmgGDS and the beta-subunit of rPFtase.

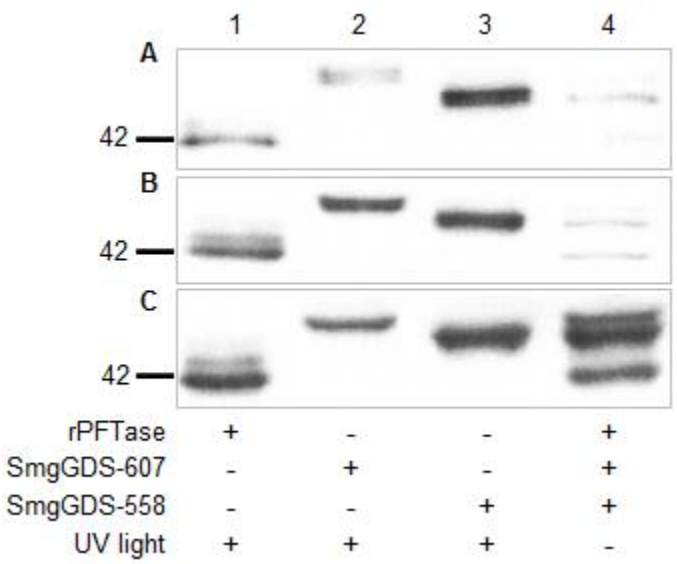

Figure 5.6. Analysis of crosslinking reactions containing rPFtase, SmgGDS-607, SmgGDS-558, and compounds **5.9** and **5.10**. (A) analogue **5.9**; (B) analogue **5.10**; (C) total protein. For this experiment, rPFTase, SmgGDS-607, and SmgGDS-558 (10 µg) was incubated with compound **5.9** or **5.10** (10 µg) for 10 mins, and then irradiated with UV light (365 nm) for 30 min in a cold room. Crosslinked material was isolated with streptavidin beads, precipitated, and resolved by SDS-Page. The resulting gel was transferred to a nitrocellulose membrane and visualized using antibodies to SmgGDS and the alpha-subunit of rPFtase.

Following SDS-PAGE resolution, immunoblot analysis with the respective protein antibody demonstrated that each protein was present in the specified lane, and at the expected molecular weight; beta-subunit of yPFtase near 42 kDa, SmgGDS proteins

near 65 kDa (Figure 5.4C). Pull down of each protein with streptavidin beads was dependent upon UV exposure (Figure 5.4, lane 4). Detection of only the beta-subunit of rPFtase suggest that **5.9** and **5.10** are crosslinking the substrate binding site (Figure 5.4, lane 1). Successful labeling and enrichment of the prenylated GTPases recognizing protein, SmgGDS-558, highlighted the ability of the phosphonophosphate analogues to identify non-prenyltransferase isoprenoid binding partners (Figure 5.4, lane 3). Given that SmgGDS-607 is thought to recognize nonprenylated GTPases, it is surprising that both **5.9** and **5.10** displayed the capability to crosslink SmgGDS-607 (Figure 5.4, lane 2). Comparing the intensity of the SmgGDS-607 band in lane 2, it is clear that **5.10** labeled more efficiently, suggesting that SmgGDS-607 has a greater capability to bind GGPP over FPP. The enhancement in GGPP recognition corralets with the finding that SmgGDS-607 forms more stable complexes with nonprenylated GTPases that will become geranylgeranylated than with nonprenylated GTPases that will become farnesylated.[219]

5.3 Conclusion

Herein, we have described the development and application of isoprenoid diphosphate analogues containing a photoexcitable diazirine moiety and phosphate or phosphonate linkages. The diphosphate analogue of FPP was synthesized in seven steps and was shown an alternative substrate for both yeast and mammalian PFTase enzymes. The phosphonophosphate analogues of FPP and GGPP were prepared over nine steps and are competitive inhibitors of PFTase with K_I's in the low micromolar range. Photolysis of yPFTase in the presence the phosphonophosphate analogues resulted in preferential

labeling of the β subunit, suggesting that the analogues interact with isoprenoid recognition site. Additionally, the phosphonophosphate analogues successfully labeled SmgGDS proteins, demonstrating their ability to identify isoprenoid binding partners other than enzymes that use isoprenoid diphosphates as substrates. These analogues should be valuable tool in identifying binding sights of know isoprenoid interacting proteins, and aid in the discovery of unknown isoprenoid binding proteins.

5.4 Materials and Methods

5.4.1 General. All solvents and reagents used for the synthesis of the diazirine isoprenoid analogues were of analytical grade and purchased from Sigma-Aldrich (St.Louis, MO). NHS-PEG_4-Biotin was obtained from Thermo Scientific. Flash chromatography was performed with silica gel (60-120 mesh) was obtained from E. M. Science. Preparative HPLC separations were performed with a Rainin Dynamax Microsorb C_{18} column (2.14 × 25 cm) while analytical separations employed a Varian c18 resin (Microsorb-MW 5 μm, 4.6 × 250 mm). ^{1}H NMR spectra were obtained at 300 or 500 MHz and ^{31}P NMR spectra were obtained at 121 MHz.'. HR-ESI-MS analysis was performed using a Bio-TOF-II (Bruker) mass spectrometer. Concentrations of FPP and the varius analogues were determined by phosphate analysis as described by Reed and Rilling employing KH_2PO_4 as a standard.[223] OD_{600} of cells was taken with a DU 720 UV/vis spectrophotometer (Beckman Coulter). Protein concentration was determined using a standard Bradford assay with a DTX 880 Multimode Detector plate reader (Beckman Coulter)

5.4.2 Synthesis of compound 5.12: 3-(3-methyldiaziridin-3-yl)propanoic acid. Levulinic acid **5.11** (1.61 g, 13.8 mmol, 1 eq) was dissolved in 7 N NH_3 in CH_3OH (13.5 mL, 91.0 mmol, 7 eq). The resulting solution was stirred under N_2 on ice for 3 h. A solution of hydrolxylamine-O-sulfonic acid (1.80 g, 15.9 mmol, 1.2 eq) in CH_3OH (12 mL) was added dropwise at a rate of 1 s^{-1}. The reaction mixture was stirred for 20 h and allowed to warm to rt. N_2 was bubbled through the solution for 1 h to remove NH_3 gas. Vacuum filtration and concentration resulted in a yellow oil that was used in the next step without purification.

5.4.3 Synthesis of compound 5.13 : 3-(3-methyl-3H-diazirin-3-yl)propanoic acid. The diaziridine **5.12** was redissolved in CH_3OH (10 mL) and stirred on ice for 5 min in a tin foil covered flask. Triethylamine (3.00 mL, 21.5 mmol) was added and allowed to stir for 5 min. Slowly, chips of I_2 were added until the solution remained a brown-red color for longer than 5 min after the last addition. The reaction solution was diluted with EtOAc, washed with 1 M HCl, and with aqueous 10% sodium thiosulfate until the organic layer was colorless. The aqueous layer was further extracted with EtOAc (2x 20 ml). The organic layers were combined, dried over $MgSO_4$, and concentrated to afford the diazirine acid **5** as a brown residue (0.785 g, 45%). ^1H NMR (300 MHz, $CDCl_3$) δ: 1.05 (s, 3H), 1.73 (t, 2H, J = 6.8 Hz), 2.23 (t, 2H, J = 6.8 Hz). HR-ESI-MS; calcd for $C_5H_8N_2O_2$ $[M-H]^-$: 127.0513, found 126.0493.

5.4.4 Synthesis of compound 5.15: (E)-2-((3,7-dimethylocta-2,6-dien-1-yl)oxy)tetrahydro-2H-pyran. This compound was prepared via a modification of a previously described procedure.[76] To a solution of geraniol **5.14** (3.11 g, 20.2 mmol, 1 eq) in CH_2Cl_2 (3.5 mL) were added DHP (2.54 g, 30.3 mmol, 1.5 eq) and PPTS (0.502 g, 2.0 mmol. 0.1 eq), and the resulting solution was stirred overnight at rt. The reaction mixture was quenched with saturated aqueous $NaHCO_3$ and extracted with CH_2Cl_2. The organic layer was dried over $MgSO_4$ and concentrated to afford **8** as a clear oil (4.79 g, 99%). ^{1}H NMR (300 MHz, $CDCl_3$) δ 1.58 (s, 3H), 1.65 (s, 6H), 1.48 – 1.85 (m, 6H), 2.04 – 2.22 (m, 4H), 3.47 – 3.54 (m, 1H), 3.85 – 3.92 (m, 1H), 3.98 – 4.05 (dd, 1H, J = 7.2, 12 Hz), 4.21 – 4.27 (dd, 1H, J = 6.3, 12 Hz), 4.62 (t, 1H, J = 2.7 Hz), 5.16 (t, 1H, J = 6.3 Hz), 5.39 (t, 1H, J = 6.2 Hz). HR-ESI-MS; calcd for $C_{15}H_{26}O_2$ $[M+H]^+$: 239.1919, found 239.1932

5.4.5 Synthesis of compound 5.16: (2E,6E)-2,6-dimethyl-8-((tetrahydro-2H-pyran-2-yl)oxy)octa-2,6-dien-1-ol. This compound was prepared via a modification of a previously described procedure.[76] The protected geraniol **5.15** was dissolved in CH_2Cl_2 (28 mL). In turn, 70% *t*-Bu-OOH in H_2O (8.5 mL, 60.9 mmol, 3eq), salicylic acid (0.279 g, 2.02 mmol, 0.1 eq), and SeO_2 (0.205 g, 2.03 mmol, 0.1eq) were added, and the resulting solution was stirred overnight at rt. The reaction mixture was quenched with saturated aqueous $NaHCO_3$, extracted with CH_2Cl_2, and dried over $MgSO_4$. After concentration, the residue was purified by flash chromatography (Hexanes: Et_2O, 3:2, v/v) on silica gel to obtain 2.36 g (46%) of alcohol **9** as a clear oil. ^{1}H NMR (300 MHz,

$CDCl_3$) δ 1.65 (s, 6H), 1.48 – 1.85 (m, 6H), 2.04 – 2.22 (m, 4H), 3.47 – 3.54 (m, 1H), 3.85 – 3.92 (m, 1H), 3.91 (s, 2H), 3.98 – 4.05 (dd, 1H, J = 7.2, 12 Hz), 4.21 – 4.27 (dd, 1H, J = 6.3, 12 Hz), 4.62 (t, 1H, J = 2.7 Hz), 5.16 (t, 1H, J = 6.3 Hz), 5.39 (t, 1H, J = 6.2 Hz). HR-ESI-MS; calcd for $C_{15}H_{26}O_3Na$ $[M+Na]^{+1}$: 277.1790, found 277.1763

5.4.6 Synthesis of compound 5.17: (2E,6E)-2,6-dimethyl-8-((tetrahydro-2H-pyran-2-yl)oxy)octa-2,6-dien-1-yl3-(3-methyl-3H-diazirin-3-yl)propanoate. This compound was prepared via a modification of a previously described procedure.[155] To a solution of protected alcohol **5.16** (1.94 g, 7.60 mmol,1 eq) and DMAP (92.8 mg, 0.76 mmol, 0.1 eq) in CH_2Cl_2 (7 mL) was added a solution of the diazirine acid **5.13** (0.97 g, 7.60 mmol, 1 eq) in CH_2Cl_2 (10 mL). DIC (0.959 g, 7.6 mmol0, 1eq) was added and the resulting solution was stirred at rt for 16 hours. The reaction mixture was filtered and concentrated. Purification by flash chromatography (hexanes: EtOAc, 5:1) afforded 1.07 g (57%) of diazirine **5.17** as a clear oil. ^{1}H NMR (300 MHz, $CDCl_3$) δ: 1.03 (s, 3H), 1.48 – 1.85 (m, 14H), 2.04 – 2.22 (m, 6H), 3.47 – 3.54 (m, 1H), 3.85 – 3.92 (m, 1H), 3.98 – 4.05 (dd, 1H, J = 7.2, 12 Hz), 4.21 – 4.27 (dd, 1H, J = 6.3, 12 Hz), 4.46 (s, 2H), 4.62 (t, 1H, J = 2.7 Hz), 5.36 (t, 1H, J = 6.3 Hz), 5.44 (t, 1H, J = 6.2 Hz); HR-ESI-MS: calcd for $C_{20}H_{32}N_2O_4Na$ $[M+Na]^+$: 387.2260, found 387.2234.

5.4.7 Synthesis of compound 5.18: (2E,6E)-8-hydroxy-2,6-dimethylocta-2,6-dien-1-yl 3-(3-methyl-3H-diazirin-3-yl)propanoate. This compound was prepared via a modification of a previously described procedure.[155] To a solution of **5.17** (99 mg, 0.271

mmol, 1 eq) in EtOH (1.60 mL) was added PPTS (6.81 mg, 271 µmol, 0.1 eq). The reaction flask was fitted with a septum and stirred at 60 °C for 4 h. The reaction mixture was concentrated *in vacuo* and purified by flash chromatography (hexanes: EtOAc, 2:1) to afford 75 mg (99%) of diazirine alcohol **5.18** as a clear oil. ^{1}H NMR (300 MHz, $CDCl_3$) δ: 1.03 (s, 3H), 1.58 – 1.75 (m, 8H), 2.05 – 2.22 (m, 6H), 4.15 (t, 2H, J = 6.0 Hz), 4.47 (s, 2H), 5.38 – 5.45 (m, 2H). HR-ESI-MS: calcd for $C_{15}H_{24}N_2O_3Na$ $[M+Na]^+$: 303.1685, found 303.1649.

5.4.8 Synthesis of compound 5.19: (2E,6E)-3,7-Dimethyl-8-((3-(3-methyl-3H-diazirin-3-yl)propanoyl)oxy)octa-2,6-dien-1-yl diphosphate. To a solution of diazirine alcohol **5.18** (69.5 mg, 247 µmol) in Et_2O (4 mL) was added PBr_3 (73 mg, 270 µmol, 1.2 eq). The resulting solution was allowed to stir in an ice bath for 30 min. The mixture was concentrated and redissolved in CH_3CN. TTBHPP (0.445 g, 494 µmol, 2.0 eq) was added, and the solution was stirred for 16 hat RT. The reaction solution was concentrated and applied to an ion exchange column (Dowex 50WX8-100 Resin) equilibrated with 25 mM NH_4HCO_3 /isopropanol (49:1, v/v). The column was eluted with 25 mM NH_4HCO_3/isopropanol (49:1, v/v), and the fractions containing the desired mass were lyophilized for 48 h to obtain a white powder. Additional purification by reverse-phase HPLC with a gradient of 0 to 40% CH_3CN in 25 mM NH_4HCO_3 over 50 min at a flow rate of 5 mL/min resulted in the elution of desired diphosphate **8** at 12.8 – 14.4% CH_3CN. The fractions containing the desired mass were lyophilized to afford 21 mg (18%) of a white solid. ^{1}H NMR (300 MHz, D_2O) δ: 1.03 (s, 3H), 1.58 – 1.75 (m, 8H), 2.05 – 2.22 (m, 6H), 4.31 (t, 2H, J = 6.6 Hz), 4.38 (s, 2H), 5.31 (t, 1H, J = 6.3 Hz), and 5.39 (t, 1H, J

= 6.3 Hz); ^{31}P NMR (300 MHz, D_2O) δ -5.83 (d, 1P, J = 54.6 Hz), and -9.83 (d, 1P, J = 54.6 Hz). HR-ESI-MS: calcd for $C_{15}H_{24}N_2O_9P_2$ $[M-H]^-$: 439.1041, found 439.1160.

5.4.9 Synthesis of compound 5.23: 1-Bromo-6-(prop-2-yn-1-yloxy)hexane. Propargyl alcohol **5.22** (0.840 g, 15.0 mmol, 1 eq) was dissolved in anhydrous THF (15 mL) under nitrogen atmosphere. N-butyllithium in hexane (2.5 M, 15.0 mmol, 1 eq) was added and the resulting solution was stirred for 90 min while cooling on an ice bath. 1,6 dibromohexane (7.32 g, 30 mmol, 2 eq) and tetrabutylammonium iodide (0.55 g, 1.5 mmol, 0.1 eq) were added, and the mixture was stirred at 50 °C for 16 h. Purification by flash chromatography (hexanes: Et_2O 20:1) afforded compound **5.23** as clear oil (1.043g, 32%). ^{1}H-NMR (300 MHz, $CDCl_3$) δ 1.37 – 1.51 (m, 4H), 1.57 – 1.66 (m, 2H), 1.82 – 1.91 (m, 2H), 2.42 (m, 1H), 3.41 (t, 2H, J = 6.6 Hz), 3.52 (t, 2H J = 6.6 Hz), and 4.14 (s, 2H). Compound was unable to be visualized by ESI-MS.

5.4.10 Synthesis of compound 5.24 6-(prop-2-yn-1-yloxy)Hexyl dihydrogen phosphate. Bromide **5.23** (0.504 g, 2.30 mmol) and $Bu_4NH_4PO_4$ (2.34 g, 6.88 mmol, 3.0 eq) were dissolved in anhydrous CH_3CN (30 mL) and stirred at 40 °C for 48 h. The reaction solution was concentrated and applied to an ion exchange column (Dowex 50WX8-100 Resin) equilibrated with 25 mM NH_4HCO_3/isopropanol (49:1, v/v). The column was eluted with 25 mM NH_4HCO_3/isopropanol (49:1, v/v), and the fractions containing the desired mass were lyophilized for 48 hours. Additional purification by reverse-phase HPLC (25 mM NH_4HCO_3) and lyophilization resulted in phosphate **5.24** (0.216 g, 40%). ^{1}H NMR (300 MHz, D_2O) δ: 1.21 (m, 4H), 1.44 (m, 4H), 3.46(t, 2H, J

= 6.6 Hz), 3.57(q, 2H, J = 6.9 Hz), and 4.04 (s, 2H); ^{31}P NMR (300 MHz, D_2O) δ: 4.504 (s, 1P). HR-ESI-MS: calcd for $C_9H_{16}O_5P$ $[M-H]^-$: 235.0694, found 235.0741.

5.4.11 Synthesis of compound 5.27: (E)-Dimethyl (3,7-dimethylocta-2,6-dien-1-yl)phosphonate. This compound was prepared via a modification of a previously described procedure.[185] A solution of geranyl bromide **5.25** (7.66 g, 35.3 mmol, 1.0 eq) in $P(OCH_3)_3$ (4.60 ml, 38.8 mmol 1.2 eq) was heated to reflux for 16 h. The reaction mixture was purified by flash chromatography (hexanes: EtOAc, 1:3) on silica gel to obtain **5.27** (5.85 g, 67.3%) as a clear oil. ^{1}H NMR (300 MHz, $CDCl_3$) δ: 1.56 (s, 3H), 1.65 (m, 6H), 2.04 (m, 4H), 2.57 (dd, 2H, J = 7.8 Hz, 22.2 Hz), 3.72 (d, 6H, J = 12.6 Hz), 5.06 (t, 1H, J = 4.2 Hz), and 5.16 (m, 1H); ^{31}P NMR (300 MHz, $CDCl_3$) δ 31.883 (s, 1P). HR-ESI-MS: calcd for $C_{12}H_{23}O_3PNa$ $[M+Na]^+$: 269.1277, found 269.2143.

5.4.12 Synthesis of compound 5.29: Dimethyl ((2E,6E)-8-hydroxy-3,7-dimethylocta-2,6-dien-1-yl) phosphonate. This compound was prepared via a modification of a previously described procedure.[185] Phosphonate **5.27** (5.85 g, 23.8 mmol, 1.0 eq) was then dissolved in CH_2Cl_2 (32 mL). In turn, 70% tBu-OOH in H_2O (10.9 mL, 76.0 mmol, 2.5 eq), salicylic acid (0.328 g, 2.38 mmol, 0.1 eq), and SeO_2 (0.261 g, 2.38 mmol, 0.1 eq) were added, and the resulting solution was stirred at rt for 22 h. The reaction mixture was quenched with saturated $NaHCO_3$ (30 mL), extracted thrice with CH_2Cl_2 (30 mL), and dried over $MgSO_4$. After concentration, the residue was purified by flash chromatography (CH_3OH:CH_2Cl_2, 1:10) on silica gel to obtain **5.29** (1.53 g, 24.6%) as a clear oil. ^{1}H NMR (300 MHz, $CDCl_3$) δ: 1.68 (m, 6H), 2.12 – 2.19 (m, 4H), 2.55 (dd, 2H,

J = 7.8 Hz, 21.6 Hz), 3.72 (d, 6H, J = 12.6 Hz), 3.96 (s, 2H), 5.15 (m, 1H), and 5.30 (m, 1H); ^{31}P NMR (300 MHz $CDCl_3$) δ 32.033 (s, 1P); HR-ESI-MS: calcd for $C_{12}H_{23}O_4PNa$ $[M+Na]^+$: 285.1226, found 285.1068.

5.4.13 Synthesis of compound 5.31: (2E,6E)-8-(dimethoxyphosphoryl)-2,6-dimethylocta-2,6-dien-1-yl 3-(3-methyl-3H-diazirin-3-yl)propanoate. To a solution of **5.29** (0.900 g, 3.44 mmol, 1.0 eq) and DMAP (42 mg, 0.34 mmol, 0.1 eq) in CH_2Cl_2 (5 mL) was added a solution of the diazirine acid **5.13** (0.55 g, 4.3 mmol, 1.5 eq) in CH_2Cl_2 (6 mL). DIC (0.510 mL, 3.44 mmol, 1.0 eq) was added and the resulting solution was stirred at rt for 18 h. The reaction mixture was filtered and concentrated. Purification by flash chromatography (EtOAc) afforded diazirine **5.31** as clear oil (0.79 g, 61%). ^{1}H NMR (300 MHz, $CDCl_3$) δ: 1.03 (s, 3H), 1.64 (m, 6H), 1.74 (t, 2H, J = 5.4 Hz), 2.04 (m, 4H), 2.19 (t, 2H, J = 5.4 Hz) 2.57 (dd, 2H**,** J = 7.8 Hz, 22.2 Hz), 3.73 (d, 6H, J = 12.6 Hz), 4.45 (s, 2H), 5.20 (m, 1H), and 5.42 (t, 1H, J = 6.6 Hz); ^{31}P NMR (300 MHz, $CDCl_3$) δ: 31.760 (s, 1P). Compound was unable to be visualized by ESI-MS

5.4.14 Synthesis of compound 5.33: ((2E,6E)-3,7-Dimethyl-8-((3-(3-methyl-3H-diazirin-3-yl)propanoyl)oxy)octa-2,6-dien-1-yl)phosphonic acid. Compound **5.31** (0.77 g, 2.0 mmol, 1.0 eq) was dissolved in anhydrous CH_2Cl_2 (28mL). In turn, $(CH_3)_3SiCH_2CHCH_2$ (0.491 mL, 3.09 mmol, 1.5 eq) and $(CH_3)_3SiBr$ (0.815 mL, 6.18 mmol, 3.0 eq) were added. The resulting solution was stirred for 40 h at RT. The reaction mixture was then concentrated and quenched with 25 mM NH_4HCO_3 (20 mL). After lyophilization, purification by reverse-phase HPLC with a gradient of 0 to 40% CH_3CN

in 25 mM NH_4HCO_3 over 50 min at a flow rate of 5 mL/min resulted in the elution of the desired phosphonate **5.33** at 20-26% CH_3CN. Lyophilization yielded a white solid (0.502 g, 73.2%). HR-ESI-MS: calcd for $C_{12}H_{24}N_2O_5P$ $[M-H]^-$: 343.1428, found 343.1297.

5.4.15 Synthesis of compound 5.7: ((2E,6E)-3,7-Dimethyl-8-((3-(3-methyl-3H-diazirin-3-yl)propanoyl)oxy)octa-2,6-dien-1-yl)phosphonic(6-(prop-2-yn-1-yloxy)hexyl phosphoric) anhydride. Phosphonate **5.33** (47.1 mg, 0.137 mmol, 1.0 eq) and DIEA (17.7 mg, 0.137 mmol, 1.0 eq) were dissolved in dry DMF (3 mL) and stirred at room temperature for 30 min. CDI (111 mg, 0.684 mmol, 5.0eq) was added and the resulting solution was stirred for 3.5 h. CH_3OH (35 mg, 1.11 mmol, 8.0 eq) was added and stirred for 30 min to decompose excess CDI. Phosphate **5.24** (40.5 mg, 0.172 mmol 1.2 eq) was added and stirred for 16 h. The reaction mixture was quenched with 25 mM NH_4HCO_3 (7 mL). Purification by reverse-phase HPLC with a gradient of 0 to 50% CH_3CN in 25 mM NH_4HCO_3 over 50 min at a flow rate of 5 mL/min resulted in the elution of the desired product **5.7** at 30-34% CH_3CN. Lyophilization yielded a white solid (6 mg, 7.8%). ^1H NMR (300 MHz, D_2O) δ: 0.89 (s, 3H), 1.25 (m, 6H), 1.45 (m, 8 H) 1.61 (t, 2H, J = 5.2 Hz), 2.4 (m, 4H), 2.19 (t, 2H, *J* = 7.2 Hz), 2.41 (dd, 2H, J = 7.8 Hz, 21.9 Hz), 3.47 (t, 2H, J = 6.6 Hz), 3.77 (m, 2H), 4.05 (s, 2H), 4.40 (s, 2H), 5.15 (q, 1H, J = 7.5 Hz), and 5.43 (t, 1H, J = 6.3 Hz); ^{31}P NMR (300 MHz, D_2O) δ: 16.65 (d, 1P), -10.28 (d, 1P). HR-ESI-MS: calcd for $C_{24}H_{40}N_2O_9P_2$ $[M-H]^-$: 561.2136, found 561.2033.

5.4.16 Synthesis of compound 5.35: N-(2-(2-(2-(2-azidoethoxy)ethoxy)ethoxy)ethyl)-1-(5-((3aS,4S,6aR)-2-oxohexahydro-1H-thieno[3,4-d]imidazol-4-yl)pentanamido)-

3,6,9,12-tetraoxapentadecan-15-amide. Commercial available NHS-PEG_4-Biotin (148 mg, 0.252 mmol, 1eq), N_3-Peg_2-NH2 (55 mg, 0.252 mmol, 1eq) and DIEA (1 mL, 25.2 µmol, 0.1 eq) were dissolved in anhydrous DMF (5 mL) and stirred at rt for 12 h. The reaction was filtered and concentrated. Purification by reverse-phase HPLC with a gradient of 0 to 40% CH_3CN in H_2O (0.1% TFA) over 60 min at a flow rate of 5 mL/min resulted in the elution of the desired product **5.35** at 19-21% CH_3CN. Lyophilization yielded a white solid (128 mg, 73.6%). ^1H NMR (300 MHz, $CDCl_3$) δ: 1.36 (m, 2H), 1.43 (m, 4H), 1.59 (t, 2H, J = 7.9 Hz), 2.19 (t, 2H, J = 7.5 Hz), 2.45 (t, 2H, J = 6.0 Hz), 2.72 (d, 1H, 12.9 J = Hz), 2.86 (dd, 1H, J = 4.5 Hz, 12.9 Hz), 3.08 (q, 1H, J = 7.5 Hz), 3.36 (dt, 4H, J = 4.5 Hz, 7.5 Hz), 3.52 (t, 2H, J = 5.1 Hz), 3.61 (m, 24H), 3.71 (t, 2H, J = 6.0 Hz), 4.28 (dd, 1H, J = 4.5 Hz ,7.5 Hz), 4. 46 (dd, 1H, J = 4.5 Hz ,7.5 Hz), 5.69 (s, 1H), 6.38 (s, 1H), 6.91 (t, 1H, J = 4.5 Hz) 7.02 (t, 1H, J = 4.5 Hz). HR-ESI-MS: calcd for $C_{29}H_{53}N_7O_{10}S$ $[M+H]^+$: 692.3653, found 692.3598

5.4.17 Synthesis of compound 5.9: 5.(6-((1-(13,29-dioxo-33-((3aS,4S,6aR)-2-oxohexahydro-1H-thieno[3,4-d]imidazol-4-yl)-3,6,9,16,19,22,25-heptaoxa-12,28-diazatritriacontyl)-1H-1,2,3-triazol-4-yl)methoxy)hexyl phosphoric) ((2E,6E)-3,7-dimethyl-8-((3-(3-methyl-3H-diazirin-3-yl)propanoyl)oxy)octa-2,6-dien-1-yl)phosphonic anhydride. Phosphonophosphate **5.7** (3.5 mg, 6.18 µmol, 1 eq) was dissolved with azide **5.35** (5.1 mg, 7.37 µmol, 1.2 eq) in 25 mM NH_4HCO_3 (3 mL). In turn, $CuSO_4$ (77.1 µg, 3.09 µmole, 0.5 eq), TCEP (77.2 µg, 3.09 µmol, 0.5 eq), and TBTA (22.8 µg, 0.43 µmol, .07 eq) was added to the solution and stirred at rt for 5 h.

Purification by reverse-phase HPLC with a gradient of 0 to 50% CH_3CN in 25 mM NH_4HCO_3 over 50 min at a flow rate of 5 mL/min resulted in the elution of the desired product **5.9** at 23-25% CH_3CN. Lyophilization yielded a white solid (7.4 mg, 9.5%). ^1H NMR (300 MHz, D_2O) δ: 0.84 (s, 3H), 1.25 (m, 6H), 1.45 – 1.55 (m, 16 H), 1.90 – 2.20 (m, 10H), 2.32-2.41 (m, 4H,), 2.58 (d, 1H, J = 13.2 Hz), 2.80 (dd, 1H, J = 4.8 Hz, 13.2 Hz), 3.14 (q, 1H, J = 6.0 Hz) 3.21 (t, 4H, J = 5.1 Hz), 3.37-3.48 (m, 24H), 3.61 (t, 2H, J = 6.3 Hz), 3.71 (q, 2H, J = 6.6 Hz), 3.79 (t, 2H, J = 5.1 Hz), 4.24 (dd, 1H, J = 4.5 Hz ,7.5 Hz) 4.33 (s, 2H), 4.42 (dd, 1H, J = 4.5 Hz ,7.5 Hz), 4.46 (s, 2H), 5.15 (q, 1H, J = 7.5 Hz), 5.34 (t, 1H, J = 6.3 Hz), and 7.89 (s, 1H). HR-ESI-MS: calcd for $C_{53}H_{92}N_9O_{19}P_2S$ $[M-H]^-$:1252.5711, found 1252.5695

5.4.18 Synthesis of compound 5.28: Dimethyl ((2E,6E)-3,7,11-trimethyldodeca-2,6,10-trien-1-yl)phosphonate. Compound **5.28** was synthesized using the same conditions and quantities as used for **5.27** with replacement of geranyl bromide **5.25** with farnesyl bromide **5.26**. ^1H NMR (500 MHz, $CDCl_3$) δ: 1.59 (s 3H), 1.61 (s, 3H), 1.67(s, 6H), 2.04 (m, 8H), 2.57 (dd, 2H, J = 7.8 Hz, 22.2 Hz), 3.73 (d, 6H, J = 12.6 Hz), 5.08 (m, 2H,), and 5.17 (q, 1H, J = 6.6 Hz); ^{31}P NMR (300 MHz, $CDCl_3$) δ 32.235 (s, 1P). HR-ESI-MS: calcd for $C_{17}H_{31}O_3PNa$ $[M+Na]^+$:337.1909, found 337.1894

5.4.19 Synthesis of compound 5.30 Dimethyl ((2E,6E,10E)-12-hydroxy-3,7,11-trimethyldodeca-2,6,10-trien-1-yl)phosphonate. Compound **5.30** was synthesized using the same conditions and quantities as used for **5.29**. ^1H NMR (500 MHz, $CDCl_3$) δ:

1.59 (s 3H), 1.65 (s, 6H), 2.06 (m, 8H), 2.58 (dd, 2H, J = 7.5 Hz, 21.9 Hz), 3.73 (d, 6H, J = 12.6 Hz), 3.98 (s, 2H), 5.10 (t, 1H, J = 6.6 Hz), 5.18 (q, 1H, J = 5.0 Hz), and 5.39 (t, 1H, J = 6.6 Hz); ^{31}P NMR (300 MHz, $CDCl_3$) δ 32.230 (s, 1P). HR-ESI-MS: calcd for $C_{17}H_{32}O_4PNa$ $[M+Na]^+$: 353.1858, found 353.1849.

5.4.20 Synthesis of compound 5.32: (2E,6E,10E)-12-(dimethoxyphosphoryl)-2,6,10-trimethyldodeca-2,6,10-trien-1-yl3-(3-methyl-3H-diazirin-3-yl)propanoate.

Compound **5.32** was synthesized using the same conditions and quantities as used for **5.31.** ^{1}H NMR (300 MHz, $CDCl_3$) δ: 1.02 (s, 3H) 1.61 (s 3H), 1.65 (s, 3H), 1.68 (m, 5H), 2.18 (m, 8H), 2.26 (t, 2H, J = 4.5 Hz) 2.55 (dd, 2H, J = 7.6 Hz, 21.9 Hz), 3.65 (d, 6H, J = 12.6 Hz), 4.51 (s, 2H) 5.15 (t, 2H, J = 6.6 Hz), and 5.46 (t, 1H, J = 6.6 Hz); ^{31}P NMR (300 MHz, $CDCl_3$) δ 31.648 (s, 1P). Compound was unable to be visualized by ESI-MS.

5.4.21 Synthesis of compound 5.34: (2E,6E,10E)-3,7,11-trimethyl-12-((3-(3-methyl-3H-diazirin-3-yl)propanoyl)oxy)dodeca-2,6,10-trien-1-yl)phosphonic acid.

Compound **5.34** was synthesized using the same conditions and quantities as used for **5.33**. HR-ESI-MS: calcd for $C_{20}H_{32}N_2O_5P$ $[M-H]^-$: 411.2054, found 411.1982

5.4.22 Synthesis of compound 5.8: ((2E,6E,10E)-3,7,11-trimethyl-12-((3-(3-methyl-3H-diazirin-3-yl)propanoyl)oxy)dodeca-2,6,10-trien-1-yl)phosphonic (6-(prop-2-yn-1-yloxy)hexyl phosphoric) anhydride. Compound **5.8** was synthesized using the same conditions and quantities as used for **5.7**. ^{1}H NMR (300 MHz, D_2O) δ: 0.84 (s, 3H), 1.25 (m, 6H), 1.40 (s, 3H), 1.51 (s, 6H) 1.54 (t, 2H, J = 7.2Hz) 1.98 (m, 8H), 2.13 (t, 2H, *J* =

7.2 Hz), 2.39 (dd, 2H, J = 7.8 Hz, 21.9 Hz), 2.68 (t, 1H, J = 2.2 Hz), 3.41 (t, 2H, J = 6.6 Hz), 3.72 (q, 2H, J = 6.3 Hz), 4.01 (d, 2H, J = 2.2 Hz), 4.34 (s, 2H), 5.06 (t, 1H, J = 6.6 Hz), 5.09 (t, 1H, J = 6.3 Hz), and 5.55 (t, 1H, J = 6.6 Hz) ; ^{31}P NMR (300 MHz, D_2O) δ: 16.05 (d, 1P), -10.97 (d, 1P). HR-ESI-MS: calcd for $C_{29}H_{47}N_2O_9P_2$ $[M-H]^-$: 629.2762, found 626.2698.

5.4.23 Synthesis of compound 5.10: 6-((1-(13,29-dioxo-33-((3aS,4S,6aR)-2-oxohexahydro-1H-thieno[3,4-d]imidazol-4-yl)-3,6,9,16,19,22,25-heptaoxa-12,28-diazatritriacontyl)-1H-1,2,3-triazol-4-yl)methoxy)hexyl phosphoric) ((2E,6E,10E)-3,7,11-trimethyl-12-((3-(3-methyl-3H-diazirin-3-yl)propanoyl)oxy)dodeca-2,6,10-trien-1-yl)phosphonic anhydride. Compound **5.10** was synthesized using the same conditions and quantities as used for **5.9**. ^{1}H NMR (300 MHz, D_2O) δ: 0.84 (s, 3H), 1.25 (m, 6H), 1.45 – 1.55 (m, 16 H), 1.90 – 2.20 (m, 14H), 2.32-2.41 (m, 4H,), 2.60 (d, 1H, J = 13.2 Hz), 2.80 (dd, 1H, J = 4.8 Hz, 13.2 Hz), 3.14 (q, 1H, J = 6.0 Hz) 3.20 (t, 4H, J = 5.4 Hz), 3.37-3.48 (m, 24H), 3.59 (t, 2H, J = 6.0 Hz), 3.70 (q, 2H, J = 6.6 Hz), 3.79 (t, 2H, J = 4.5 Hz), 4.24 (dd, 1H, J = 4.5 Hz ,7.5 Hz) 4.32 (s, 2H), 4.42(dd, 1H, J = 4.5 Hz ,7.5 Hz), 4.43 (s, 2H),), 5.02 (t, 1H, J = 6.6 Hz), 5.08 (q, 1H, J = 5.0 Hz), and 5.29 (t, 1H, J = 6.6 Hz) and 7.89 (s, 1H). HR-ESI-MS: calcd for $C_{58}H_{100}N_9O_{19}P_2S$ $[M-H]^{-1}$: 1320.6337, found 1320.6297

5.4.24 yPFTase Expression and Purification. was expressed and purified following a previously reported procedure.[224] A frozen stock of BL21(DE3)pLysS *E. coli* cells

containing yeast PFTase on a CDF-Duet1 vector, created by the Lorena Beese lab using a design previously employed for the mammalian PFTase,[225] was used to inoculate a small culture of LB containing 50 μg/mL of streptomycin and grown overnight at 37 °C with shaking at 240 rpm. The next morning, flasks containing 1 L LB media were inoculated with 10 mL of the overnight culture and grown to an OD_{600} of approximately 0.8. Cells were then induced with 1 mM IPTG and supplemented with 500 μM $ZnSO_4$ followed by incubation overnight at 15 °C with shaking at 250 rpm. Cells were harvested by centrifugation at 5400*g*, and the pellets (one pellet equivalent to one liter of cell growth) were frozen and stored at −80 °C.

Two cell pellets were thawed and resuspended in 50 mL of a buffer containing 50 mM Tris–HCl (pH 7.0), 200 mM NaCl, 5 μM $ZnCl_2$, 5 mM $MgCl_2$, 20 mM imidazole, and 1 mM β-mercaptoethanol (lysis buffer). To this mixture was added 1 mL of protease inhibitor cocktail, a cocktail developed for His-tagged proteins from (Sigma Aldrich, No. P8849). Cells were pulse-sonicated for a total of 5 min (10 s on, 10 s off) at 50 W followed by centrifugation at 13,000*g* for 30 min to remove insoluble cell material. The soluble fraction was then loaded onto a 30 mL Ni-NTA column bed equilibrated with lysis buffer at a rate of approximately 2 mL/min and the column was washed with lysis buffer until the A_{280} dropped to 0.25 (approximately 200 mL). The desired protein was then eluted using buffer containing 50 mM Tris–HCl (pH 7.0), 20 mM NaCl, 5 μM $ZnCl_2$, 5 mM $MgCl_2$, 250 mM imidazole, and 1 mM β-mercaptoethanol. Fractions containing PFTase were pooled in an Amicon Ultra-15 centrifugal filter from Millipore, and concentrated to 4 mL. This was diluted three times at a 10-fold dilution with 50 mM

Tris–HCl, 200 mM NaCl, 5 μM $ZnCl_2$, 5 mM $MgCl_2$, and 1 mM β-mercaptoethanol buffer and stored in the latter buffer containing 50% glycerol at −80 °C. This purification typically yielded 100 mg/L of liquid culture of PFTase with a purity of 90%.

5.4.25 rPFTase Expression and Purification. rPFTase was expressed and purified following a previously reported procedure,[224] and is similar to that described for yPFTase Streptomycin (50 μg/mL) was used as the selection antibiotic for cell growth. IPTG and $ZnSO_4$ were added, both with final concentration of 0.5 mM to induce protein expression. To purify the enzymes, lysis buffer (50 mM Tris·HCl, pH 7.5, 200 mM NaCl, 5 μM $ZnCl_2$, 5 mM $MgCl_2$, and 20 mM imidazole) and elution buffer (50 mM Tris·HCl, pH 7.5, 200 mM NaCl, 5 μM $ZnCl_2$, 5 mM $MgCl_2$, and 250 mM imidazole) were used. 1 mM β-mercaptoethanol was added to these two buffers before use. Fractions containing rPFTase were collected and concentrated. Buffer exchange was performed with lysis buffer and the rPFTase was stored in 50% glycerol at −80 °C.

5.4.26 Continuous Fluorescence Assay for yPFTase Activity Measurement. *N*-dansyl-GCVIA, prepared as previously described,[170] was preincubated with DTT for 1h. After incubation, the peptide DTT solution was used to make a PFTase assay solution that had a final concentration of 2 μM dansyl-CVIA, 5 mM DTT, 50 mM Tris–HCl (pH 7.5), 10 mM $MgCl_2$, 10 μM $ZnCl_2$, 0.04% *n*-dodecyl β-d-maltoside and 10 μM of **5.1** or **5.2**.). For the enzyme concentration 70 nM of yPFTase was used. All these reagent concentrations were standard for all unless otherwise noted.

The reactions were performed in 96-well microtiter plates and the fluorescence emission for each sample was obtained using a DTX 880 Multimode Detector plate reader (Beckman Coulter). The reaction was performed in a black 96-well pinch bar plate (Nunc, No. 237105) with no top. The total volume of each reaction was 250 μL. Reactions were performed by adding 100 μL of a concentrated assay solution (5 μM dansyl-GCVIA, 12.5 mM DTT, 125 mM Tris–HCl (pH 7.5), 25 mM $MgCl_2$, 25 μM $ZnCl_2$, 0.1% *n*-dodecyl β-d-maltoside and 50 μM of **5.1** or **5.2**) and 30 μL of H_2O without enzyme to each well using a multichannel pipette. The initial fluorescence reading was recorded (λ_{ex} = 340 nm, λ_{em} = 505 nm) followed by initiation of the reaction through the addition of 20 μL yPFTase in enzyme buffer (50 mM Tris–HCl (pH 7.5), 5 mM $MgCl_2$, 50 μM $ZnCl_2$, 20 mM KCl, 1mM DTT, 1mg/mL BSA). The flourescense was monitored until it reached a plateau signifying that the reaction was complete. Initial velocities were obtained from linear regression analysis of the time-dependent fluorescence emission data using the fluorimeter software

5.4.27 Continuous Fluorescence Assay for rPFTase Activity Measurement. The same the continuous fluorescence assay conditions except the enzyme concentration was altered to 50 nM, rPFTase was used, and the peptide N-dansyl GCVLS was used instead of N-dansyl GCVIA. The assay was performed in triplicate at differing concentrations of the diazirine substrate: 0.02, 0.3, 0.5, 1.0, 2.0, 3.0, and 5.0 μM The increase in fluorescence was monitored until completion.

5.4.28 Product Studies. Large-scale reactions contained 50 mM Tris·HCl, pH 7.0, 10

mM $MgCl_2$, 10 μM $ZnCl_2$, 5.0 mM DTT, 2.4 μM *N*-dansyl-GCVIA, 70 nM PFTase, and **5.2** (10 μM), where appropriate, in a final reaction volume of 10 mL. The reactions were equilibrated to 30 °C, initiated by the addition of PFTase, and allowed to react for 1 h. To desalt the samples, each reaction mixture was applied to a Sep-Pak C_{18} cartridge, and eluted with in 10% increments of acetonitrile in 25 mM NH_4HCO_3 The fluorescent fractions were assessed by ESI-MS.

5.4.29 Enzyme Inhibition Experiments. To determine if **5.7** and **5.8** were competitive inhibitors of PFTase, a 4 × 6 grid of duplicate assays were run in which *N*-dansyl-GCVIA (2.4 μM) and FPP (5.0μM) maintained at a set of fixed concentrations and the inhibitor (**5.8** or **5.8**) concentrations were varied at each FPP concentration. Concentrations of 0, 3.0, 5.0, 10.0, 25.0 and 30.0 μM for FPP and 0, 1.8, 3.6, 9.0, 18.0, and 40.0 μM for **5.7** and **5.8** were chosen; the PFTase concentration in these experiments was 2.0 nM. The rates were determined from initial velocity measurements performed as described above.

5.4.30 Photocrosslinking of SmgGDS-607, SmgGDS-558, and rPFTase Recombinant SmgGDS-607, SmgGDS-558, and rPFTase (10 μg) was incubated with compound **5.9** or **5.10** (10 μg) for 10 mins, and then irradiated with UV light (365 nm) for 30 min at a distance of 3 cm. Photo-cross-linking reaction was quenched in liquid nitrogen. A control sample was prepared as described above, and the tube was wrapped in tin foil before exposure to UV light. After the cross-linking procedure, the peptides were immunoprecipitated using streptavidin-Sepharose 4B beads (434341; Invitrogen) and subjected to ECL-Western blotting.

5.4 Supporting Information

5.5.1 Characterization of compound 5.19

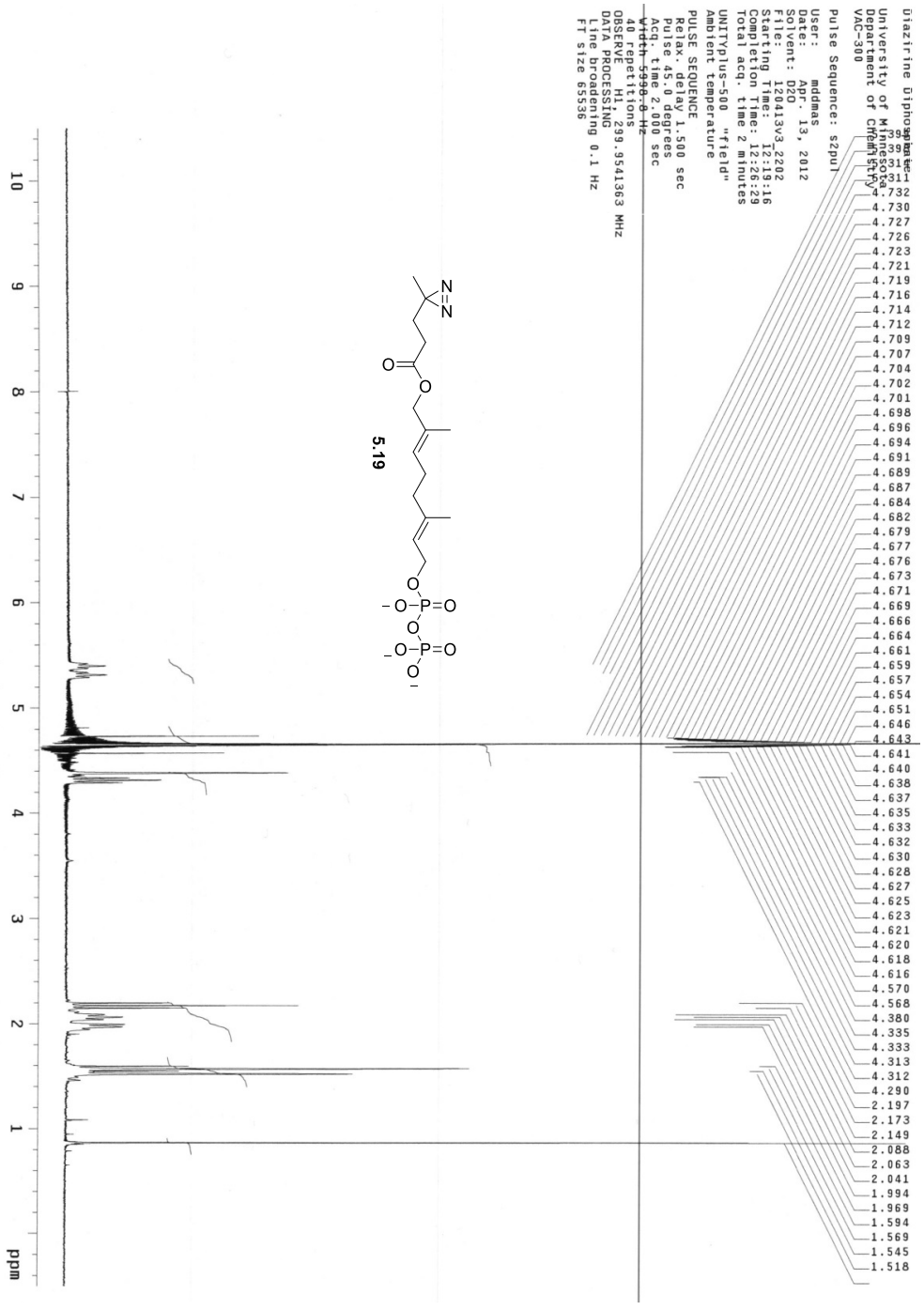

Figure 5.7. ^{1}H NMR spectrum of compound **5.19**.

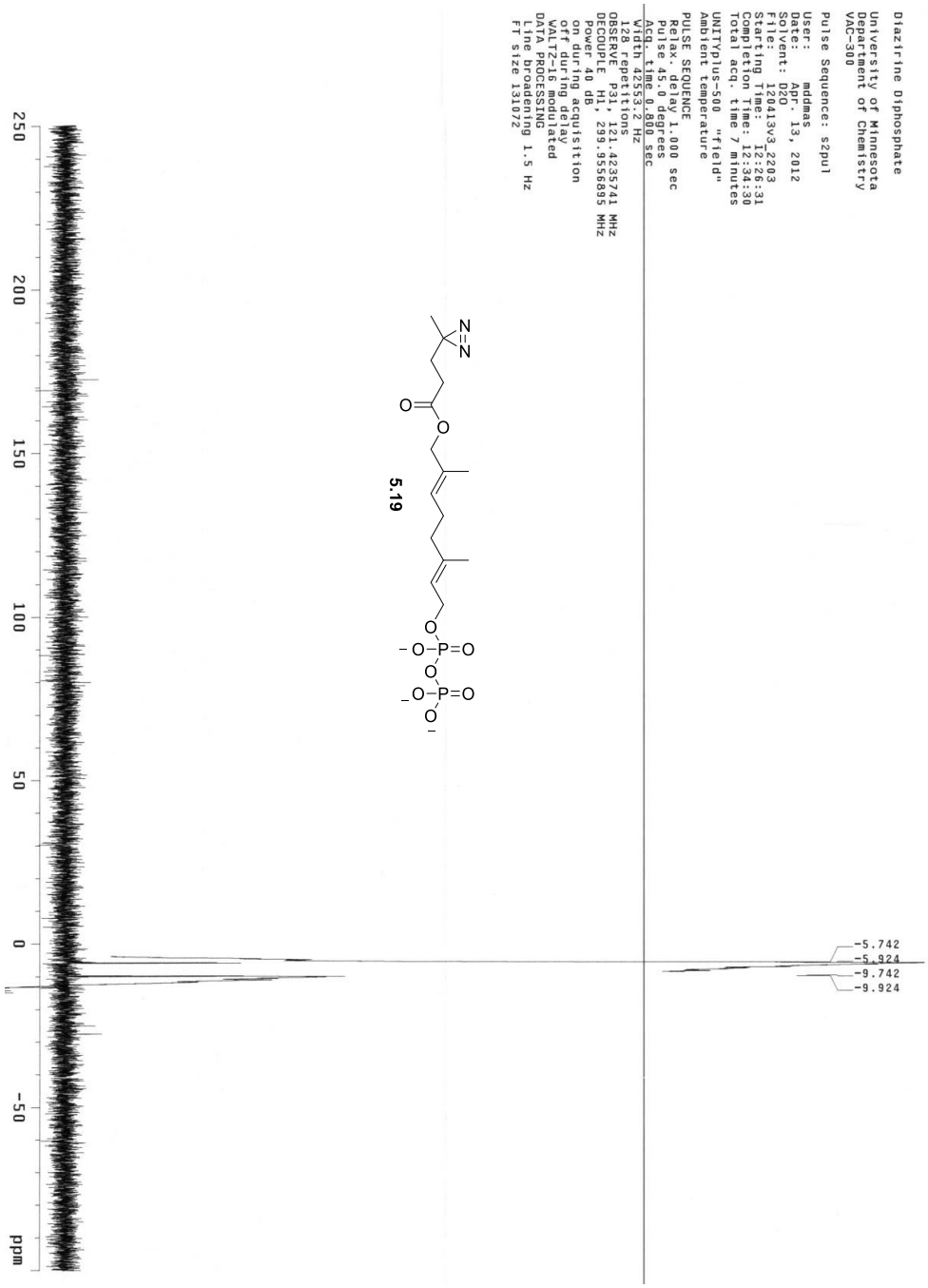

Figure 5.8. ^{31}P NMR spectrum of compound **5.19**.

5.5.2 Characterization of compound 5.23

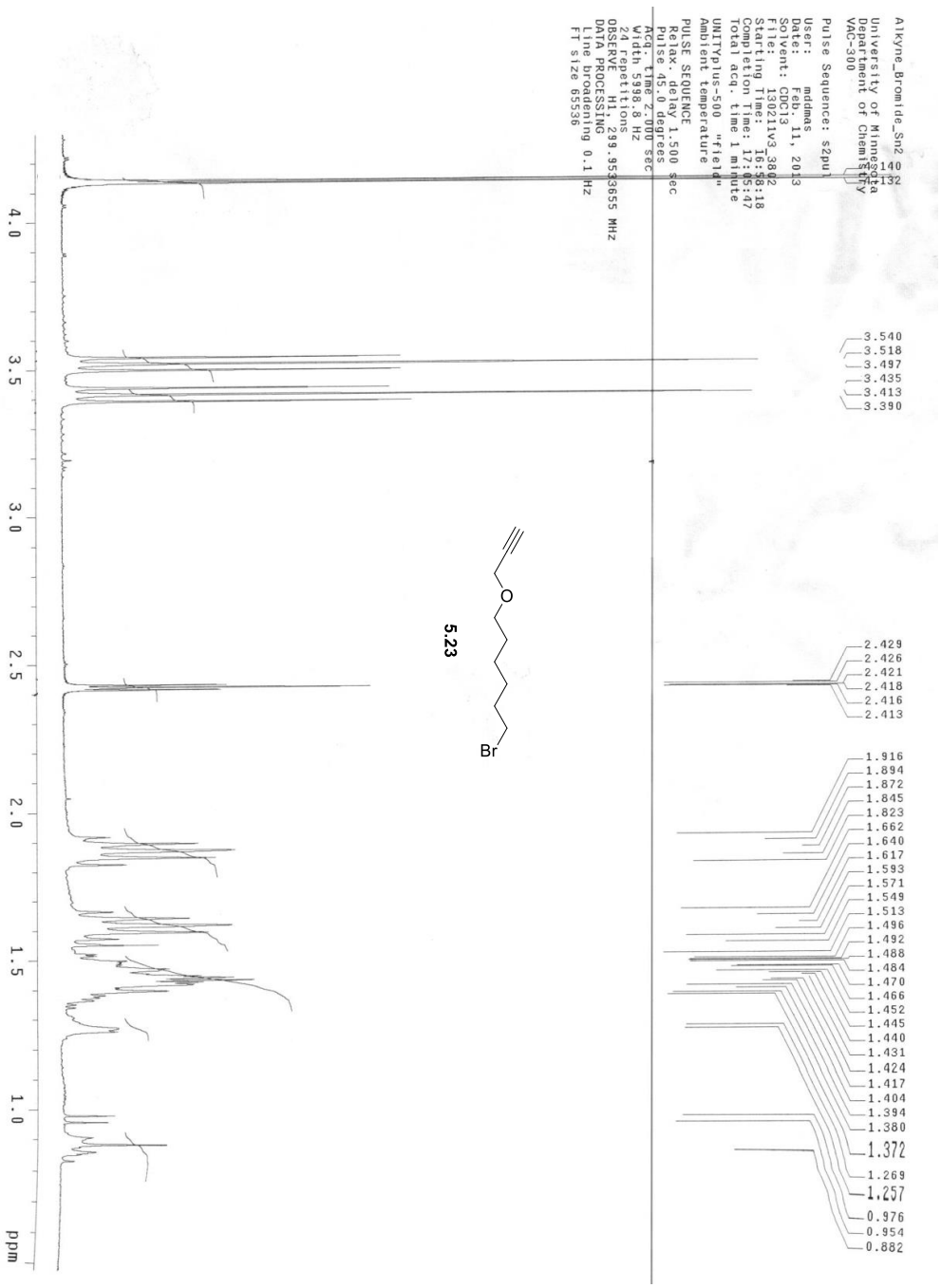

Figure 5.9. ^{1}H NMR spectrum of compound **5.23**.

5.5.3 Characterization of compound 5.24

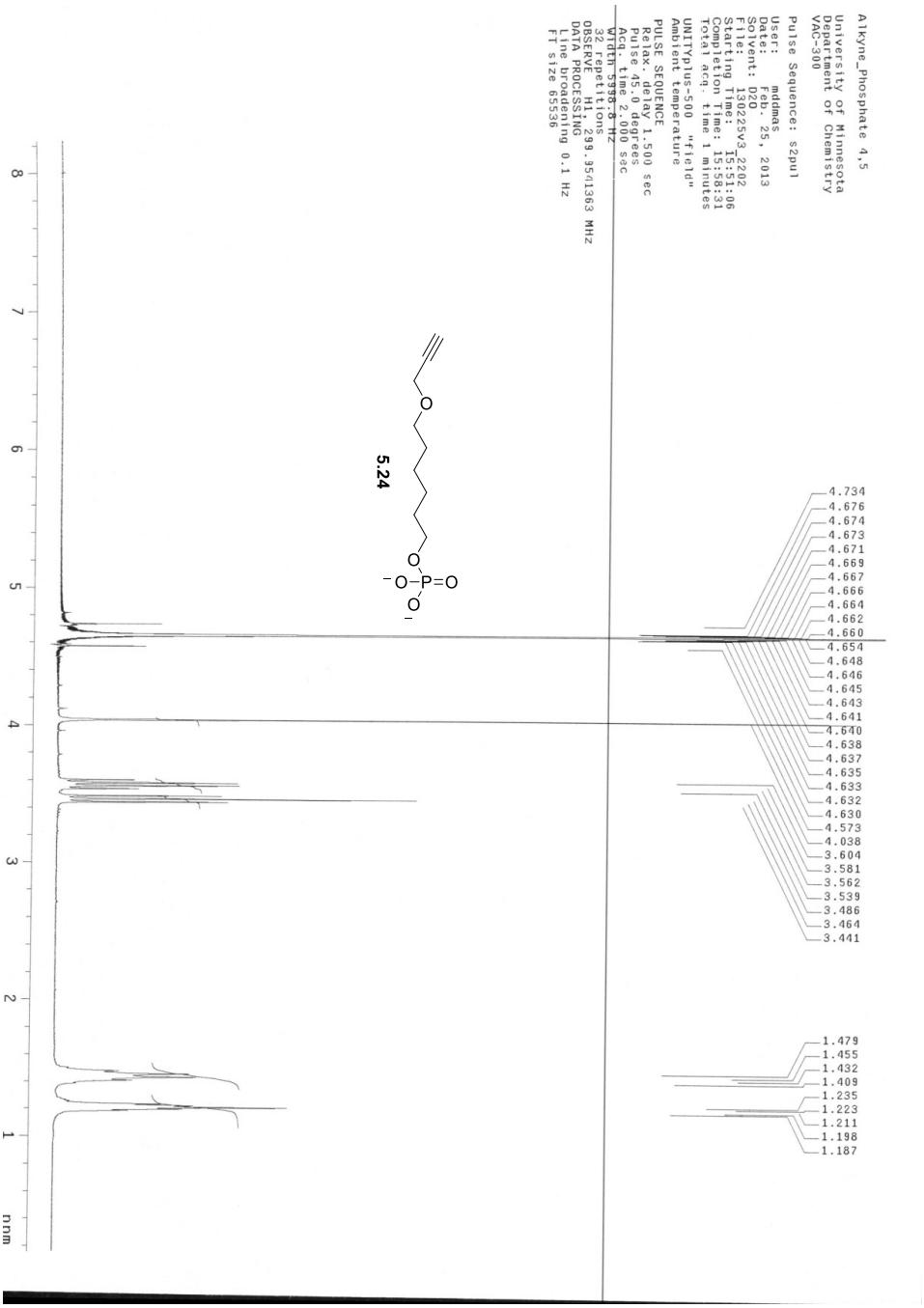

Figure 5.10. ^{1}H NMR spectrum of compound **5.24**.

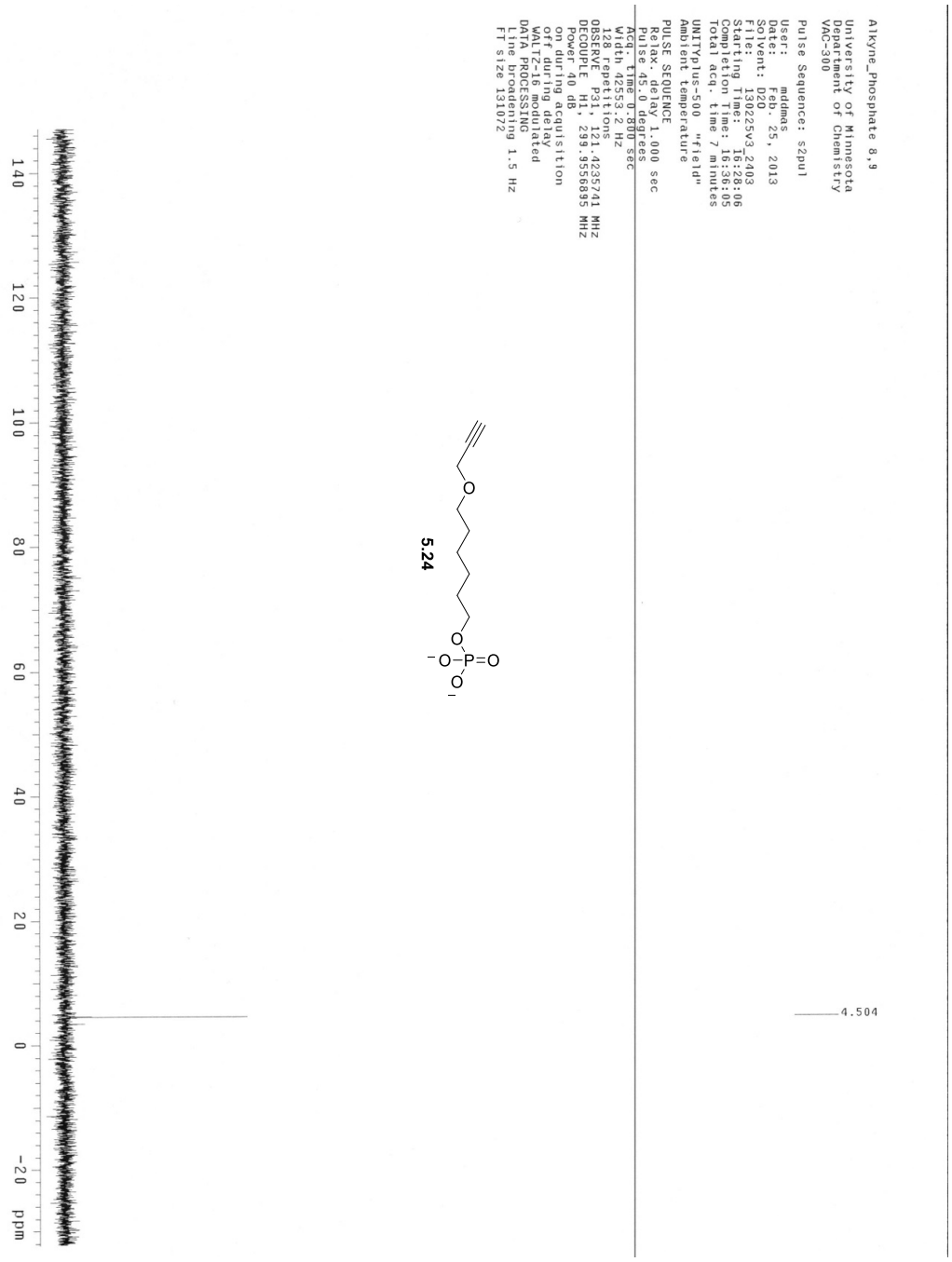

Figure 5.11. ^{31}P NMR spectrum of compound **5.24**.

5.5.4 Characterization of compound 5.27

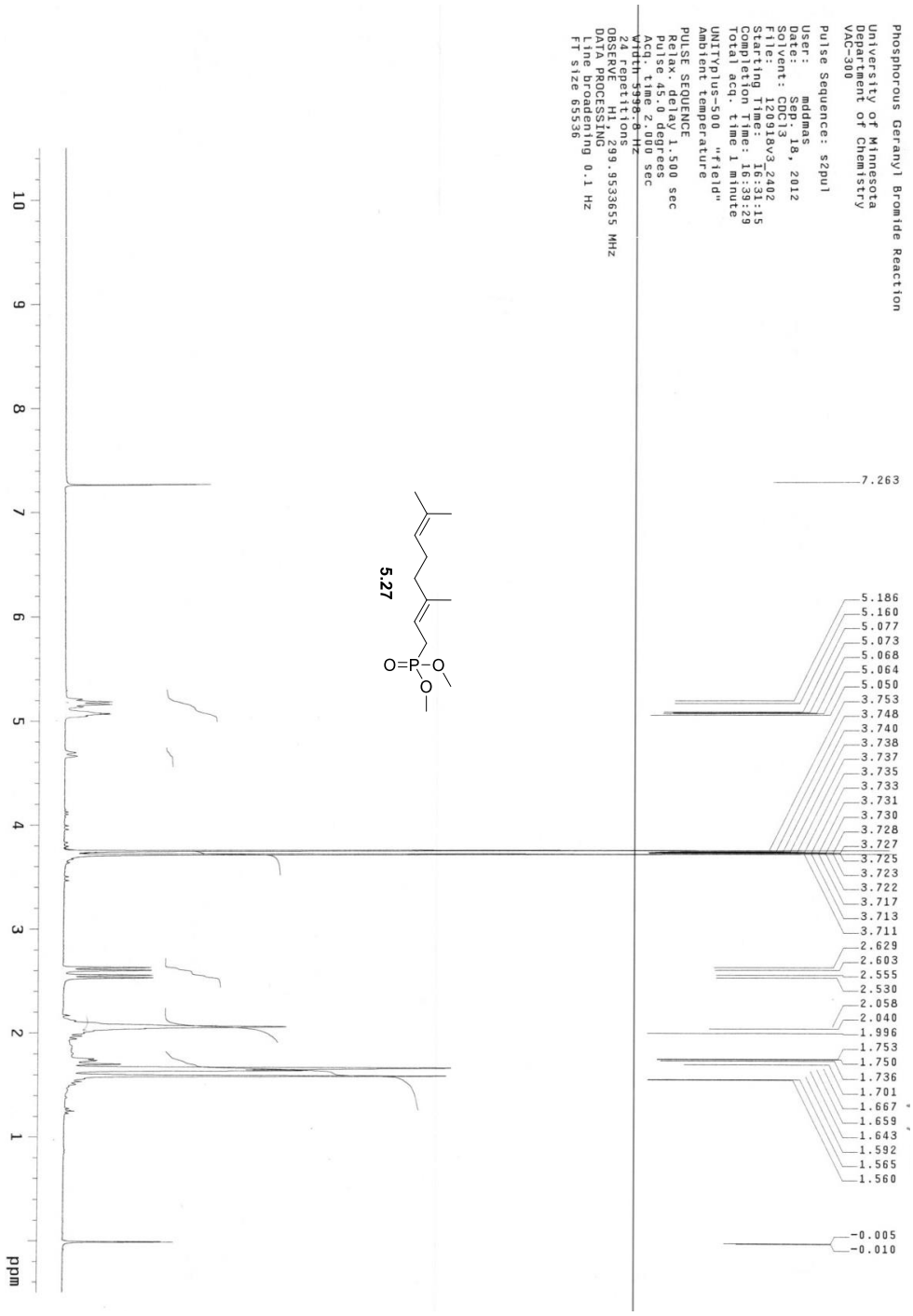

Figure 5.12. ^{1}H NMR spectrum of compound **5.27**.

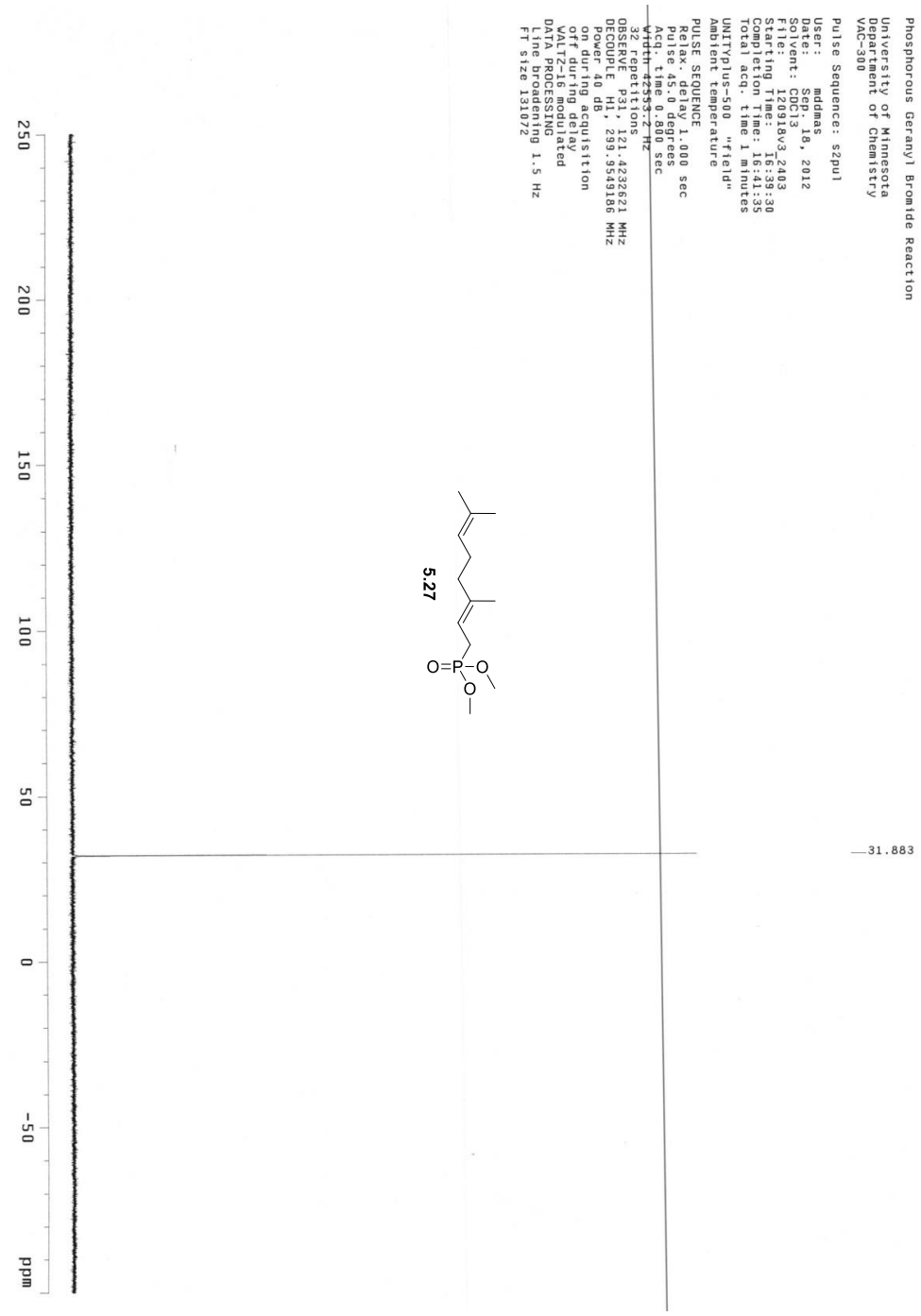

Figure 5.13. ^{31}P NMR spectrum of compound **5.27**.

5.5.5 Characterization of compound 5.29

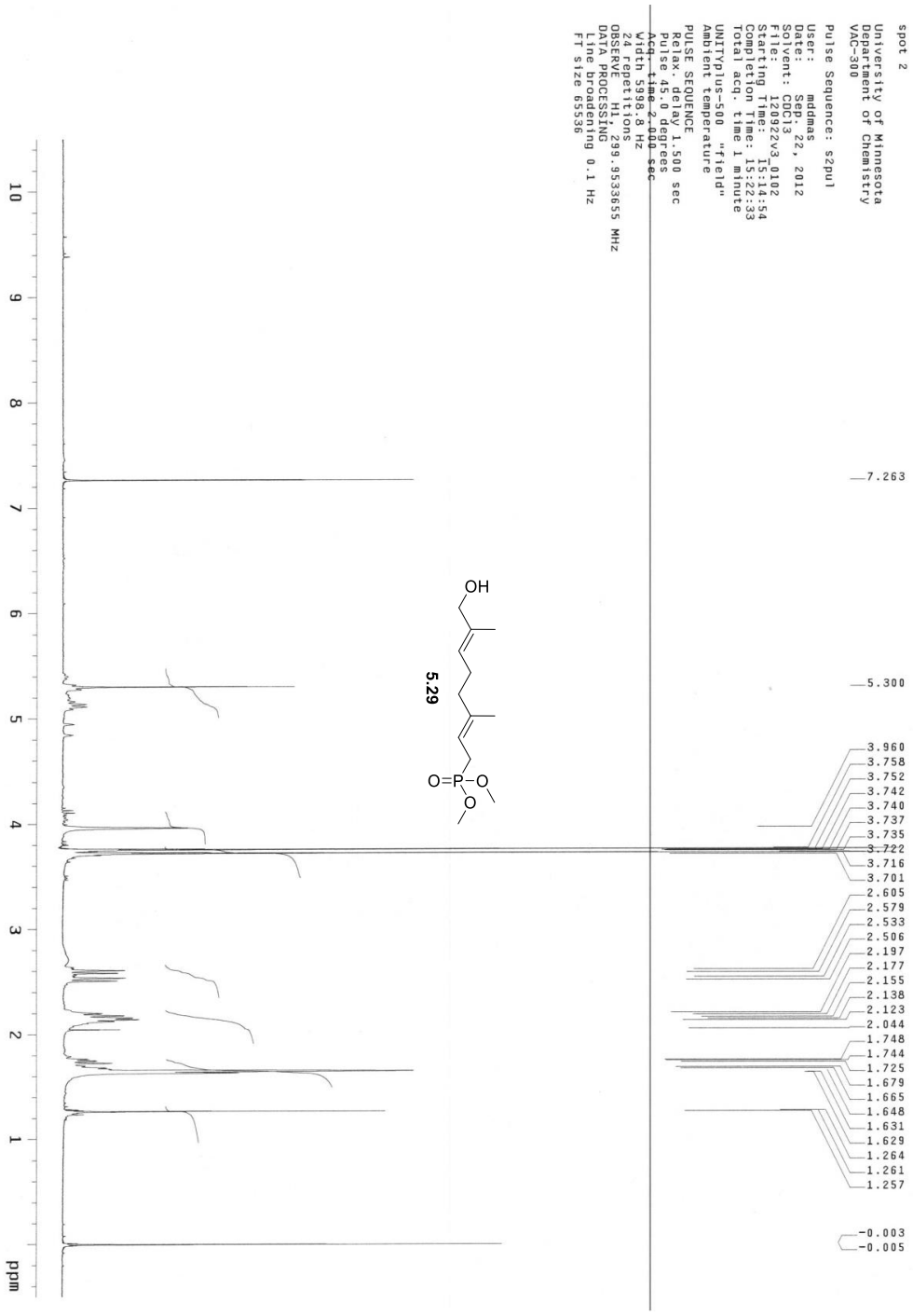

Figure 5.14. ^{1}H NMR spectrum of compound **5.29**.

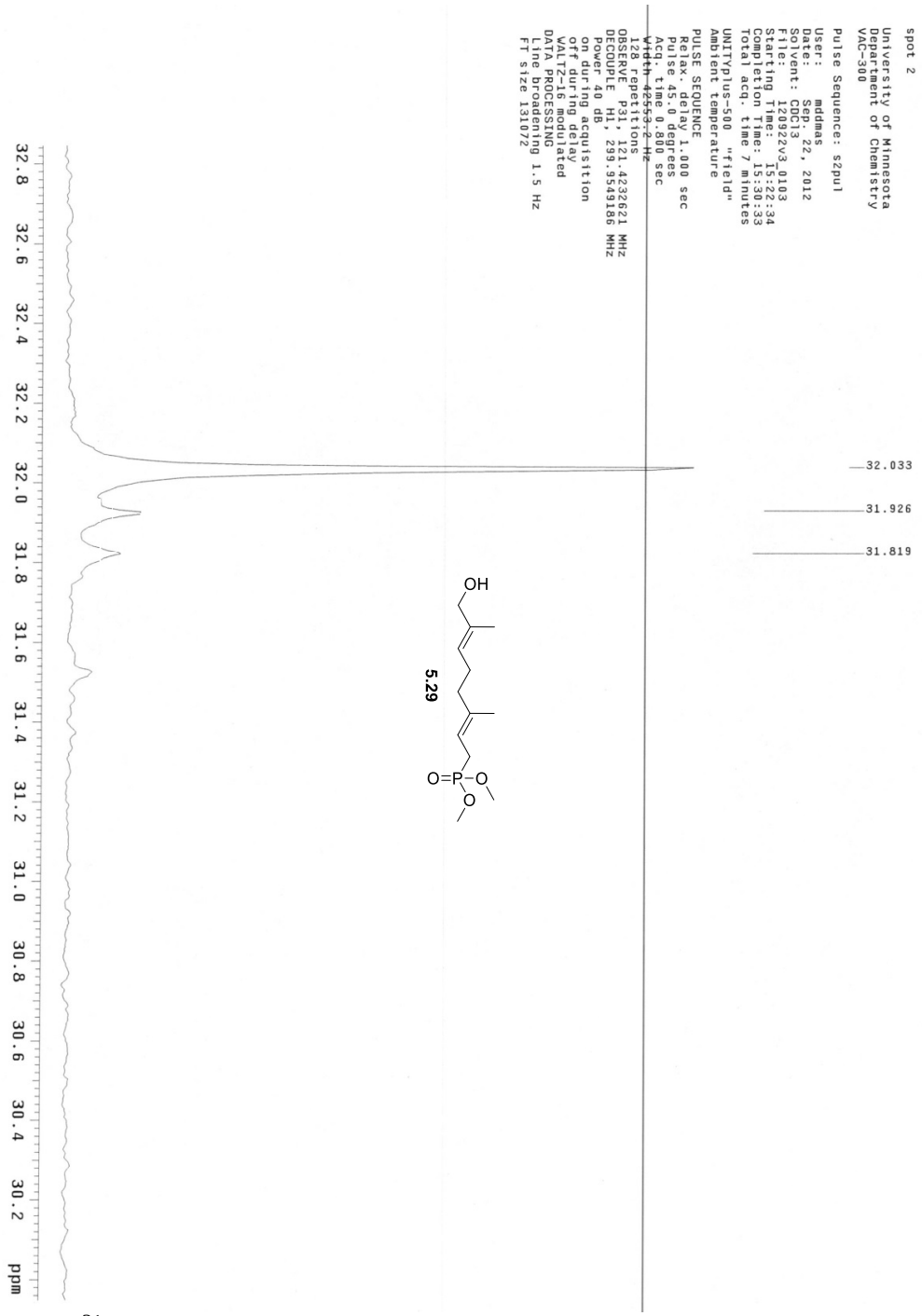

Figure 5.15. ^{31}P NMR spectrum of compound **5.29**.

5.5.6 Characterization of compound 5.31

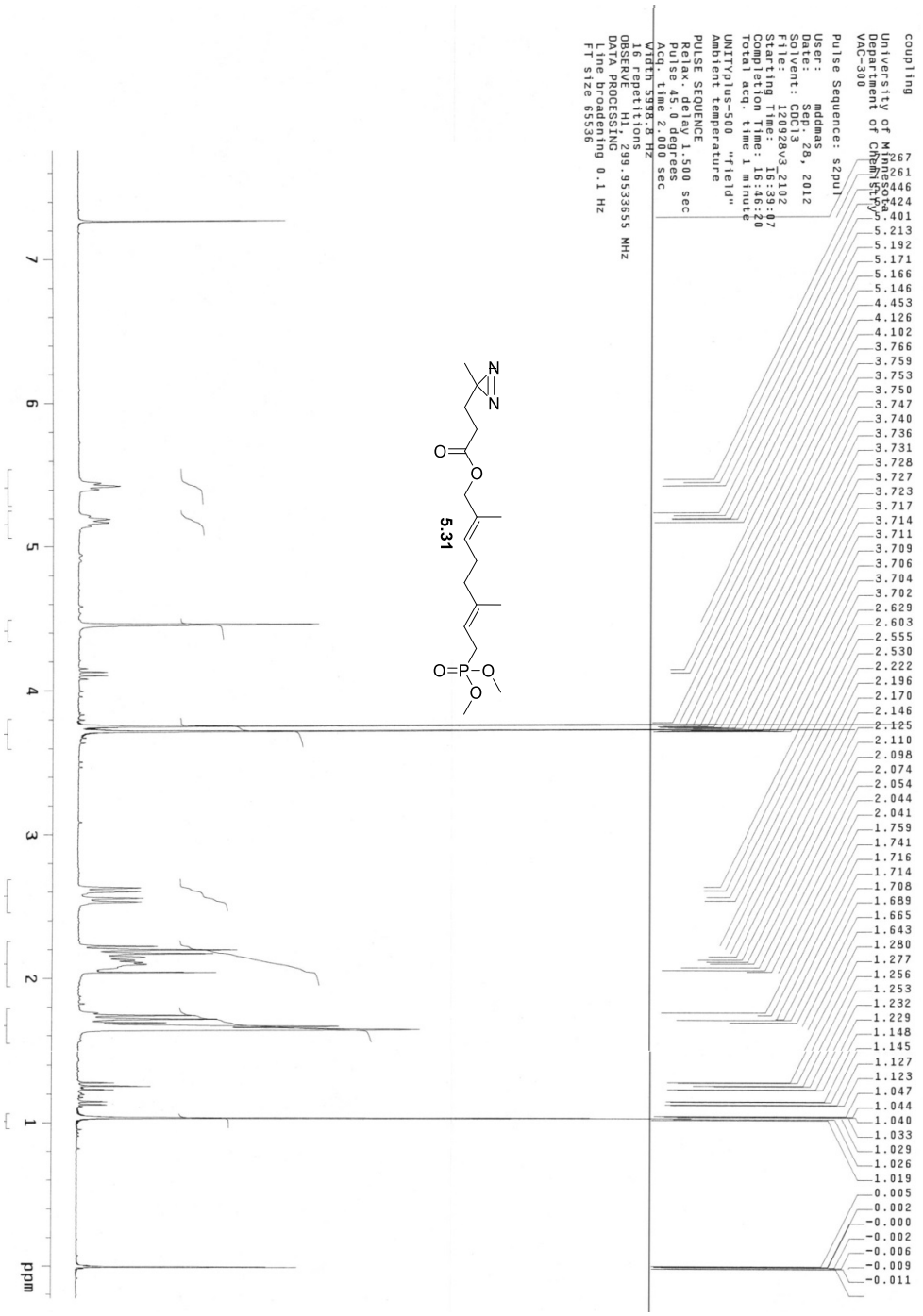

Figure 5.16. ^{1}H NMR spectrum of compound **5.31**.

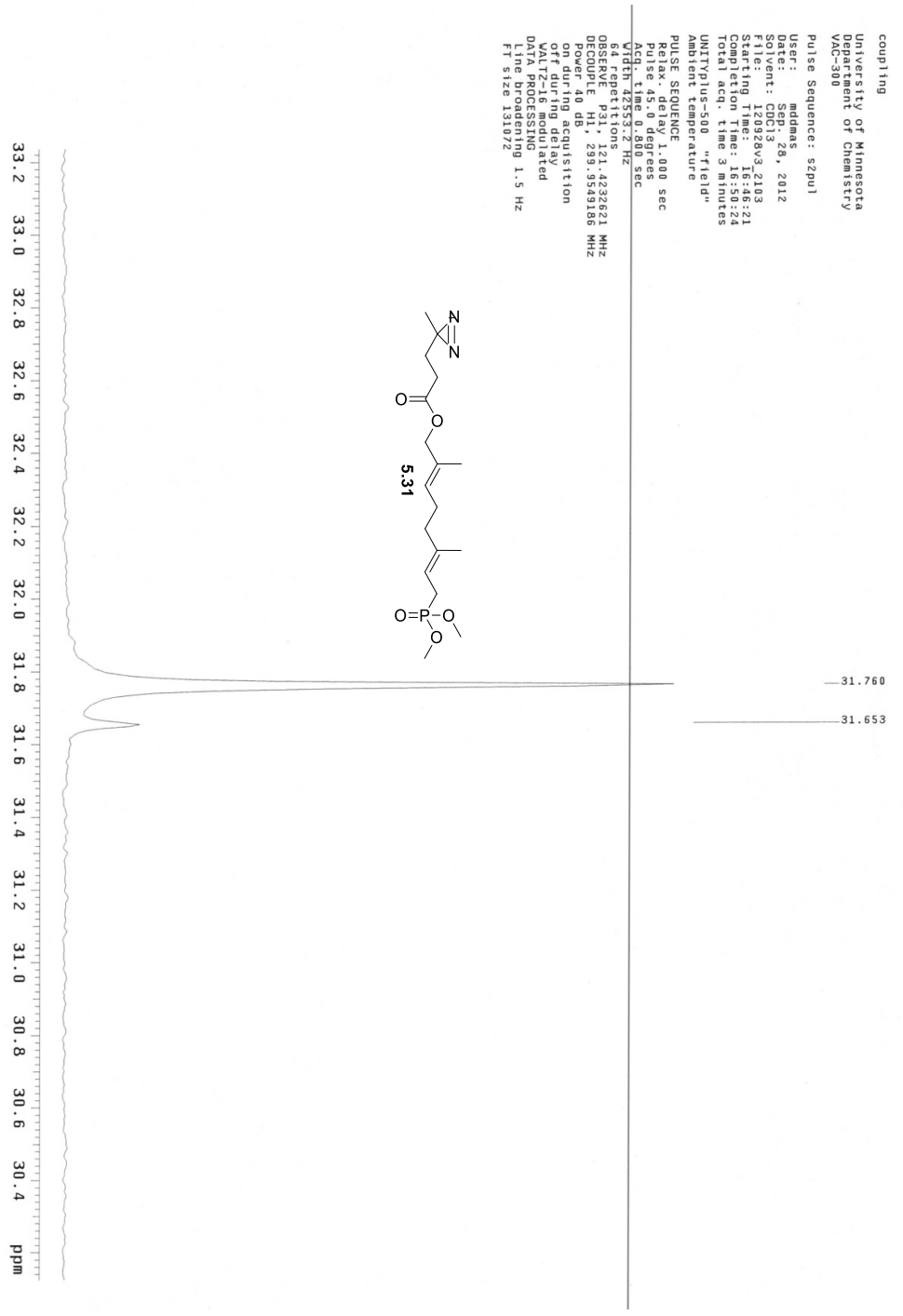

Figure 5.17. ^{31}P NMR spectrum of compound **5.31**.

5.5.7 Characterization of compound 5.7

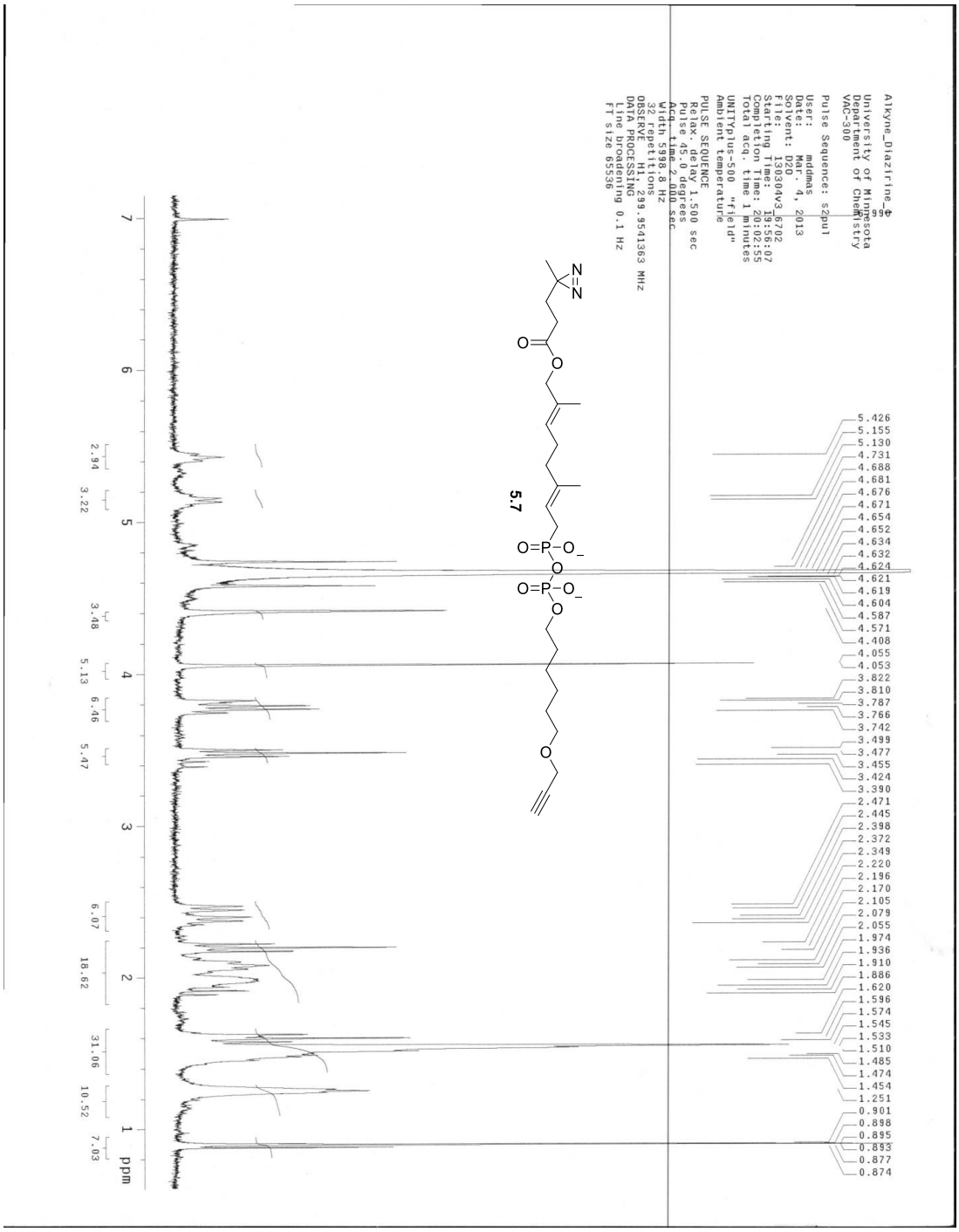

Figure 5.18. ^{1}H NMR spectrum of compound **5.7**.

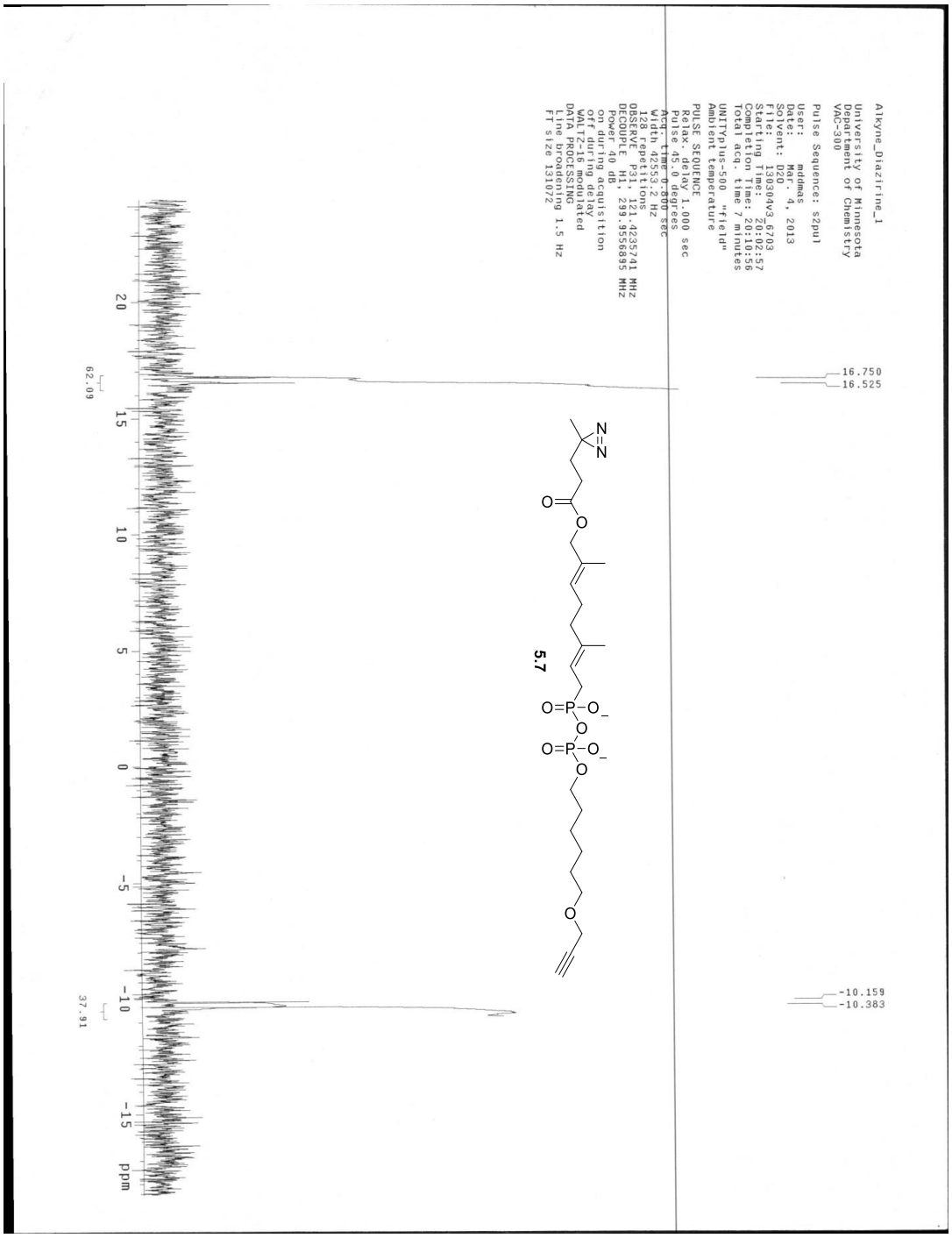

Figure 5.19. ^{31}P NMR spectrum of compound **5.7**.

5.5.8 Characterization of compound 5.35

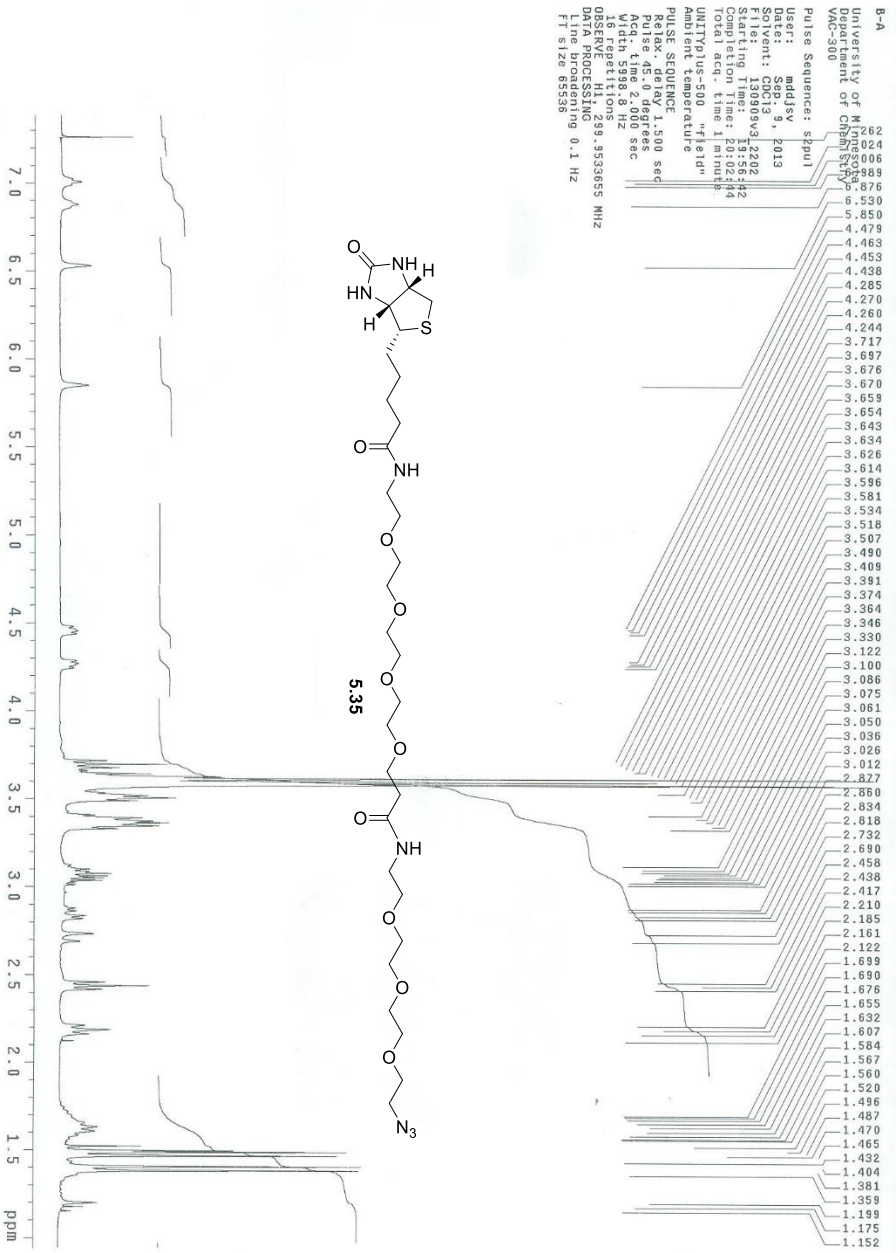

Figure 5.20. ^{1}H NMR spectrum of compound **5.35**.

5.5.9 Characterization of compound 5.9

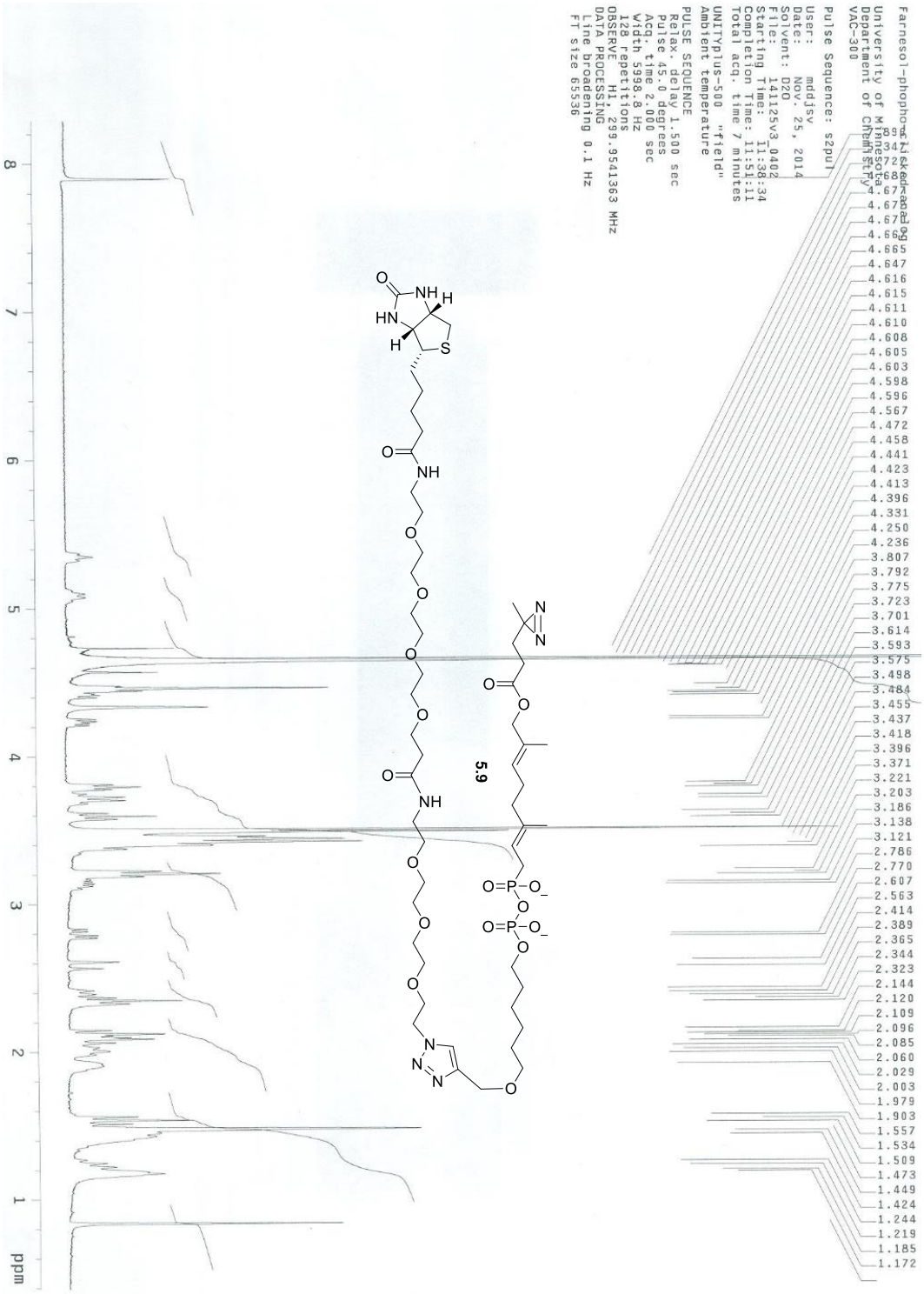

Figure 5.21. ^{1}H NMR spectrum of compound **5.9**.

5.5.10 Characterization of compound 5.28

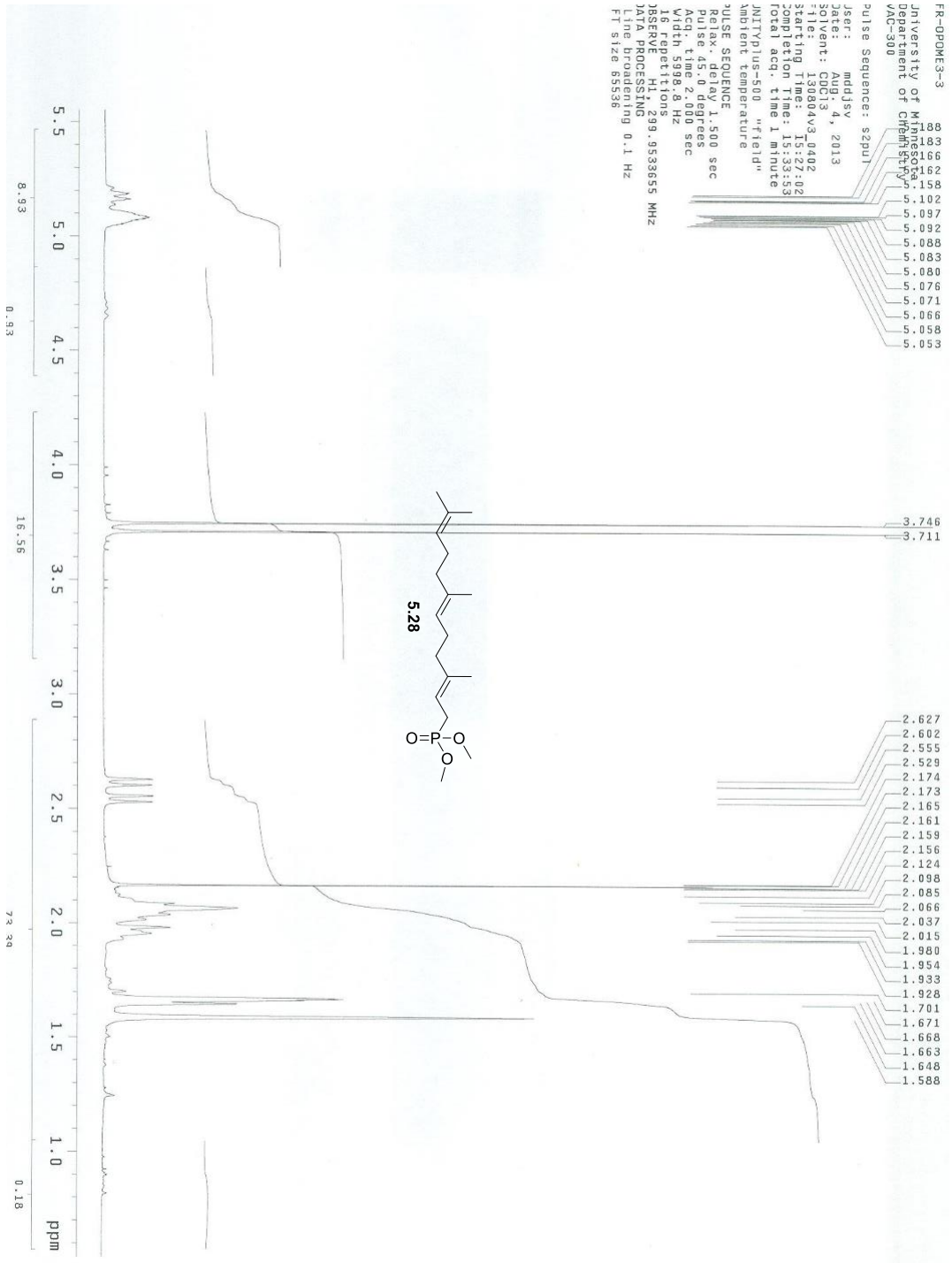

Figure 5.22. ^{1}H NMR spectrum of compound **5.28**.

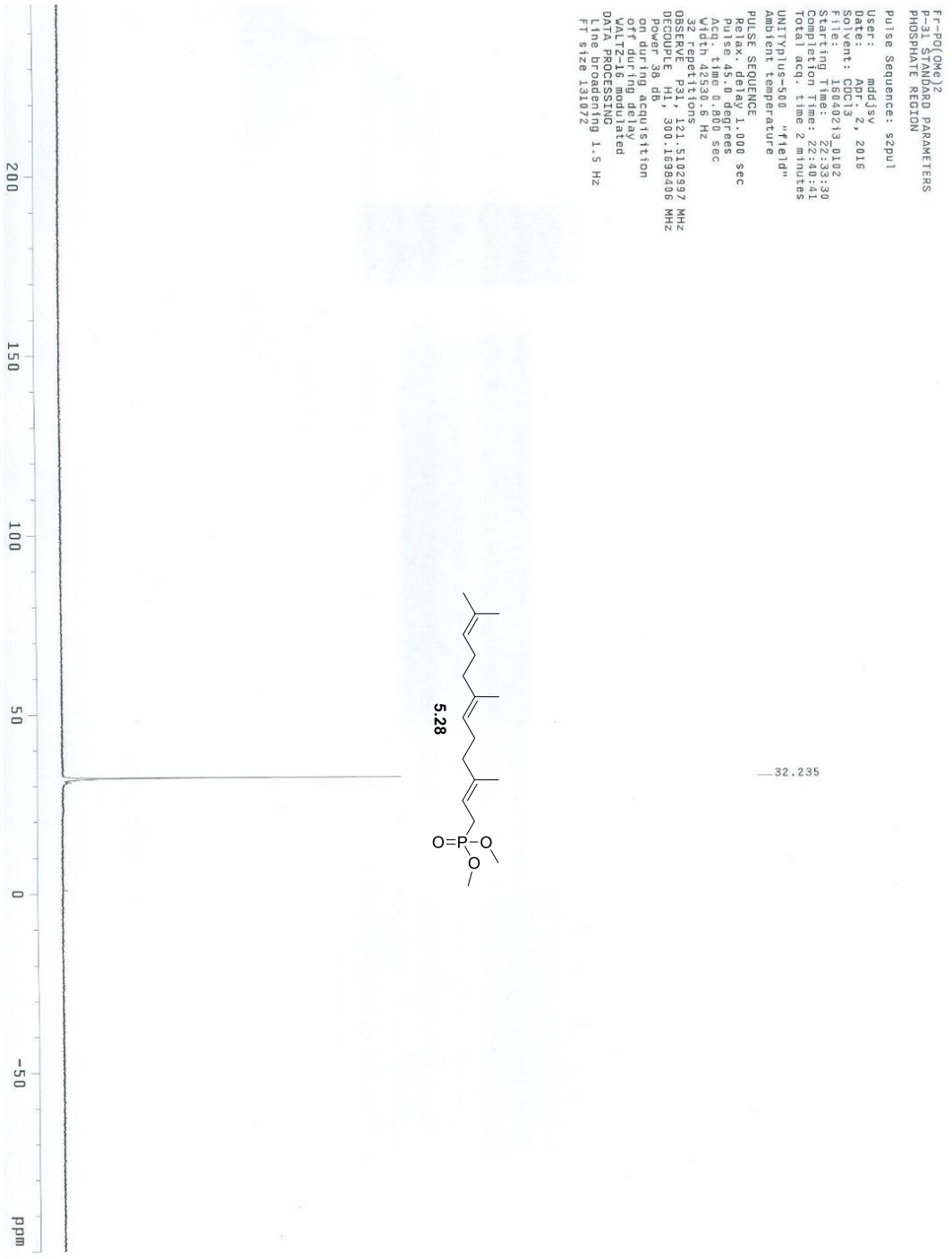

Figure 5.23. ^{31}P NMR spectrum of compound **5.28**.

5.5.11 Characterization of compound 5.30

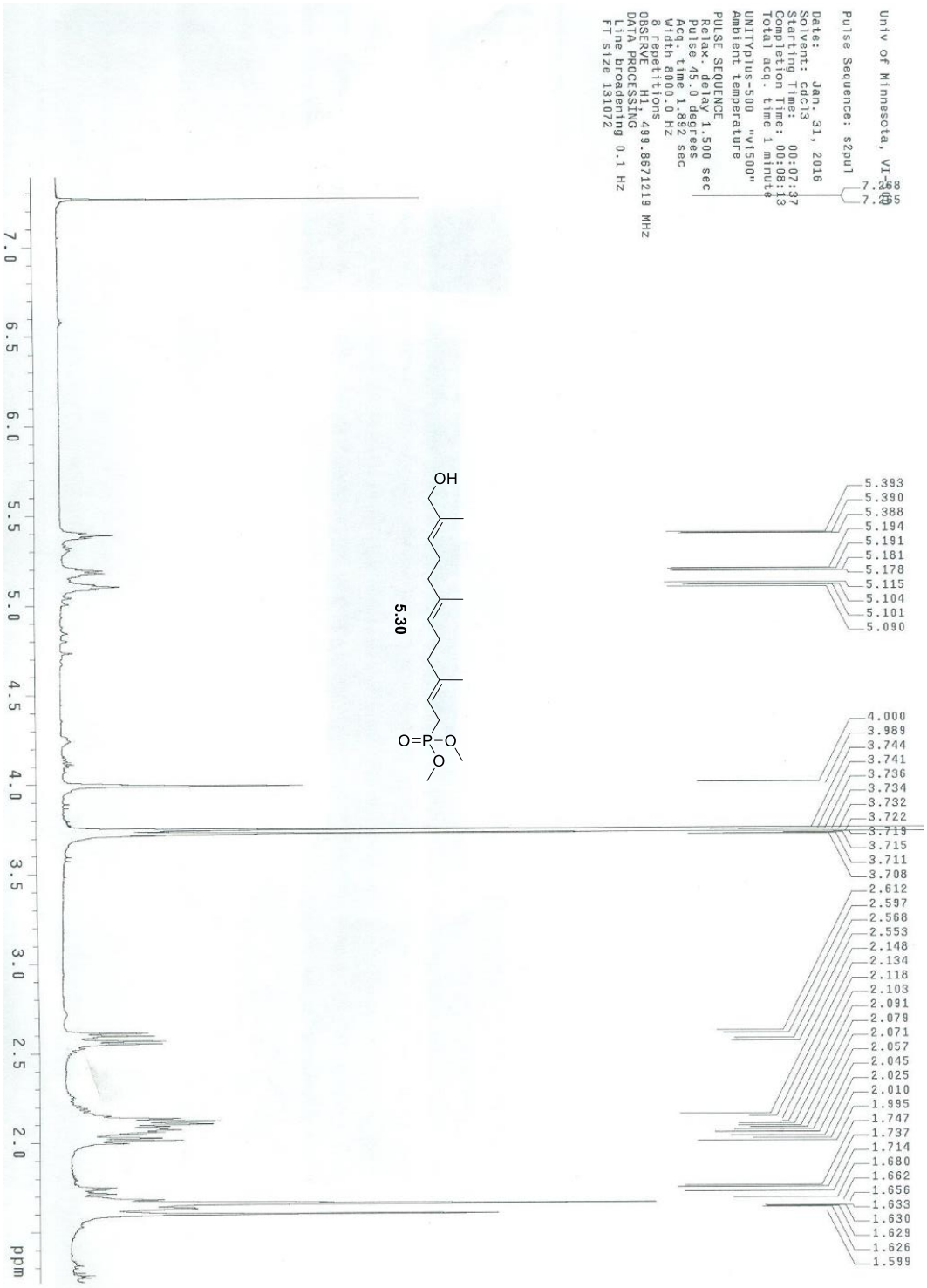

Figure 5.24. ^{1}H NMR spectrum of compound **5.30**.

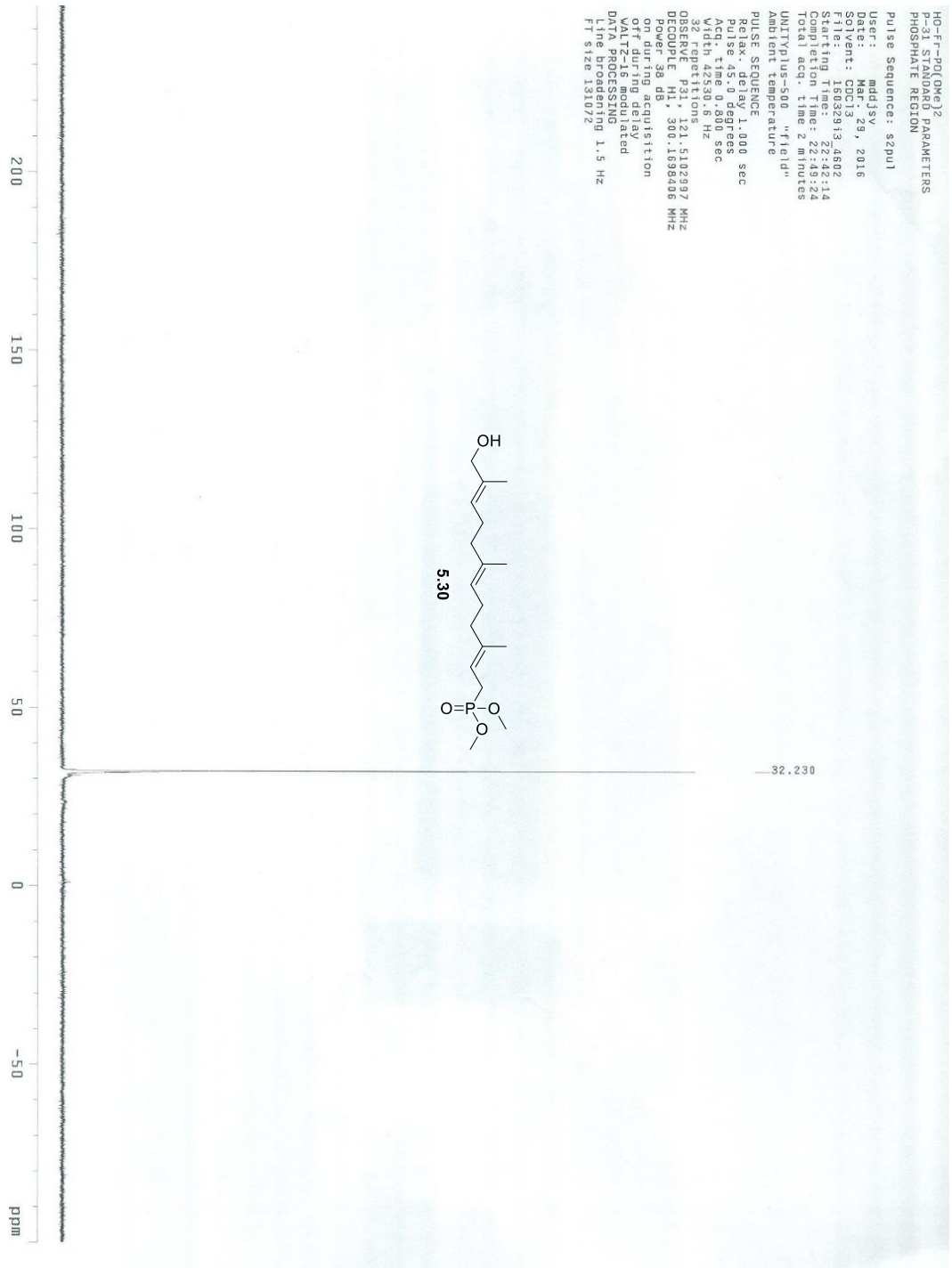

Figure 5.25. ^{31}P NMR spectrum of compound **5.30**.

5.5.12 Characterization of compound 5.32

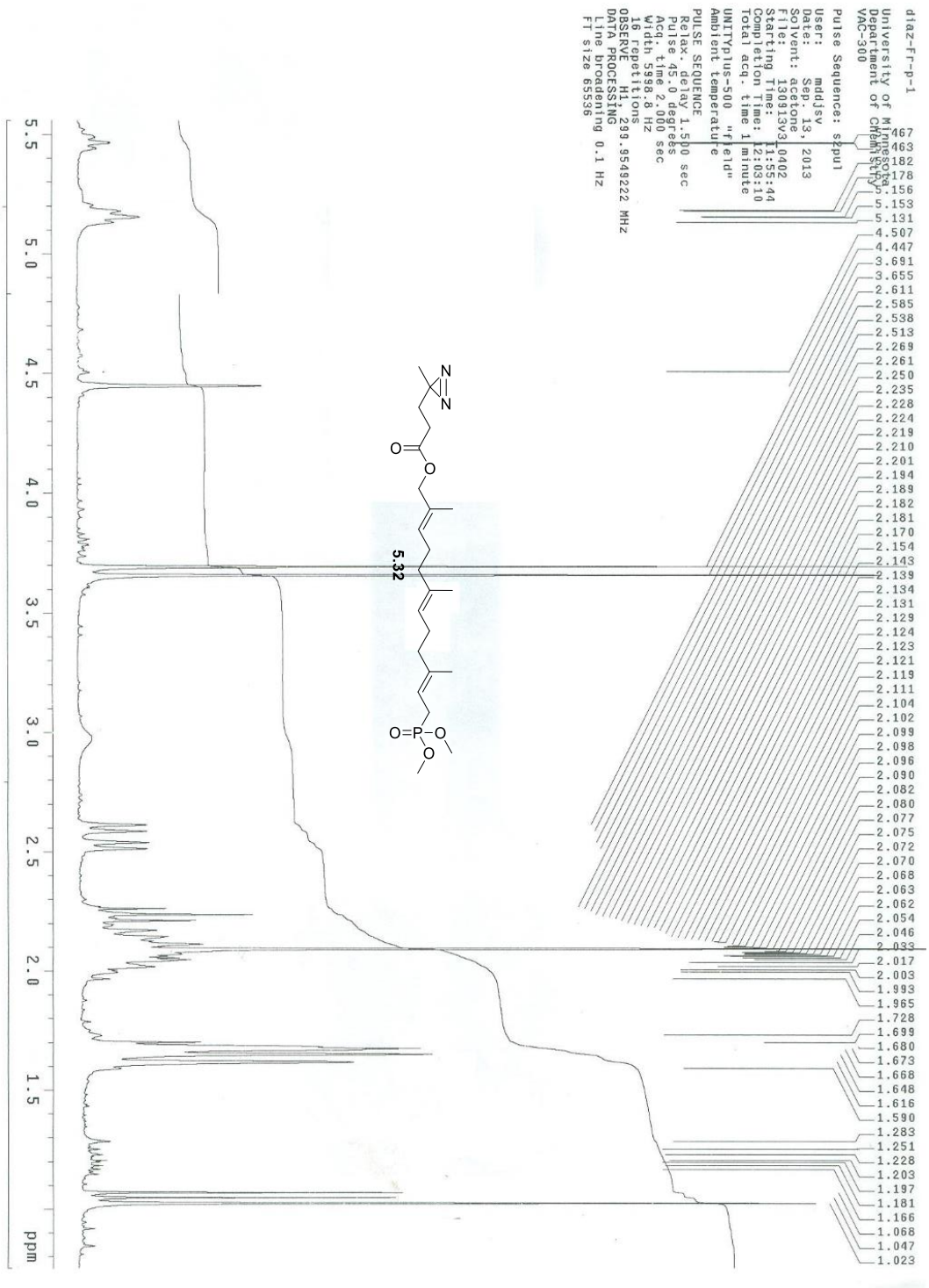

Figure 5.26. ^{1}H NMR spectra of compound **5.32**.

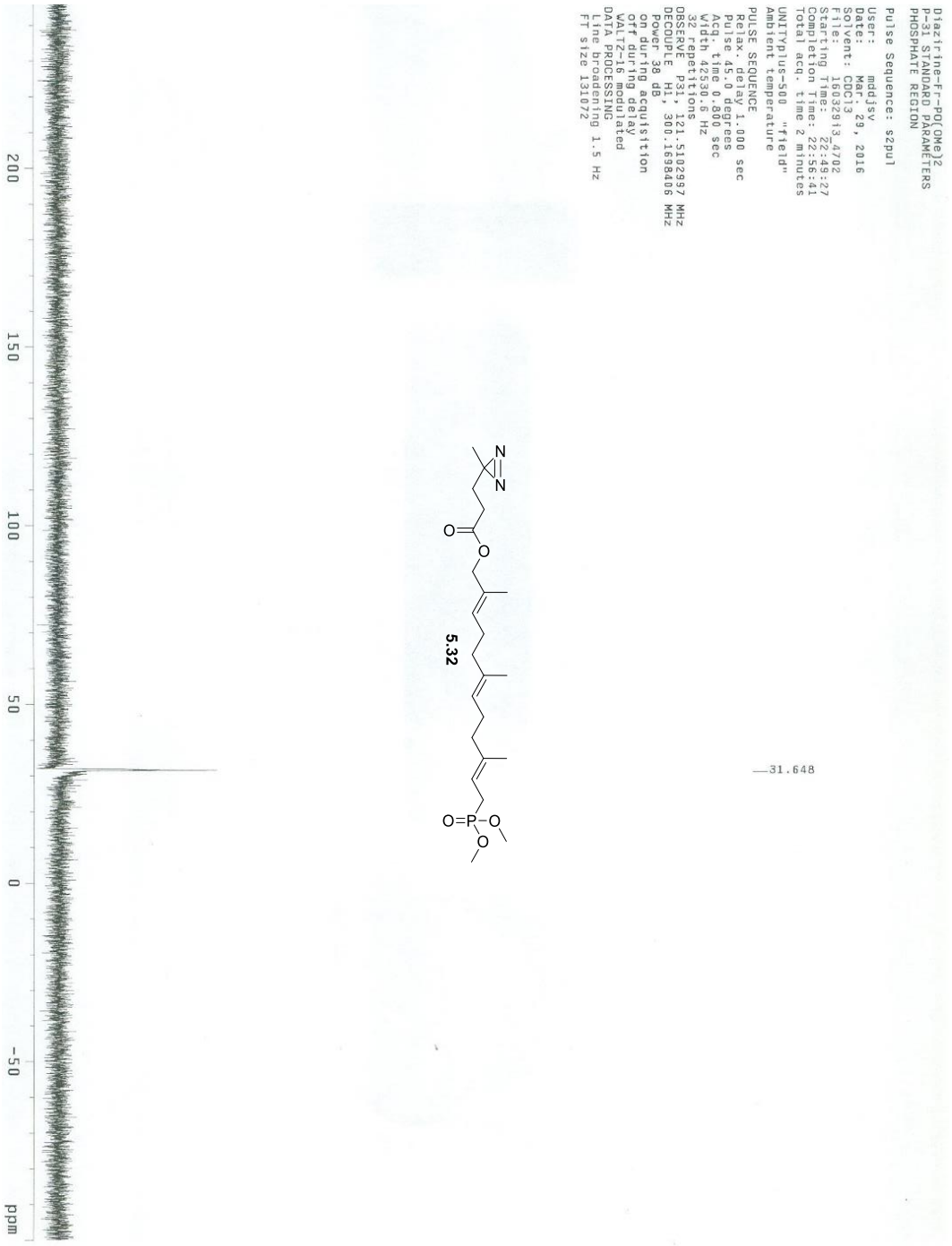

Figure 5.27. ^{31}P NMR spectrum of compound **5.32**.

5.5.13 Characterization of compound 5.8

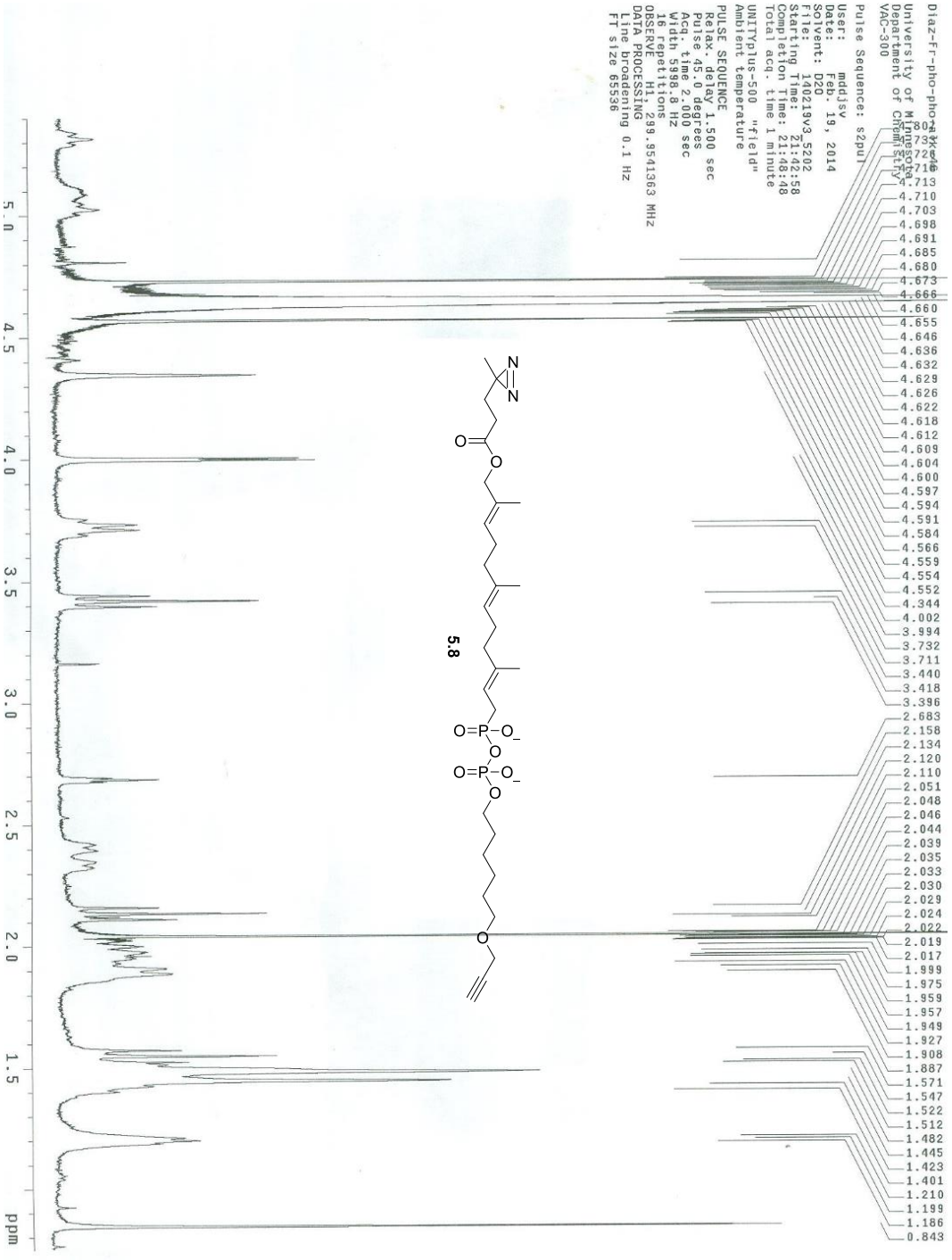

Figure 5.28. ^{1}H NMR spectrum of compound **5.8**.

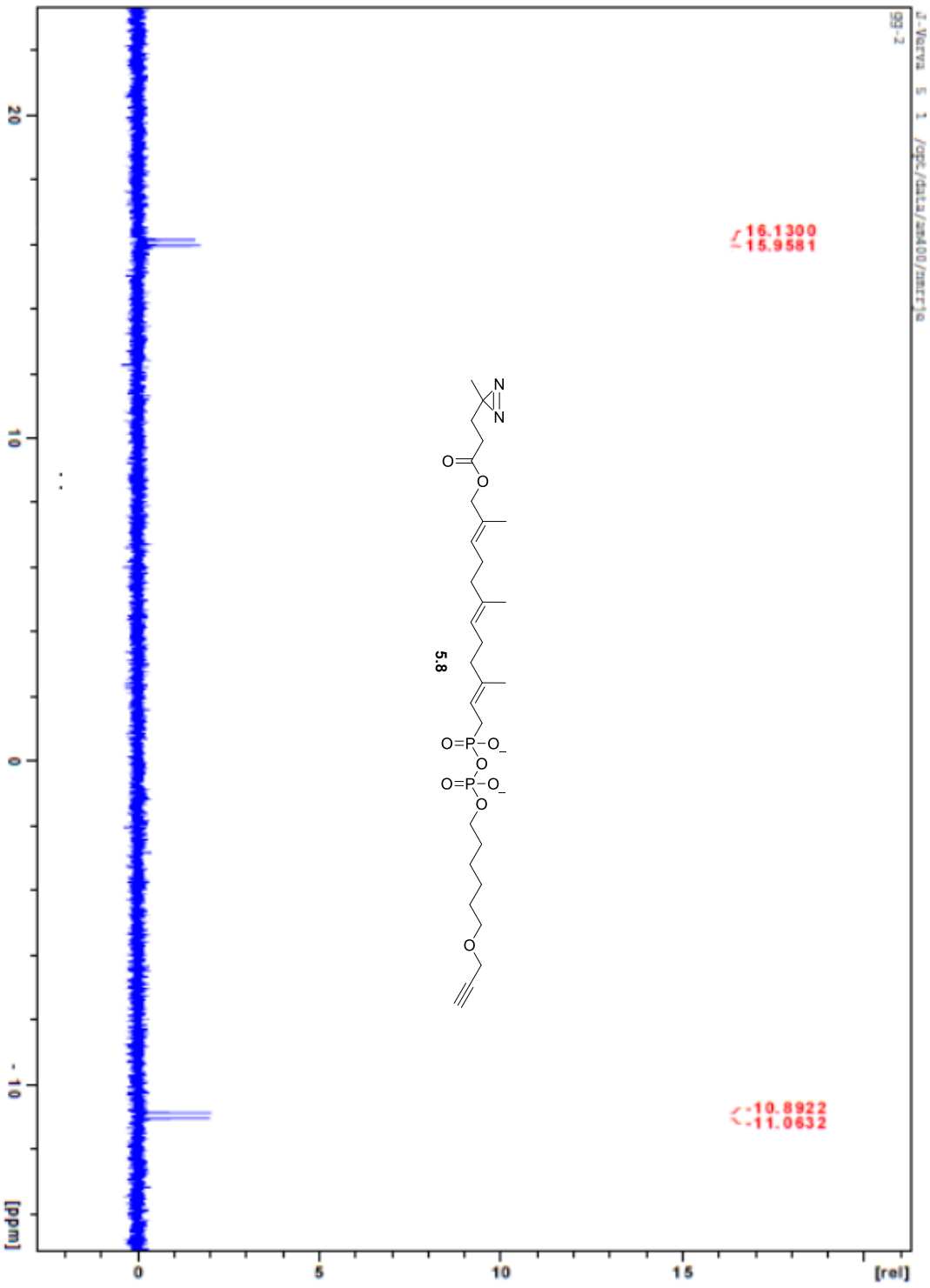

Figure 5.29 ^{31}P NMR spectrum of compound **5.8**.

5.5.14 Characterization of compound 5.10

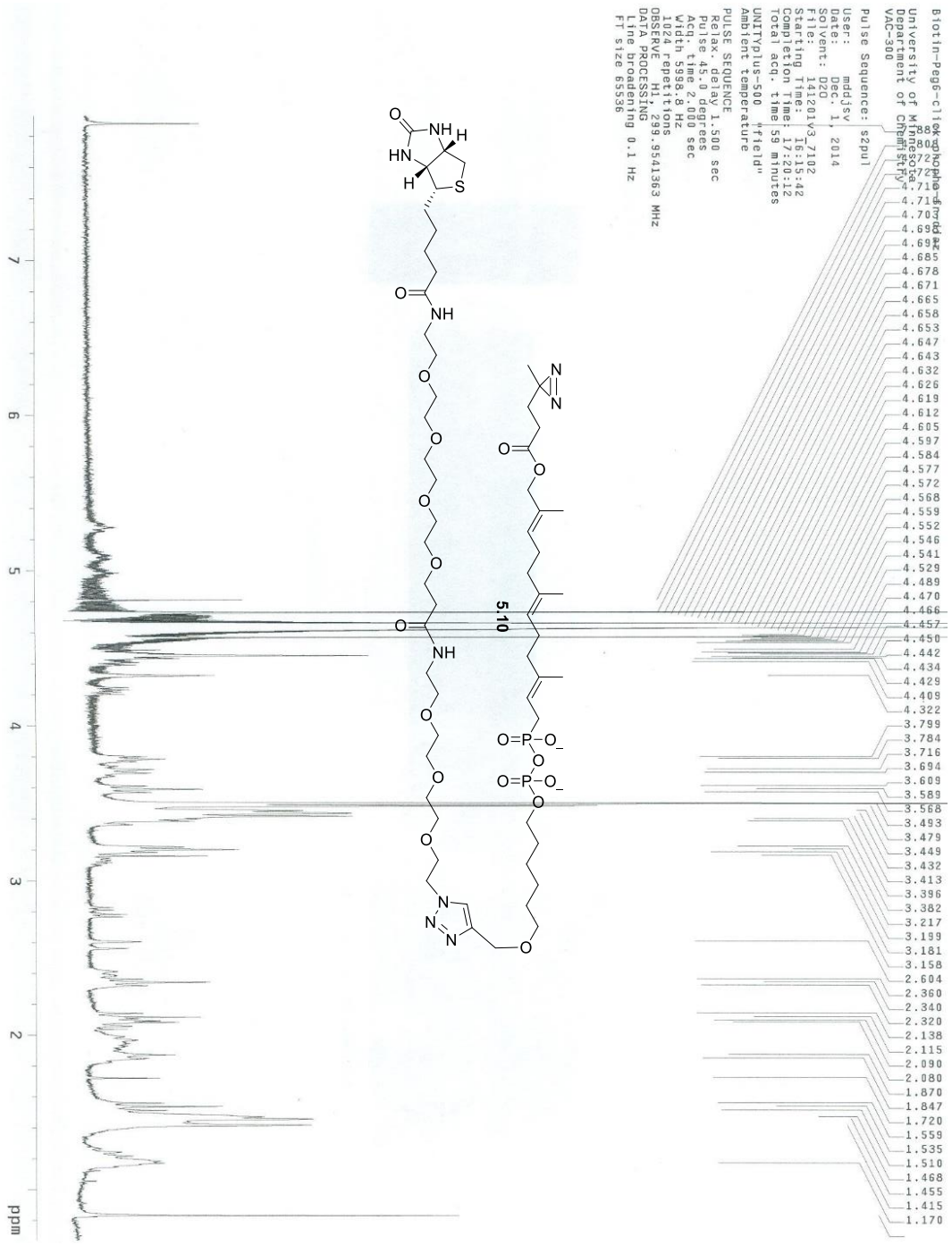

Figure 5.30. ^{1}H NMR spectrum of compound **5.10**.

Chapter 6: Synthesis and Evaluation of Bisubstrate Inhibitor for Icmt

6.1 Introduction

Among the many proteins in a mammalian host, roughly 2% of the proteome undergo the post-translational modification known as prenylation.[5] A specific superfamily of prenylated proteins, known as Ras, has been a focus for anti-cancer research, due to studies relating Ras mutations with approximately 20-30% of known cancer.[6] Ras proteins are translated with a CAAX motif that is first prenylated though a thioether bond to the C-terminal cysteine residue with either a farnesyl or geranylgeranyl group catalyzed by farnesyltransferase (FTase) or geranylgenaryltransferase (GGtase), respectively.[22-24] After prenylation, the Ras protein is further processed at the endoplasmic reticulum by the endoprotease Ras converting enzyme 1 (Rce1) that cleaves the AAX tripeptide.[26,27] The new prenylcysteine carboxylate C-terminus is then methylated by the *S*-adenosyl-methionine (SAM)-dependent enzyme isoprenylcysteine carboxylmethyltransferase (Icmt).[82,83] These modifications increase protein hydrophobicity, assist in membrane localization, and facilitate signal transduction.

Following the discovery that oncogenic Ras requires prenylation for its membrane association and transforming capabilities,[201] the enzymes associated with the prenylation pathway have been targets for drug development. Of the three classes of enzymes, the protein prenyltransferases have been the primary focus for inhibitor development, with an emphasis on FTase.[5,30] To date, several FTase inhibitors have reached clinical trials; however, due to the process of alternative prenylation by GGtase, the effect of inhibitors on oncogenic Ras suppression has been limited. Turning efforts toward Rce1 and Icmt,

mice knockout studies showed that in their absence, Ras proteins were mislocalized and tumorigenesis was impaired.[36,37,103,104] Rce1 knockouts also have been shown to cause adverse effects compared to Icmt, with studies reporting induced cardiomyopathy and accelerated myeloproliferative diseases.[39,79] Given these results, attention was directed at Icmt as a target in oncogenesis.

Work to inhibit Icmt began with determining its substrate specificity. Initial studies worked with the small molecules *N*-acetyl-*S*-farnesyl-cysteine (AFC) and *N*-acetyl-*S*-geranlygeranyl-cysteine (AGGC),[19] and later S-farnesyl thiopropionic acid (FTP),[98] to show that Icmt recognition was dependent upon the isoprenylcysteine motif. With this key requirement in mind, many different structural derivatives were designed and tested as Icmt inhibitors. These derivatives of AFC and FTP included heteroatom replacements,[98,110,111] rigid carboxylic acid analogues,[123,124] amino functionality variants,[122,126-129] and modifications to the isoprenyl motif,[111,130,131,171] all of which produced inhibitors of varying effect. Advancement in high-throughput screening techniques afforded effective non-prenylcysteine inhibitors, such as cysmethynil,[138] and natural product derived inhibitors, like spermatinamine.[148-150] In addition, inhibition attempts with the byproduct of the methylation reaction, *S*-adenosylhomocysteine (SAH), were also explored. With either direct treatment of SAH or compounds that increase its endogenous pool, studies confirmed that elevated concentration of the byproduct inhibited Icmt activity;[132-135] however, other cellular SAM-dependent methyltransferases were also inhibited.

Bisubstrate analogues have been a popular approach in substrate and inhibitor design, due to their increased binding kinetics. As the name implies, bisubstrate analogues integrate the structural features of each of the two substrates, or products, into a single molecule. The substrates should bind to their target as one entity, affording stronger binding than each substrate individually. Stark et al. pioneered this approach with the development of *N*-(phosphonacetyl)-L-aspartate (PALA), which binds to aspartate transcarbamylase about 1000 times more tightly than carbamoyl phosphate alone, and similarly to L aspartate.[226] More recently, the bisubstrate approach has been shown to elucidate substrate binding sites in crystal structures,[227-229] study protein reaction mechanics,[230-232] and develop inhibitors for a wide range of enzymes.[233-237]

The importance of Icmt inhibition as a cancer therapeutic, and the lack of any Icmt specific bisubstrate inhibitor development inspired our efforts to produce compound **6.1** (Figure 6.1.) By conjugating the adenosine motif though an amide bond to *N*-acetyl-*S*-farnesyl-cysteine the first bisubstrate Icmt inhibitor was developed. Compound **6.1** was versioned to elevate the non-specific inhibition of cellular (SAM)-Dependent methyltransferases by increasing its specificity for Icmt through the affiliation with farnesylcysteine. Reaction kinetics were evaluated using mammalian Icmt and yeast Ste14p. Herein, we describe the synthesis and application the bisubstrate Icmt inhibitor **6.1**

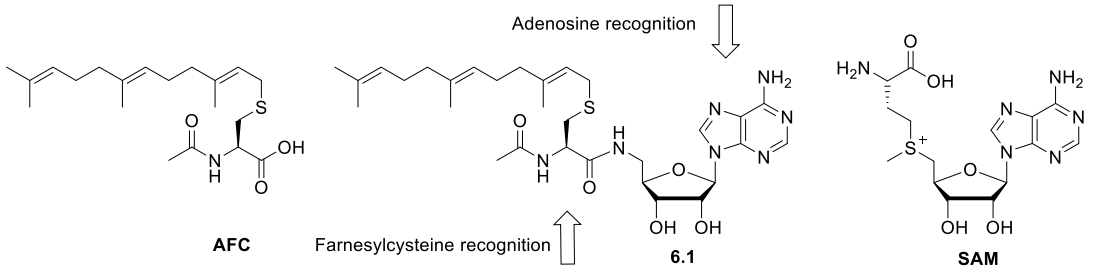

Figure 6.1. Structure of bisubstrate Icmt inhibitor **6.1**.

6.2 Results and Discussion

6.2.1 Design and synthesis of Icmt inhibitor. To prepare the desired bifunctional inhibitor for *in vitro* kinetic analyses of Ste14p and Icmt, the initial strategy was to first design a small molecule that embodied the isoprenylcysteine and *S*-adenosyl-methionine motifs. Compound **6.1** was selected as the target molecule to take advantage of the commercial availability of *N*-acetyl-*S*-farnesyl-cysteine, **6.2**, and the established synthesis of the adenosine analogue, **6.3**. Unfortunately, the coupling reaction (Scheme 6.1) produced a complex mixture of products, due to the number of exposed nucleophiles in compound **6.2**, that were too difficult to resolve by chromatographic techniques.

Scheme 6.1. Original strategy for the synthesis of bifunctional Icmt inhibitor

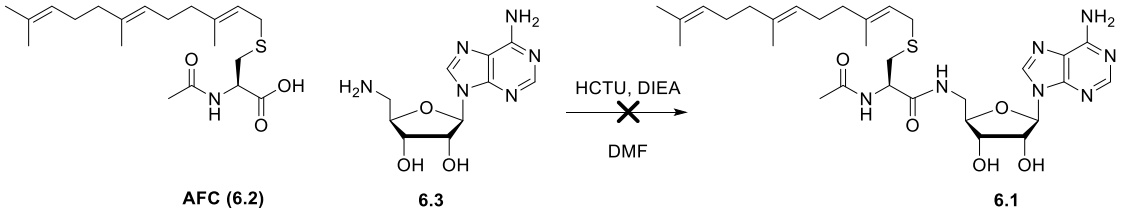

Based on the above observations, it was decided to redesign the synthesis strategy to the target compound that installs the desired amide linkage selectively by blocking reactivity of the other nucleophiles with protecting groups (Scheme 6.2). Synthesis began following the previously reported route to the protected adenosine analogue **6.7**.[238] Coupling of **6.7** and *N*-acetyl-*S*-trityl-cysteine in the presence of HCTU and DIEA

afforded the amide **6.8**. Cleavage of the acid labile protecting groups by treatment with a mixture of TFA-CH_2Cl_2-H_2O afforded compound **6.9.** Alkylation of the free thiol was performed using farnesyl bromide in the presence of $Zn(OAc)_2$ in acidic DMF to yield the prenylated molecule **6.1** whose identity was determined via ^1H NMR and ESI-MS analysis. The complex splitting patterns observed in the NMR spectra for **6.1** was deconvoluted by COSY (Figure 6.10), which showed the correct orientation of the 5 stereocenters.

Scheme 6.2. Revised synthesis of bifunctional Icmt inhibitor

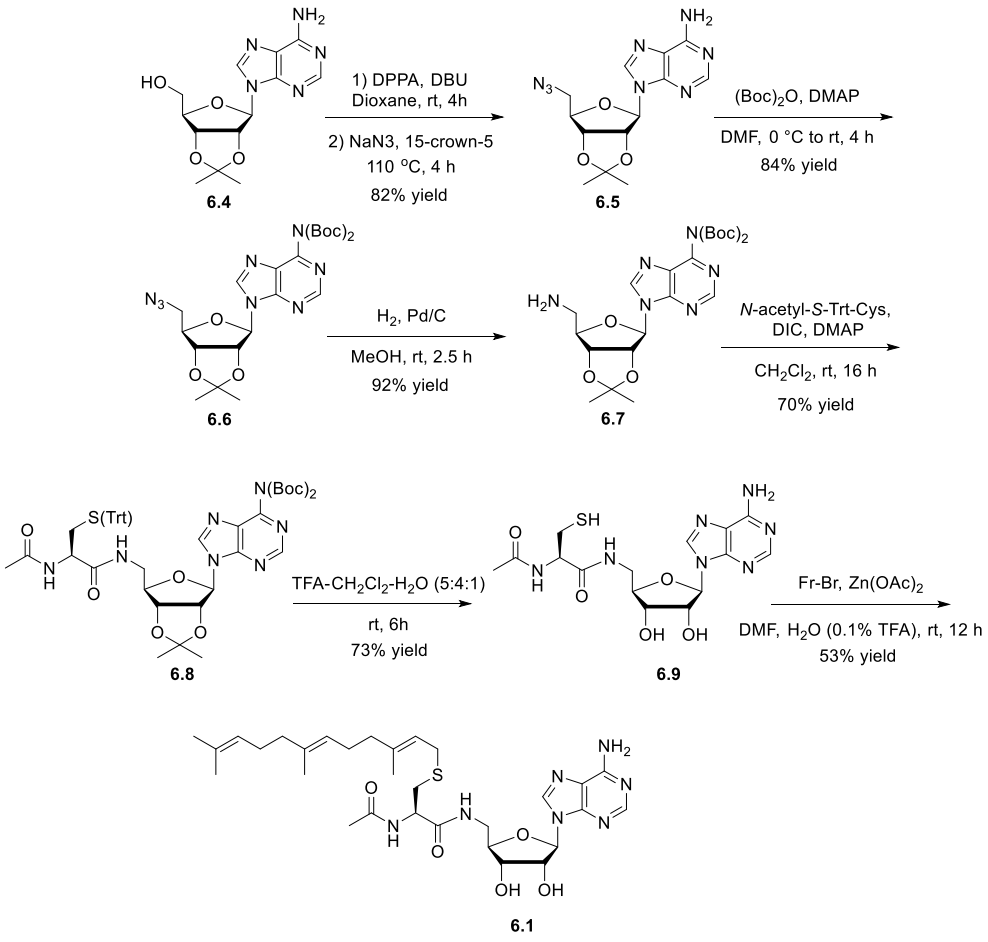

6.2.3 Bisubstrate inhibitor affects Icmt processing but not Ste14p. To test the bisubstrate compound, **6.1**, as an inhibitor for Icmt, we used recombinant $His_{10}myc_3N$-Icmt (His-Icmt) and $His_{10}myc_3N$-Ste14p (His-Ste14p). The ability of **6.1** to act as an inhibitor for His-Icmt and His-Ste14p was determined using an *in vitro* methyltransferase vapor diffusion assay.[88] The IC_{50} value (Figure 6.2) for **6.1** was measured using crude membrane extracts overexpressing hIcmt or Ste14 (5µg) in the presence of N-acetyl-S-farnesylcysteine (AFC) (10 µM), and [^{14}C]-SAM (60 µM) were added to 1 µl of inhibitor at increasing concentrations. Interestingly, inhibitor **6.1** affected mammalian Icmt activity (IC_{50} = 30 µM), but had little effect of yeast Ste14p (Figure 6.2). Although the resulting inhibitor effect is milder than other reported Icmt inhibitors, **6.1** highlights previously unappreciated inhibitor specificity differences between the different Icmts.

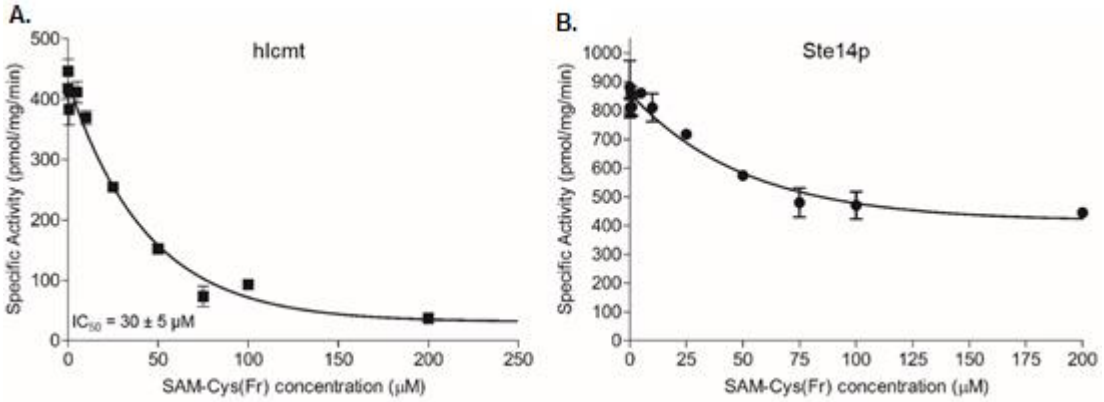

Figure 6.2. Inhibition of hIcmt and Ste14p activity by **6.1**. **6.1** was evaluated as an inhibitor in an *in vitro* methyltransferase vapor diffusion assay with hIcmt (A) and the yeast homolog, Ste14p (B). Methyltransferase activity values were plotted against inhibitor concentration and an IC_{50} value was calculated using GraphPad Prism 4.0.

6.3 Future Direction

Having determined the ability of compound **6.1** to act as a mild inhibitor for Icmt, a new bisubstrate target was envisioned that resembles the reaction transition state to a

greater extent. The design of the new bisubstrate inhibitor, **6.10** (Figure 6.3), incorporates an ethylene diamine linker between the isoprenoid and adenosine motifs. Similar to **6.1**, compound **6.10** conjugates the AFC component though an amide bond; however, the distance between AFC and the adenosine component would increase by two methane units. Additionally, the linkage to the adenosine motif facilitated though a secondary amine, which under cellular conditions is protonated, allowing the positively charged sulfur in SAM to be more accurately represented. When comparing **6.1** and **6.10**, it should also be noted that **6.1** is one methylene unit shorter than the actual transition state, and **6.10** being one methylene unit longer (Figure 6.3). Never the less, given the increased degree of rotational freedom, and the cationic element afforded through the new diamine linker, bisubstrate **6.10** should be a superior Icmt inhibitor. Efforts are underway to synthesize the new bisubstrate target.

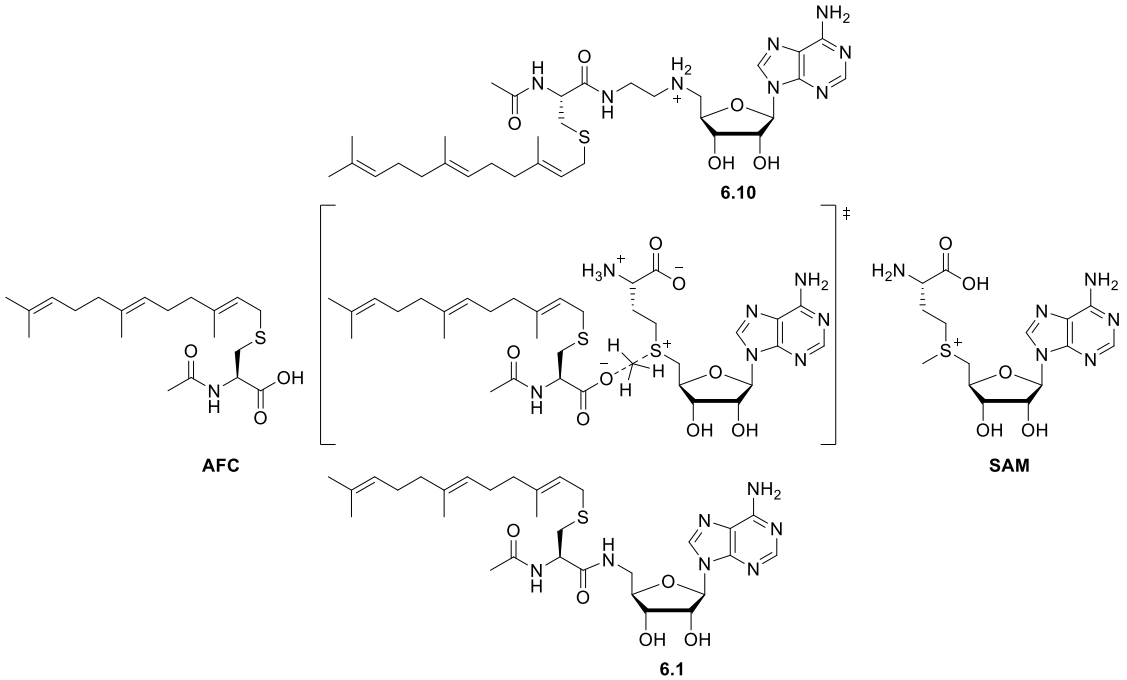

Figure 6.3. Design of new bisubstrate inhibitor **6.10**.

6.4 Materials and Methods

6.4.1 General. AFC was purchased from Enzo Life Sciences, Inc. (Farmingdale, NY). [^{14}C]-SAM was purchased from Perkin-Elmer (Waltham, MA). The anti-myc monoclonal antibody and goat antirabbit IgG were purchased from Invitrogen. Cell lines were purchased from ATCC. All other reagents and chemicals were purchased from either Sigma-Aldrich (St. Louis, MO) or Invitroge (Carlsbad, CA). Flash chromatography was performed with silica gel, 60-120 mesh. HPLC purification was performed on reverse phase c18 resin from. ^{1}H NMR spectra were obtained at 300 or 500 MHz. HR-ESI-MS analysis was performed using a Bio-TOF-II (Bruker) mass spectrometer

6.4.2 Synthesis of compound 6.5: 9-((3aR,4R,6R,6aR)-6-(azidomethyl)-2,2-dimethyltetrahydrofuro [3,4-d][1,3]dioxol-4-yl)-9H-purin-6-amine. This compound was prepared via a modification of a previously described procedure.[238] 2′,3′-*O*-Isopropylideneadenosine **6.4** (1.0 g, 3.26 mmol, 1eq) was suspended in dry 1,4-dioxane (1o mL) at room temperature under nitrogen. DPPA (1.89 g, 6.49 mmol, 2 eq) and DBU (1.49 g, 9.76 mmol, 3 eq) were added dropwise to the suspension, and the reaction mixture stirred at rt for 4 h. Sodium azide (1.06 g, 16.28 mmol, 5 eq) and 15-crown-5 (71.8 mg, 0.326 mmol, 0.1 eq) were added, and the mixture heated at 110 °C for 4 h under nitrogen. The reaction was filtered, evaporated, and then re-dissolved in $CHCl_3$ (30mL). The $CHCl_3$ solution was washed three times with water (15 mL), sat. NaCl (20 mL), and then dried over $MgSO_4$. Purification by flash column chromatography on silica gel ($CHCl_3$: MeOH, 10:1) afforded the azide **6.2** as an amorphous, yellow solid

(0.98 g, 91%): ^{1}H NMR (300 MHz, $CDCl_3$) δ: 1.40 (s, 3H), 1.62 (s, 3H), 3.60 (d, 2H, J = 5.1 Hz), 4.41 (dt, 1H, J = 3.9 Hz, 9 Hz), 5.06 (dd, *J* = 3.3 and 6.3 Hz, 1H, 3′-H), 5.43 (dd, *J* = 2.1 and 6.3 Hz, 1H, 2′-H), 5.83 (s, 2H), 6.18 (d, 1H, *J*= 1.8 Hz), 8.21 (s, 1H), 8.88 (s, 1H). HR-ESI-MS; calcd for $C_{13}H_{17}N_8O_3$ $[M+H]^+$: 333.1423, found 333.1409

6.4.3 Synthesis of compound 6.6: (9-((3aR,4R,6R,6aR)-6-(azidomethyl)-2,2-dimethyltetrahydrofuro[3,4-d][1,3]dioxol-4-yl)-9H-purin-6-yl)-N,N-bis(*tert*-butoxycarbonyl)-amide. This compound was prepared via a modification of a previously described procedure.[238] DMAP (72 mg, 0.592 mmol, 0.2 eq) and Et_3N (0.93 g, 9.14 mmol, 3.0 eq) were added to a solution of azide **6.5** (0.98 g, 2.96 mmol, 1.0 eq) in anhydrous DMF (25 mL) at 0 °C under nitrogen. Boc_2O (2.61 g, 12.0 mmol, 4.0 eq) was then added to this solution, and the mixture stirred at 0 °C for 1 h and then at rt for 4 h. The reaction mixture was filtered and evaporated. Purification by flash column chromatography on silica gel (Hexane: EtOAc, 1:1) afford compound **6.6** as an amorphous solid (1.29 g, 82%). ^{1}H NMR (300 MHz, $CDCl_3$) δ: 1.40 (s, 3H), 1.57 (2, 18H) 1.62 (s, 3H), 3.60 (d, 2H, J = 5.1 Hz), 4.41 (dt, 1H, J = 3.9 Hz, 9 Hz), 5.06 (dd, *J* = 3.3 and 6.3 Hz, 1H, 3′-H), 5.43 (dd, *J* = 2.1 and 6.3 Hz), 5.83 (s, 2H), 6.18 (d, 1H, *J*= 1.8 Hz), 8.21 (s, 1H), 8.88 (s, 1H). HR-ESI-MS; calcd for $C_{23}H_{33}N_8O_7$ $[M+H]^+$: 533.2472, found 533.2453

6.4.4 Synthesis of compound 6.7: (9-((3aR,4R,6R,6aR)-6-(aminomethyl)-2,2-dimethyltetrahydrofuro[3,4-d][1,3]dioxol-4-yl)-9H-purin-6-yl)-N,N- bis(*tert*-

butoxycarbonyl)-amide. This compound was prepared via a modification of a previously described procedure.[238] Compound **6.6** (1.29 g, 2.42 mmol, 1.0 eq) and 10% Pd on carbon (300 mg) were suspended in 9:1 MeOH–H_2O (50 mL). A balloon of hydrogen gas was attached to the reaction flask and the mixture was stirred at rt for 5 h. After reaction was judged complete by TLC ($CHCl_3$: MeOH, 10:1), the mixture was filtered through celite® 545, and evaporated affording amine **6.7** that was used in the next step without further purification (1.12g, 92%). ^{1}H NMR (300 MHz, $CDCl_3$) δ: 1.23 (s, 3H), 1.45 (2, 18H) 1.57 (s, 3H), 3.33 – 3.52 (m, 2H), 4.52 (m, 1H) , 5.33 (m, 2H), 6.18 (d, 1H, *J*= 1.8 Hz), 8.44 (s, 1H), 8.86 (s, 1H). HR-ESI-MS; calcd for $C_{23}H_{35}N_6O_7$ $[M+H]^+$: 507.2567, found 507.2589

6.4.5 Synthesis of compound 6.8: (9-((3aR,4R,6R,6aR)-6-(((S)-2-acetamido-3-(tritylthio)propanamido)methyl)-2,2-dimethyltetrahydrofuro[3,4-d][1,3]dioxol-4-yl)-9H-purin-6-yl)-*N*,N-bis(*tert*-butoxycarbonyl)-amide. *N*-acetyl-*S*-trityl-cysteine (0.213 g, 0.420 mmol, 1.0 eq), HCTU (0.174 g, 0.420 mmol, 1.0 eq), and DIEA (0.110 mg, 0.840 mmol, 2.0 eq) were dissolved in anhydrous DMF (5 mL) and stirred for 30 mins under nitrogen at rt. Amine **6.7** (0.171, 0.420 mmol, 1.0 eq) dissolved in anhydrous DMF (5 mL) was added to the mixture and stirred overnight at rt. DMF was removed under high vacuum resulting in a yellow oil. Purification my flash chromatography on silica gel (Hexane: EtOAc, 1:1) affording the coupled product **6.5** (0.263 g, 70%). ^{1}H NMR (300 MHz, $CDCl_3$) 1.31 (s, 3H), 1.55 (s, 18H), 1.583 (s, 3H), 1.88 (s, 3H), 2.53 – 2.69 (m, 2H), 3.18 (m, 2H), 4.23 (m, 1H), 4.68 (dd, 1H, J = 1.2 Hz, 6 Hz), 4.76 (m, 1H) 5.02 (t,

1H, J = 6.0 Hz), 5.38 (t, 1H, J = 4.3 Hz), 5.72 (d, 1H, J = 5.4 Hz), 6.35 (s, 1H), 6.97 – 7.40 (m, 15H), 7.84 (s, 1H), 8.34 (s, 1H). HR-ESI-MS; calcd for $C_{47}H_{55}N_7O_9S$ $[M+H]^+$: 894.3860, found 894.3823.

6.4.6 Synthesis of compound 6.9: (S)-2-acetamido-N-(((2R,3S,4R,5R)-5-(6-amino-9H-purin-9-yl)-3,4-dihydroxytetrahydrofuran-2-yl)methyl)-3-mercaptopropanamide. Compound **6.8** (0.100 g, 0.112 mmol, 1.0 eq) was dissolved in a solution of 5:1:4 TFA–H_2O–CH_2Cl_2 (10 mL) and stirred for 6h at rt. The reaction was judged complete by TLC ($CHCl_3$: MeOH, 10:1) and then diluted with H_2O (10 mL). Purification by reverse-phase HPLC with a gradient of 0 to 25% CH_3CN in H_2O (0.1% TFA) over 50 min at a flow rate of 5 mL/min afforded the deprotected product 6.6 at 10 – 12.4% CH_3CN. Lyophilization yielded a white solid (40 mg, 80%) HR-ESI-MS; calcd for $C_{15}H_{22}N_7O_5S$ $[M+H]^+$: 412.1403, found 412.1385

6.4.7 Synthesis of compound 6.1: (S)-2-acetamido-N-(((2R,3S,4R,5R)-5-(6-amino-9H-purin-9-yl)-3,4-dihydroxytetrahydrofuran-2-yl)methyl)-3-(((2E,6E)-3,7,11-trimethyldodeca-2,6,10-trien-1-yl)thio)propanamide (6.1) 1he free thiol compound 6.6 (40 mg, 92.2 µmol**,** 1eq) was dissolved in DMF/n-Butanol/H_2O (0.10% TFA) (5:1:1 v/v/v, 7 mL). Farnesyl bromide (66 mg, 0.312 mmol, 3.2 eq) and $Zn(OAc)_2 \cdot 2H_2O$ (67 mg, 0.233 µmol, 2.5 eq) was then added to initiate the alkylation reaction that was stirred overnight at rt. Purification by reverse-phase HPLC with a gradient of 0 to 25% CH_3CN in H_2O (0.1% TFA) over 50 min at a flow rate 5 mL/min resulted in the elution of the

desired product **6.1** at 19 – 21% CH_3CN. Lyophilization yielded a clear amorphous solid (29 mg 52%). ^1H NMR (300 MHz, $CDCl_3$) 1.56 (s, 6H), 1.58 (s, 3H), 1.65 (s 3H), 1.97 (2, 3H), 2.00 (dt, 8H, J = 7.2 Hz, 23.1 Hz,) 2.65 (dd, 1H, J = 6.6 Hz, 13.6 Hz), 2.84 (dd, 1H, J = 8.4 Hz, 13.5 Hz), 3.01 (dd, 1H, J = 6.9 Hz, 13.5 Hz), 3.13 (dd, 1H, J = 6.9 Hz, 13.5 Hz), 3.35 (m, 2H), 3.98 (dd, 1H, J = 3.9 Hz, 14.4 Hz), 4.17 (d, 1H, J = 14.4 Hz), 4.66 (t, 1H, J = 6.3 Hz), 4.84 (d, 1H, J = 7.2 Hz) 5.08 (m, 3H), 5.88 (d, 1H, 7.2 Hz), 8.22 (s, 1H), 8.55 (s, 1H). HR-ESI-MS; calcd for $C_{30}H_{46}N_7O_5S$ $[M+H]^+$: 616.3281, found 616.3254.

6.4.8 Crude Membrane Preparation. Crude membrane extracts were prepared as previously described from $His_{10}myc_3N$-Icmt (His-Icmt) and $His_{10}myc_3N$-Ste14p (His-Ste14p) yeast strains.[239,240] Briefly, yeast cells were cultured in SC-URA medium to an OD_{600} of 4.0-5.0. The cells were then harvested by centrifugation and the resulting pellet was stored at -80 °C until use. Upon thawing, the pellet was resuspended in lysis buffer (0.3 M sorbitol, 10 mM Tris-HCl, pH 7.5, 0.1 M NaCl, 5 mM $MgCl_2$, 1% aprotinin, and 2 mM AEBSF) and allowed to swell on ice for 15 min. The cells were rapidly frozen and thawed twice by submersion into liquid N_2 and room temperature respectively. The cells were then lysed by two passes through a French press at 18,000 p.s.i. The lysate was then centrifuged at 500xg to removed cell debris. The supernatant was then ultracentrifuged at 100,000xg for 1 h at 4 °C. The supernatant was then removed and the pellet was resuspended in 10 mM Tris-HCl, pH 7.5. The crude membrane extracts were separated

into aliquots, flash frozen in liquid N_2 and stored at -80 °C. Total protein concentration was determined using Coomassie Plus protein reagent (Pierce).

6.4.9 IC_{50} Methyltransferase Assays. Crude membrane extracts overexpressing hIcmt or Ste14(5µg) in the presence of a solution of Tris-HCl buffer (100 mM, pH 7.4), 10 µM *N*-acetyl-*S*-farnesylcysteine (AFC), and [^{14}C]-SAM (60 µM) were added to 1 µl of inhibitor at increasing concentrations. After incubating the samples at 37°C for 30 min, the reaction was stopped by the addition of 50 µl of 1 M NaOH/1% SDS. The reaction mixture was spotted onto filter paper. The filter paper was lodged into the neck of a scintillation tube filled with 10 mL of scintillation fluid and capped. The filter papers were removed after 2.5h and the radioactivity was quantified using a Packard 1600CA Liquid Scintillation Analyzer. IC_{50} values were calculated using GraphPad Prism 4. DMSO concentrations were kept constant at 5%

6.5 Supporting information

6.5.1 Characterization of compound 6.5

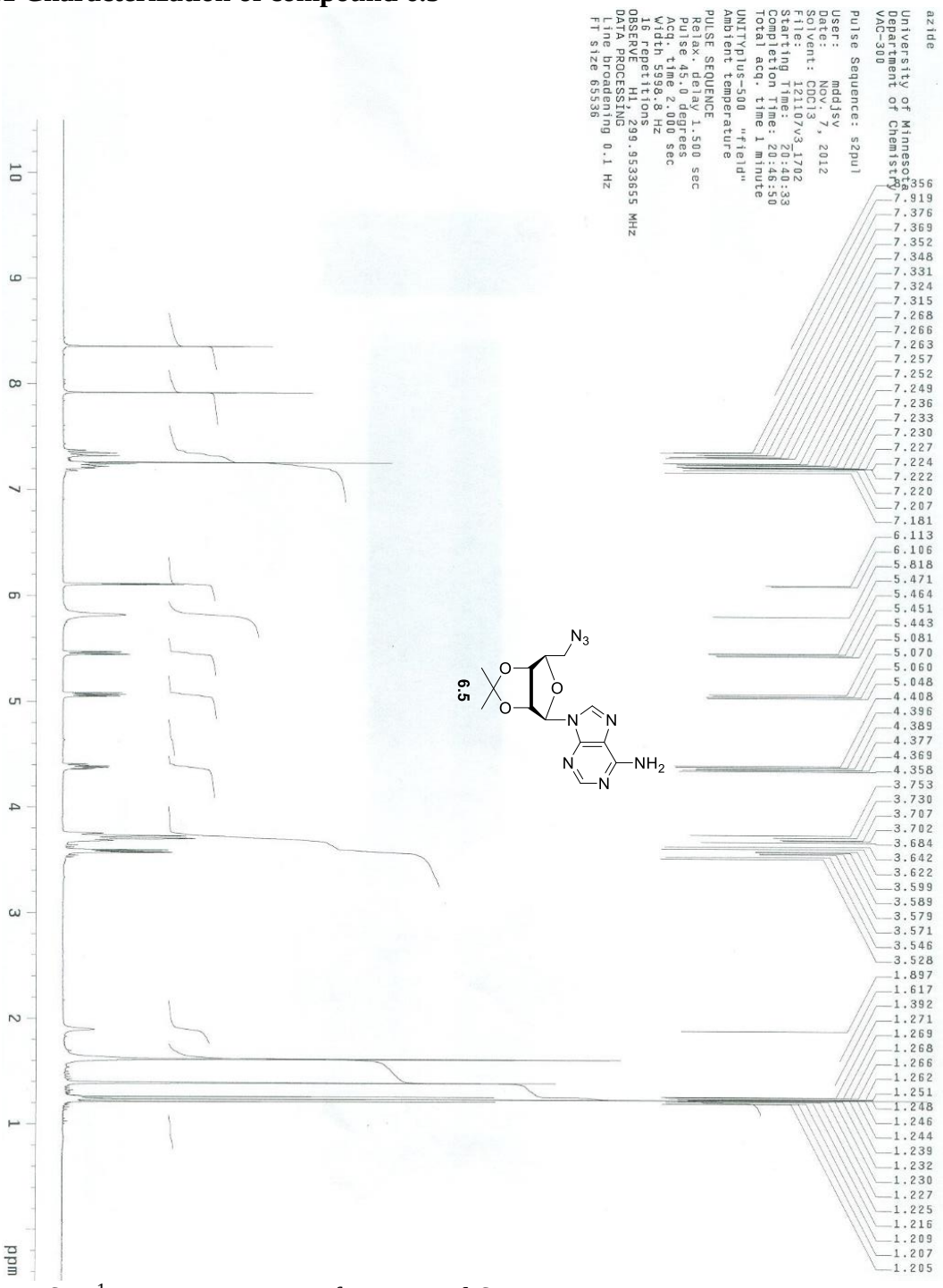

Figure 6.4. ^{1}H NMR spectrum of compound **6.5**.

6.5.2 Characterization of compound 6.6

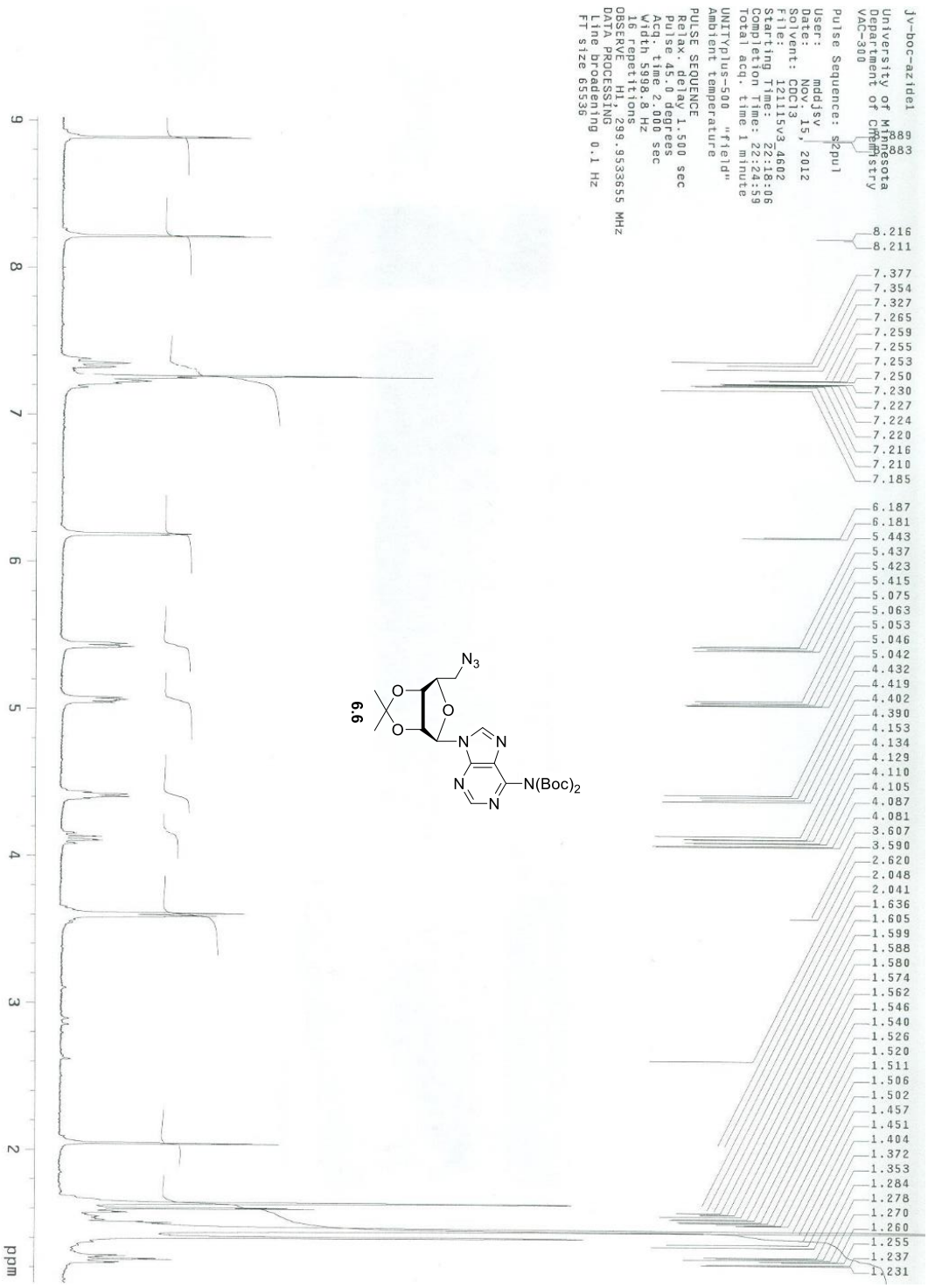

Figure 6.5. ^{1}H NMR of compound **6.6**.

6.5.3 Characterization of compound 6.7

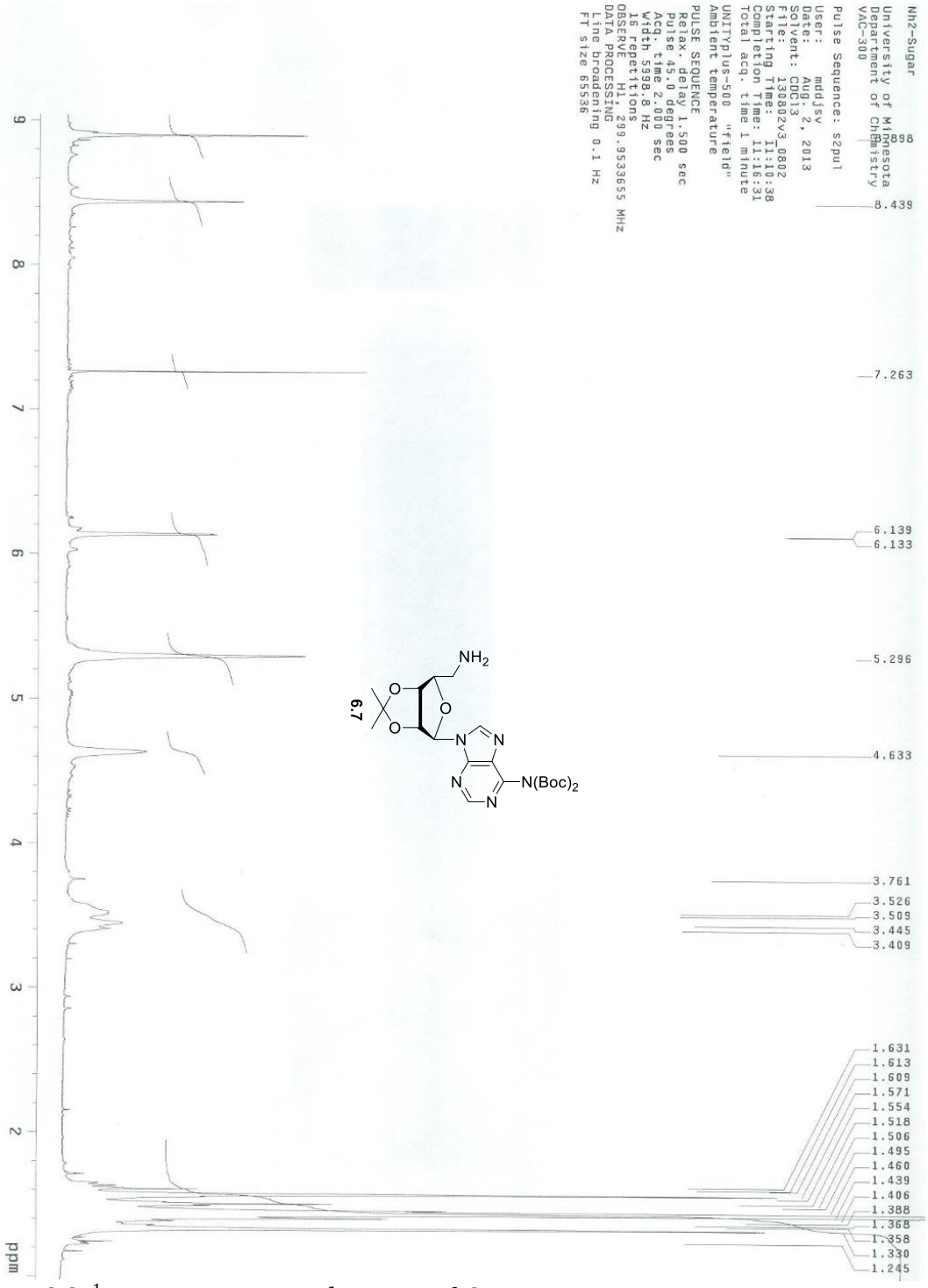

Figure 6.6. ^{1}H NMR spectrum of compound **6.7**.

6.5.4 Characterization of compound 6.8

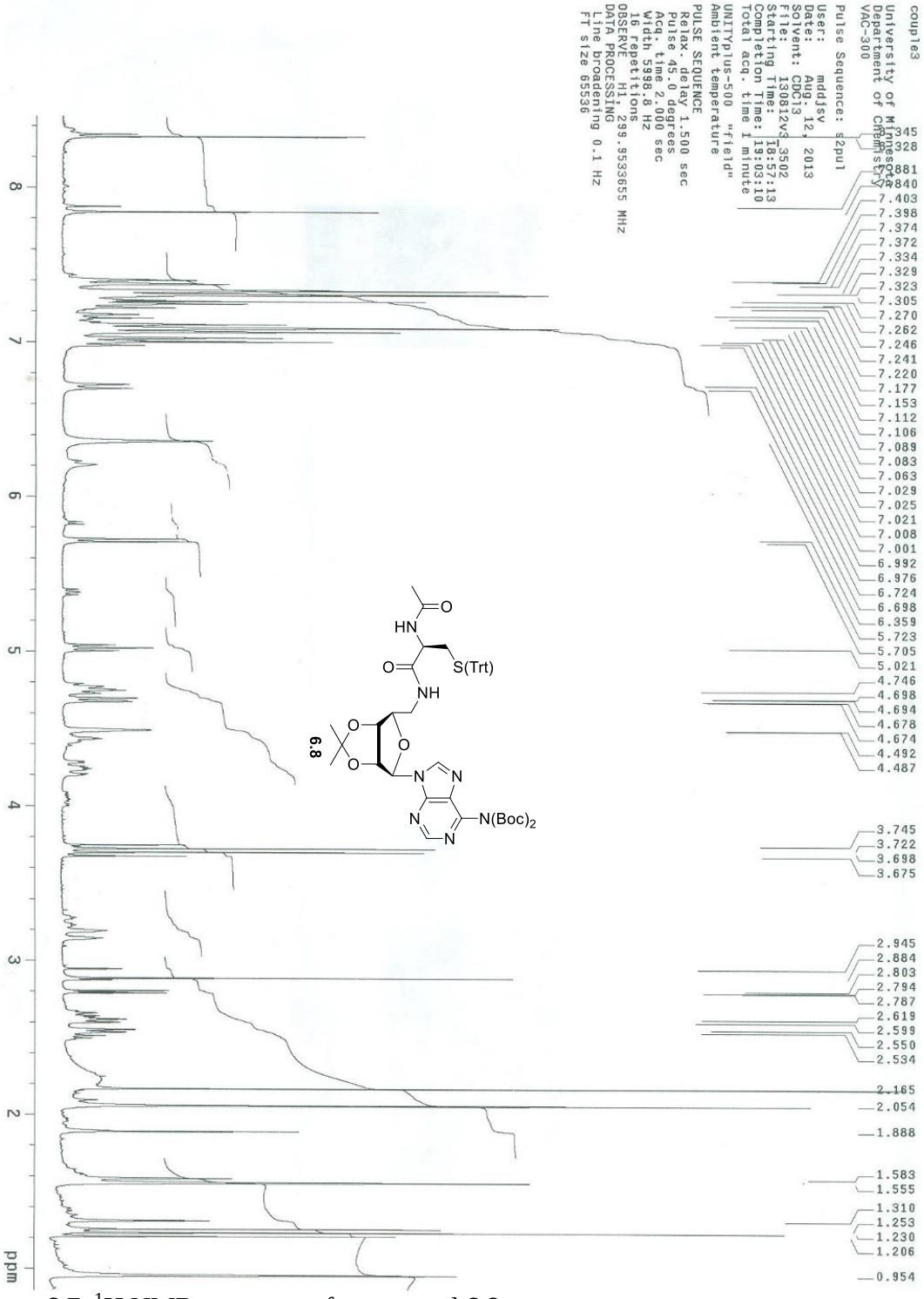

Figure 6.7. ^{1}H NMR spectrum of compound **6.8**.

6.5.5 Characterization of compound 6.9

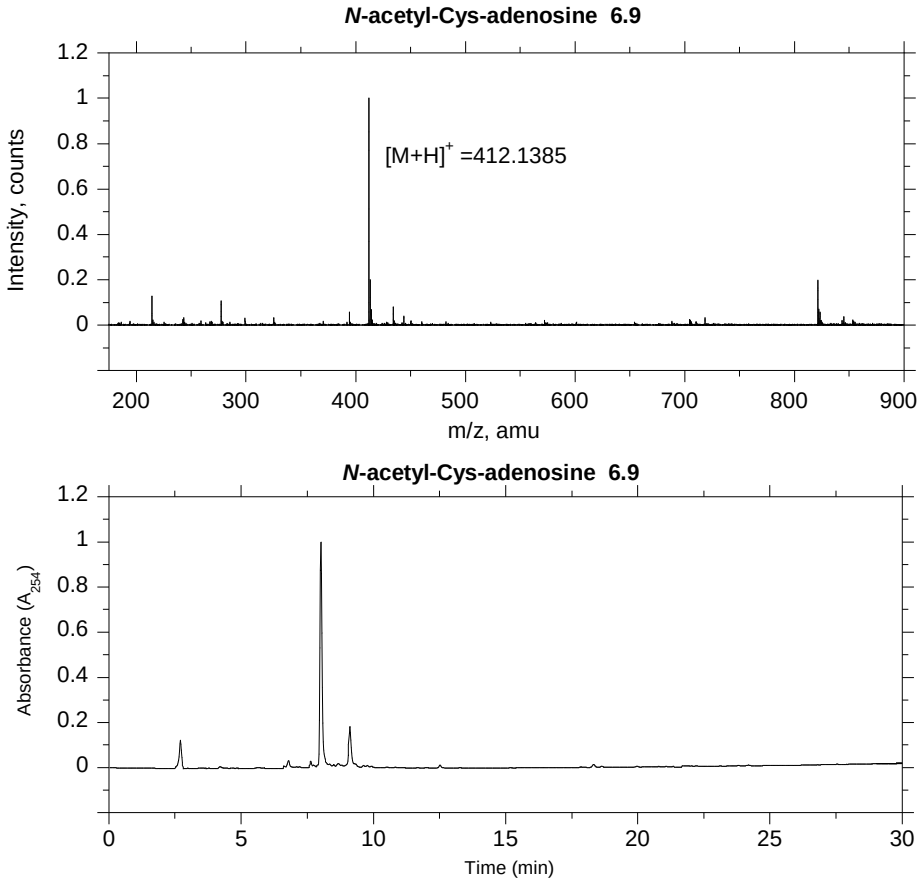

Figure 6.8. Mass spectrum and analytical RP-HPLC chromatogram for compound **6.9**. Linear gradient 0-100% CH_3CN (0.1%TFA) in 60 min, detected at 254 nm.

6.5.6 Characterization of compound 6.1

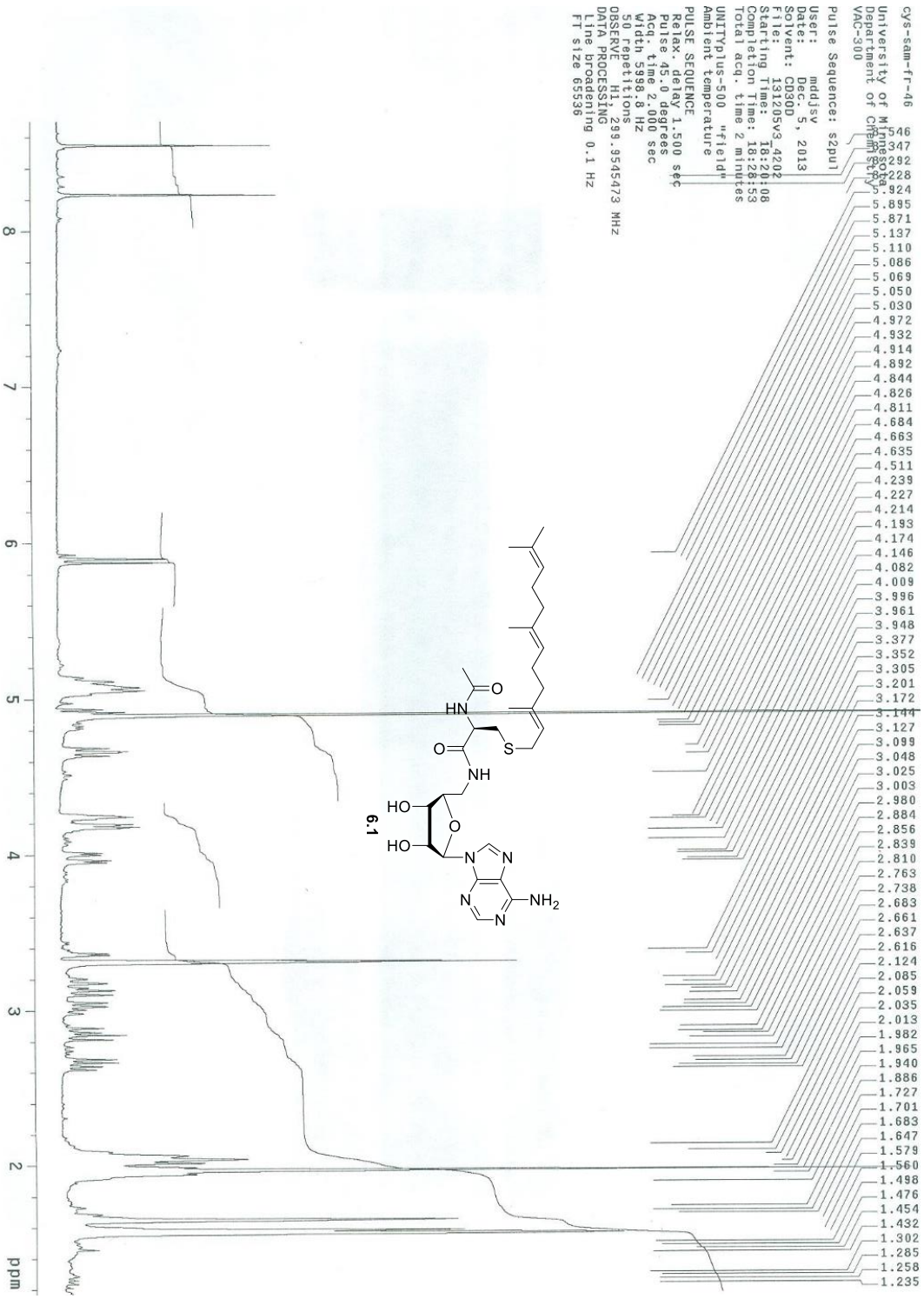

Figure 6.9. ^{1}H NMR spectrum of compound **6.1**.

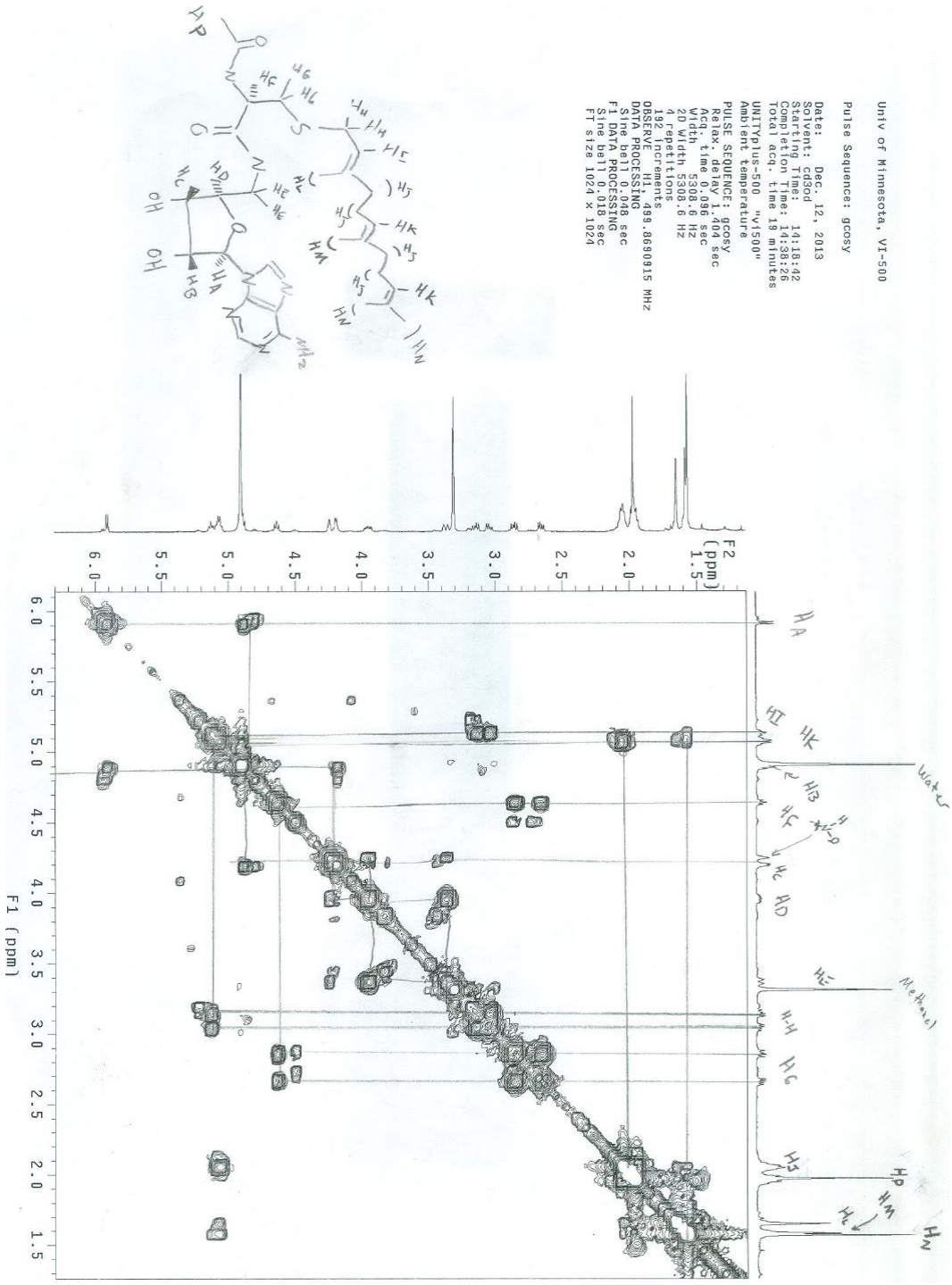

Figure 6.10. ^{1}H-^{1}H COSY NMR spectrum of compound **6.1**.

Bibilography

(1) Walsh, C. T.; Garneau-Tsodikova, S.; Gatto, G. J. *Angew. Chem Int. Edit.* **2005**, *44*, 7342-7372.
(2) Khoury, G. A.; Baliban, R. C.; Floudas, C. A. *Scientific Reports* **2011**, *1*, 90.
(3) Boyartchuk, V. L.; Ashby, M. N.; Rine, J. *Science* **1997**, *275*, 1796-1800.
(4) Nelson, D. L.; Cox, M. M. *Lehninger principles of biochemistry*; 4th ed.; W.H.Freeman & CO: New York, 2005.
(5) Ohkanda, J.; Knowles, D. B.; Blaskovich, M. A.; Sebti, S. M.; Hamilton, A. D. *Curr. Top. Med. Chem.* **2002**, *2*, 20.
(6) Bos, J. *Cancer Res.* **1989**, *49*, 843-846.
(7) Harvey, J. J. *Nature* **1964**, *204*, 1104-1105.
(8) Kirsten, W. H.; Schauf, V.; McCoy, J. *Bibl. Haematol* **1970**, *36*, 246-249.
(9) Rounds, S.; Lu, Q.; Harrington, E. O.; Newton, J.; Casserly, B. *T. Am. Clinic. Climat. Assoc.* **2008**, *119*, 155-169.
(10) Lodish, H.; Berk, A.; Zipursky, S. L.; Matsudaira, P.; Baltimore, D.; Darnell, J. *Mol. Cell Biol.*; 4th ed.; W. H. Freeman: San Francisco, 2000.
(11) McTaggart, S. J. *Cell. Mol. Life Sci.* **2006**, *63*, 255-267.
(12) Malumbres, M.; Barbacid, M. *Nat. Rev. Cancer* **2003**, *3*, 459-465.
(13) Chang, E. H.; Gonda, M. A.; Ellis, R. W.; Scolnick, E. M.; Lowy, D. R. *Proc. Natl. Acad. Sci. USA* **1982**, *79*, 4848-4852.
(14) Prior, I. A.; Lewis, P. D.; Mattos, C. *Cancer Res.* **2012**, *72*, 2457-2467.
(15) Casey, P. J.; Solski, P. A.; Der, C. J.; Buss, J. E. *Proc. Natl. Acad. Sci. USA* **1989**, *86*, 8323-8327.
(16) Hancock, J. F.; Magee, A. I.; Childs, J. E.; Marshall, C. J. *Cell* **1989**, *57*, 1167-1177.
(17) Schafer, W. R.; Kim, R.; Sterne, R.; Thorner, J.; Kim, S.-H. R., J. *Science* **1989**, *245*, 379-384.
(18) Farnsworth, C. C.; Gelb, M. H.; Glomset, J. A. *Trends Biochem. Sci.* **1990**, *15*, 139-142.
(19) Lai, R. K.; Perez-Sala, D.; Cafiada, F. J.; Rando, R. R. *Proc. Natl. Acad. Sci. USA* **1990**, *87*, 7673-7677.
(20) Maltese, W. A. *FASEB J* **1990**, *4*, 3319-3328.
(21) Mumby, S. M.; Casey, P. J.; Gilman, A. G.; Gutowski, S.; Sternweis, P. C. *Proc. Natl. Acad. Sci. USA* **1990**, *87*, 5873-5877.
(22) Manne, W.; Roberts, D.; Tobin, A.; O'Rourke, E.; De Virgilio, M.; Meyers, C.; Ahmed, N.; Kurz, B.; Resh, M.; Kung, H.-F.; Barbacid, M. *Proc. Natl. Acad. Sci. USA* **1990**, *87*, 7541-7544.
(23) Reiss, Y.; Stradley, S. J.; Gierasch, L. M. B., M. S.Goldstein, J. L. *Proc. Natl. Acad. Sci. USA* **1991**, *88*, 732-736.
(24) Schaber, M. D.; OHara, M. B.; Garsky, W. M.; Mosser, S. D.; Bergstrom, J. D.; Moores, S. L.; Marshall, M. S.; Friedman, P. A.; Dixon, R. A.; Gibbs, J. B. *J. Biol. Chem.* **1990**, *265*, 14701-14704.

(25) Ashby, M. N. *Curr. Opin. Lipidol.* **1998**, *9*, 99-102.
(26) Hrycyna, C. A.; Clarke, S. *J. Biol. Chem.* **1992**, *267*, 10457-10464.
(27) Hrycyna, C. A.; Clarke, S. *Pharmacol. Ther.* **1993**, *59*, 281-300.
(28) Hrycyna, C. A.; Clarke, S. *Mol. Cell Biol.* **1990**, *10*, 5071-5076.
(29) Hrycyna, C. A.; Sapperstein, S. K.; Clarke, S.; Michaelis, S. *Embo. J.* **1991**, *10*, 1699-1709.
(30) Zhu, K.; Hamilton, A. D.; Sebti, S. M. *Curr. Opin. Invest. Drugs* **2003**, *4*, 1428-1435.
(31) Otto, J. C.; Kim, E.; Young, S. G.; Casey, P. J. *J. Biol. Chem.* **1999**, *274*, 8379-8382.
(32) Brown, M. S.; Goldstein, J. L. *Proc. Natl. Acad. Sci. USA* **1999**, *96*, 11041-11048.
(33) Schmidt, W. K.; Tam, A.; Fujimura-Kamada, K.; Michaelis, S. *Proc. Natl. Acad. Sci. USA* **1998**, *95*, 11175-11180.
(34) Trueblood, C. E.; Boyartchuk, V. L.; Picologlou, E. A.; Rozema, D.; Poulter, C. D.; Rine, J. *Mol. Cell Biol.* **2000**, *20*, 4381-4392.
(35) Ast, T.; Michaelis, S.; Schuldiner, M. *Cell* **2016**, *164*, 103-114.
(36) Leung, G. K.; Schmidt, W. K.; Bergo, M. O.; Gavino, B.; Wong, D. H.; Tam, A.; Ashby, M. N.; Michaelis, S.; Young, S. G. *J. Biol. Chem.* **2001**, *276*, 29051-29058.
(37) Bergo, M. O.; Ambroziak, P.; Gregory, C.; George, A.; Otto, J. C.; Kim, E.; Nagase, H.; Casey, P. J.; Balmain, A.; Young, S. G. *Mol. Cell Biol.* **2002**, *22*, 171-175.
(38) Kim, E.; Ambroziak, P.; Otto, J. C.; Talyor, B.; Ashby, M. N.; Shannon, K.; Casey, P. J.; Young, S. G. *J. Biol. Chem.* **1999**, *274*, 8383-8387.
(39) Christiansen, J. R.; Kolandaivelu, S. B., M. O.; Ramamurthy, V. *Proc. Natl. Acad. Sci. USA* **2011**, *108*, 8862-8866.
(40) Dittmer, T. A.; Misteli, T. *Gernome Biol.* **2011**, *12*, 222-228.
(41) Bergo, M. O.; Gavino, B.; Ross, J.; Schmidt, W. K.; Hong, C.; Kendall, L. V.; Mohr, A.; Meta, M.; Genant, H.; Jiang, Y.; Wisner, E. R.; van Bruggen, N.; Carano, R. A. D.; Michaelis, S.; Griffey, S. M.; Young, S. G. *Proc. Natl. Acad. Sci. USA* **2002**, *99*, 13049-13054.
(42) Navarro, C. L.; Cadiñanos, J.; Sandre-Giovannoli, A. D.; Bernard, R.; Courrier, S.; Boccaccio, I.; Boyer, A.; Kleijer, W. J.; Wagner, A.; Giuliano, F.; Beemer, F. A.; Freije, J. M.; Cau, P.; Hennekam, R. C. M.; López-Otín, C.; Badens, C.; Lévy, N. *Hum. Mol. Genet.* **2005**, *14*, 1503-1513.
(43) Barrowman, J.; Michaelis, S. In *Biol. Chem.* 2009; Vol. 390, p 761.
(44) Agarwal, A. K.; Fryns, J.-P.; Auchus, R. J.; Garg, A. *Hum. Mol. Genet.* **2003**, *12*, 1995-2001.
(45) Denecke, J.; Brune, T.; Feldhaus, T.; Robenek, H.; Kranz, C.; Auchus, R. J.; Agarwal, A. K.; Marquardt, T. *Hum. Mutati.* **2006**, *27*, 524-531.
(46) Dutour, A.; Roll, P.; Gaborit, B.; Courrier, S.; Alessi, M.-C.; Tregouet, D.-A.; Angelis, F.; Robaglia-Schlupp, A.; Lesavre, N.; Cau, P.; Lévy, N.; Badens, C.; Morange, P.-E. *Hum. Mol. Genet.* **2011**, *20*, 3779-3786.

(47) Barrowman, J.; Wiley, P. A.; Hudon-Miller, S. E.; Hrycyna, C. A.; Michaelis, S. *Hum. Mol. Genet.* **2012**, *21*, 4084-4093.
(48) Tam, A.; Nouvet, F. J.; Fujimura-Kamada, K.; Slunt, H.; Sisodia, S. S.; Michaelis, S. *J. Cell Biol.* **1998**, *142*, 635-649.
(49) Ashby, M. N.; King, D. S.; Rine, J. *proc. Natl. Acad. Sci. USA* **1992**, *89*, 4613-4617.
(50) Fujimura-Kamada, K.; Nouvet, F. J.; Michaelis, S. *J. Biol. Chem.* **1997**, *136*, 271-276.
(51) Huyer, G.; Kistler, A.; Nouvet, F. J.; George, C. M.; Boyle, M. L.; Michaelis, S. *Eukaryot. Cell* **2006**, *5*, 1560-1570.
(52) Schmidt, W. K.; Tam, A.; Michaelis, S. *J. Biol. Chem.* **2000**, *275*, 6227-6233.
(53) Tam, A.; Schmidt, W. K.; Michaelis, S. *J. Biol. Chem.* **2001**, *276*, 46798-46806.
(54) Dolence, J. M.; Steward, L. E.; Dolence, E. K.; Wong, D. H.; Poulter, C. D. *Biochemistry* **2000**, *39*, 4096-4104.
(55) Plummer, L. J.; Hildebrandt, E. R.; Porter, S. B.; Rogers, V. A.; McCracken, J.; Schmidt, W. K. *J. Biol. Chem.* **2006**, *281*, 4596-4605.
(56) Kyro, K.; Manandhar, S. P.; Mullen, D.; Schmidt, W. K.; Distefano, M. D. *Bioorgan. Med. Chem.* **2010**, *18*, 5675-5684.
(57) Ma, Y.-T.; Rando, R. R. *Proc. Natl. Acad. Sci. USA* **1992**, *89*, 6275-6279.
(58) Ma, Y. T.; Chaudhuri, A.; Rando, R. R. *Biochemistry* **1992**, *31*, 11772-11777.
(59) Jang, G.-F.; Gelb, M. H. *Biochemistry* **1998**, *37*, 4473-4478.
(60) Ma, Y. T.; Gilber, B. A.; Rando, R. R. *Biochemistry* **1993**, *32*, 2386-2393.
(61) Westerik, J. O.; Wolfenden, R. *J. Biol. Chem.* **1972**, *247*, 8195-8197.
(62) Hurley, J. B.; Simon, M. I.; Teplow, D. B.; Robishaw, J. D.; Gilman, A. G. *Science* **1984**, *226*, 860-862.
(63) Chen, Y.; Ma, Y.-T.; Rando, R. R. *Biochemistry* **1996**, *35*, 3227-3237.
(64) Chen, Y. *Cancer Lett.* **1998**, *131*, 191-200.
(65) Porter, S. B.; Hildebrandt, E. R.; Breevoort, S. R.; Mokry, D. Z.; Dore, T. M.; Schmidt, W. K. *BBA-Mol. Cell Res.* **2007**, *1773*, 853-862.
(66) Dechert, A.-M. R.; MacNamara, J. P.; Breevoort, S. R.; Hildebrandt, E. R.; Hembree, N. W.; Rea, A. C.; McLain, D. E.; Porter, S. B.; Schmidt, W. K.; Dore, T. M. *Bioorgan. Med. Chem.* **2010**, *18*, 6230-6237.
(67) Schlitzer, M.; Winter-Vann, A.; Casey, P. J. *Bioorgan. Med. Chem. Lett.* **2001**, *11*, 425-427.
(68) Manandhar, S. P.; Hildebrandt, E. R.; Schmidt, W. K. *J. Biomol. Screen* **2007**, *12*, 983-9932.
(69) Manandhar, S. P.; Hildebrandt, E. R.; Jacobsen, W. H.; Santangelo, G. M.; Schmidt, W. K. *Yeast* **2010**, *27*, 327-343.
(70) Mohammed, I.; Hampton, S. E.; Ashall, L.; Hildebrandt, E. R.; Kutlik, R. A.; Manandhar, S. P.; Floyd, B. J.; Smith, H. E.; Dozier, J. K.; Distefano, M. D.; Schmidt, W. K.; Dore, T. M. *Bioorgan. Med. Chem.* **2016**, *24*, 160-178.
(71) Coffinier, C.; Hudon, S. E.; Farber, E. A.; Chang, S. Y.; Hrycyna, C. A.; Young, S. G.; Fong, L. G. *Proc. Natl. Acad. Sci. USA* **2007**, *104*, 13432-13437.

(72) Coffinier, C.; Hudon, S. E.; Lee, R.; Farber, E. A.; Nobumori, C.; Miner, J. H.; Andres, D. A.; Spielmann, H. P.; Hrycyna, C. A.; Fong, L. G.; Young, S. G. *J. Biol. Chem.* **2008**, *283*, 9797-9804.
(73) Hudon, S. E.; Coffinier, C.; Michaelis, S.; Fong, L. G.; Young, S. G.; Hrycyna, C. A. *Biochem. and Bioph. Res. Co.* **2008**, *374*, 365-368.
(74) Son, C. D.; Sargsyan, H.; Naider, F.; Becker, J. M. *Biochemistry* **2004**, *43*, 13193-13203.
(75) Li, L.; Tang, W.; Zhao, Z. *Chin. J. Chem.* **2009**, *27*, 1391-1396.
(76) Turek, T. C.; Gaon, I.; Distefano, M. D. *Tetrahedron Lett.* **1996**, *37*, 4845-4848.
(77) Gaon, I.; Turek, T. C.; Distefano, M. D. *Tetrahedron Lett.* **1997**, *37*, 8833-8836.
(78) Kyro, K.; Manandhar, S. P.; Mullen, D.; Schmidt, W. K.; Distefano, M. D. *Bioorgan. Med. Chem.* **2011**, *19*, 7559-7569.
(79) Bergo, M. O.; Lieu, H. D.; Gavino, B. J.; Ambroziak, P.; Otto, J. C.; Casey, P. J.; Walker, Q. M.; Young, S. G. *J. Biol. Chem.* **2004**, *279*, 4729-4736.
(80) Pryor, E. E.; Horanyi, P. S.; Clark, K. M.; Fedoriw, N.; Connelly, S. M.; Koszelak-Rosenblum, M.; Zhu, G.; Malkowski, M. G.; Wiener, M. C.; Dumont, M. E. *Science* **2013**, *339*, 1600-1604.
(81) Quigley, A.; Dong, Y. Y.; Pike, A. C. W.; Dong, L.; Shrestha, L.; Berridge, G.; Stansfeld, P. J.; Sansom, M. S. P.; Edwards, A. M.; Bountra, C.; von Delft, F.; Bullock, A. N.; Burgess-Brown, N. A.; Carpenter, E. P. *Science* **2013**, *339*, 1604-1607.
(82) Clarke, S.; Vogel, J. P.; Deschenes, R. J.; Stock, J. *Proc. Natl. Acad. Sci. USA* **1988**, *85*, 4643-4647.
(83) Gutierrez, L.; Magee, A. I.; Marshall, C. J.; Hancock, J. F. *EMBO. J.* **1989**, *8*, 1093-1098.
(84) Romano, J. D.; Schmidt, W. K.; Michaelis, S. *Mol. Biol. Cell* **1998**, *9*, 2231-2247.
(85) Dai, Q.; Choy, E.; Chiu, V.; Romano, J.; Slivka, S. R.; Michaelis, S.; Philips, M. R. *J. Biol. Chem.* **1998**, *273*, 15030-15034.
(86) Shi, Y. Q.; Rando, R. R. *J. Biol. Chem.* **1992**, *267*, 9547-9551.
(87) Baron, R. A.; Casey, P. J. *BMC BioChem.* **2004**, *5*, 19.
(88) Anderson, J. L.; Frase, H.; Michaelis, S.; Hrycyna, C. A. *J. Biol. Chem.* **2005**, *280*, 7336-7345.
(89) Romano, J.; Michaelis, S. *Mol. Biol. Cell* **2001**, *12*, 1957-1971.
(90) Wright, L. P.; Court, H.; Mor, A.; Ahearn, I. M.; Casey, P. J.; Philips, M. R. *Mol. Biol. Cell* **2009**, *29*, 1826-1833.
(91) Desrosiers, R. R.; Nguyen, Q. T.; Beliveau, R. *Biochem. Biophs. Res. Commun.* **1999**, *261*, 270-279.
(92) Schmitt, L.; Dietrich, C.; Tampe, R. *J. Am. Chem. Soc.* **1994**, *116*, 8485-8491.
(93) Hodges, H. B.; Zhou, M. K.; Haldar, S.; Anderson, J. L.; Thompson, D. H.; Hrycyna, C. A. *Bioconjug. Chem* **2005**, *16*, 490-943.
(94) Sakagami, Y.; Yoshida, M.; Isogai, A.; Suzuki, A. *Science* **1981**, *212*, 1525-1527.
(95) Ishibashi, Y.; Sakagami, Y. I., A.; Suzuki, A. *Biochemistry* **1984**, *23*, 1399-1404.
(96) Murr, R. S.; Blair, L. C.; Thorner, J. **1990**.
(97) Stephenson, R. C.; Clarke, S. *J. Biol. Chem.* **1990**, *265*, 16248-16254.

(98) Tan, E. W.; Perezsala, D.; Canada, F. J.; Rando, R. R. *J. Biol. Chem.* **1991**, *266*, 10719-10722.
(99) Stephenson, R. C.; Clarke, S. *J. Biol. Chem.* **1992**, *267*, 13314-13319.
(100) Clarke, S. *Annu. Rev. Biochem.* **1992**, *61*, 355.
(101) Zhang, F. L.; Casey, P. J. *Annu. Rev. Biochem.* **1996**, *65*, 241-269.
(102) Bergo, M. O.; Leung, G. K.; Ambroziak, P.; Otto, J. C.; Casey, P. J.; Gomes, A. Q.; Seabra, M. C.; Young, S. G. *J. Biol. Chem.* **2001**, *276*, 5841-5845.
(103) Bergo, M. O.; Leung, G. K.; Ambroziak, P.; Otto, J. C.; Casey, P. J.; Young, S. G. *J. Biol. Chem.* **2000**, *275*.
(104) Bergo, M. O. G., B. J.; Hong, C.; Beigneux, A. P.; McMahon, M.; Casey, P. J.; Young, S. G. *J. Clin. Invest.* **2004**, *113*, 539-550.
(105) Ibrahim, M. X.; Sayin, V. I.; Akula, M. K.; Liu, M.; Fong, L. G.; Young, S. G.; Bergo, M. O. *Science* **2013**, *340*, 1330-1333.
(106) Clarke, S.; Tamanoi, F. *J. Clin. Invest.* **2004**, *113*, 513-515.
(107) Perez-Sala, D.; Gilbert, B. A.; Tan, E. W.; Rando, R. R. *Biochem. J.* **1992**, *284*, 835-840.
(108) Young, S. G.; Ambroziak, P.; Kim, E.; Clarke, S. *The Enzymes*; 3rd ed.; Academic Press: San Diego, CA, 2000; Vol. 21.
(109) Abad-Zapatero, C.; Metz, J. T. *Drug Discov. Today* **2005**, *10*, 464-469.
(110) Henriksen, B. S.; Anderson, J. L.; Hrycyna, C. A.; Gibbs, R. A. *Bioorg. Med. Chem. Lett.* **2005**, *15*, 5080-5083.
(111) Bergman, J. A.; Hahne, K.; Hrycyna, C. A.; Gibbs, R. A. *Bioorg. Med. Chem. Lett.* **2011**, *21*, 5616-5619.
(112) Volker, C.; Lane, P.; Kwee, C.; Johnson, M.; Stock, J. *FEBS Lett.* **1991**, *295*, 189-194.
(113) Volker, C.; Miller, R. A.; McCleary, W. R.; Rao, A.; Poenie, M.; Backer, J. M.; Stock, J. B. *J. Biol. Chem.* **1991**, *266*, 21515-21522.
(114) Philips, M. R.; Pillinger, M. H.; Staud, R.; Volker, C.; Rosenfeld, M. G.; Weissmann, G.; Stock, J. B. *Science* **1993**, *259*, 977-980.
(115) Huzoor-Akbar; Wang, W.; Kornhauser, R.; Volker, C.; Stock, J. B. *Proc. Natl. Acad. Sci. USA* **1993**, *90*, 868-871.
(116) Scheer, A.; Gierschik, P. *FEBS Lett.* **1993**, *319*, 110-114.
(117) Scheer, A.; Gierschik, P. *Biochemistry* **1995**, *34*, 4952-4956.
(118) Kramer, K.; Harrington, E. O.; Lu, Q.; Bellas, R.; Newton, J.; Sheahan, K. L.; Rounds, S. *Mol. Biol. Cell* **2003**, *14*, 848-857.
(119) Chiu, V. K.; Silletti, J.; Dinsell, V.; Wiener, H.; Loukeris, K.; Ou, G.; Philips, M. R.; Pillinger, M. H. *J. Biol. Chem.* **2004**, *279*, 7346-7352.
(120) Philips, M. R.; Staud, R.; Pillinger, M.; Feoktistov, A.; Volker, C.; Stock, J. B.; Weissmann, G. *Proc. Natl. Acad. Sci. USA* **1995**, *92*, 2283-2288.
(121) Ding, J.; Lu, D. J.; Perezsala, D.; Ma, Y.-T.; Maddox, J. F.; Gilbert, B. A.; Badwey, J. A.; Rando, R. R. *J. Biol. Chem.* **1994**, *269*, 16837-16842.
(122) Ma, Y.-T.; Shi, Y.-Q.; Lim, Y. H.; McGrail, S. H.; Ware, J. A.; Rando, R. R. *Biochemistry* **1994**, *33*, 5414-5420.

(123) Marciano, D.; Benbaruch, G. M., M.; Egozi, Y.; Haklai, R.; Kloog, Y. *J. Med. Chem* **1995**, *38*, 1267-1272.
(124) Marciano, D.; Aharonson, Z.; Varsano, T.; Haklai, R.; Kloog, Y. *Bioorg. Med. Chem. Lett.* **1997**, *7*, 1709-1714.
(125) Marom, M.; Haklai, R.; Ben-Baruch, G.; Marciano, D.; Egozi, Y.; Kloog, Y. *J. Biol. Chem.* **1995**, *270*, 22263-22270.
(126) Ma, Y.-T.; Gilbert, B. A.; Rando, R. R. *Methods Enzymol* **1995**, *250*, 226-234.
(127) Donelson, J. L.; Hodges, H. B.; MacDougall, D. D.; Henriksen, B. S.; Hrycyna, C. A.; Gibbs, R. A. *Bioorg. Med. Chem. Lett.* **2006**, *16*, 4420-4423.
(128) Donelson, J. L. H.-L., H. B.; Henriksen, B. S.; Hrycyna, C. A.; Gibbs, R. A. *J. Org. Chem.* **2009**, *74*, 2975-2981.
(129) Majmudar, J. D.; Hahne, K.; Hrycyna, C. A.; Gibbs, R. A. *Bioorg. Med. Chem. Lett.* **2011**, *21*, 2616-2620.
(130) Anderson, J. L.; Henriksen, B. S.; Gibbs, R. A.; Hrycyna, C. A. *J. Biol. Chem.* **2005**, *280*, 29454-29461.
(131) Bergman, J. A.; Hahne, K.; Song, J.; Hrycyna, C. A.; Gibbs, R. A. *Med. Chem. Lett.* **2012**, *3*, 15-19.
(132) Chiang, P. K.; Gordon, R. K.; Tal, J.; Zeng, G. C.; Doctor, B. P.; Pardhasaradhi, K.; McCann, P. P. *FASEB J.* **1996**, *10*, 471-480.
(133) Lederer, E. D.; Jacobs, A. A.; Hoffman, J. L.; Harding, G. B.; Robishaw, J. D.; Mcleish, K. R. *Biochem. Biophs. Res. Commun.* **1994**, *200*, 1604-1609.
(134) Wang, H.; Yoshizumi, M.; Lai, K.; Tsai, J.-C.; Perrella, M. A.; Haber, E.; Lee, M.-E. *J. Biol. Chem.* **1997**, *272*, 25380-25385.
(135) Winter-Vann, A. M.; Kamen, B. A.; Bergo, M. O.; Young, S. G.; Melnyk, S.; James, S. J.; Casey, P. J. *Proc. Natl. Acad. Sci. USA* **2003**, *100*, 6529-6534.
(136) Kim, J. H.; Kim, J. H.; Kim, S. C.; Yi, Y.-S.; Yang, W. S.; Yang, Y.; Kim, H. G.; Lee, J. Y.; Kim, K.-H.; Yoo, B. C.; Hong, S.; Cho, J. Y. *Biochem. Pharmacol.* **2013**, *86*, 1285-1300.
(137) Hoffman, D. R.; Cornatzer, W. E.; Duerre, J. A. *Can. J. Biochem.* **1979**, *57*, 56-65.
(138) Winter-Vann, A. M.; Baron, R. A.; Wong, W.; dela Cruz, J.; York, J. D.; Gooden, D. M.; Bergo, M. O.; Young, S. G.; Toone, E. J.; Casey, P. J. *Proc. Natl. Acad. Sci. USA* **2005**, *102*, 4336-4341.
(139) Baron, R. A.; Peterson, Y. i. K.; Otto, J. C.; Rudolph, J.; Casey, P. J. *Biochemistry* **2007**, *46*, 554-560.
(140) Wang, M. In *The Enzymes*; Christine A. Hrycyna, M. O. B., Fuyuhiko, T., Eds.; Academic Press: 2011; Vol. Volume 30, p 259-278.
(141) Wang, M.; Tan, W.; Zhou, J.; Leow, J.; Go, M.; Lee, H. S.; Casey, P. J. *J. Biol. Chem.* **2008**, *283*, 18678-18684.
(142) Cushman, I.; Casey, P. J. *J. Biol. Chem.* **2009**, *284*, 27964-27973.
(143) Wang, M.; Hossain, M. S.; Tan, W.; Coolman, B.; Zhou, J.; Liu, S.; Casey, P. J. *Oncogene* **2010**, *29*, 4959-4970.
(144) Lau, H. Y.; Ramanujulu, P. M.; Guo, D.; Yang, T.; Wirawan, M.; Casey, P. J.; Go, M.-L.; Wang, M. *Cancer Biol. Ther.* **2014**, 1280-1291.

(145) Sun, W. T.; Xiang, W.; Ng, B. L.; Asari, K.; Bunte, R. M.; Casey, P. J.; Wang, M.; Chuah, C. *Exp. Hematol.* **2016**, *44*, 189-193.
(146) Wang, M.; Khoo, Y. M.; Zhou, J.; Casey, P. J.; Lee, H. S. *J. Chromatogr. B.* **2009**, *877*, 553-557.
(147) Go, M.-L.; Leow, J. L.; Gorla, S. K.; Schüller, A. P.; Wang, M.; Casey, P. J. *J. Med. Chem.* **2010**, *53*, 6838-6850.
(148) Buchanan, M. S.; Carroll, A. R.; Fechner, G. A.; Boyle, A.; Simpson, M. M.; Addepalli, R.; Avery, V. M.; Hooper, J. N. A.; Su, N.; Chen, H.; Quinn, R. J. *Bioorg. Med. Chem. Lett.* **2007**, *17*, 6860-6863.
(149) Buchanan, M. S. *J. Nat. Prod* **2008**, *71*, 1066-1070.
(150) Buchanan, M. S.; Carroll, A. R.; Fechner, G. A.; Boyle, A.; Simpson, M. M.; Addepalli, R.; Avery, V. M.; Forster, P. I.; Guymer, G. P.; Cheung, T.; Chen, H.; Quinn, R. J. *Phytochemistry* **2008**, *69*, 1886-1889.
(151) García, J.; Pereira, R.; de Lera, A. R. *Tetrahedron Lett.* **2009**, *50*, 5028-5030.
(152) Ullah, N.; Arafeh, K. M. *Tetrahedron Lett.* **2009**, *50*, 158-160.
(153) Ullah, N.; Haladu, S. A.; Mosa, B. A. *Tetrahedron Lett* **2011**, *52*, 212-214.
(154) Hahne, K.; Vervacke, J. S.; Shrestha, L.; Donelson, J. L.; Gibbs, R. A.; Distefano, M. D.; Hrycyna, C. A. *Biochem. Biophs. Res. Commun.* **2012**, *423*, 98-103.
(155) Vervacke, J. S.; Funk, A. L.; Wang, Y.-C.; Strom, M.; Hrycyna, C. A.; Distefano, M. D. *J. Org. Chem.* **2014**, *79*, 1971-1978.
(156) Vetter, I. R.; Wittinghofer, A. *Science* **2001**, *294*, 1299-1304.
(157) Wennerberg, K.; Rossman, K. L.; Der, C. J. *J. Cell. Sci.* **2005**, *118*, 843-846.
(158) Court, H.; Hahne, K.; Philips, M. R.; Hrycyna, C. A. In *The Enzymes*; Christine A. Hrycyna, M. O. B., Fuyuhiko, T., Eds.; Academic Press: 2011; Vol. Volume 30, p 71-90.
(159) Hrycyna, C. A.; Wait, S. J.; Backlund, P. S.; Michaelis, S. *Methods Enzymol* **1995**, *250*, 251-266.
(160) Reid, T. S.; Terry, K. L.; Casey, P. J.; Beese, L. S. *J. Mol. Biol.* **2004**, *343*, 417-433.
(161) Yang, J.; Kulkarni, K.; Manolaridis, I.; Zhang, Z.; Dodd, R. B.; Mas-Droux, C.; Barford, D. *Mol. Cell* **2011**, *44*, 997-1004.
(162) Kale, T. A.; Raab, C.; Yu, N.; Dean, D. C.; Distefano, M. D. *J. Am. Chem. Soc.* **2001**, *123*, 4373-4381.
(163) Mullen, D. G.; Kyro, K.; Hauser, M.; Gustavsson, M.; Veglia, G.; Becker, J. M.; Naider, F.; Distefano, M. D. *Bioorg. Med. Chem.* **2011**, *19*, 490-497.
(164) Cheng, Y.; Prusoff, W. H. *Biochem. Pharmacol.* **1973**, *22*, 3099-3108.
(165) Ballell, L.; Alink, K. J.; Slijper, M.; Versluis, C.; Liskamp, R. M.; Pieters, R. J. *ChemBioChem* **2005**, *6*, 261-295.
(166) Rowland, M. M., University of Tennessee, 2011.
(167) P.D.M.; Brown, M. J.; Lever, D. J.; Epstein, W. W.; Poulter, D. C. *J. Am. Chem. Soc.* **1991**, *113*, 3176-3177.
(168) Turek, T. C.; Gaon, I.; Distefano, M. D.; Strickland, C. L. *J. Org. Chem.* **2001**, *66*, 3253-3264.

(169) Turek-Etienne, T. C.; Strickland, C. L.; Distefano, M. D. *Biochemistry* **2003**, *42*, 3716-3724.
(170) Gaon, I.; Turek, T. C.; Weller, V. A.; Edelstein, R. L.; Singh, S. K.; Distefano, M. D. *J. Org. Chem.* **2001**, *61*, 7738-7745.
(171) Donelson, J. L.; Hodges-Loaiza, H. B.; Henriksen, B. S.; Hrycyna, C. A.; Gibbs, R. A. *J. Org. Chem.* **2009**, *74*, 2975-2981.
(172) Volkert, M.; Uwai, K.; Tebbe, A.; Popkirova, B.; Wagner, M.; Kuhlmann, J.; Waldmann, H. *J. Am. Chem. Soc.* **2003**, *125*, 12749-12758.
(173) Kaiser, E.; Colescott, R. L.; Bossinger, C. D.; Cook, P. I. *Anal. Biochem.* **1970**, *34*, 595-598.
(174) Griggs, A. M.; Hahne, K.; Hrycyna, C. A. *J. Biol. Chem.* **2010**, *285*, 13380-13387.
(175) Wessel, D.; Flugge, U. I. *Anal. Biochem.* **1984**, *285*, 13380-13387.
(176) Vervacke, J. S.; Wang, Y.-C.; Distefano, M. D. *Curr. Med. Chem.* **2013**, *20*, 1585-1594.
(177) Berndt, N.; Hamilton, A. D.; Sebti, S. M. *Nat. Rev. Cancer* **2011**, *11*, 775-791.
(178) Ochocki, J. D., M. D. *MedChemComm*, *4*, 476-492.
(179) Chehade, K. A. H.; Kiegiel, K.; Isaacs, R. J.; Pickett, J. S.; Bowers, K. E.; Fierke, C. A.; Andres, D. A.; Spielmann, H. P. *J. Am. Chem. Soc.* **2002**, *124*, 8206-8219.
(180) Baba, T. A., C. M. *Biochemistry* **1984**, *23*, 1312-1322.
(181) Bikhtiyarov, Y. E.; Omer, C. A. A., C. M. *J. Biol. Chem.* **1995**, *270*, 19035-19040.
(182) Hovlid, M. L.; Edelstein, R. L.; Henry, O. O., J.Talbot, T.; Lopez-Gallego, F.; Schmidt-Dannert, C.; Distefano, M. D. *Chem. Biol. Drug Des.* **2010**, *75*, 51-67.
(183) Yokoyama, K.; McGeady, P.; Gelb, M. H. *Biochemistry* **1995**, *34*, 1344-1354.
(184) Alexander, M.; Gerauer, M.; Pechlivanis, M.; Popkirova, B.; Dvorsky, R.; Brunsveld, L.; Waldmann, H.; Kuhlmann, J. *ChemBioChem* **2009**, *10*, 98-108.
(185) DeGraw, A. J.; Zhao, Z.; Strickland, C. L.; Taban, A. H.; Hsieh, J.; Jefferies, M.; Xie, W.; Shintani, D. K.; McMahan, C. M.; Cornish, K.; Distefano, M. D. *J. Org. Chem.* **2007**, *72*, 4587-4595.
(186) Chowdhry, V.; Vaughan, R.; Westheimer, F. H. *Proc. Natl. Acad. Sci. USA* **1976**, *73*, 1406-1408.
(187) Michaelis, S.; Barrowman, J. *Microbiol. Mol. Biol. R.* **2012**, *76*, 626-651.
(188) Bond, M. R.; Zhang, H.; Vu, P. D.; Kohler, J. J. *Nat. Protocols* **2009**, *4*, 1044-1063.
(189) Atherton, E.; Hardy, P. M.; Harris, D. E.; Matthews, B. H. In *American Peptide Syposium*; Giralt, E., Andreu, D., Eds. 1990.
(190) Anderegg, R. J.; Betz, R.; Carr, S. A.; Crabb, J. W.; Duntze, W. *J. Biol. Chem.* **1988**, *19*, 7559-7569.
(191) Ding, F.-X.; Lee, B. K.; Hauser, M.; Davenport, L.; Becker, J. M.; Naider, F. *Biochemistry* **2001**, *40*, 1102-1108.
(192) Diaz-Rodriguez, V.; Ganusova, E.; Rappe, T. M.; Becker, J. M.; Distefano, M. D. *J. Org. Chem.* **2015**, *80*, 11266-11274.

(193) Diaz-Rodriguez, V.; Mullen, D. G.; Ganusova, E.; Becker, J. M.; Distefano, M. D. *Org. Lett.* **2012**, *14*, 5648-5651.
(194) Atherton, E.; Hardy, P. M.; Harris, D. E.; Matthews, B. H. In *American Peptide Syposium*; Giralt, E., Andreu, D., Eds. 1990.
(195) Hollander, I.; Frommer, E.; Mallon, R. *Anal. Biochem.* **2000**, *286*, 129-137.
(196) Poulter, D. C. *Accounts Chem. Res.* **1990**, *23*, 70-77.
(197) Rupar, C. A.; Ravi, K.; Carroll, K. K. *Prog. Lipid. Res.* **1985**, *24*, 269-309.
(198) Cornish, K. In *Regulation of Isopentenoid Metabolism*; American Chemical Society: 1992; Vol. 497, p 18-26.
(199) Christianson, D. W. *Curr. Opin. Chem. Biol.* **2008**, *12*, 141-150.
(200) Loomis, W. D. C., R., *Biochem. Plants* **1980**, *4*, 363-418.
(201) Kato, K.; Cox, A. D.; Hisaka, M. M.; Graham, S. M.; Buss, J. E.; Der, C. J. *Proc. Natl. Acad. Sci. USA* **1992**, *89*, 6403-6407.
(202) Sebti, S. M.; Hamilton, A. D. *Oncogene* **2000**, *19*, 6584-6593.
(203) Crul, M.; J., d. K. G.; Beijnen, J. H.; Schellens, J. H. *Anti-cancer Drugs* **2001**, *12*, 163-184.
(204) Baba, T.; Allen, C. M. *Biochemistry* **1984**, *23*, 1312-1322.
(205) Baba, T.; Muth, J.; Allen, C. M. *J. Biol. Chem.* **1985**, *260*, 10467-10473.
(206) Das, N. P.; Allen, C. M. *Biochem. Biophys. Res. Comm.* **1991**, *181*, 729-735.
(207) Edelstein, R. L.; Distefano, M. D. *Biochem. Biophys. Res. Comm.* **1997**, *235*, 377-382.
(208) Liu, J.; Stipanovic, R. D.; Benedict, C. R. *J. Labelled Compd. Radiopharm.* **1996**, *38*, 139-148.
(209) Ohno, K.; Mori, K.; Orita, M. T., M., *Curr. Med. Chem.* **2011**, *18*, 220-233.
(210) Omer, C. A.; Kral, A. M. D., R. E.Prendergast, G. C.Powers, S.; Allen, C. M. G., J. B.; Kohl, N. E. *Biochemistry* **1993**, *32*, 5167-5176.
(211) Quellhorst, G. J., Jr.Allen, C. M.; Wessling-Resnick, M. *J. Biol. Chem.* **2001**, *276*, 40727-40733.
(212) Das, D.; Tnimov, Z.; Nguyen, U. T. T.; Thimmaiah, G.; Lo, H.; Abankwa, D.; Wu, Y.; Goody, R. S.; Waldmann, H.; Alexandrov, K. *ChemBioChem* **2012**, *13*, 674-683.
(213) Edelstein, R. L.; Singh, S. K.; Distefano, M. D. *J. Org. Chem.* **1996**, *61*, 7738-7745.
(214) Turek, T. C.; Gaon, I.; Distefano, M. D. *J. Labelled Compd. Radiopharm.* **1997**, *1997*, 140-146.
(215) Turek, T. C.; Gaon, I.; Gamache, D.; Distefano, M. D. *Bioorg. Med. Chem. Lett.* **1997**, *7*, 2125-2130.
(216) Blau, N. F.; Wang, T. T. S.; Buess, C. M. *J. Chem. Eng. Data* **1970**, *15*, 206-208.
(217) Popjak, G.; Hadley, C. *J. Lipid Res.* **1985**, *26*, 1151-1159.
(218) Tian, R.; Li, L.; Tang, W.; Liu, H.; Ye, M.; Zhao, Z. K.; Zou, H. *Proteomics* **2008**, *8*, 3094-3104.

(219) Schuld, N. J.; Vervacke, J. S.; Lorimer, E. L.; Simon, N. C.; Hauser, A. D.; Barbieri, J. T.; Distefano, M. D.; Williams, C. L. *J. Biol. Chem.* **2014**, *289*, 6862-6876.
(220) Bond, P. D.; Dolence, J. M.; Poulter, C. D. *Methods Enzymol* **1995**, *250*, 30-43.
(221) Pompliano, D. L.; Gomez, R. P.; Anthony, N. J. *J. Am. Chem. Soc.* **1992**, *114*, 7945-7946.
(222) Bond, M. R.; Zhang, H.; Vu, P. D.; Kohler, J. J. *Nat. Protocols* **2009**, *4*, 1044-1063.
(223) Reed, B. C.; Rilling, H. C. *Biochemistry* **1976**, *15*, 3739-3745.
(224) Dozier, J. K.; Distefano, M. D. *Anal. Biochem.* **2012**, *421*, 158-163.
(225) DeGraw, A. J.; Hast, M. A.; Xu, J.; Mullen, D.; Beese, L. S.; Barany, G.; Distefano, M. D. *Chem. Biol. Drug Des.* **2008**, *72*, 171-181.
(226) Collins, K. D.; Stark, G. R. *J. Biol. Chem.* **1971**, *246*, 6599-6605.
(227) Lavogina, D.; Lust, M.; Viil, I.; König, N.; Raidaru, G.; Rogozina, J.; Enkvist, E.; Uri, A.; Bossemeyer, D. *J. Med. Chem.* **2009**, *52*, 308-321.
(228) Cassera, M. B.; Ho, M.-C.; Merino, E. F.; Burgos, E. S.; Rinaldo-Matthis, A.; Almo, S. C.; Schramm, V. L. *Biochemistry* **2011**, *50*, 1885-1893.
(229) Szyk, A.; Deaconescu, A. M.; Spector, J.; Goodman, B.; Valenstein, M. L.; Ziolkowska, N. E.; Kormendi, V.; Grigorieff, N.; Roll-Mecak, A. *Cell* **2014**, *157*, 1405-1415.
(230) Frankel, B. A.; Kruger, R. G.; Robinson, D. E.; Kelleher, N. L.; McCafferty, D. G. *Biochemistry* **2005**, *44*, 11188-11200.
(231) Due, A. V.; Kuper, J.; Geerlof, A.; Kries, J. P.; Wilmanns, M. *Proc. Natl. Acad. Sci. USA* **2011**, *108*, 3554-3559.
(232) Evjenth, R. H.; Brenner, A. K.; Thompson, P. R.; Arnesen, T.; Frøystein, N. Å.; Lillehaug, J. R. *J. Biol. Chem.* **2012**, *287*, 10081-10088.
(233) Schlitzer, M.; Sattler, I. *Angew. Chem.* **1999**, *38*, 2032-2040.
(234) Armstrong, J. I.; Ge, X.; Verdugo, D. E.; Winans, K. A.; Leary, J. A.; Bertozzi, C. R. *Org. Lett.* **2001**, *3*, 2657-2660.
(235) Barnett, B. P.; Hwang, Y.; Taylor, M. S.; Kirchner, H.; Pfluger, P. T.; Bernard, V.; Lin, Y.-Y.; Bowers, E. M.; Mukherjee, C.; Song, W.-J.; Longo, P. A.; Leahy, D. J.; Hussain, M. A.; H., M.; Boeke, J. D.; Cole, P. A. *Science* **2010**, *330*, 1689-1692.
(236) Brandvold, K. R.; Santos, S. M.; Breen, M. E.; Lachacz, E. J.; Steffey, M. E.; Soellner, M. B. *ACS Chem. Biol.* **2015**, *10*, 1387-1391.
(237) Dong, Q.; Ernst, S. E.; Ostedgaard, L. S.; Shah, V. S.; Ver Heul, A. R.; Welsh, M. J.; Randak, C. O. *J. Biol. Chem.* **2015**, *290*, 14140-14153.
(238) Ikeuchi, H.; Meyer, M. E.; Ding, Y.; Hiratake, J.; Richards, N. G. J. *Bioorganic & Medicinal Chemistry* **2009**, *17*, 6641-6650.
(239) Anderson, J. L.; Frase, H.; Michaelis, S.; Hrycyna, C. A. *J. Biol. Chem.* **2005**, *280*, 7336-7345.
(240) Anderson, J. L.; Henriksen, B. S.; Gibbs, R. A.; Hrycyna, C. A. *J. Biol. Chem.* **2005**, *280*, 29454-29461.